

**Evaluation of Novel Glass-Ionomer Cements
for Hard Tissue Repair using *In Vitro* and
In Vivo methods**

A thesis submitted as the requirement for the

Doctor of Philosophy

by

Kámel K Johal

**Department of Oral & Maxillofacial Surgery,
Department of Restorative Dentistry,
Department of Oral Pathology,
University of Sheffield.**

August 1998

IMAGING SERVICES NORTH

Boston Spa, Wetherby

West Yorkshire, LS23 7BQ

www.bl.uk

**BRITISH
LIBRARY**

**ORIGINAL COPY TIGHTLY
BOUND**

IMAGING SERVICES NORTH

Boston Spa, Wetherby

West Yorkshire, LS23 7BQ

www.bl.uk

BEST COPY AVAILABLE.

VARIABLE PRINT QUALITY

CONTENTS

	Page
Acknowledgements	xviii
Summary	xix
1. Introduction	1
1.1 Glass-ionomer (polyalkenoate) cements	5
1.1.1 History	5
1.1.2 Properties	7
1.1.3 Applications for medical and dental use	9
1.1.4 Ion release	12
1.2 Bone cements and substitutes for hard tissue augmentation	18
1.2.1 Polymethylmethacrylate	19
1.2.2 Calcium phosphates	20
1.3 The evaluation of biocompatibility	22
1.3.1 Evaluation of ICs <i>in vitro</i>	23
1.3.2 Evaluation of ICs <i>in vivo</i>	25
1.3.3 Bone proteins	25
1.4 Hypothesis	27
1.5 Aims	27
2. Materials and Methods	29
2.1 Materials	29
2.1.1 Glass polyalkenoate cements	30
2.1.2 Ion release experiments	33
2.1.3 Tissue culture	34
2.1.4 <i>In vivo</i> implantation	38
2.1.5 Immunohistochemical techniques	40
2.2 Methods	41
2.2.1 Mechanical testing of glass polyalkenoates	41
2.2.2 Ion release methods	41
2.2.3 Tissue culture method	48
2.2.4 <i>In vivo</i> techniques	57

CONTENTS

	Page
3. Results	65
3.1 Material properties	65
3.2 Ion release studies	69
(a) Fluoride	69
(b) Sodium	82
(c) Potassium	85
(d) Aluminium	86
(e) Silicon	94
(f) Calcium	102
(g) Phosphate	106
(h) pH of autoclaved and non-autoclaved discs in solution	111
3.3 Tissue culture/ <i>in vitro</i>	115
3.3.1 Bone marrow cell culture	115
3.3.2 Quantitative assessment of cytocompatibility	119
3.4 <i>In vivo</i> implantation	134
3.4.1 Histological assessment of <i>in vivo</i> Surgical implantation	134
3.4.2 Histomorphometric results	153
3.4.3 Immunohistochemical assessment	155
4. General Discussion	165
4.1 Setting and working times	166
4.2 Ion release	168
4.3 Tissue culture	192
4.4 <i>In vivo</i>	197
4.4(a) Set ionomeric cements	198
4.4(b) Wet ionomeric cements	202
4.4(c) Bone proteins	207
5. Final Discussion	210
6 Conclusion	214
7 Future Considerations	217
8 References	219
9 Appendix	239

TABLES

	Page
<i>Table 1.1.1:</i> Significant published studies showing the history of the development of ionomeric cements	5
<i>Table 2.1:</i> Commercial materials used for <i>in vitro</i> studies	29
<i>Table 2.2:</i> Ionomeric cements tested for surgical implantation	38
<i>Table 2.3:</i> Instrument Conditions for Ca analysis	44
<i>Table 2.4:</i> Instrument Conditions for Si analysis	45
<i>Table 2.5:</i> Furnace parameters	46
<i>Table 2.6:</i> Protein concentrations	54
<i>Table 3.1:</i> Working and setting time (s) for the monovalent cation series of ICs	65
<i>Table 3.2:</i> Working and setting time test (s) for the apatite-stoichiometric based ICs	66
<i>Table 3.3:</i> Working and setting time test (s) for the radiopaque strontium based ICs	67
<i>Table 3.4:</i> Working and setting time test (s) for the zinc based ICs	67
<i>Table 3.5:</i> Working and setting time test for the acrylic cement (control)	68
<i>Table 3.6:</i> Fluoride ion release ($\mu\text{mol/g}$) over time from discs of ionomeric cements from the monovalent cation based series	69
<i>Table 3.7:</i> Fluoride ion release ($\mu\text{mol/g}$) over time from discs of ionomeric cements from the apatite-stoichiometric based series (Ca:P~1.66)	75

TABLES (continued)

	Page
<i>Table 3.8:</i> Fluoride ion release ($\mu\text{mol/g}$) over time from discs of ionomeric cements from the series varying in calcium fluoride	77
<i>Table 3.9:</i> Fluoride ion release ($\mu\text{mol/g}$) over time from discs of ionomeric cements from the series varying in silica:alumina and calcium	77
<i>Table 3.10:</i> Fluoride ion release ($\mu\text{mol/g}$) over time from discs of ionomeric cements from the series varying in silica:alumina ratios.	77
<i>Table 3.11:</i> Fluoride ion release ($\mu\text{mol/g}$) over time from discs of ionomeric cements from the series varying in generic compositions derived from the apatite-stoichiometric based glass LG26	78
<i>Table 3.12:</i> Fluoride ion release ($\mu\text{mol/g}$) over time from discs of ionomeric cements from the calcium based series	79
<i>Table 3.13:</i> Fluoride ion release ($\mu\text{mol/g}$) over time from discs of ionomeric cements from LG2 and LG26 in α -MEM	79
<i>Table 3.14:</i> Fluoride ion release ($\mu\text{mol/g}$) over time from discs of glass ionomeric cements controls	80
<i>Table 3.15:</i> Fluoride ion release ($\mu\text{mol/g}$) over time from discs of autoclaved ionomeric cements	80
<i>Table 3.16:</i> Fluoride ion release ($\mu\text{mol/g}$) over time from discs of monovalent cation based series (without TISAB)	81
<i>Table 3.17:</i> Fluoride ion release ($\mu\text{mol/g}$) over time from discs of apatite stoichiometric based series without TISAB	81
<i>Table 3.18:</i> Sodium ion release ($\mu\text{mol/g}$) over time from discs of ionomeric cements of the monovalent cation series	82

TABLES (continued)

	Page
<i>Table 3.19:</i> Sodium ion release ($\mu\text{mol/g}$) over time from discs of ionomeric cements of the apatite stoichiometric based series	84
<i>Table 3.20:</i> Potassium ion release ($\mu\text{mol/g}$) over time from discs of ionomeric cements of the monovalent cation series	85
<i>Table 3.21:</i> Potassium ion release ($\mu\text{mol/g}$) over time from discs of ionomeric cements of the apatite stoichiometric based series	85
<i>Table 3.22:</i> Aluminium ion release ($\mu\text{mol/g}$) over time from discs ionomeric cements of the monovalent cation series	86
<i>Table 3.23:</i> Aluminium ion release ($\mu\text{mol/g}$) over time from discs of ionomeric cements from the series varying in silica/alumina and calcium	92
<i>Table 3.24:</i> Aluminium ion release ($\mu\text{mol/g}$) over time from discs of ionomeric cements from the series varying in silica/alumina ratios.	92
<i>Table 3.25:</i> Aluminium ion release ($\mu\text{mol/g}$) over time from discs of ionomeric cements from the series varying in generic compositions derived from the apatite stoichiometric based glass LG26	92
<i>Table 3.26:</i> Aluminium ion release ($\mu\text{mol/g}$) over time from discs of ionomeric cements from the calcium based series	93
<i>Table 3.27:</i> Aluminium ion release ($\mu\text{mol/g}$) over time from discs of glass ionomeric cements controls	94
<i>Table 3.28:</i> Silicon release ($\mu\text{mol/g}$) over time from discs of ionomeric cements of the monovalent cation series	94
<i>Table 3.29:</i> Silicon release ($\mu\text{mol/g}$) over time from discs of ionomeric cements from apatite stoichiometric series	97

TABLES (continued)

	Page
<i>Table 3.30:</i> Silicon release ($\mu\text{mol/g}$) over time from discs of ionomeric cements from the series varying in calcium fluoride	97
<i>Table 3.31:</i> Silicon release ($\mu\text{mol/g}$) over time from discs of ionomeric cements from the series varying in silica/alumina and calcium	98
<i>Table 3.32:</i> Silicon ion release ($\mu\text{mol/g}$) over time from discs of ionomeric cements from the series varying in silica/alumina ratios	98
<i>Table 3.33:</i> Silicon release ($\mu\text{mol/g}$) over time from discs of ionomeric cements from the series varying in generic compositions derived from the apatite stoichiometric based glass LG26	100
<i>Table 3.34:</i> Silicon release ($\mu\text{mol/g}$) over time from discs of ionomeric cements from the calcium based series	100
<i>Table 3.35:</i> Silicon over time ($\mu\text{mol/g}$) from discs of glass ionomeric cement controls	101
<i>Table 3.36:</i> Calcium ion release ($\mu\text{mol/g}$) over time from discs of ionomeric cements of the monovalent cation series	102
<i>Table 3.37:</i> Calcium ion release ($\mu\text{mol/g}$) over time from discs of ionomeric cements from the apatite stoichiometric series	103
<i>Table 3.38:</i> Calcium ion release ($\mu\text{mol/g}$) over time from discs of ionomeric cements from the series varying in calcium fluoride up to the same period	103
<i>Table 3.39:</i> Calcium ion release ($\mu\text{mol/g}$) over time from discs of ionomeric cements for the series varying in silica/alumina and calcium	104

TABLES (continued)

	Page
<i>Table 3.40:</i> Calcium ion release ($\mu\text{mol/g}$) over time from discs of ionomeric cements from the series varying in silica/alumina ratios	104
<i>Table 3.41:</i> Calcium ion release ($\mu\text{mol/g}$) over time from discs of ionomeric cements from the series varying in generic compositions derived from the apatite stoichiometric series glass LG26	105
<i>Table 3.42:</i> Calcium ion release ($\mu\text{mol/g}$) over time from discs of ionomeric cements from the calcium based series	105
<i>Table 3.43:</i> Phosphate ion release ($\mu\text{mol/g}$) over time from discs of ionomeric cements of the monovalent cation series	106
<i>Table 3.44:</i> Phosphate ion release ($\mu\text{mol/g}$) over time from discs of ionomeric cements from the apatite stoichiometric series	107
<i>Table 3.45:</i> Phosphate ion release ($\mu\text{mol/g}$) over time from discs of ionomeric cements from the series varying in calcium fluoride	107
<i>Table 3.46:</i> Phosphate ion release ($\mu\text{mol/g}$) over time from discs of ionomeric cements from the series varying in silica:alumina and calcium	108
<i>Table 3.47:</i> Phosphate ion release ($\mu\text{mol/g}$) over time from discs of ionomeric cements from the series varying in silica:alumina ratio	108
<i>Table 3.48:</i> Phosphate ion release ($\mu\text{mol/g}$) over time from discs of ionomeric cements from the series varying in generic compositions derived from the apatite stoichiometric based glass LG26	109

TABLES (continued)

	Page
<i>Table 3.49</i> Phosphate ion release ($\mu\text{mol/g}$) over time from discs of ionomeric cements from the Calcium based series	111
<i>Table 3.50:</i> pH of eluting water as a function of cement disc Immersion time	111
<i>Table 3.51:</i> Mean pH of eluted water of autoclaved ICs at 7 days	112
<i>Table 3.52:</i> pH of LG2 and LG26 in 50ml water	113
<i>Table 3.53:</i> pH of LG2 and LG26 in 50ml of α -minimal essential media	113
<i>Table 3.54:</i> Summary of mean and SD for each set Ionomeric cement at four weeks implantation N=5	153
<i>Table 3.55:</i> Summary mean and SD of each wet ionomeric cement at four weeks implantation N=5	153
<i>Table 3.56:</i> Summary mean and SD of each of the acrylic cements at four weeks implantation N=5	154
<i>Table A1</i> The % osseointegration and the degree of osteoconductivity of the set sodium based ionomeric cement rods Materials: LG2	240
<i>Table A2</i> The % osseointegration and the degree of osteoconductivity of the set sodium based ionomeric cement rods Materials: LG6	240
<i>Table A3</i> The % osseointegration and the degree of osteoconductivity of the set sodium based ionomeric cement rods Materials: LG63	240
<i>Table A4</i> The % osseointegration and the degree of osteoconductivity of the apatite-stoichiometric based series (Ca:P~1.66) ionomeric set cement rods Materials: LG26	241

TABLES (continued)

	Page
<i>Table A5</i> The % osseointegration and the degree of osteoconductivity of the apatite-stoichiometric based series (Ca:P~1.66) ionomeric set cement rods Materials: LG27	241
<i>Table A6</i> The % osseointegration and the degree of osteoconductivity of the apatite-stoichiometric based series (Ca:P~1.66) ionomeric set cement rods Materials: LG30	241
<i>Table A7</i> The % osseointegration and the degree of osteoconductivity of the sodium based wet ionomeric cement Materials: LG23 1:2:3	242
<i>Table A8</i> The % osseointegration and the degree of osteoconductivity of the sodium based wet ionomeric cement Materials: LG23 1:2:2	242
<i>Table A9</i> The % osseointegration and the degree of osteoconductivity of the apatite-stoichiometric based wet ionomeric cements Materials: LG26	243
<i>Table A10</i> The % osseointegration and the degree of osteoconductivity of the apatite-stoichiometric based wet ionomeric cements Materials: LG30	243
<i>Table A11</i> The % osseointegration and the degree of osteoconductivity for the strontium based radiopaque based wet ionomeric cements Materials: LG119	244
<i>Table A12</i> The % osseointegration and the degree of osteoconductivity for the strontium based radiopaque based wet ionomeric cements Materials: LG125	244
<i>Table A13</i> The % osseointegration and the degree of osteoconductivity for the Zinc based radiopaque based wet ionomeric cements Materials: LG130	245

TABLES (continued)

	Page
<i>Table A14</i> The % osseointegration and the degree of osteoconductivity for the Zinc based radiopaque based wet ionomeric cements Materials: LG132	245
<i>Table A15</i> The % osseointegration and the degree of osteoconductivity of the set Acrylic controls	246
<i>Table A16</i> The % osseointegration and the degree of osteoconductivity of the wet Acrylic controls	246

FIGURES

	Page
<i>Figure 2.1:</i> Poly(acrylic acid)	29
<i>Figure 2.2:</i> Poly(methylmethacrylate)	33
<i>Figure 2.3:</i> Set rod cutter used to cut Ionomeric cement rods (1mm in diameter) covered in medical silicone grade tubing to 1mm, 2mm, 3mm and 4mm in lengths. Metal ring device pushes out the IC rod with the medical silicone grade tubing.	64
<i>Figure 3.1:</i> Fluoride ion release of varying compositions of Sodium based ICs at day 1. Linear regression, $y=9.45x+0$. Correlation coefficient=0.56 (n=6).	71
<i>Figure 3.2:</i> Relation of Sodium glass composition and Fluoride ion release at 7 days. Linear regression, $y=52.1x+5$. Correlation coefficient=0.49 (n=6).	72
<i>Figure 3.3:</i> Relation between sodium glass composition and Fluoride ion release at 21 days. Linear regression, $y=93.01x+29$. Correlation coefficient=0.33 (n=6).	73
<i>Figure 3.4:</i> Fluoride ion release of LG26 up to a period of 42 days Linear regression, $y=0.59x+(-1)$. Correlation coefficient=0.97 (n=6).	74
<i>Figure 3.5:</i> Relation between Fluoride glass composition and Fluoride ion release at 42 days. Linear regression, $y=12.5x+0$. Correlation coefficient=1 (n=6)	76
<i>Figure 3.6:</i> Relation between Sodium glass content and Sodium ion release at 84 days. Linear regression, $y=543.4x+5$. Correlation coefficient=0.99 (n=6)	83
<i>Figure 3.7:</i> Relation between Aluminium ion release and Sodium glass composition, $y=0.67x+0$. Correlation coefficient=0.97 (n=6)	88
<i>Figure 3.8:</i> Relation between Aluminium ion release and Sodium glass composition at 21 days. Linear regression, $y=3.89x+0.22$. Correlation coefficient=0.96 (n=6).	89

FIGURES (continued)

	Page
<p><i>Figure 3.9:</i> Relation between Aluminium ion release and Potassium glass composition at day 7. Linear regression, $y=2.32x+0.09$. Correlation coefficient=0.87 (n=6).</p>	90
<p><i>Figure 3.10:</i> Aluminium ion release of LG26 up to a period of 42 days. Linear regression, $y=0.032x+(-0.05)$. Correlation coefficient=0.82 (n=6)</p>	91
<p><i>Figure 3.11:</i> Relation between measured Silicon release and Sodium glass composition at day 42. Linear regression, $y=222.0x+49$. Correlation coefficient=-0.3 (n=6).</p>	96
<p><i>Figure 3.12:</i> Relation between Phosphorus pentoxide glass composition and Silicon release at 42 days. Linear regression, $y=28.8x+46.5$. Correlation coefficient=0.96 (n=6).</p>	99
<p><i>Figure 3.13:</i> Relation between Phosphorus pentoxide glass composition and phosphorus ion release at 3 days. Linear regression, $y=0.69x-6$. Correlation coefficient=0.97 (n=6)</p>	110
<p><i>Figure 3.14:</i> Scanning electron micrograph of a 14 day rat osteoblast-type cell derived from bone marrow culture : disc of ionomeric cement (LG27). Cell processes in close apposition to surface of IC (Field of width 40μm) Original magnification x 1000.</p>	116
<p><i>Figure 3.15:</i> Scanning electron photomicrograph at high power showing defect on surface of a typical set ionomeric cement used for tissue culture (LG26) after 14 days (Field width 200μm) Original magnification x 1850</p>	117
<p><i>Figure 3.16:</i> Scanning electron photomicrograph showing confluent osteoblast-like cells on the surface of set ionomeric cement (LG26) after 14 days tissue culture (Field width=120μm) Original magnification x 800</p>	118

FIGURES (continued)

	Page
<i>Figure 3.17:</i> Total protein of bone marrow cells cultured with monovalent cation series of ICs	120
<i>Figure 3.18:</i> Cell activity of bone marrow cells with monovalent cation ICs	121
<i>Figure 3.19:</i> Total protein of Bone marrow cells with apatite stoichiometric based ICs	122
<i>Figure 3.20:</i> Cell activity of bone marrow cells with apatite stoichiometric based ICs	123
<i>Figure 3.21:</i> Total protein of bone marrow cells with commercial based cements	124
<i>Figure 3.22:</i> Cell activity of bone marrow cells with commercial cements	125
<i>Figure 3.23:</i> Total protein of Ros cells cultured with monovalent cation series of ICs	126
<i>Figure 3.24:</i> Cell activity of Ros cells with monovalent cation ICs	127
<i>Figure 3.25:</i> Total protein of Ros cells cultured with varying silica/alumina and calcium based ICs	128
<i>Figure 3.26:</i> Cell activity of Ros cells with varying Silica/alumina and calcium based ICs	129
<i>Figure 3.27:</i> Total protein of Ros cells with ICs varying in calcium fluoride	130
<i>Figure 3.28:</i> Cell activity of Ros cells with ICs varying in calcium fluoride	131
<i>Figure 3.29:</i> Total protein of Ros cells with commercial cements	132

FIGURES (continued)

	Page
<i>Figure 3.30:</i> Cell activity of Ros cells with commercial cements	133
<i>Figure 3.31:</i> Transverse section through mid-shaft of femur showing extent of normal marrow and minimal cancellous trabeculae; Haematoxylin and Eosin x 42	138
<i>Figure 3.32:</i> Detail from Figure 3.31 showing interface between normal marrow tissue and mature cancellous trabeculae (CT); Haematoxylin and Eosin x 212	139
<i>Figure 3.33:</i> Transverse section of femur showing rod of ionomeric cement LG63 (IC) completely surrounded by bone; arrow depict six points around the perimeter at which osteoconduction might be evaluated; Haematoxylin and Eosin x 16.	140
<i>Figure 3.34:</i> Interface between “set” ionomeric cement LG63 (IC) and bone; the opposing arrows demarcate the thickness of newly formed bone and its measurement formed the basis for evaluating osteoconductive potential; Haematoxylin and Eosin x 162	141
<i>Figure 3.35:</i> Interface (narrow arrows) between the set ionomeric cement LG26 (IC) and newly formed bone; note its cellularity and the woven appearance seen focally (small wide arrow); osteoblasts line marrow spaces adjacent to the interface (large wide arrow); Haematoxylin and Eosin x 162.	142
<i>Figure 3.36:</i> Partly remodelled cortex and new bone (arrows) at the periosteal interface of the set IC implant LG26 (IC); P=Periosteum; M=voluntary muscle; Haematoxylin and Eosin x 162	143
<i>Figure 3.37.</i> Set IC implant LG26 (IC) projecting into marrow cavity and separated from vital marrow (M) by a thin layer of new bone (wide arrows); Haematoxylin and Eosin x 16	144

FIGURES (continued)

	Page
<i>Figure 3.38:</i> Detail from Figure 3.37 showing a thin layer of partly mineralized woven bone (arrows) separating the set implant implant LG26 (IC) from vital marrow tissue; Haematoxylin and Eosin x 162	145
<i>Figure 3.39:</i> Particles of the wet cement LG125 (IC) surrounded by newly formed bone (arrow) and separated from the adjacent healthy marrow tissue (M); Haematoxylin and Eosin x 42	146
<i>Figure 3.40:</i> Higher power view of Figure 3.39 showing the wet cement LG125 (IC) surrounded by a combination of woven (W) and more mature bone (M) with partially mineralized osteoid (O) situated more peripherally. The wide arrows demarcate the thickness of newly formed bone and its measurement formed the basis for evaluating osteoconductive potential; Haematoxylin and Eosin x 106	147
<i>Figure 3.41:</i> Detail from Figure 3.40 showing interface between the wet cement LG125 (IC) and relatively mature bone; Haematoxylin and Eosin x 212	148
<i>Figure 3.42:</i> Wet cement LG119 (IC) surrounded by a combination of mature bone (MB), osteoid (O) and cellular osteogenic connective tissue (C); Haematoxylin and Eosin x 42	149
<i>Figure 3.43:</i> Interface between the wet cement LG119 (IC) and notably cellular osteogenic connective tissue (c) (bold arrow); Haematoxylin and Eosin x 212	150
<i>Figure 3.44:</i> Particle of the wet cement LG130 (IC) surrounded by compressed cellular connective tissue (C) with minimal evidence of new bone apposition; Haematoxylin and Eosin x106	151
<i>Figure 3.45:</i> The wet cement LG26 (IC) surrounded by acellular connective tissue (C); new bone formation is present peripherally (arrow); Haematoxylin and Eosin x 212	152

FIGURES (continued)

	Page
<i>Figure 3.46:</i> OPN immunofluorescence stain at the new bone (NB) and with less brightly stained mature bone (MB) with the IC-implant LG23 (IC); x 200	158
<i>Figure 3.47:</i> OPN immunofluorescence stain at new woven bone brightly staining the reversal lines (R) signified by pointed arrows in new bone (NB) and stain in mature bone (MB) with the IC-implant LG23; x 400	159
<i>Figure 3.48:</i> FN immunofluorescence stain at the mineralized matrix of woven bone diffuse granular arrangement indicated by arrows pointing at the new woven bone in contact with the IC-implant LG23; x 200	160
<i>Figure 3.49:</i> OPN immunofluorescence stain at the reversal line (indicated by arrow) in close proximity to the IC-implant LG6 x 200	161
<i>Figure 3.50:</i> TN immunofluorescence stain at the periphery of the endosteum (P) arrows indicate the granular appearance with close contact to the bone associated with the IC implant (I) LG6; x 100	162
<i>Figure 3.51:</i> OPN immunofluorescent stain in new woven bone (NB) in comparison to mature bone (MB) with the IC implant (I) LG2; x 300	163
<i>Figure 3.52:</i> TN (T) immunofluorescent stain at the periphery of the endosteum. Note a diffused granular appearance of the new woven bone (NB) associated with the IC implant LG2 (I) (indicated by arrows); x 400	164

ACKNOWLEDGEMENTS

Thank you to my main supervisor Professor Ian M Brook who has guided me throughout the three years of working with him. I would like to thank my assistant supervisors Dr Paul V Hatton in the Department of Restorative Dentistry and Dr Geoff T Craig in the Department of Oral Pathology for their helpful and constructive comments. Thank you to Dr AJ Devlin for all her help and support.

I would also like to thank everyone at the Dental School and the Department of Biomedical Science who have been involved in this research, and who have supported me throughout these studies. Thank you to all other Departments (outside the University of Sheffield) involved with research in this thesis.

I am eternally grateful to my mother, father and brother who have always been there for me. Thanks to my close friends who have supported me and have been patiently waiting! A memorable three years!

Evaluation of Novel Glass-Ionomer Cements for Hard tissue Repair using *In Vitro* and *In Vivo* methods

SUMMARY

Ionometric cements (ICs) have a successful history as restorative materials in dentistry where they are called glass-ionomer cements (GICs). More recently they have potential for use as bone substitutes and cements in orthopaedic, otolaryngology and maxillofacial surgery. The influence of glass composition on IC properties such as biocompatibility has not been adequately studied. The broad aim of this research was to characterise a series of ICs of defined composition and evaluate their biocompatibility *in vitro* and *in vivo*. The hypothesis was that ICs could be optimised through their glass composition for clinical use as bone substitutes or cements.

ICs are formed by the neutralisation reaction of an inorganic basic glass and organic polyelectrolyte acid. *In vitro* studies involved the determination of ions eluted from set cement discs and evaluation of the toxicology and biocompatibility of the ICs using cell culture techniques. *In vivo* studies involved the implantation of set and wet ICs into the midshaft of the rat femur. The osteoconduction and osseointegration of specified ICs were determined by histomorphometric analysis. Additionally, the role of noncollagenous extracellular matrix bone proteins were studied as they play an important role in the interactions of the healing of hard tissues with implants.

The response of bone was dependent upon IC formulation with increase in fluoride and phosphate stimulating bone cell response. Bone response was negatively correlated with aluminium. It was concluded that the IC from the apatite stoichiometric series (designated LG26) had the most promising formulation for biomedical applications. This study confirmed that ICs have some potential clinical use as a bone substitute and cement. However, *in vitro* studies suggested that aluminium ions released from set ICs were responsible for some cytotoxicity and further work might usefully be directed at reducing the release of this ion from the cement.

Evaluation of Novel Glass-Ionomer Cements for Hard Tissue Repair using *In Vitro* and *In Vivo* methods

“The biocompatibility of glass-ionomer cements with living tissue is a subject of some importance”

AD Wilson (1988)

1. INTRODUCTION

Biomaterials are used in various medical devices and new materials are continuously being developed and introduced for biomedical application. A wide variety of materials have been used for the repair and augmentation of bone that has been damaged by trauma or disease.¹⁻¹⁰ For both hard and soft tissue implants, the biocompatibility of the material used has to be considered. A biomaterial has been defined as ‘a non-viable material used in a biomedical device intended to interact with biological systems’.^{11, 12} The material of choice for bone augmentation is the patient’s own bone tissue. This is not always practical and often necessitates the opening of a second surgical site for harvesting autogenous (bone from the patient’s own body) grafts with associated increased morbidity. It is for this reason that alloplastic materials (other materials) are often employed. The most popular bone substitute material for filling defects is hydroxyapatite (HA) because of its apparent ability to enable bone to osseointegrate on their surface, a process described as

“bioactivity” or osteoconduction.¹³⁻¹⁵ Despite this advantage over traditionally more biologically inert materials, problems remain with accurate surgical placement and migration of particulate forms of HA or infection of porous blocks of HA.¹⁶⁻¹⁹ For these reasons, a number of alternative bone substitutes have been proposed, they include bioglass.²⁰⁻²³ Despite many of these materials exhibiting bioactive properties, there remains much debate on the underlying mechanisms responsible for osteoconduction and osseointegration.

Bioactive glasses have been shown to be a potential bone substitute material, integrating well with bone *in vivo*.^{22, 24} Osteoblasts cultured on 45S5 bioglass demonstrate a high proliferation rate and expression of osteoblast-like phenotype.²⁵

In contrast to the applications of bone substitutes, bone cement is used in order to obtain stable fixation to bone and to reduce the number of patients from the pain of weight-bearing after surgery due to micromotion of metal prosthesis. The major disadvantage of the most commonly used bone cement, poly(methylmethacrylate) (PMMA), results from its exotherm on setting and creep²⁶⁻³² as at a high temperature there is an increase in cement volume and when the temperature is lowered there is a reduction in cement volume causing creep. Despite improvements in bone cement with the introduction of systems based on poly(ethyl methacrylate) and n-butyl methacrylate monomer an ideal bone cement has not yet been produced.^{9, 10, 33}

There is a need for improved materials for hard tissue repair and replacement.³⁴⁻⁴⁴

In addition, it is essential that we also improve our understanding of how so-called bioactive or osteoconductive materials interact with bone tissue.

Ionomeric Cements (ICs) are a group of biomaterials used in restorative dentistry.^{39,}

^{40, 45, 46, 47} They offer several potential advantages over ceramic or glass-based materials as they can be moulded into a variety of shapes.⁴⁸ They are formed by the neutralisation reaction of a basic ion leachable inorganic glass and an organic polyelectrolyte (poly(acrylic) acid). They set without an exotherm on mixing, are chemically adhesive to enamel, dentine and bone.^{36, 45, 46, 48} These attributes and their apparent osteoconductive potential have led to the use of ICs as preformed implants and cement in otolaryngology and cranial surgery.^{39, 40}

The reason why ICs integrate with bone and in certain cases appear to stimulate bone formation is unclear. The release of potentially osteoconductive ions (e.g. fluoride, calcium and phosphate) and the biological effects of other ions (e.g. aluminium and silicate) have been linked with the biological response to ICs following implantation.⁴⁹ However, we lack a sound understanding of the mechanisms which are responsible for the biocompatibility and clinical performance of ICs.

The overall aim of this thesis was to evaluate biocompatibility of novel ICs for biomedical applications as bone substitutes and cement material (see section 1.5 Aims). It is helpful to firstly review the literature on ICs.

1.1 Glass -ionomer (polyalkenoate) cements

The most important landmarks in the development of ICs are in Table 1.1.1, pages 5-6

Table 1.1.1 Significant published studies showing the history of the development of ionomeric cements

Author	Observation	Reference
Wilson AD 1965	Cements were prepared by mixing dental silicate glass powder with aqueous solutions of various organic acids.	50
Kent BE & Lewis BG 1968	Poly(acrylate) cement pastes set slowly and were hydrolytically stable. Hydrolytically stable cements could be produced by altering Al_2O_3/SiO_2 ratio, which was crucial as it determines whether the glass network breaks down if exposed to acids, and the rate of breakdown.	51
Wilson AD & Kent BE 1969	Original development of ICs	50
Wilson AD & Kent BE 1971	ICs first reported	52
McLean JW & Wilson AD 1974	ICs first reported to release fluoride and bond to enamel	53
Wilson AD & Crisp S 1976	Tartaric acid modified the cement-forming reaction, improving working time First practical material: ASPA II	50 54
McLean JW & Wilson AD 1977	ICs first used in restorative dentistry	55
Powis DR, Folleras T, Merson SA & Wilson AD 1982	Improved adhesion of ICs to dentine and enamel	53

Table 1.1.1 (continued)

Author	Observation	Reference
Aboush YEY & Jenkins CBG 1986	Cements based on poly(acrylic acid (PAA) bond strongly to enamel and dentine	56
Jonck LM, Grobelaar CJ & Strating H 1989	First screening test for ICs (Ketac-O) to be used as a bone cement for orthopaedic use.	35
Jonck LM, Grobelaar CJ & Strating H 1989	Bulk testing of ICs (Ketac-O) for use as joint replacement. where ICs were found to be non-toxic in bulk. Normal haemopoietic and osteoblastic activity took place on the cement surface.	48
Jonck LM & Grobelaar CJ 1990	Experimental and clinical evaluation of ICs, Ionos bone cement, in joint replacement reported in baboon model and in selected patients in whom poly(methylmethacrylate) cement was contra-indicated. A direct bone-bonding was demonstrated, and clinical results were satisfactory.	45
Brook IM, Craig GT & Lamb DJ 1991	Initial <i>in vivo</i> evaluation of ICs cements for use as alveolar bone substitutes. Leaching of fluoride may stimulate osseointegration <i>in vivo</i> .	46
Brook IM, Craig GT, Hatton PV and Jonck LM 1992	Granular IC in primate baboon model and in <i>in vitro</i> primary bone organ cultures derived from neonate rat calvaria, both formed osteoblast-like cells colonising the surface of the implant producing a collagenous extracellular matrix.	57
Hatton PV & Brook IM 1992	Glass particles surrounded by a siliceous layer set in a hydrogel matrix. Mobility of ions from ICs in the matrix phase are important in determining the biocompatibility and adhesive properties of ICs.	58
Hatton PV, Craig GT & Brook IM 1992	X-ray microanalysis (XRMA) provided evidence for the formation of a bioactive bone/IC bond, with movement of ions across the interface being demonstrated.	59

1.1.2 Properties

ICs show a wide range of physical properties. The composition of the cement affects its properties. For example, compressive strength increases with an increase in alumina content.⁵¹ A high powder/liquid (P/L) ratio produces thickly mixed materials with an increased strength and a shorter setting time.⁶⁰

The temperature at which the cement is mixed affects its working time. The working time is prolonged as the temperature of cement and its surroundings is reduced.⁵¹

ICs are regarded as brittle materials. In the first few minutes after mixing they deform slightly under load.⁵¹ Set ICs lack toughness, and although they can have a relatively high compressive strength (~200MP) they are comparatively weak in flexural strength (5 to 40 MP).⁵¹ It has been reported that a twelve month old cement is approximately twice as strong as a one day old cement and approaches 400 MP in compressive strength.⁶¹ However, it may be possible in the future to improve the physical properties of ICs.⁶²

At present, ICs are not suited for load-bearing purposes such as total hip replacement because of their poor mechanical properties. ICs are more suited to non-weight bearing applications where the ability exists to biomechanically match the IC to the bone. This can be done by varying the volume fraction of the glass and

polymer components of the cement.⁶¹ Attempts are now being made by colleagues at The University of Limerick to improve the mechanical properties by altering the compositions of ICs.^{20, 22, 23, 63, 64}

The clinical success of implanted biomaterials, such as ICs, for hard tissue replacement is dependent upon the formation of a stable bone-implant interface. A prerequisite for formation of this interface is believed to be the ability of the surface of the material to bind certain biological molecules and attract bone cells. The surface of set IC is hydrophilic.⁵¹

The biological properties of an IC result from its surface chemistry, physical structure and bulk composition. Setting occurs by gelation of the cement with transfer of ions from the glass to the acidic matrix. Unset IC is able to chemically bond to both bone (apatite) and metals^{51,65} and during gelation the IC does not undergo appreciable shrinkage.^{5, 65, 66} ICs, if used as a bone cement would not have to rely exclusively on a mechanical bond to achieve fixation, unlike acrylics. The adhesive properties of ICs and their stability in an aqueous environment have potential as a bone cement although they are mechanically inferior to acrylic cements. The stability of ICs and the increasing strength with time may mean that ICs would be less susceptible to the problems of late failure that is associated with the acrylic cements.⁶⁷⁻⁷¹

1.1.3 Applications of ICs for dental and medical use

ICs have remained an important class of dental restorative materials for almost 30 years.^{51, 65, 72} In this role their attributes include adhesion to untreated tooth mineral and release of fluoride ions that are thought to confer resistance against recurrent and/or secondary dental caries.⁶⁵ The favourable biological responses reported by Jonck *et al*^{35, 45, 48} led to their limited clinical application in orthopaedic surgery.⁴⁵ Set IC bone substitutes used as granules and cement were applied successfully to cases where conventional care had failed.⁴⁵ ICs are suited to situations where the strength of the cement is not a major factor in determining clinical success. IC has also been used to reinforce osteoporotic femoral heads to improve the primary stability of hip screws.³⁶

It has been shown *in vitro* that a slow release of fluoride over a long time period may have clinical advantages, fluoride released from IC restorations may reduce microbial activity.⁷³⁻⁷⁵ This antimicrobial property could also be beneficial to ICs implanted in bone reducing infections after surgery.⁷⁶

Implanted ICs have made the most clinical impact in otological surgery, proving highly successful in several otologic procedures when used either as a cement or as preformed prosthetic implants, for example, ear ossicles or granular bone substitute.³⁷⁻⁴³ Geyer and Helms in 1990 reported 167 patients on whom they had performed reconstructive middle ear surgery, including reconstruction of the

auditory canal with IC, reducing the size of the mastoid cavity with set IC bone substitute, and rebuilding of the ossicular chain.³⁷

Further reports on the use of IC in otologic surgery followed a 94% initial four year success rate being reported in 945 cases of IC ossicular implant placement.⁴⁰

Revision surgery had to be undertaken in only 12 out of 74 cases of posterior canal wall repair using IC.⁴⁰ The major applications in otologic surgery, where IC has no near rival for clinical efficacy, are in reconstruction of the ossicular chain where the cement can be used to repair the bony ossicles in their normal position and in cementation of cochlear implants.^{38, 39, 41-43}

The early clinical reports of the successful use of IC led to their wider application in neuro-otological and skull base surgery, and for repair of cerebrospinal fluid (CSF) fistulas and skull defects.^{39, 77} Concurrent with these developments, IC were being evaluated for their biological effect on neural tissue using neurophysiological techniques. The results of these *in vitro* tests conflicted with the positive clinical data, in that, following exposure of nerves to viscous IC a block in nerve conduction (which may not be reversible) occurred.^{66, 78} However, it should be noted that for clinical use the manufacturers recommend that unset IC should not come into contact with soft tissues and that it should be placed in a 'dry field'.

As a result of these studies the use of IC as a bone cement was restricted to avoid all direct contact with neural tissue. Unfortunately this warning came too late to prevent four reported cases of post-otoneurosurgery aluminium encephalopathy (2 deaths) following repair of skull base defects (post- acoustic neuroma or vestibular neurectomy surgery).⁷⁹ The exact details of these and subsequent cases are difficult to establish. In all cases there appeared to have been a massive release of aluminium ions from the IC into the CSF resulting in encephalopathy. ⁷⁹

Direct interaction of unset IC with neural tissue would, as seen in laboratory studies, be expected to produce tissue damage due to the release of polyacid.^{67, 79} This together with possible disruption of the setting reaction by contamination of unset IC with CSF and/or blood is a possible explanation for the tragic consequences reported. ⁷⁹ The large surface area of IC's allows release of polyacid, large quantities of metal ions and glass particle.⁷⁹

IC has found application in oral surgery as a set pre-formed particulate bone substitute where it has been shown to be of particular benefit in prevention of bone loss following tooth extraction and as a filler for graft donor sites and cyst cavities.⁸⁰ As a cement the use of IC as a surgical dressing has been reported following exposure of teeth prior to orthodontic alignment.⁴⁴

1.1.4 Ion release

The main effect of IC composition on bioactivity is as a reservoir for ion release.^{49, 62, 81} In general, the ionic species that are present are fluoride, sodium, potassium, aluminium, silicate, calcium, phosphate, strontium and zinc. Several investigators have proposed that ion release is a major factor in the bioactivity of different ICs.⁴⁶⁻

116

X-ray microanalytical (XRMA) studies of set IC have shown that ions released from the glass particles during the gelation process are present in the matrix of the cement⁵⁹ and in adjacent bone.⁸² Even after gelation has occurred, there is mobility of ions within the IC and exchange of ions takes place with the (aqueous) environment.^{65, 70, 83} Early work into the bioactivity of ICs and their effects on osteogenic cells demonstrated that IC composition was important, with non-fluoride glasses being the least toxic to cells *in vitro*³⁴ but the least osteoconductive *in vivo*.⁴⁶

1.1.4 (a) Fluoride

Fluoride is an essential constituent of ICs. The chemical and biological actions of fluoride on bone mineral are complex and imperfectly understood. The slow and sustained release of fluoride^{84, 85} from a bone cement may provide the stimulus for sustained osteoblastic activity for the osteoconduction of the insert. It has been

shown that fluoride strengthens the adhesive bond of the cement to both enamel and dentine and probably bone.⁸⁶

Jonck *et al* found that ICs used in patients for total joint replacement gave positive clinical results.⁴⁵ This was postulated to be from the ICs fluoride releasing osteoconductive properties.⁴⁵ Fluoride has been used successfully in the treatment of osteoporosis by stimulating osteoid formation^{45, 87} inhibiting resorption⁸⁸ and by increasing trabecular bone density. Fluoride and calcitonin have synergistic mitogenic activities and they increase proline incorporation into bone matrix.⁸⁹

It is possible to speculate that the presence of a fluoride releasing IC at the time of bone formation would result in mineralization with fluorapatite.⁴⁵ Fluorapatite is more resistant to resorption than apatite, as bone formation is a dynamic process of deposition and resorption, a greater volume of bone should form in association with implanted IC compared to more inert ceramic bone substitutes. This hypothesis was confirmed by studies that have compared IC implants to ceramic implants and by more recent work which proposed increased fluoride release to increased bone formation.⁴⁶

The study of fluoride ion release from IC has been extensive but mainly related to the dental applications.^{50, 51, 70, 83} Dentally, the incorporation during formation and later uptake of fluoride by enamel increases the acid resistance of the

hydroxyapatite.⁹⁰ Fluoride has an effect on bacterial enzymes by combining with various trace metals that are necessary for activation of the bacterial enzymes. These enzymes are deprived of these trace metals as a result, they remain inactive and caries is reduced.⁹¹

The slow release of fluoride, over a sustained period from the IC,^{84, 85, 92} has a similar beneficial effect on osteogenesis. Fluoride ions released from IC appear to act in a dose-dependant manner. At relatively high concentration, fluoride acts as an enzyme inhibitor *in vitro* but *in vivo* it stimulates proliferation and alkaline phosphatase activity of bone-forming cells (osteoblasts).^{46, 93-95}

It has been reported that sodium fluoride strengthens the bond of hydroxyapatite to both enamel and dentine,^{50, 86} and that the fluoride-hydrogen bond may be of consequence in promoting the calcification process on the IC. Further evidence shows that fluoride is potentially osteoconductive as there is an increase in endosteal bone resorption and periosteal bone formation in rats that were exposed to 30-100 mg F/l in drinking water.⁹⁶⁻⁹⁹

The lack of fluoride in *in vivo* studies has been shown to interfere with the integration of IC.⁴⁶ The slow release of fluoride ions at low doses is reported to stimulate bone formation in the chick and rat, however higher doses of fluoride are reported to inhibit bone formation.^{83, 84}

1.1.4 (b) Sodium

The sodium monovalent cation has been reported to promote the release of fluoride from ICs.⁵⁰ Sodium fluoride is an effective stimulator of osteoblastic proliferation in low turnover osteoporosis.¹⁰⁰ Sodium ions in the body are important in extracellular fluid accounting for over 90% of the osmotic pressure of the extracellular fluid.⁹¹

1.1.4 (c) Potassium

The effects of potassium, also a monovalent cation, on bone needs further investigation. Physiologically, potassium channels play an important role in causing the voltage changes of nerve action potentials.⁹¹ Potassium also has further important functions in the body as a low potassium concentration in the brain interstitial fluid is required for the correct functioning of neurones in the brain as they require an exact controlled environment, for normal function. The blood-brain barrier protects the cerebral tissue from detrimental substances in the blood, and the transport processes of the choroid plexuses and the brain capillary endothelium help provide the appropriate fluid environment for the brain.⁹¹

Experiments have shown that even when the circulating blood potassium rises to values almost two times normal, the potassium concentration in the cerebral spinal fluid still remains at its normal low value. Thus the barrier system, along with its carrier-mediated transport of potassium, not only maintains a low potassium concentration but also keeps this concentration constant, allowing the neurons to

generate very high electrical potentials that do not change with the vagaries of the rest of the body.⁹¹ Any potassium release from ICs would thus be unlikely to affect the central nervous system (CNS).

1.1.4 (d) Aluminium

The effect of aluminium is more controversial. At low concentrations aluminium ions enhance stimulation and proliferation of osteoblasts and new bone formation.^{101, 102} These findings are supported by the observations *in vitro* of aluminium particles inside cultured osteoblast cells without any impairment of bone formation or detrimental effect on the cells.^{82, 103, 104} Aluminium ion release from ICs play an important role in *in vivo* biocompatibility, increasing the amount of osteoid formed.^{102, 104, 105} Aluminium enhances the mobilisation of calcium from bone by a cell-independent mechanism and exerts an indirect effect on bone formation through the inhibition of collagen synthesis.^{106, 107}

Aluminium reduces bone mineralization by interfering with the early stages of this process^{102, 104, 105} and is the least biologically acceptable of all the inorganic species leached from these cements, compared to other ions such as fluoride, sodium, potassium, silicate, calcium and phosphate. Aluminium at high concentration has been associated with Alzheimers disease.⁸¹ Increased aluminium levels in the brain can lead to aluminium encephalopathy.¹⁰⁸ Cases of subacute aluminium

encephalopathy have been reported after the implantation of IC during translabyrinthine otoneurosurgery.¹⁰⁸

1.1.4 (e) Silicate

Silicate ion species leach from IC's⁸¹ and in gel-form, has been reported to induce apatite nucleation on its surface *in vitro*. This ion may thus be important in determining the *in vitro* biocompatibility of IC's.^{34, 109}

1.1.4 (f) Calcium

Calcium is released from ICs in very small amounts. It is the main inorganic constituent of both the teeth and bones as hydroxyapatite ($\text{Ca}_{10}(\text{PO}_4)_6(\text{OH})_2$). Apatite (calcium phosphate) seems to be the only calcium phosphate able to incorporate fluoride ions,¹¹⁰ as natural non- biological calcium phosphate contains a lot of fluoride and the incorporation of this element occurs in apatite phases.¹¹⁰

1.1.4 (g) Phosphate

Phosphate is involved with the mineral hydroxyapatite, so the IC acts as a source of natural mineralised tissue as hydroxyapatite is calcium phosphate. Phosphate improves translucency and adds body to the cement.⁵¹

1.1.4 (viii) Strontium

Strontium at high concentrations in the diet has been known to cause rickets.

Strontium's release from ICs needs to be carefully controlled.¹¹¹ Strontium at low doses is used to treat osteoporosis.¹¹² Strontium stimulates osteoblast proliferation.

Radioactive strontium enables the detection of differences in the relative compartments in bone diseases like osteoporosis¹¹³ and other bone disorders.¹¹⁴

The strontium in ICs would be useful in a dental cement enabling detection of microleakage and secondary caries using x-rays.^{115, 116}

1.1.4 (I) Zinc

Zinc is an integral part of many enzymes.⁹¹ Zinc is a component of lactic dehydrogenase and is therefore important for the conversion between pyruvic acid and lactic acid. Zinc is important in some peptidases for the digestion of proteins in the gastrointestinal tract.⁹¹

1.2 Bone cements and substitutes for hard tissue augmentation

A wide range of materials, such as cements, ceramics, metals, and polymers are used for bone implants in many different applications including tissue augmentation, fracture fixation and joint replacement.¹¹⁷ The bone-biomaterial interaction may be

significantly different for all these materials. For load-bearing implants, their superior fracture and fatigue resistance has made metals the materials of choice.¹¹⁸

Development is proceeding on cements, ceramics, composites, polymers and biologically derived materials such as collagen, but suitable alternatives for metal for

general use have yet to be introduced.¹¹⁸ This section will focus on only a few current bone cements and substitutes.

1.2.1 Poly(methylmethacrylate)

Techniques were pioneered by Charnley in the 1960s for the treatment of hip joint dysfunction utilising PMMA for cementing prosthetic hips.^{1, 2} PMMA has been used widely as a bone cement and has enabled significant success with the rehabilitation of many elderly patients,³⁻⁵ and only in some cases for reconstructive surgery for diseased bone,¹¹⁹⁻¹²⁴ and in cases where bone has lessened.^{125, 126}

PMMA polymerisation continues after the placement of the primary insert with PMMA infiltrating the surrounding alveolar spaces, resulting in further bone-implant interlocking.^{48, 127, 128}

The main clinical problem with PMMA is with loosening of the implants, often associated with fragmentation and fracture of the supporting cement.^{123, 129-133}

PMMA's exothermic polymerisation, creep and the presence of excess methacrylate monomer have been implicated as the major factor in the loosening and subsequent failure of hip prostheses.^{26, 122, 133, 134} PMMA causes thermal necrosis^{27, 28} and chemical necrosis of bone due to the unreacted monomer,^{29, 30} and from the toxic leaching effects of this residual monomer on the osteoblast cells.^{31, 32} PMMA cement has thus been identified as a cause of implant failure, and the cement is particularly unsuitable for bone reconstruction following cancer.^{119, 133} In cases of

catastrophic failure, the subsequent need for revision surgery leads to loss of bone volume in which to place a second device.¹²⁵ The mechanical properties of PMMA decrease 10-15% over one year contributing to implant loosening.⁴⁵

1.2.2 Calcium phosphates

These materials are divided into two main groups: **hydroxyapatite (HA)** ($\text{Ca}_{10}[\text{PO}_4]_6[\text{OH}]_2$) and **β -tricalcium phosphate** ($\text{Ca}_3[\text{PO}_4]_2$). Calcium phosphates are described as bioactive not because they are osteogenic, but because they are connected to the surrounding bone tissue by a strong chemical bond.¹⁰ Calcium phosphates are probably the most commonly utilised bone substitutes in oral surgery and may give satisfactory results in many cases. The major advantage of the calcium phosphates is their capacity to become functionally integrated with host bone without fibrous tissue encapsulation and with little inflammatory or foreign body response.^{13, 135-146} The favourable response seen on implantation of the calcium phosphate ceramics is attributed to the calcium and phosphate ions, the commonest constituents of vertebrate hard tissue.¹⁴¹⁻¹⁴⁵ Calcium phosphate ceramics appear to allow normal 'wound' healing following implantation on or in bone defects.^{130, 147, 148}

1.2.2(a) Hydroxyapatite

HA is the most popular artificial material used for bone augmentation and has proved well suited for use as a filler in low weight bearing situations in oral and orthopedic surgery. It is used as a bone substitute in otolaryngology.^{142, 146, 149}

HA shows osseointegration when implanted in either soft tissue^{147, 150, 151} or hard tissue^{142, 146} and can form strong and intimate bonds with bone.^{141, 142, 146} Driskell *et al*¹⁵¹ were the first to report that a chemical bond exists between bone and HA. LeGeros *et al* reported that the bioactivity of HA may be related to its dissolution rate.¹⁵² It is generally accepted that degradation of HA can occur to a certain extent.^{146, 153}

HA has been implanted together with autogenous iliac bone grafts for jaw reconstruction but failed to achieve HA-bonding.¹⁵⁴ Problems remain with HA as it lacks adhesiveness and plasticity. Difficulties also exist with accurate clinical placement of HA and involve migration of the material or its loss from the implant site. HA can stress shield bone due to its high elastic modulus compared to that of bone.¹⁵⁵⁻¹⁵⁹ HA is mechanically weak in tension, which limits its use for load bearing applications.^{160, 161}

1.2.2 (b) β -Tricalcium phosphate

β -Tricalcium phosphate (β -TCP or whitlockite) is one of the most widely investigated calcium phosphate ceramics. It has been reported to exhibit good hard tissue integration¹⁶²⁻¹⁶⁵ and does not cause any significant inflammatory reactions *in vivo*.⁶⁻⁹ It is considered less suitable as a plasma sprayed layer on metal implants than HA, due to its degradation characteristics,¹⁶⁶ and is currently used primarily as a bone filler.

1.3 The evaluation of biocompatibility

Despite the fact that various biomaterials have been used for many years there is still a limited knowledge of the reactions which occur after the implantation of a non-biological material, in particular those occurring in the interface zone within a few microns from the implant surface. One reason for this is the difficulty of obtaining intact implant-tissue interfaces which permit analysis at a subcellular level.

Biocompatibility is defined as “the ability of a material to perform with an appropriate host response in a specific application”.^{11, 12} The initial host response after implantation of a non-biological material is characterised by an inflammatory reaction. This reaction is elicited by the inevitable surgical trauma and subsequently modified by the presence of the implant. In normal tissues and most experimental implant models an inflammatory phase occurs prior to repair and integration of the

implant. Initially *in vitro* cell and tissue culture tests provide essential information on the cellular and tissue response. Materials when implanted attain and maintain contact with the body environment through their surfaces; the interfacial interaction between the implant bed and surface could be a determinant of the implant's performance. The next section looks at *in vitro* and *in vivo* studies evaluating the biocompatibility of ICs as implants.

1.3.1 (a) Evaluation of ICs *in vitro*

A wide variety of cell culture models have been used to test medical materials. In using these methods to evaluate ICs, and in interpreting the results, it is important to realise that this class of materials should be classified as bioactive rather than inert. It is now generally recognised that bioactive materials often perform less well in tissue culture tests than the more inert materials that they are designed to replace in clinical use.³⁴ *In vitro* testing is not always effective in surface-active materials, hence *in vivo* testing is necessary.

The biocompatibility of set ICs has been investigated by several groups using *in vitro* methods. Ideally, initial *in vitro* evaluation should be carried out using a model which mirrors the clinical situation. Through selection of cell source and culture conditions, and by addition of β -glycerophosphate and ascorbic acid into the medium, *in vitro* formation of a bone-like tissue may be induced. These techniques have been used to evaluate the response of cells and "hard tissue biocompatibility"

of a range of ICs including dental materials, bone substitutes and bone cements. Tissues or cells used include neonate rat calvaria, osteoblasts, fibroblasts, bone marrow cells and osteoclasts.^{110, 167, 168}

Previous studies of dental ICs show that toxicity appears to be due to the presence of a toxic leachate or rough fracture surface.^{34, 168, 169} Fluoride has been suggested as the most likely cause of cytotoxicity.¹⁶⁹ The improved *in vitro* biocompatibility of ICs based on non-fluoride MP4 glass supports this hypothesis.³⁴ Metal ions have been suggested as a possible inhibitory factor. Aluminium has been localised in cells cultured on the surface of set ICs where it had no visible detrimental effect.^{82, 168} Aluminium and fluoride are both reported to influence bone cells *in vitro*.¹⁷⁰ These effects may be stimulatory or inhibitory, depending upon ion concentration and culture conditions.¹⁷⁰ Further work on the factors influencing ion release from ICs would be beneficial in producing the optimal formulation for a bioactive bone cement/substitute.

In vitro investigation of unset ICs has been hampered because of the extreme sensitivity of cultured cells to wet cements. Wet cements have been placed directly onto neonate rat calvaria cultures where consequently the calvaria cultures died.³⁴ It is likely that meaningful results will be obtained from *in vivo* testing of unset ionomeric bone cements.

1.3.2 (b) Evaluation of ICs *in vivo*

It is essential that clinical trials of a new biomaterial are preceded by adequate *in vivo* testing, especially given the limitations of tissue culture models. Set ICs have undergone initial *in vivo* evaluation with encouraging results.⁴⁶ Osteoconduction was observed on the surface of certain formulations after only six weeks implantation in rat femora. This tissue was apparently stable over the course of one year.⁸² In addition to demonstrating the osteoconductive nature of certain formulations, these experiments highlighted the danger of relying on tissue experiments when evaluating bioactive materials. An IC based on non-fluoride MP4 glass was apparently biocompatible *in vitro*, yet failed to osseointegrate with bone after surgical placement.³⁴ Direct contact between bone and material was only observed with ICs containing fluoride. The transmission electron microscope (TEM) confirmed that bone tissue was in direct apposition to the ICs and a stable interface was formed.⁴⁶

58, 82

1.3.3 Bone proteins

It is desirable in implanted materials, where the aim is to establish osseointegration, that the material is able to bind factors that recruit osteogenic cells. There are many cell types involved in the response of the body to a polymeric implant. The early recruitment of osteogenic cells essential to this process is mediated by the extracellular matrix bone proteins. Noncollagenous extracellular matrix (ECM) proteins osteopontin (OPN), fibronectin (FN), and tenascin (TN) are known to

play an important role in the integration of biomaterials with bone¹⁷¹⁻¹⁸³ as with ICs.

OPN is involved in the ossification process through its role in osteogenesis and chondrogenesis.¹⁷¹ OPN messenger ribonucleic acid (mRNA) and the OPN protein have been detected in the premature osteoblasts and chondrocytes during embryogenesis.^{172, 173} In adult bone, OPN mRNA is expressed in the osteoblasts of primitive woven bone formed in the initial phase of fracture healing suggesting it has a role in early bone formation.¹⁷³

FN appears to be important during wound healing and provides a substrate for fibroblasts migrating into wounds to initiate the repair process.¹⁷⁴ FN is reported to play an important role in maintaining the structure and relationship of mineralised tissues with soft connective tissues during skeletal morphogenesis and remodelling.¹⁷⁵⁻¹⁷⁷

TN, an extracellular glycoprotein, is localised in hard tissues during wound healing and tissue remodelling.¹⁷⁸⁻¹⁸³ It is prominent during embryogenesis,¹⁷⁸ and tumorigenesis,¹⁷⁸ suggesting it may have a role in tissue growth,¹⁸² and cell migration.^{182, 183} TN has been localised in new bone adjacent to implants and is thought to have a role in cell adhesion.¹⁸³

1.4 Hypothesis

Biocompatibility of ICs is dependent on their chemical formulation and related to ion release.

Ionomeric cements of different chemical formulations can be optimised for use as bone cements or substitutes.

1.5 Aims

The aim of this project is to investigate the relationship between composition and the biocompatibility of novel model formulations of ICs designed for use as bone substitutes or cements. This will give valuable information on the development of novel adhesive bone cements for use in medicine and dentistry; improved bone substitutes for use in plastic and maxillofacial surgery and improved dental cements for use as a restorative materials. The investigation will be undertaken using *in vitro* and *in vivo* models to differentiate between defined formulations of novel ICs produced by the Department of Materials, University of Limerick, Eire. In addition, a feature of these ICs is their ability to release ions. A major part of this study will therefore determine the effect of these ions on biocompatibility.

Specific objectives will be:

(a) To determine if ICs can be selected on the basis of their setting and working times to produce an ideal bone substitute/cement.

(b) To evaluate and define parameters that determine the release of ions from IC's and relate ion release to initial composition and formulation of the IC, and to biocompatibility.

(c) To observe the *in vitro* cellular response to products released from ICs.

(d) To observe the *in vivo* cellular response to products released during the transition from wet to the solid phase of ICs.

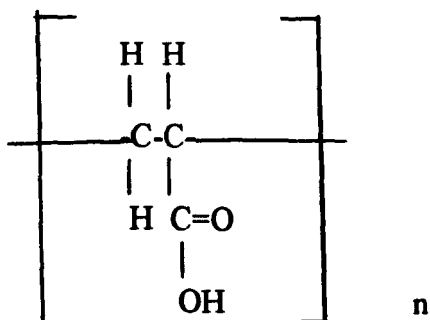
2. MATERIALS AND METHODS

2.1 Materials

All experimental glasses for preparation of glass polyalkenoate cements were obtained from Dr Robert Hill (Department of Materials Science, University of Limerick, Eire).

The medical grade mercaptan-free freeze-dried poly(acrylic acid) (PAA) was obtained from Advanced Healthcare (Tonbridge, Kent, UK). PAA has the following general formula:-

Figure 2.1 Poly(acrylic acid)



The PAA used had a weight average molar mass of 1.68×10^5 g and a number average molar mass of 2.29×10^4 .

Table 2.1 Commercial materials used for *in vitro* studies

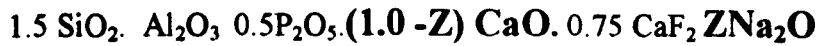
Cement Type	Manufacturer
Chemfil Chemfil Express	Dentsply Ltd, De Trey Division, (Surrey, UK)
Hydroxyapatite	Howmedica GmbH (Germany)
Poly(tetrafluoroethylene) (PTFE)	ICI (UK)
Vo-cem	ESPE GmbH (Germany)
Poly(methylmethacrylate) (PMMA)	Howmedica GmbH (Germany) Surgical Simplex [®] RO

2.1.1 Glass polyalkenoate cements

The glass compositions are summarised from section 2.1.1 a) to j).

a) Monovalent cation based :Sodium

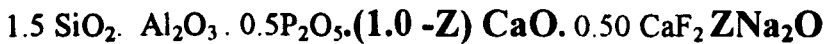
(i) General formula for the following glasses was as follows:



Glass code	LG2	LG6	LG4	LG5
Z (mole fraction) Na ₂ O	0	0.1	0.025	0.05

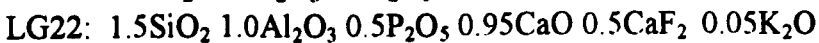
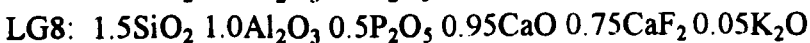
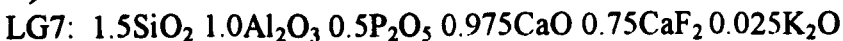
Glass code	LG23	LG63
Z (mole fraction) Na ₂ O	0.15	0.2

(ii) General formula for the following glasses was as follows:

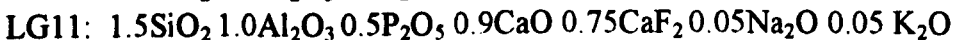
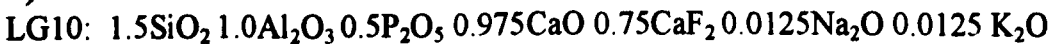


Glass code	LG65	LG66	LG67	LG68	LG69	LG70
Z (mole fraction) Na ₂ O	0.1	0.2	0.3	0.4	0.5	0.45

iii) Monovalent cation based:Potassium

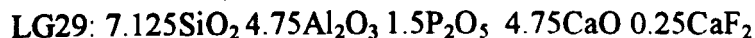
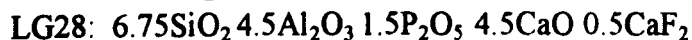
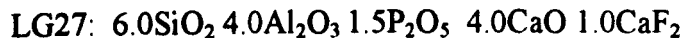
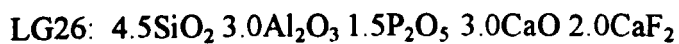
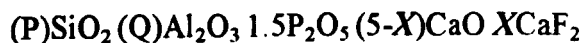


iv) Monovalent cation based:Sodium/Potassium



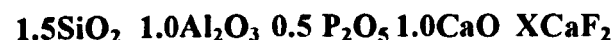
b) Apatite-stoichiometric series

General formula was as follows:



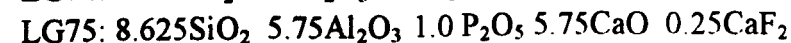
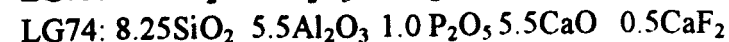
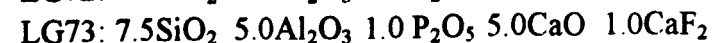
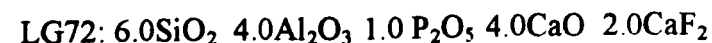
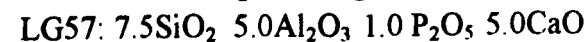
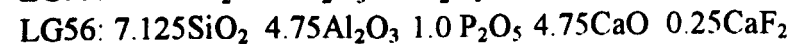
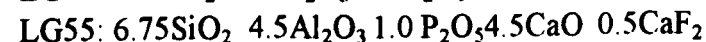
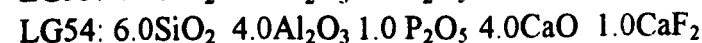
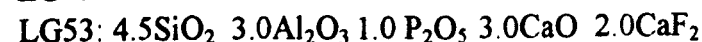
c) Varying Calcium fluoride series

General formula for the following glasses was as follows:

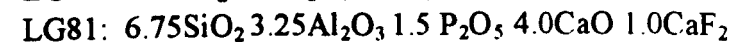
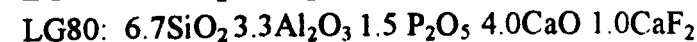
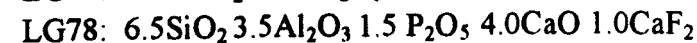
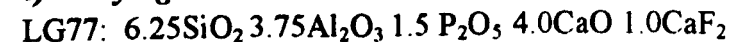


Glass code	LG3	LG26	LG2	LG42	LG44	LG45
X (mole fraction) CaF ₂	0.5	0.67	0.75	1.0	0.25	0

d) Varying Silica/Alumina and Calcium series of glasses LG53-LG57 and LG72-LG75



e) Varying Silica:Alumina ratio based



f) Generic compositions derived from LG26

LG83: 4.1 SiO₂ 3.0 Al₂O₃ 1.7P₂O₅ 2.8 CaO 2.0CaF₂
LG84: 3.7 SiO₂ 3.0 Al₂O₃ 1.9P₂O₅ 2.6 CaO 2.0CaF₂
LG85: 3.3 SiO₂ 3.0 Al₂O₃ 2.1P₂O₅ 2.4 CaO 2.0CaF₂
LG86: 2.9 SiO₂ 3.0 Al₂O₃ 2.3P₂O₅ 2.2 CaO 2.0CaF₂
LG26: 4.5 SiO₂ 3.0 Al₂O₃ 1.5P₂O₅ 3.0 CaO 2.0CaF₂

g) High Calcium based series

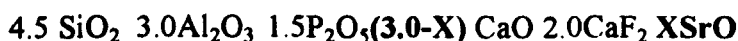
LG95: 4.5SiO₂ 3.0Al₂O₃ 1.5 P₂O₅ 2.8CaO 2.2CaF₂
LG96: 4.5SiO₂ 3.0Al₂O₃ 1.5 P₂O₅ 2.6CaO 2.4CaF₂
LG97: 4.5SiO₂ 3.0Al₂O₃ 1.5 P₂O₅ 2.4CaO 2.6CaF₂
LG98: 4.5SiO₂ 3.0Al₂O₃ 1.5 P₂O₅ 2.2CaO 2.8CaF₂
LG99: 4.5SiO₂ 3.0Al₂O₃ 1.5 P₂O₅ 2.0CaO 3.0CaF₂

h) High phosphate based series

LG91: 3.3SiO₂ 3.0Al₂O₃ 2.1 P₂O₅ 2.2CaO 2.2CaF₂
LG92: 3.3SiO₂ 3.0Al₂O₃ 2.1 P₂O₅ 2.0CaO 2.4CaF₂
LG93: 3.3SiO₂ 3.0Al₂O₃ 2.1 P₂O₅ 1.8CaO 2.6CaF₂
LG94: 3.3SiO₂ 3.0Al₂O₃ 2.1 P₂O₅ 1.6CaO 2.8CaF₂

i) Radiopaque Strontium based

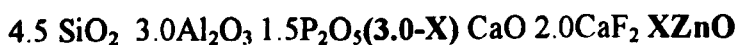
General formula was as follows:



Glass code	LG26	LG119	LG125
X(mole fraction) SrO	0	1.5	3.0

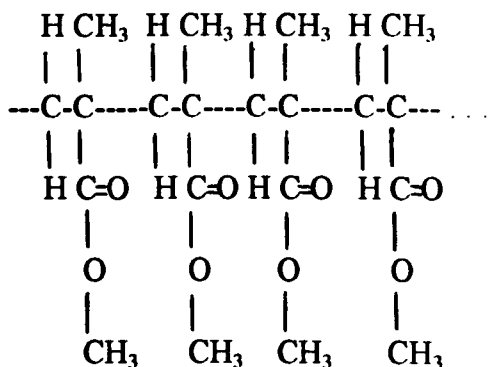
j) Zinc based

General formula was as follows :



Glass code	LG130	LG132
X(mole fraction) ZnO	1.5	0.75

Figure 2.2 Poly(methylmethacrylate) as the control has the general formula as shown below:



Surgical PMMA consisted of the following:-

Poly(methylmethacrylate)	6.0 g
Methyl-methacrylate	30.0 g
Barium sulphate USP	4.0 g

2.1.2 Ion release

Distilled sterile highly pure water (Baxter's Healthcare Ltd, UK).

Weighing machine (Mettler Bas Ba/BB2400Wycombe, Buckinghamshire, USA).

Concentration/conductivity/pH direct readout meter (Orion SA 720 pH/ISE, USA).

Incubator (Harvard/LTE).

Nalgene® bottles (Rochester, NY, USA).

Fluoride electrode (Orion Model 94-09).

Sodium electrode (Orion Model 84-11, 86-11 Ross™).

Electrode solution (Orion, USA).

Total ionic strength adjustment buffer (TISAB, Boston, USA).

Atomic absorption spectrometer (Perkin-Elmer M2100).

10.0 ml plastic clinical sampling tubes (Rochester, NY, USA).

α -Minimal essential media (Sigma, USA).

2.1.3 Cell culture

Wash medium

Ascorbic acid (Sigma, USA)	50.0 μ g/ml
Foetal calf-serum (heat-inactivated) (Gibco BRL, UK)	15.0 %
Penicillin (Sigma, USA)	50.0 IU/ml
Streptomycin (Sigma, USA)	50.0 IU/ml
Amphotericin B (Sigma, USA)	0.3 μ g/ml
Fungizone (Sigma, USA)	2.0 ml

Basic medium(BM)

α -Minimal Essential Medium (Sigma, USA)	85.0 ml
Foetal Calf Serum	15.0 ml
Penicillin/Streptomycin	1.0 ml
Fungizone (ug/ml)	120 μ l

20.0 ml of BM was supplemented (BSM) with

Dexamethasone(Sigma, USA)	200 μ l
Ascorbic acid/ β -glycerophosphate	200 μ l
Glutamine	200 μ l

Ascorbic acid/β-Glycerophosphate was made up of:

Ascorbic acid	5.0 mg
β-Glycerophosphate	2.16 g
Water (Baxter's Healthcare Ltd, UK)	10.0 ml

Fresh β-glycerophosphate and ascorbic acid solutions were freshly made up before use and were added to the culture media to give 10.0 mM and 50.0 μg/ml concentrations.

Ascorbic acid (Vitamin C) was used in the media as it is essential for normal formation of collagen .

β-Glycerophosphate was used for metabolic reasons as a phosphate donor for the process of mineralization.

Dexamethasone is a defined medium supplement aiding mineralization by stimulating the differentiation of progenitor cells into osteoblasts, and induces expression of tyrosine aminotransferase activity constitutively. Dexamethasone, 2.5×10^{-5} M, 10 μg/ml (asoluble synthetic hydrocortisone analogue), improves the plating efficacy of human normal glia, glioma, fibroblasts, and melanoma, and chick myoblasts, and will give increased clonal growth (colony size) if removed 5 days after plating. Lower concentrations (10^{-7} M) have been found preferable for epithelial cells.

Foetal calf serum was used to support the growth of the cells.

Streptomycin /penicillin were used to inhibit bacterial growth by interfering with the final stage of synthesis of the cell wall.

Amphotericin B (fungizone) was used to interfere with the permeability of cell membrane sensitive fungi by binding sterols.

Glutamine is an amino acid and was used in the exogenous form as serially cultured cells, growing in the customary medium containing glutamine, typically exhibit low levels of the enzyme which catalyses the synthesis of glutamine from glutamic acid. Glutamine unlike most other amino acids, is labile in solution.

Ros cell nutrient media

Nutrient mixture F-12 (HAM) with l-Glutamine (Gibco BRL,UK) 500 ml

Foetal Calf Serum 30.0 ml

Penicillin/Streptomycin 5.0 ml

Fungizone 600 µl

200 µl glutamine was added to 20.0 ml media as glutamine degrades with time.

Protein assay reagents

A) Lowry reagent solution

40 ml water was added to a bottle of Lowry reagent (Sigma catalogue number L1013). The bottle was not shaken to minimise foaming and kept at room temperature to keep the reagent stable.

B) Folin and Ciocalteu's Phenol reagent working solution

5.0 ml distilled water

90.0 ml 2.0 N Folin and Ciocalteu's Phenol reagent (sigma catalogue number F9252). Stored in the dark at room temperature (wrapped aluminium foil around the bottle, stored it in a cupboard).

Protein standard solution (400 µg/ml)

This is a reconstituted protein standard (Sigma catalogue number P7656) with the amount of water indicated on the vial label. The mixture was dissolved by gently mixing.

Sodium Dodecyl solution (SDS solution)

Sodium dodecyl sulphate (SDS) was dissolved in sufficient distilled water to produce a 0.1 % solution of SDS (for example, 300 mg in 300 ml).

Phosphate buffered saline solution

Phosphate buffered saline solution was warmed in a warm water bath (37 °C).

MTT reagents

A) MTT solution

MTT powder* was dissolved in phosphate buffered saline to a concentration of 5.0 mg/ml, and filtered through a sterile 0.2 µm membrane filter. Spare MTT solution was frozen at -20°C.

*MTT powder=(3-[4,5-Dimethylthiazol-2-yl]-2,5-diphenyltetrazolium bromide; thiazolylblue). Sigma catalogue number M5655.

B) MTT solvent

10 % Triton X-100 was prepared in acidic isopropanol (0.1 N HCl in absolute isopropanol).

2.1.4 *In vivo*

Table 2.2 Ionomeric cements tested for surgical implantation

Cement type	Composition	Series type	Set	Wet
LG2	1.5 SiO ₂ , Al ₂ O ₃ , 0.5P ₂ O ₅ , CaO 0.75 CaF ₂	Monovalent	*	
LG6	1.5 SiO ₂ , Al ₂ O ₃ , 0.5P ₂ O ₅ , 0.9 CaO 0.75 CaF ₂ , 0.1Na ₂ O	Monovalent	*	
LG63	1.5 SiO ₂ , Al ₂ O ₃ , 0.5P ₂ O ₅ , 0.8 CaO, 0.75 CaF ₂ , 0.2Na ₂ O	Monovalent	*	
LG23 1:2:3	1.5 SiO ₂ , Al ₂ O ₃ , 0.5P ₂ O ₅ , 0.85 CaO, 0.75 CaF ₂ , 0.15Na ₂ O	Monovalent		*
LG23 1:2:2	1.5 SiO ₂ , Al ₂ O ₃ , 0.5P ₂ O ₅ , 0.85 CaO, 0.75 CaF ₂ , 0.15Na ₂ O	Monovalent		*
LG26	4.5 SiO ₂ , 3Al ₂ O ₃ , 1.5P ₂ O ₅ , 3 CaO, 2 CaF ₂	Apatite-S	*	*
LG27	6 SiO ₂ , 4Al ₂ O ₃ , 1.5P ₂ O ₅ , 4 CaO 1CaF ₂	Apatite-S	*	
LG30	7.5 SiO ₂ , 5Al ₂ O ₃ , 1.5P ₂ O ₅ , 5CaO	Apatite-S	*	*
LG119	4.5 SiO ₂ , 3Al ₂ O ₃ , 1.5P ₂ O ₅ , 1.5 CaO, 2 CaF ₂ , 1.5Sr ₂ O	Strontium		*
LG125	4.5 SiO ₂ , 3Al ₂ O ₃ , 1.5P ₂ O ₅ , 2 CaF ₂ , 3Sr ₂ O	Strontium		*
LG130	4.5 SiO ₂ , 3Al ₂ O ₃ , 1.5P ₂ O ₅ , 1.5 CaO, 2 CaF ₂ , 1.5ZnO	Zinc		*
LG132	4.5 SiO ₂ , 3Al ₂ O ₃ , 1.5P ₂ O ₅ , 2.25 CaO, 2 CaF ₂ , 0.75ZnO	Zinc		*
Acrylic	CH₂-CH-COOH	Polymer	*	*

The monovalent cation (monovalent) cements were selected on the basis of their varying monovalent cation sodium concentrations. LG23 was tested using a composition of 1:0.2:0.3 ratio and at a high powder/liquid ratio i.e. 1:0.2:0.2 as wet cements to investigate any difference in the cements adhesive properties and thus in osseointegration. Apatite-stoichiometric cements were selected on the basis of their varying CaF₂ concentrations with LG26 having a high fluoride content. Apatite-stoichiometric cements were chosen as they have the same calcium:phosphate ratio as that of apatite (1.67). LG26 a high apatite stoichiometry glass, was chosen for substitution by strontium because it is known that strontium can substitute for calcium in the apatite lattice. LG119 and LG125 cements were chosen as strontium

is known to stimulate osteoblast proliferation.¹¹¹⁻¹¹⁴ Zinc cements were selected to determine its osteoconductive properties¹⁸⁴.

Stains used for histological sections:

Harris hematoxylin

Hematoxylin	2.5 g
Absolute alcohol	25.0 ml
Potassium alum	50.0 g
Distilled water	500 ml
Mercuric acid	1.25 g
Glacial acetic acid	20.0 ml

The hematoxylin was dissolved in the absolute alcohol, and was then added to the alum which had previously been dissolved in the warm distilled water in a two-litre flask. The mixture was rapidly brought to the boil and the mercuric oxide was then added. The stain was rapidly cooled by plunging the flask into cold water. When the solution was cold the acetic acid was added. The stain was then ready for immediate use. The glacial acetic acid was optimal but its inclusion gives more precise and selective staining of nuclei. For the best results a fresh batch of stain was made up every week.

***Eosin Y* (Eosin yellowish, eosin water soluble)**

Eosin	0.2 %
Calcium chloride	0.2 %
Distilled water	1000 ml

As a cytoplasmic stain it is usually used as a 0.5 or 1.0% solution in distilled water, with a crystal of thymol added to inhibit the growth of fungi. The addition of a little acetic acid (0.5ml to 1000 ml stain) is said to sharpen the staining.

Differentiation of the eosin staining occurs in the subsequent tap water wash, and a little further differentiation occurs during the dehydration through the alcohols.

2.15 Immunohistochemical techniques materials

Rabbit polyclonal primary antibodies raised against fibronectin (Dako, UK, dilution 1:100)

Rabbit polyclonal primary antibodies raised against tenascin (Chemicon, UK, dilution 1:100)

Monoclonal mouse primary antibodies raised against osteopontin (Ohio Hybridoma Bank, USA, Dilution 1:100)

Secondary FITC conjugated antibodies raised against mouse immunoglobulins (Sigma, UK)

2.2 Methods

2.2.1 Material properties testing of glass ionomer (polyalkenoate) cements

To obtain quantitative measurements for the handling properties assessed clinically, the setting and working times of all the ICs surgically implanted were determined.

The **working time** (seconds) was from the point where the glass, polyacrylic acid and water were all mixed until the wet IC was successfully implanted into the bone. For set ICs working time was from the point where the set IC rod was extracted from the silicone mould to the point where the set IC rod was implanted into the bone. The **setting time** was from the point where the IC ingredients were mixed till the IC had successfully set in the medical grade silicone tubing or was set in the bone. Nine tests for the working and setting times were performed.

2.2.2 Ion release

Ionomeric cements were made up in fractions of the following ratio:

1.0 g Glass

0.2 g Poly(acrylic acid)

0.3 ml Water.

For ion release studies cement discs (20.0 mm diameter x 2.0 mm thick) were prepared by mixing 6.0 g of the appropriate glass powder with 1.2 g of mercaptan - free freeze dried PAA and 1.8 ml of distilled sterile highly purified water on a pre-cooled, clean slab. Discs were then cured for at least 24 hours at 37°C at 100 % humidity in a Harvard/LTE incubator.

Cement discs were then placed into Nalgene bottles with 50.0 ml aliquots of sterile non-pyrogenic water (Baxter's Healthcare Ltd, UK) at 37 °C, for elution to take place under sink conditions i.e. in the mechanical shaker. Samples of the solutions with IC discs were collected at 1 day, 3 days, 5 days, 7 days, and 84 days.

2.2.2 (a) Ion selective electrode

The ion selective electrode was used by:

- 1) Connecting electrodes to the Orion SA 720 pH/ISE direct readout meter (USA).
- 2) The mains connected to the meter were switched on.
- 3) Electrode solution (Orion, USA) was placed into the electrode and left for at least 2 hours for the electrode to stabilise.
- 4) The standards were prepared with a ten-fold difference in concentration in the range of the expected sample concentration i.e. 10.0 parts per million (ppm) and 100 ppm. 100 ppm was prepared by using 5.0ml of Total ionic strength adjustment buffer (TISAB III) (Orion, Boston, USA) in 50ml of water, and 10.0 ppm would be prepared by using 0.5 ml of TISAB III in 50ml of highly purified water. TISAB III contains a reagent, CDTA that preferentially complexes Al^{3+} or Fe^{3+} in the sample. Thus, higher levels of Al^{3+} and Fe^{3+} were complexed, obtaining the total fluoride concentration of the solution. This was carried out for sodium ion measurements, where sodium ionic adjustor (ISA, Orion cat. number 841111*) was used in place of TISAB III.

- 5) The 'calibration' button on the meter was switched on and the electrode was placed into the 10.0 ppm solution until the reading on the meter was 10.0 ppm or near 10.0 ppm, the lowest concentration. This was repeated for the 100 ppm solution, the higher concentration.
- 6) The 'sample' button was then pressed and the electrode was placed into the sample solution and the reading was taken.
- 7) The electrode was then rinsed in highly pure water and the next sample reading was measured.
- 8) Baxter's highly pure water was used as a control, and was also sampled at the given times.

Fluoride ion measurements were taken, using an Orion model 94-09, 96-09 fluoride/combination fluoride electrode with reference filling solution (Orion cat. number 900001(see Figure 2.3). Sodium measurements were taken using an Orion model 84-11, 86-11 ROSS™ sodium electrode with reference filling solution (Orion cat. number 900012). Fluoride and sodium detection limits were in the range 10 ppm to 100 ppm) and the percentage accuracy for fluoride measurements were 97.3% accurate and for sodium 95.4% accurate.

2.2.2 (b) Atomic absorption spectroscopy

The atomic absorption spectroscopy (AAS) procedures were carried out by Analytical services at the University of Sheffield. Ions such as calcium, aluminium, silicon, phosphate and potassium were measured by AAS. The

samples requiring calcium were analysed on a Perkin-Elmer M2100 AAS with an AS-50 autosampler. The samples were measured using a Perkin-Elmer calcium hollow cathode lamp, and the instrument was calibrated (1 ppm to 10 ppm) using standards prepared from a pre-concentrated calcium standard (10,000 ppm) purchased from the Laboratory of the Government chemist.

Five standards were used to calibrate the instrument, these were 0.5 ppm, 1.0 ppm , 2.0 ppm, 3.0 ppm and 5.0 ppm of Analytical Quality Control Standard (AQCS) . After every five samples an AQCS standard was run whose value is noted on control charts to ensure accuracy. After every ten samples the instrument was re-calibrated to avoid drift. Detection limits for calcium measurements were in the range of 1 ppm to 10 ppm and were 92.1% accurate.

Table 2.3 Instrument Conditions for Ca Analysis

Wavelength	422.8
Slit Width (nm)	0.7 High
Lamp Current(mA)	1.5
Integration Time (sec)	4
Hold Time (sec)	4
Replicates	2
Oxidant	Air
Fuel	Acetylene
Oxidant Flow (L/min)	12.0
Fuel Flow (L/min)	3.4
Standard Units	(ppm)
Sample Units	(ppm)

The samples requiring silicon (Si) were analysed on a Perkin-Elmer M2100 AAS with a HGA-700 graphite furnace and an AS-70 autosampler. The samples were measured using a S&J Juniper silicon hollow cathode lamp, and the instrument was calibrated using standards prepared from a pre-concentrated silicon standard (1000 ppm) purchased from the Sigma chemicals.

Five standards were used to calibrate the instrument, these were 100 ppm, 200 ppm, 300 ppm, 400 ppm and 500 ppm. After every five samples a separate standard was run, this was a separately prepared AQC, whose value is noted on control charts to ensure accuracy. Again, after every ten samples the instrument was re-calibrated to avoid drift. Detection limits for silicon measurements were in the range 100-500 ppm and were 91.2% accurate.

Table 2.4 Instrument Conditions for Si Analysis

Wavelength (nm)	251.6
Slit Width (nm)	0.7 Low
Lamp Current (mA)	30
Signal Processing	Peak Area
Integration Time (sec)	5.0
Replicates	4
Standard Units	ppm
Sample Units	ppm

Table 2.5 Furnace Parameters

Step Number	Furnace Temp(°C)	Ramp Time (sec)	Hold Time (sec)	Gas Flow (l/min)	Read On	Description
1	140	10	40	300		Drying
2	1400	5	10	300		Ashing
3	2650	0.1	10	0	0	Atomisation
4	3000	1	3	300		Clean-up
5	30	1	5	300		Cool

The samples requiring aluminium were analysed on a Perkin-Elmer M2100 AAS with an AS-50 autosampler. The samples were measured using a Perkin-Elmer aluminium hollow cathode lamp, and the instrument was calibrated (0.1 ppm to 1.0 ppm) using standards prepared from a pre-concentrated aluminium standard (10,000 ppm) purchased from the Laboratory of the Government chemist. Standards were analysed using the same method as that of calcium. Aluminium detection limits were in the range 0.1 ppm to 1.0 ppm and were 93.3 % accurate.

The samples requiring potassium were analysed on a Perkin-Elmer M2100AAS with an AS-50 autosampler. The samples were measured using a hollow cathode lamp, and the instrument was calibrated (1 ppm to 10 ppm) using standards prepared from a pre-concentrated potassium standard (10,000 ppm) purchased from the Laboratory of the Government chemist. The procedure followed was the

same as described in calcium analysis. Potassium detection limits were in the range of 1 ppm to 10 ppm and were 94.1% accurate.

The samples requiring phosphate were analysed on a DIONEX 200001 high pressure liquid chromatography (HPLC) with an autosampler and Trivector integration package. The instrument was calibrated using standards prepared from the separate salts purchased from BDH chemicals. Five mixed standards were used to calibrate the instrument, (containing chloride, nitrate, sulphate and phosphate) these were 5.0 ppm, 10.0 ppm, 15.0 ppm, 25.0 ppm and 40.0 ppm.

After every seven samples a separate AQCS was run, this was a separately prepared AQC, whose value is noted on control charts to ensure accuracy. After every twenty samples the instrument was re-calibrated to avoid drift. The Dionex uses an ASA4 Dionex ionpac anion chromatography column. The eluent is a 1.98 mM sodium bicarbonate mixture with 0.025N sulphuric acid as the suppresser regenerant inhibiting the measurement of recycling ions. Phosphate detection limits were from 5 ppm to 40 ppm and were 94.8% accurate.

2.2.2 (c) pH readings

The pH and conductivity was measured for selected solutions with IC discs.

Measurements were taken using a pH electrode using an Orion SA 720 pH/ISE direct meter (USA).

2.2.3 Cell culture techniques

This was supervised by Dr AJ Devlin.

(i) Making discs for *in vitro* studies

Cement discs were made using the same method as that for the ion release studies (10.0 mm diameter x 1.0 mm depth). The cement discs were cleaned by rinsing them with 15.0 ml of 1 % Decon 90 (E.Sussex, England) in separate universals. The discs were then ultrasonicated for 5 minutes (F5100b Decon, UK). This wash was then repeated and then rinsed with highly pure water (water that had been purified giving water with the least number of contaminant ions, such as calcium, sodium, potassium, aluminium, chlorides, nitrates, sulphates and bicarbonates making it highly pure water, Baxters, UK) three times. The discs were then autoclaved at 120 °C for 20 minutes at 100 % humidity for sterilisation.

2.2.3 a) Bone marrow culture

2.2.3 a) i) Dissection of the femur

Weaned Wistar rats (3 weeks old) (Field Laboratories, University of Sheffield, UK) were harvested using Schedule I killing (a method used to kill protected animals rapidly and in a painless manner). The rats were initially overdosed with a general anaesthetic, halothane, then dislocation of the cervical vertebrae was carried out. The overlying fur and skin of the right femur was cut away working towards the pelvis to expose the right femur. The tibia just below the tibiofemoral joint

(knee) was initially snapped off and again above the coxal joint (hip). The whole of the right femur was then removed cutting away soft tissues from the femur. The femur was then placed into the sterile wash medium. This whole procedure was then repeated for the left femur.

2.2.3 a) ii) Extraction of the bone marrow cells

Asceptic techniques were used to reduce infection from bacteria and fungi by carrying out work in the ICN flow TC4 (USA) laminar flow cabinet to make media and extract cells. The femora together with the wash medium were placed in a water bath at 37 °C for ten minutes. The femora were then washed three times every ten minutes. The muscle and periosteum were asceptically removed by carefully cutting and teasing away the tissues. Each femur was then placed in 10.0 ml of basic medium to rinse off antibiotics in the laminar flow cabinet.

The marrow tissue was then gently flushed out of the bone using 20.0 ml of basic medium in a syringe. The cellular debris was allowed to settle, and the medium containing the cell suspension was then decanted into a vented 135 cm² tissue culture polystyrene disposable sterile flask [T75](Corning, UK). The whole procedure was then repeated for the remaining femur and labelled as such. 10.0 ml of BSM was then added, so that mixed bone cells were suspending in 30.0 ml of medium. The flasks were placed in an LEEC incubator at 37 °C in an atmosphere of 5 % CO₂. Every two-three days the flasks were checked for normal growth and

for any bacterial and fungal infections. β -glycerophosphate 1M solution and ascorbic acid were made up and added to media prior to use. The media was replenished every three to five days with 30.0 ml fresh BSM per flask.

2.2.3.a) iii) Trypsinisation of bone marrow cells

When cells were confluent they were washed twice with 20.0 ml of 1 % PBS. To remove any remaining debris in the culture flask. Cells were then treated with 20.0 ml of 0.25 % trypsin in a 37 °C mechanical shaker for 5 minutes to lift cells off the surface of the flask. The cells were then observed under the inverted phase-contrast microscope (Nikon TMS/TMS-F, Japan) at x 10 magnification. Round-shaped cells indicated that the cells were trypsinised.

The trypsinised cells were placed into a sterile 20.0 ml universal container (Catalogue No. 3276 and 3376, Costar, Cambridge, MA, USA), and centrifuged at 1500 rpm for 5 minutes. The trypsin media was then removed with a sterile pipette and placed into bleach prior to disposing. The pelleted cells in the bottom of the universal container were resuspended by adding 20.0 ml of BSM.

2.2.3 b) Ros Cell line

In addition to primary cells ICs were studied using a cell line ROS 17/2.8, which has well-defined osteoblastic properties.¹⁸⁵ ROS cells have many advantages such as having no cellular heterogeneity, no phenotypic changes in culture and they are a

permanent cell line and they give more consistent results in toxicology testing than primary cell lines. ROS cells were kindly donated by Dr GA Rodan (Merck- Sharp and Dohme, Philadelphia, USA). Studies were carried out in the same way as for the bone marrow cultures, except that cells were grown in Ham's F12 containing 5 % foetal calf serum, 50 IU/ml penicillin, 50 µl Streptomycin, 0.3 µg/ml amphotericin B and 2 mM glutamine (Materials section 2.1.3, Ros cell media).

2.2.3 b) i) Chamber Slide Cultures

The same procedure was used as above to grow Ros cells in Chamber slide culture chambers (Lab-Tek, Nunc Inc, Illinois, USA). This method was used for staining the cells, and determining calcium deposits in live cells by staining with Alizarin Red S. The objective of the Alizarin Red S method is to detect calcium deposits. After fixation with 4% neutral buffered formalin for 10-15 minutes, cell layers were rinsed in distilled water. 2% Alizarin Red S (Sigma, UK) solution (pH 4.2) was added for 1-5 minutes and the reaction monitored under an inverted phase-contrast microscope (Nikon TMS/TMS-F, Japan) until completion. The layers were differentiated in a 0.05% hydrochloric acid/95% ethanol solution for 15 seconds. The layers were rinsed in 100% ethanol two times and rinsed in histoclear twice for 5 minutes.

2.2.3 b) ii) Multiwell plates

Multiwell plates were set up for both bone marrow cells and Ros cells. Sterile cement discs were placed into individual wells of the multiwell tissue culture plates (Costar, Cambridge, MA, 02140, USA). 1.0 ml of sterile BSM and 0.5 ml of dilute media with bone marrow cells and Ros cells were placed into each of the wells. The plate was placed into the incubator, and was regularly observed for the healthy growth of bone marrow cells and Ros cells, and for the attachment of cells to the cement discs under the Nikon phase-contrast microscope. Media was changed every two or three days to feed the cells.

2.2.3 b) iii) Scanning electron microscopical examination of cultures

This was supervised by Mr John Proctor. Specimens were fixed by replacing the culture medium with 2.5% glutaraldehyde in 0.1M cacodylate buffer (pH 7.2-7.4) for 24 hours. Cultures were secondarily fixed with 2% aqueous osmium tetroxide for 1 hour, followed by dehydration through a graded acetone series, critical-point from CO₂ (Polaron critical point drier) and coated with a thin layer (approximately 20nm) of gold (Nanotech sputter coater) for scanning electron microscopy (SEM) (Cambridge Stereoscan 600, set at 25kV).

2.2.3 c) Quantitative assessment of cytocompatibility

2.2.3 c) i) Total protein

The Lowry procedure has been found to be the most reliable and satisfactory method for quantification of soluble proteins.¹⁸⁶ The procedure used was based on Peterson's modification of the micro-Lowry method and utilised sodium dodecylsulfate, included in the Lowry reagent, to facilitate the dissolution of relatively insoluble lipoproteins.¹⁸⁶

For many proteins, the Lowry reaction can be run directly on the protein solution. However, interference in the direct Lowry procedure is caused by commonly used chemicals, such as Tris, ammonium sulphate, EDTA, sucrose, citrate, amino acid and peptide buffers and aromatic amino acids such as tyrosine and phenylalanine are detected. The procedure with protein precipitation, which uses deoxycholate (DOC) and trichloroacetic acid (TCA), eliminates these interferences with the exception of phenols. However, the amount of various proteins recovered through the precipitation step may vary depending on the particular protein assayed.

A purple-blue colour is formed when alkaline cupric tartrate reagent complexes with the peptide bonds when the phenol reagent is added. Wavelengths at which the absorbances are read are between 500 nm and 800 nm, and the protein concentration is determined by a calibration curve.

Direct protein procedure-without Protein precipitation

1) Standard tubes were prepared by diluting Protein Standard Solution with water to a volume of 1.0 ml in appropriately labelled test tubes:

Table 2.6 Protein concentrations

Protein Standard Solution (ml)	Water(ml)	Protein Concentration($\mu\text{g/ml}$)
0.125	0.875	50
0.250	0.750	100
0.500	0.500	200
0.750	0.250	300
1.000	0	400

2) 1.0 ml of water in a test tube was labelled 'Blank'.

3) Samples were added to appropriately labelled test tubes and diluted to 1.0 ml with water.

4) 1.0 ml of Lowry reagent solution was added to the standard, blank and sample tubes, and were then well mixed.

5) Solutions were then left to stand for 20 minutes.

6) 0.5ml of Folin & Ciocalteu's phenol reagent working solution samples were added to each tube and mixed rapidly.

7) The colour was allowed to develop for 30 minutes.

8) Solutions were then transferred to cuvettes and the absorbance was measured for all the standards and sample tubes vs. the blank at a wavelength from 500 nm to 800 nm. Readings were completed within 30 minutes.

9) The absorbance values of the standards vs. their corresponding protein concentrations were plotted to prepare a calibration curve.

10) The protein concentration of the sample tube was determined from the calibration curve. The result was multiplied by the appropriate dilution factor to obtain the protein concentration in the original sample.

2.2.3 c) ii) Methyltetrazolium Test (MTT)

Traditionally, *in vitro* determination of toxic effects of unknown compounds have been performed by counting viable cells after staining with a vital dye.¹⁸⁷

Alternative methods have been to measure the radioisotope incorporation as a measurement of DNA synthesis, counting by automated counters and others which rely on dyes and cellular activity. The MTT system is a means of measuring the activity of living cells via mitochondrial dehydrogenases.¹⁸⁷

The key component is (3-[4,5-dimethylthiazol-2-yl]-2,5-diphenyl tetrazolium bromide) or MTT. Solutions of MTT dissolved in medium or balanced salt solutions without phenol red, are yellowish in colour. Mitochondrial dehydrogenases of viable cells cleave the tetrazolium ring yielding purple crystals which are insoluble in aqueous solutions. The crystals are dissolved in acidified isopropanol. The resulting purple solution is measured using a spectrophotometer. An increase or decrease in cell number results in a concomitant change in the amount formed, indicating the degree of cytotoxicity caused by the test material.

The MTT method of monitoring *in vitro* cytotoxicity is well suited for use with multiwell plates. For best results, cells in the logarithmic phase of growth should be employed and the final cell number should not exceed 10^6 cells/cm². Each test included a blank containing complete medium without the cells.

1 The culture was removed from the incubator and into the laminar flow hood.

2 Each vial reconstituted with MTT was used with 3.0 ml of medium, the reconstituted MTT was added in equal amounts to 10 % of the culture medium volume.

3 The cultures were then returned to the incubator for 2-4 hours. Incubation times were consistent when compared with other samples.

4 Cultures were then removed from the incubator and the resulting formazon crystals were dissolved using an equal amount of MTT solubilization solution to that of the original culture medium.

5 The plate was then placed in the mechanical shaker to enhance dissolution.

Occasionally, pipetting up and down, i.e. titration, was required to completely dissolve the MTT formazon crystals.

6 Tests performed in multiwell plates were read by transferring the well contents to appropriate size cuvettes for spectrophotometric measurements.

7 The absorbance measurements were taken at 570 nm and 670 nm wavelengths to measure the background absorbance of the multiwell plates. The absorbances at 670 nm were then subtracted from the 570 nm absorbance measurements.

8 Plates were read within 1 hour after adding MTT solvent.

2.2.4 *In vivo* techniques

2.2.4 a) Production of set ionomeric cement rods

ICs were produced using a ratio of 1.0 g glass, 0.2 g freeze dried mercaptan free poly(acrylic) acid (Advanced Healthcare, UK) and 0.3 ml sterile non-pyrogenic water. Smooth rods (nominally 2.0 mm length x 1.0 mm diameter) were produced by placing unset material in silicone moulds. The silicon tube containing the IC was placed into a device specially made by the Department of Medical Physics (University of Sheffield, UK) (see Figure 2.3 Set rod cutter). The set rod cutter took the exact measurement of the length of the tube, i.e. 1.0 mm, 2.0 mm, 3.0 mm, and 4.0 mm. 2.0 mm lengths. A scalpel was used to cut rods. The rods were cured for at least 5 hours at 37 °C at 100 % relative humidity. The rods were then autoclaved for 20 minutes and returned to room temperature and stored overnight at 100 % humidity in an incubator (Harvard/LTE) until surgical implantation.

2.2.4 b) Formulation of wet cements for surgical implantation

Glasses and poly(acrylic) acid were weighed out into clean bijou plastic bottles and γ -irradiated (Swann Morton, Sheffield, UK) a few weeks prior to the day of implantation. ICs were produced using the same ratio for wet implants as that for set rods, i.e.

1.0 g Glass

0.2 g Poly(acrylic) acid,

0.3 ml Sterile non-pyrogenic water

with the exception of LG23 as this was tested with the above quantities and with 0.2 ml of sterile non-pyrogenic water (high powder/liquid ratio) as osseointegration in varying powder/liquid ratios was investigated.

All contents were mixed just prior to implantation and were placed into dental tubing (Odus Full Tuben-transparent, Zurich, Switzerland) where the end of the tube was snipped off and the wet cement was squeezed into the drilled hole of 1.0 mm in diameter and 2.0 mm in length. The remaining procedure was the same as that for set rod implantation.

2.2.4 c) Surgical Implantation

The Animal (Scientific Procedures) Act 1986 provided for the licensing of experimental and other scientific procedures carried out on 'protected animals'. The act aimed to provide the maximum protection for laboratory animals without

unnecessarily hindering biomedical research. The person applying the 'regulated procedures' held a personal licence. For the work carried out in this thesis the personal licence was Home office approved and given the following personal licence number PIL 50 03510. The procedures must be part of a programme of work authorised by a project licence. The Home office approved project licence number for the work carried out in this thesis was PPL 50 01281. No work was done until the procedure, the animals used, and the place where the work was done, were specifically authorised by the Home Office in both Personal and Project licences.

The room used for implantation was thoroughly cleaned the day before surgical implantation. The surgical drill and all instruments were cleaned and sterilised and gas tanks were checked for sufficient amounts of NO₂ and O₂. For each of the set materials used *in vivo* a single rod was implanted, under anaesthesia (Halothane 2.0 %, May & Baker, UK) in oxygen 25.0 % and nitrous oxide 75.0 %), into the midshaft of the femora of groups of five male weaned (3 weeks) inbred Wistar rats. The skin was initially swabbed with Chlorhexidine (DePuy® Healthcare, Leeds, UK) left to dry for approximately 1 minute and then with a pair of forceps lifted the skin orientating the cut from the the tibia below the tibiafemoral joint (knee) to the coxal joint (hip) with a sharp pair of surgical scissors.

Under saline (0.9 % w/v Sodium chloride intravenous infusion BP, Braun Medical limited, Aylesbury, Bucks, UK) irrigation a slow speed 1mm diameter tungsten

carbide burr was used to cut a hole matched to the diameter of the implant, through one cortex into the marrow space. Implants were placed to lie level with the outer surface of the bone penetrating through the cortex into the marrow cavity. The overlying periosteum and soft tissues were replaced and the wound sutured using vicryl sterile synthetic absorbable sutures (Ethicon, Edinburgh, UK) antibiotics were not used and no there was no evidence of inflammation.

Post-operatively, wounds were inspected to monitor healing and rats were maintained on a standard laboratory diet. After 4 weeks, 5 animals were sacrificed, femora removed, fixed in neutral buffered formalin, and decalcified in 4N formic acid for one week prior to trimming. Routine histological processing was carried out and paraffin wax embedded. Two femurs were fixed in neutral buffered formalin for ground sectioning. Two femurs were fixed in 3.0 % Glyceraldehyde for electron microscopy. 12 week implants were also carried out for all the radiopaque and radiolucent glasses (LG119, LG125, LG130 and LG132) in the rat femora.

2.2.4 d) Light microscopy/Histomorphometry

Five stepped serial sections 7.0 μm thick, each separated by 70.0 μm , were cut from the implant bed in each femora using a rotary microtome (Leitz 1512, Germany), dewaxed by taking the section through a series of xylene and dehydrating alcohol's and stained using Harris hematoxylin (Shandon, USA) and eosin Y

(Midland Laboratories equipment, Lichfield, Staffordshire, UK), dehydrated through alcohol's, cleared in xylol and mounted in DPX.

The biological response to the different ionomer implants was studied blind to the IC by covering the labels by determining the degree of osteoconduction (amount of new bone formed adjacent to the implant) ¹⁸⁸ and percentage osseointegration (the length of bone/implant interfacial contact), ¹⁸⁹ using the transmission Nikon Optiphot 2 microscope linked to an image analyser system (Optimas 4.1, Biosoft, USA. The software was then updated to Optimas 5.1, Biosoft, USA, 1995. In 1996 it was updated to Optimas 5.2, Biosoft, USA).

2.2.4 e) Using the Optimas Image Analysis software

The perimeter of the implant and the perimeter of bone in contact with implant was drawn using the pointer to obtain the percentage osseointegration.

Osteoconduction was determined by taking six points at random around the perimeter of each ionomeric rod measuring the thickness of new bone formed. The degree of osteoconduction being taken as the average thickness of new bone produced on the implant surface. An average of ten sections were analysed to carry out measurements for each ionomeric cement to obtain the mean bone thickness for lamellar bone. Obliquity has to be taken into account as the measurements of new bone was neither completely parallel nor perpendicular to the IC and not all sections were perfectly plane therefore obliquity had to taken into account. Fields of

interest gave the most sharp, crisp image for analysis of bone-implant interface. Statistical analysis was undertaken using the Unistatistical package (University software, UK) and by applying Student's t-Test (unpaired) for some of the implants and later the t-Test from the Excel 5.0 package was used.

2.2.4 f) Immunohistochemical detection of bone proteins

The three set ICs LG2, LG6 and LG23 of the monovalent cation sodium based glasses were produced (section 2.2.4a) and were surgically implanted as previously described in section 2.2.4c. For each set sodium based glass nine samples were implanted. After four weeks, femora were harvested snap frozen in isopentane over liquid nitrogen and embedded in carboxymethylcellulose at -25 ° C.

Serial cryosections, 10µm thick, were fixed in neutral buffered formalin, decalcified in 20% EDTA and washed in PBS then stained using rabbit polyclonal primary antibodies raised against FN (Dako, UK, dilution 1:100), TN (Chemikon, UK, dilution 1:40), using fluoroisothiocyanate (FITC) conjugated secondary antibodies to visualize the protein raised against rabbit immunoglobulins (Igs). FITC was used as a fluorescent label. Monoclonal mouse primary antibody raised against OPN (Ohio Hybridoma Bank, USA, dilution 1:100), using FITC conjugated secondary antibodies raised against mouse Igs. When the femora was embedded in carboxymethylcellulose resin at -25°C the femora may have been slightly slanted in the frozen block as a result sometimes sectioning showed that the set IC implant

was part of an oblique transverse section. Not all sections were perfectly plane therefore obliquity had to be taken into account. A secondary conjugate was used on a secondary site on an antibody as this gives a greater intensity for specific proteins such as OPN, FN, and TN coupled by FITC, the fluorescent probe, which in this case is fluorescent green under the fluorescence microscope.

Sections were mounted in DABCO and examined under UV light using a Zeiss Axoplan microscope. Micrographs were taken using Agfa 100ASA colour film.

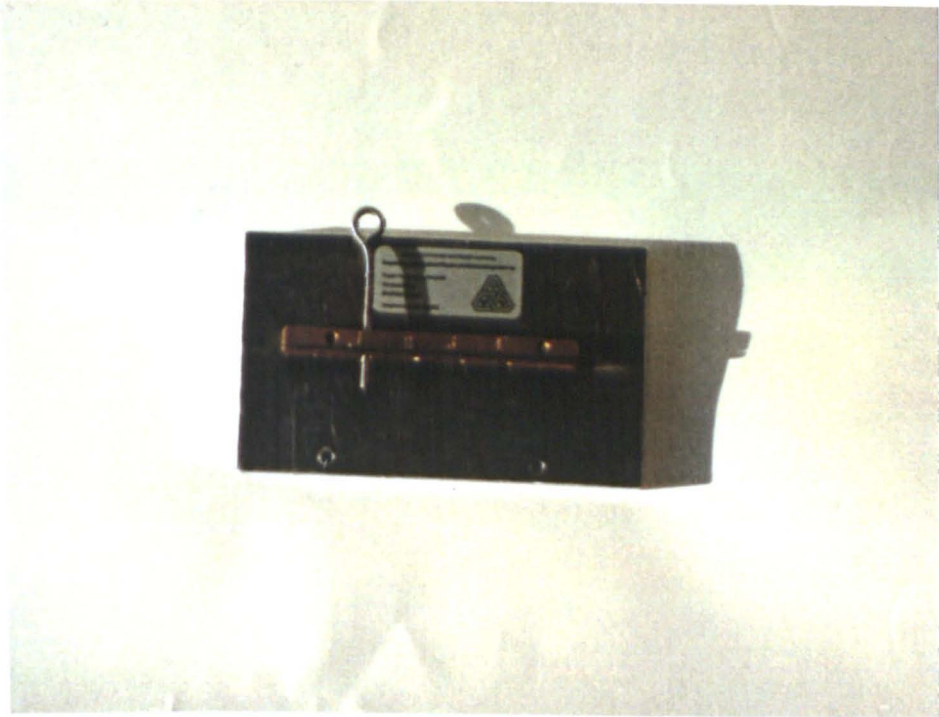


Figure 2.3 Set rod cutter used to cut Ionomeric cement rods (1mm in diameter) covered in medical siliconegrade tubing to 1mm, 2mm, 3mm and 4 mm in lengths. Metal ring device pushes out the IC rod with the medical siliconegrade tubing.

3. RESULTS

3.1 Results for Setting/ Working Time

The setting and working time required for the *in vivo* surgical placement of ICs for use as a bone substitute were studied. The setting time was from the point where the glass, poly(acrylic) acid and water were mixed until the IC had successfully set in the medical grade silicone tubing or had set in the bone. The working time for wet cements was from the point where the glass, poly(acrylic) acid and water were all mixed up to the time when the wet IC was implanted into the bone. Results are given in Table 3.1 to 3.5.

Particular results of interest for the working and setting times are added as footnotes where appropriate for Tables 3.1 to 3.5.

Table 3.1 Working and setting time (s) test for the monovalent cation series of ICs*

1.5SiO₂ Al₂O₃ 0.5P₂O₅ (1-Z) CaO 0.75CaF₂ ZNa₂O

Material		Mean	SD
LG2	Working Time	84	2.0
Z=0	Setting Time	90	3.7
LG6	Working Time	84	2.0
Z=0.1	Setting Time	102	0.9
LG23 1:0.2:0.3	Working Time	60	6.7
Z=0.15	Setting Time	63	2.1
LG23 1:0.2:0.2	Working Time	20	4.2

Z=0.15	Setting Time	35	0.4
LG63	Working Time	90	1.2
Z=0.2	Setting Time	114	0.5

Cements were mixed at room temperature at 20°C. *The data is the arithmetic mean of one analysis of each of nine specimens (n=9).

LG23, with a composition ratio of 1:0.2:0.2, had the fastest setting time of 35 seconds and the fastest working time of 20 seconds from all the ICs implanted as bone cements or bone substitutes. LG63 had the longest setting time of 114 seconds and the longest working time of 90 seconds for the monovalent cation series.

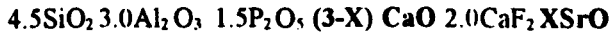
Table 3.2 Working and setting time test (S) for the apatite-stoichiometric based ICs*.
(P)SiO₂(Q)Al₂O₃ 1.5P₂O₅ (5-X)CaO XCaF₂

Material		Mean	SD
LG26	X=2 Working Time	120	0.7
	Setting Time	150	0.7
LG27	X=1 Working Time	120	0.7
	Setting Time	156	5.7
LG30	X=0 Working Time	156	5.6
	Setting Time	175	7.9

Cements were mixed at room temperature at 20°C. *The data is the arithmetic mean of one analysis of each of nine specimens (n= 9).

LG30 had the longest setting time of 175 seconds and working time of 156 seconds for the apatite-stoichiometric based ICs and from all the ICs implanted as bone cements or bone substitutes. LG26 had the shortest setting time for this series of 150 seconds, and the shortest working time of 120 seconds.

Table 3.3 Working and setting time test (S) for the radiopaque strontium based ICs*

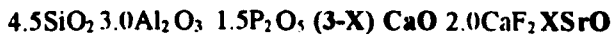


Material		Mean	SD
LG119	Working Time	90	1.2
X=1.5	Setting Time	93	3.6
LG125	Working Time	78	2.4
X=3.0	Setting Time	90	0.7

Cements were mixed at room temperature at 20°C. *The data is the arithmetic mean of one analysis of each of nine specimens (n= 9).

For the radiopaque ICs LG125 had a shorter setting time of 90 seconds and working time of 78 seconds.

Table 3.4 Working and setting time test (S) for the zinc based ICs*



Material		Mean	SD
LG130	Working Time	81	1.4
X=1.5	Setting Time	84	0.7
LG132	Working Time	73.2	0.5
X=0.75	Setting Time	90.0	0.4

Cements were mixed at room temperature at 20°C. *The data is the arithmetic mean of one analysis of each of nine specimens (n= 9).

For the zinc based ICs LG132 had the longest setting time. LG130 had a longer working time than LG132.

Table 3.5 Working and setting time test (S) for the acrylic cement (control)*

Material		Mean	SD
Acrylic	Working Time	500	0.6
	Setting Time	540	0.8

Cements were mixed at room temperature at 20°C. *The data is the arithmetic mean of one analysis of each of nine specimens (n= 9).

The acrylic cements had the longest setting time of 540 seconds and the longest working time of 500 seconds to implant into the femur.

Ideally, when formulated for use as a bone cement ICs should mix to a paste which can be loaded into a syringe and encapsulated for injection placement.

Encapsulation and machine mixing would help to standardise the mix and is usually more rapid than hand mixing in effect allowing for a longer placement time. At delivery the IC should be of sufficiently high viscosity not to flow at the shear stresses employed in manipulation/placement, preventing undue spreading of material and enabling accurate placement at the implant site. Once placed, contamination by body fluids e.g. blood would rapidly occur so a snap set is required. In achieving the above aims the mixing times are not critical but should be of sufficient length to allow manipulation. Under simulated surgical conditions this was in the order of 200 seconds, which is close to the setting time of LG30 (Table 3.2). However, the actual setting time needs to be known accurately so that placement can be timed to be followed immediately by a snap set. LG30 having the

longest working and setting time, and LG23 with a composition ratio of 1:0.2:0.2 with the least working and setting time.

3.2 *In vitro* experiments

3.2.1 Ion release studies

(a) Fluoride by ion selective electrode

A fluoride ion selective electrode was used to measure the concentration of ions released from the set discs of IC (see Section 2.2.1). Fluoride release data from all formulations examined are summarised in Table 3.6 to 3.17 on the following pages.

Particular areas of interest of fluoride ion release data are added as footnotes where appropriate in Tables 3.6 to 3.17.

Table 3.6 Fluoride ion release ($\mu\text{mol g}^{-1}$) from discs of ionomeric cements from the monovalent cation series. $1.5\text{SiO}_2 \text{ Al}_2\text{O}_3 \cdot 0.5\text{P}_2\text{O}_5 \cdot (1-Z) \text{ CaO} \cdot 0.75\text{CaF}_2 \cdot Z\text{Na}_2\text{O}$

Material	Time (d)								
	1	3	5	7	10	14	21	42	84
LG2 Z=0	0.7	na	0.8	5.4	na	na	28.4	43.2	60.1
LG3 Z=0	2.9	5.6	7.8	9.6	11.7	13.9	15.2	19.5	na
LG4 Z=0.025Na	na	na	na	13.6	na	na	26.1	39.3	53.1
LG5 Z=0.05Na	na	na	na	20.1	na	na	36.7	52.7	69.0
LG6 Z=0.1Na	na	na	na	27.1	na	na	48.3	66.4	83.8
LG7 Z=0.025K	na	na	na	11.6	na	na	22.4	36.4	50.4
LG8 Z=0.05K	na	na	na	16.2	na	na	30.3	46.6	63.6
LG10 Z=0.0125Na/K	na	na	na	12.6	na	na	22.9	35.4	49.7
LG11Z=0.05Na/K	na	na	na	17.3	na	na	33.3	49.1	64.8
LG22 Z=0.05K	3.1	5.2	8.2	9.1	10.4	12.3	14.4	18.6	22.8
LG23 Z=0.15Na	6.2	11.9	17.9	20.1	23.8	29.3	35.2	46.0	na
LG63 Z=0.2Na	8.8	17.2	25.1	28.7	33.4	38.5	46.3	64.6	na
LG65 Z=0.1Na	2.8	5.0	6.8	8.3	10.2	12.3	15.5	21.7	na
LG66 Z=0.2 Na	3.0	5.8	8.0	9.5	11.6	14.1	17.1	25.8	na
LG67 Z=0.3 Na	3.3	6.0	7.8	9.6	12.0	14.7	19.0	26.6	na

LG68 Z=0.4 Na	4.7	8.0	10.0	12.0	14.7	18.0	22.0	30.0	na
LG69 Z=0.5Na	9.3	17.0	25.0	30.0	37.0	45.0	56.0	78.0	na
LG70 Z=0.45Na	5.0	9.0	13.0	18.0	20.0	24.0	30.0	41.0	na

Data obtained from discs (20 mm by 2 mm) in 50 ml water at 37°C *. Release data is the arithmetic mean of one analysis of each of six specimens. The standard deviation did not exceed 10%.

* Analyses performed in presence of TISAB III buffer to give total fluoride concentration.

na-Not applied-reading was not taken as there was no sample

LG69 released the greatest amount of fluoride to 42 days, however LG22 eluted the least amount of fluoride up to the same time period.

Detection limits of fluoride ion selective electrode were 10 ppm to 100 ppm.

Figure 3.1 to Figure 3.3 illustrate increasing fluoride ion release and a positive relation with sodium glass content with the exception of 0.2 –0.3 mole fraction of sodium oxide glass content, where fluoride release decreases (Correlation coefficient of sodium glass content and fluoride release at day 1=0.56, day 7=0.49 and at day 21=0.33). This relation is persistent up to 21 days. This decrease in fluoride release would be an error in fluoride ion measurements as after 0.3 mole fraction of sodium oxide glass content fluoride release increases as shown in Figure 3.1 to Figure 3.3.

There is also a relation between fluoride ion release and potassium glass content (see Table 3.6, however a wider range of potassium glass concentrations were required for adequate plots). Hence, sodium and potassium increase release of fluoride.

Figure 3.4 illustrates increasing fluoride ion release from LG26 during 42 days showing a positive relation between fluoride ion release and time with a correlation coefficient of 0.97.

Figure 3.1 Fluoride ion release of varying compositions of Sodium based ICs at day 1. Linear regression, $y=9,45x+0$. Correlation coefficient=0.56 (n=6).

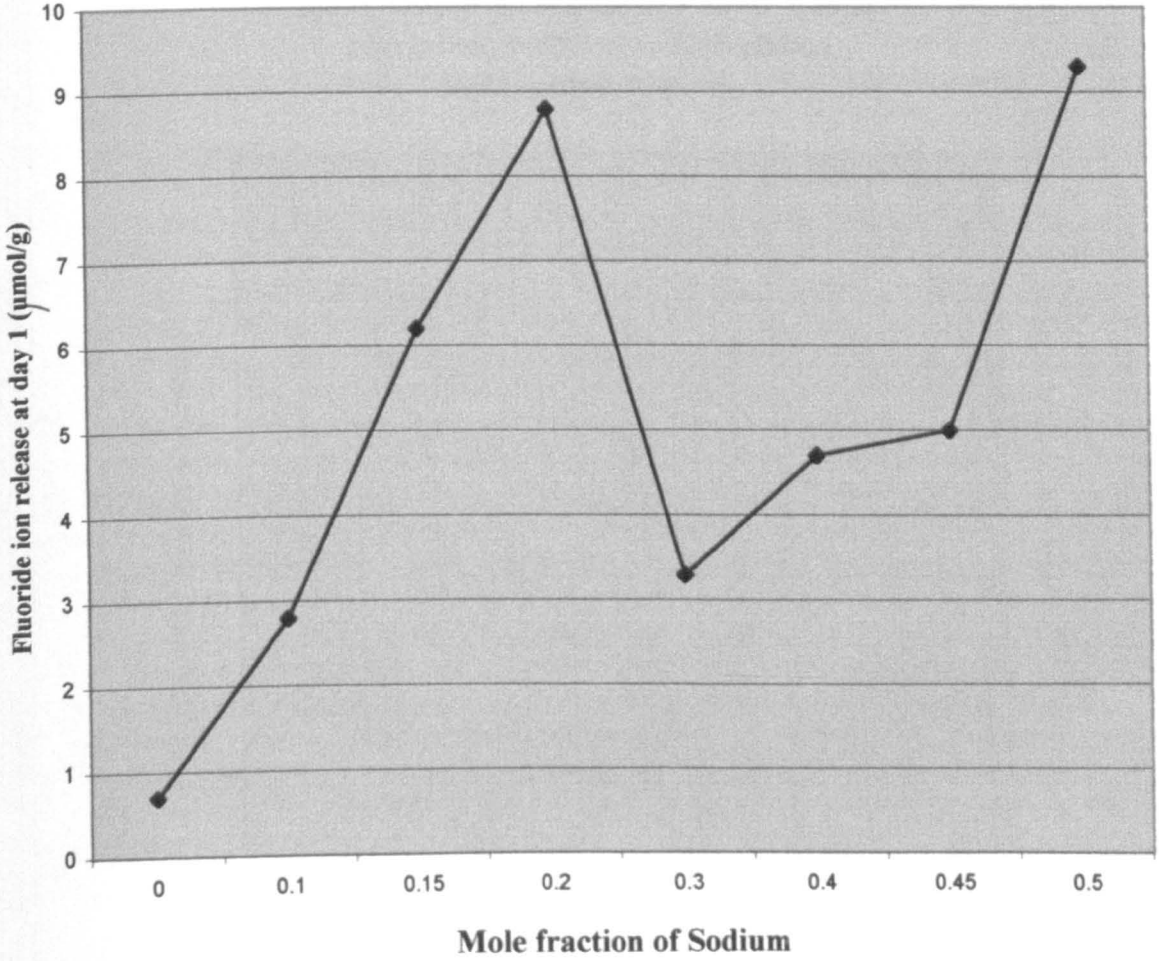


Figure 3.2 Relation of Sodium glass composition and Fluoride ion release at 7 days. Linear regression, $y=52.1x+5$. Correlation coefficient=0.49 (n=6).

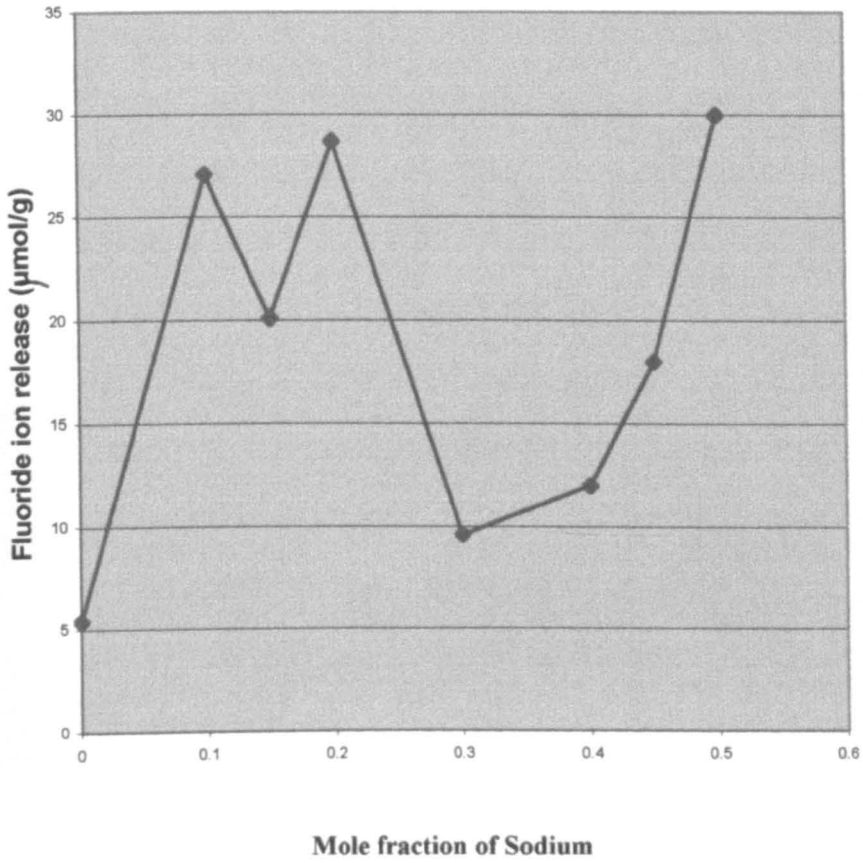


Figure 3.3 Relation between Sodium glass composition and Fluoride ion release at 21 days. Linear regression, $y=93.01x+29$. Correlation coefficient=0.33 (n=6).

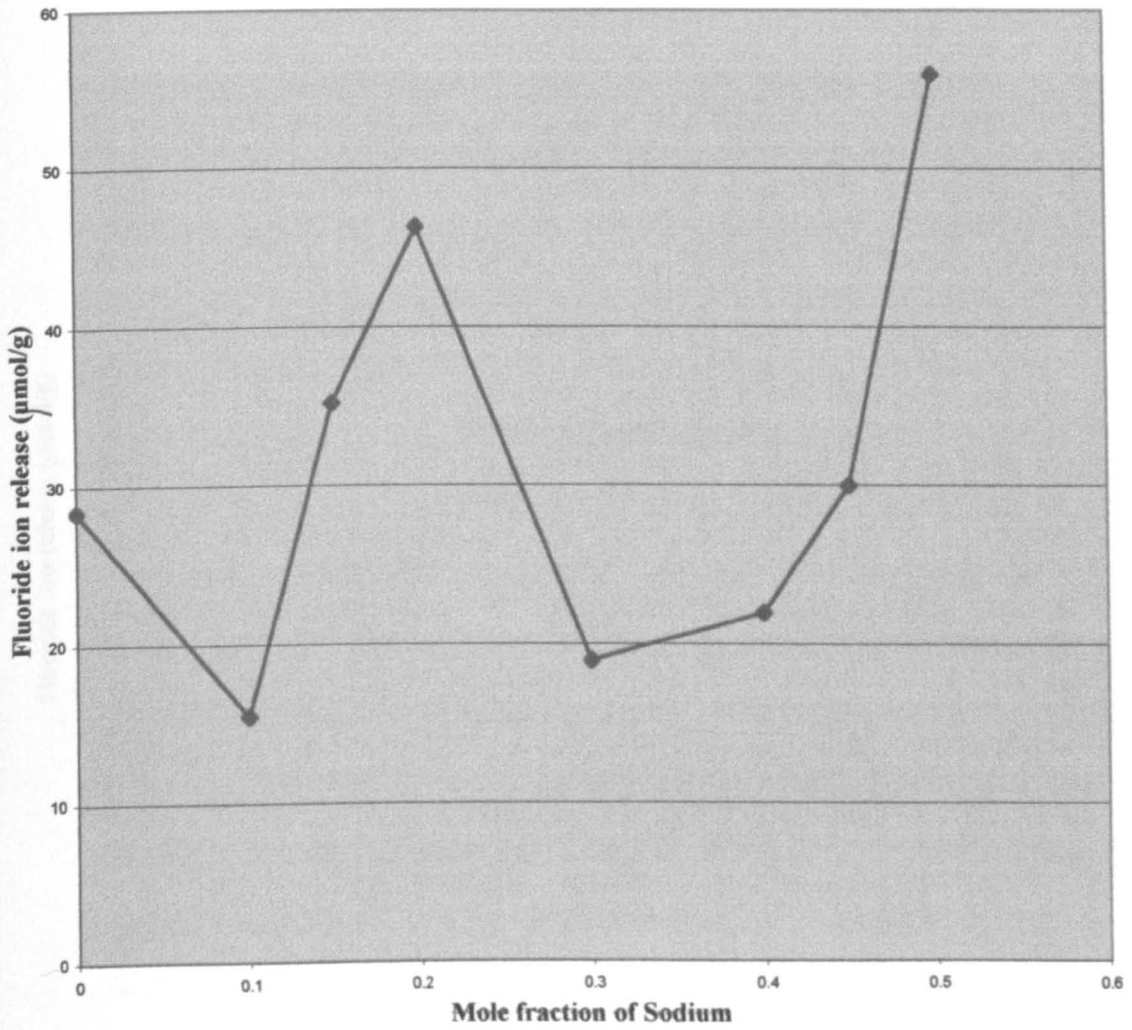


Figure 3.4 Fluoride ion release of LG26 upto a period of 42 days
Linear regression, $y=0.59x+(-1)$. Correlation coefficient=0.97
(n=6).

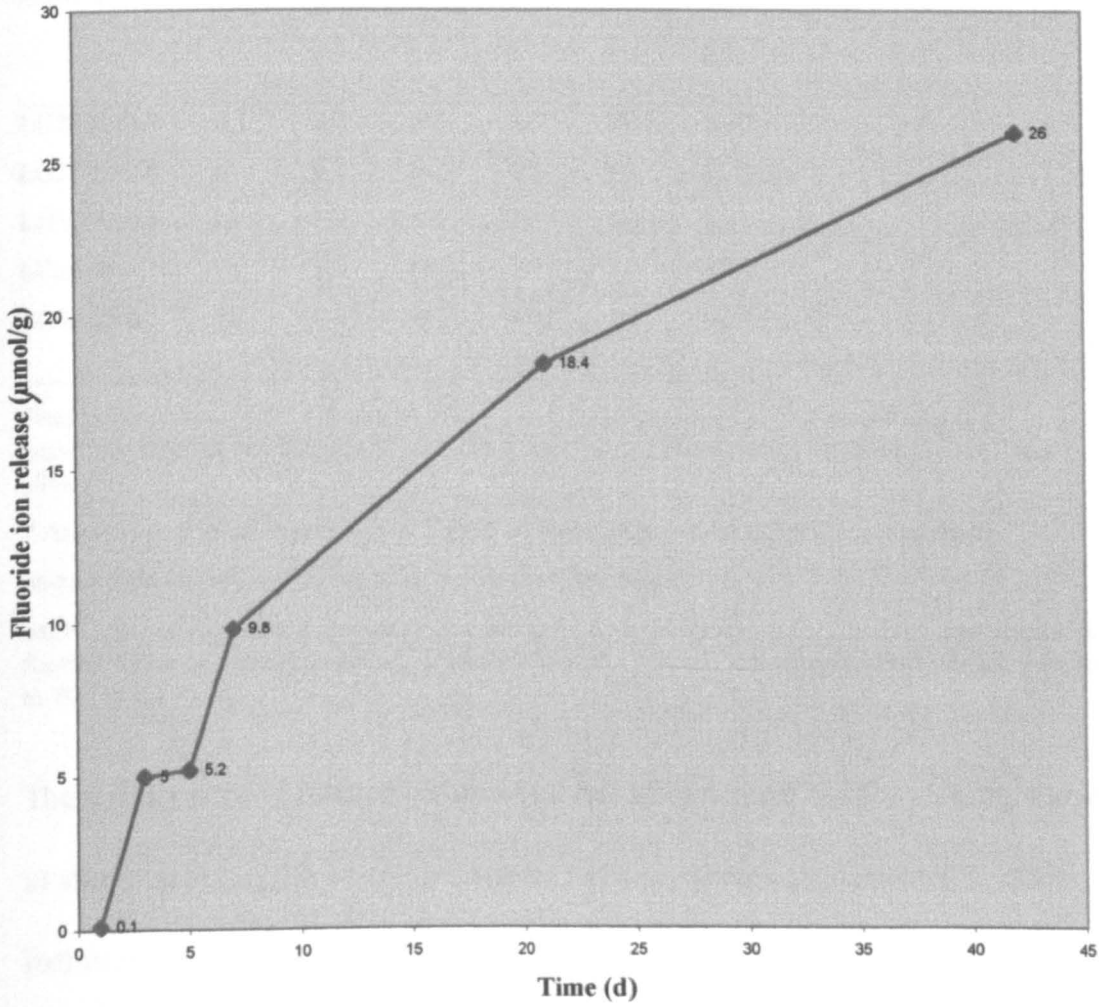


Table 3.7 Fluoride ion release ($\mu\text{mol g}^{-1}$) over time from discs of ionomeric cements from the apatite stoichiometric series (Ca:P~1.66).



Material	Time (d)					
	1	3	5	7	21	42
LG26 X=2.0	0.1	5.0	5.2	9.8	18.4	26.0
LG27 X=1.0	na	2.3	na	4.3	7.3	11.3
LG28 X=0.5	na	1.2	na	2.3	4.0	6.4
LG29 X=0.25	na	1.0	na	1.9	3.0	4.7
LG30 X=0	na	0.05	na	0.01	0.2	0.2

Data obtained from discs (20 mm by 2 mm) in 50 ml water at 37°C *. Release data is the arithmetic mean of one analysis of each of six specimens. The standard deviation did not exceed 10%.

* Analyses performed in presence of TISAB III buffer to give total fluoride concentration.

na-Not applied-reading was not taken as there was no sample.

LG26 released the greatest amount of fluoride to 42 days, however LG30 eluted the least amount of fluoride up to the same time period. Detection limits of fluoride ion selective electrode were 10 ppm to 100 ppm.

There was a positive relation between fluoride glass content and fluoride ion release as shown in Figure 3.5 where the relation has a correlation coefficient of 1. This indicates a strong relation between the two parameters and that fluoride ion release is dependent on fluoride glass content.

Figure 3.5 Relation between Fluoride glass composition and Fluoride ion release at 42 days.
Linear regression, $y=12.5x+0$. Correlation coefficient=1 (n=6)

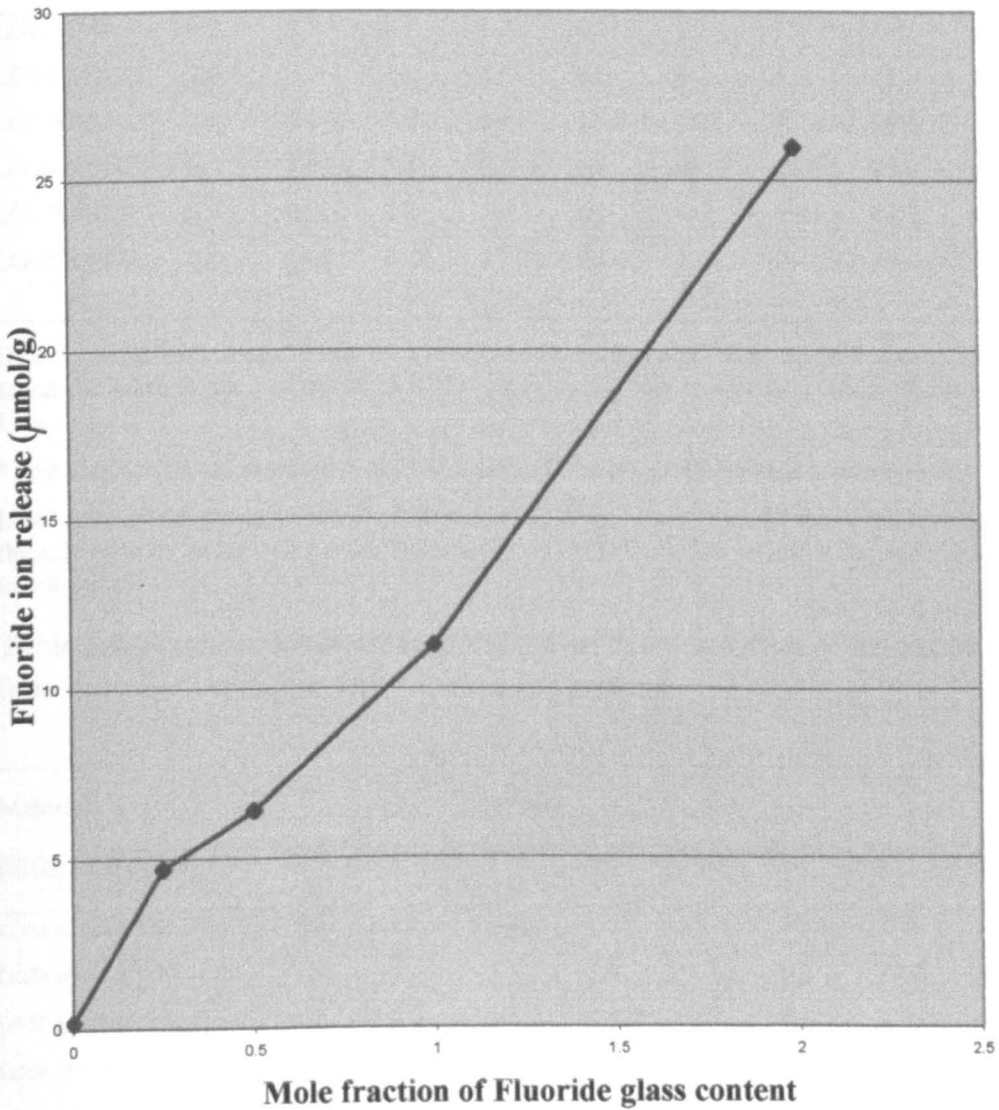


Table 3.8 Fluoride ion release ($\mu\text{mol g}^{-1}$) over time from discs of ionomeric cements from the series varying in calcium fluoride.

1.5SiO₂ 1.0Al₂O₃ 0.5P₂O₅ 1.0CaO XCaF₂

Material	Time (d)								
	1	3	5	7	10	14	21	42	84
LG45 X=0	0.2	0.3	1.1	1.2	1.2	1.2	1.3	1.4	1.4
LG44 X=0.25	2.0	5.0	7.4	8.0	8.0	8.2	9.0	11.0	11.5
LG3 X=0.5	2.9	5.6	7.8	9.6	11.7	13.9	15.2	19.5	na
LG26 X=0.67	0.1	5.0	5.2	9.8	na	na	18.4	26.0	na
LG2 X=0.75	0.7	na	0.8	5.4	na	na	28.4	43.2	60.1
LG42 X=1.0	6.0	11.0	15.7	17.7	20.4	23.2	26.1	35.0	43.8

Data obtained from discs (20 mm by 2 mm) in 50 ml water at 37°C *. Release data is the arithmetic mean of one analysis of each of six specimens. The standard deviation did not exceed 10%.

* Analyses performed in presence of TISAB III buffer to give total fluoride concentration.

LG42 released the greatest amount of fluoride to 42 days, however LG45 eluted the least amount of fluoride up to the same time period. Detection limits of fluoride ion selective electrode were 10 ppm to 100 ppm.

Table 3.9. Fluoride ion release ($\mu\text{mol g}^{-1}$) over time from discs of ionomeric cements from the series varying in silica:alumina and calcium.

Material	Time (d)								
	(SiO ₂ :Al ₂ O ₃ :CaF ₂)1	3	5	7	10	14	21	42	84
LG53 (4.5:3.0:2.0)	4.5	7.9	12.3	14.0	17.5	19.6	25.6	36.0	45.8
LG54 (6.0:4.0:1.0)	1.2	2.7	3.7	4.6	5.8	6.3	8.2	12.2	16.3
LG55 (6.75:4.5:0.5)	0.6	1.6	2.2	2.8	3.4	3.7	4.8	6.5	8.4
LG56 (7.125:4.75:0.25)0.3	0.3	0.7	0.9	1.2	1.4	1.6	2.1	2.8	3.6
LG57 (7.5:5.0:0)	0	< 0.1	< 0.1	< 0.1	< 0.1	< 0.1	< 0.1	< 0.1	< 0.1
LG72 (6.0:4.0:2.0)	3.6	7.0	9.0	11.0	13.0	15.0	18.0	24.0	na
LG73 (7.5:5.0:1.0)	1.7	3.5	4.5	5.7	6.7	7.9	10.1	12.9	na
LG74 (8.25:5.5:0.5)	0.8	1.5	1.9	2.3	2.7	3.2	4.1	5.4	na
LG75 (8.625:5.75:0.25)0.3	0.3	0.7	1.0	1.4	1.6	1.9	2.5	3.3	na

Data obtained from discs (20 mm by 2 mm) in 50 ml water at 37°C *. Release data is the arithmetic mean of one analysis of each of six specimens. The standard deviation did not exceed 10%.

* Analyses performed in presence of TISAB III buffer to give total fluoride concentration.

na-Not applied-reading was not taken as there was no sample

LG53 released the greatest amount of fluoride to 42 days, however LG57 eluted the least amount of fluoride at the same time period. Detection limits of fluoride ion selective electrode were 10 ppm to 100 ppm.

Table 3.10 Fluoride ion release ($\mu\text{mol g}^{-1}$) over time from discs of ionomeric cements from the series varying in silica:alumina ratio based.

Material	Time (d)							
	1	3	5	7	10	14	21	42
SiO₂:Al₂O₃								
LG77 (6.25:3.75)	1.7	3.3	4.7	5.6	6.7	7.5	8.9	11.4
LG78 (6.5:3.5)	1.1	1.9	2.9	3.6	4.4	5.2	6.5	8.9
LG80 (6.7:3.3)	1.5	2.8	4.1	5.3	6.6	7.9	10.0	13.0
LG81 (6.75: 3.25)	1.8	3.0	4.4	5.6	7.1	8.3	10.0	15.0

Data obtained from discs (20 mm by 2 mm) in 50 ml water at 37°C *. Release data is the arithmetic mean of one analysis of each of six specimens. The standard deviation did not exceed 10%.

* Analyses performed in presence of TISAB III buffer to give total fluoride concentration.

LG81 released the greatest amount of fluoride to 42 days, however LG78 eluted the least amount of fluoride at the same time period. Detection limits of fluoride ion selective electrode were 10 ppm to 100 ppm.

Table 3.11 Fluoride ion release ($\mu\text{mol g}^{-1}$) over time from discs of ionomeric cements from the series varying in generic compositions derived from the apatite-stoichiometric based glass LG26.

Material	Time (d)							
	1	3	5	7	10	14	21	42
SiO₂:P₂O₅:CaO								
LG26 (4.5:1.5:3.0)	0.1	5.0	5.2	9.8	na	na	18.4	26.0
LG83 (4.1:1.7:2.8)	2.2	3.9	5.4	6.7	8.4	10.1	12.4	17.2
LG84 (3.7:1.9:2.6)	3.1	6.4	9.4	12.1	15.3	18.1	22.6	28.6
LG85 (3.3:2.1:2.4)	2.6	4.6	6.2	7.4	8.6	9.9	11.8	14.7

Data obtained from discs (20 mm by 2 mm) in 50 ml water at 37°C *. Release data is the arithmetic mean of one analysis of each of six specimens. The standard deviation did not exceed 10%.

* Analyses performed in presence of TISAB III buffer to give total fluoride concentration.

LG84 released the greatest amount of fluoride to 42 days, however LG85 eluted the least amount of fluoride at the same time period. Detection limits of fluoride ion selective electrode were 10 ppm to 100 ppm.

There was a relation between fluoride ion release and phosphorus pentoxide, however the graph was not adequate enough to submit as there was an error with LG84 (1.9P₂O₅) fluoride ion measurements which gave a correlation coefficient of – 0.43 (and linear regression=11.6).

Table 3.12 Fluoride ion release ($\mu\text{mol g}^{-1}$) over time from discs of ionomeric cements from the calcium based series .

Material	Time (d)							
	1	3	5	7	10	14	21	42
CaO:CaF₂								
LG26 (3.0:2.0)	0.3	5.0	5.2	9.8	na	na	18.4	26.0
LG95 (2.8:2.2)	6.4	8.9	12.8	15.9	20.0	24.9	30.6	39.0
LG96 (2.6:2.4)	4.8	9.1	12.2	14.8	18.0	22.2	27.5	35.5
LG97 (2.4: 2.6)	4.9	8.5	11.3	13.3	16.0	19.0	23.5	21.6
LG98 (2.2: 2.8)	5.6	9.8	13.0	15.7	19.4	28.8	29.3	38.3
LG99 (2.0: 3.0)	5.0	9.2	12.6	14.8	17.8	21.3	26.7	35.0

Data obtained from discs (20 mm by 2 mm) in 50 ml water at 37°C *. Release data is the arithmetic mean of one analysis of each of six specimens. The standard deviation did not exceed 10%.

* Analyses performed in presence of TISAB III buffer to give total fluoride concentration.

LG95 released the greatest amount of fluoride to 42 days , however LG97 eluted the least amount of fluoride at the same time period. Detection limits of fluoride ion selective electrode were 10 ppm to 100 ppm.

Table 3.13 Fluoride ion release ($\mu\text{mol g}^{-1}$) over time from discs of ionomeric cements from the LG2 and LG26 in α -MEM .

Material	Time (d)		
	1	5	7
CaF₂			
LG2 (0.75)	0.3	0.7	4.7
LG26 (2.0)	2.7	3.2	6.6

Data obtained from discs (20 mm by 2 mm) in 50 ml water at 37°C *. Release data is the arithmetic mean of one analysis of each of six specimens. The standard deviation did not exceed 10%.

* Analyses performed in presence of TISAB III buffer to give total fluoride concentration.

LG26 released the greatest amount of fluoride to 7 days in α -MEM, however LG2 eluted the least amount of fluoride to the same time period. Detection limits of fluoride ion selective electrode were 10 ppm to 100 ppm.

Table 3. 14 Fluoride ion release ($\mu\text{mol g}^{-1}$) over time from discs of glass ionomeric cements controls .

Material	Time (d)							
	1	3	5	7	10	14	21	42
Chemfil	40.4	73.7	100.0	115.0	135.0	169.0	192.0	273.0
Chemfil Express	8.7	15.0	21.4	25.7	31.3	37.9	46.5	63.4
Water	0	na	0	0	na	na	na	na
α -MEM	0	na	0	0	na	na	na	na

Data obtained from discs (20 mm by 2 mm) in 50 ml water at 37°C *. Release data is the arithmetic mean of one analysis of each of six specimens. The standard deviation did not exceed 10%.

* Analyses performed in presence of TISAB III buffer to give total fluoride concentration.

na-Not applied-reading was not taken as there was no sample.

The commercial IC Chemfil released the greatest amount of fluoride to 42 days, however Chemfil Express eluted less fluoride to the same time period. Detection limits of fluoride ion selective electrode were 10 ppm to 100 ppm.

Table 3. 15 Fluoride ion release ($\mu\text{mol g}^{-1}$) over time from discs of autoclaved ionomeric cements .

Material ($\text{K}_2\text{O}:\text{CaF}_2$)	Time (d)			
	3	7	21	42
LG7 (0.025:0.75)	6.9	11.3	13.2	23.5
LG7 Autoclaved	3.5	5.79	10.6	15.3
LG8 (0.05: 0.75)	na	16.2	30.3	46.6
LG8 Autoclaved	3.4	5.5	9.9	13.6
LG26 (0:2.0)	5.0	9.8	18.4	26.0
LG26 Autoclaved	4.6	8.7	16.1	24.0

Data obtained from discs (20 mm by 2 mm) in 50 ml water at 37°C *. Release data is the arithmetic mean of one analysis of each of six specimens. The standard deviation did not exceed 10%.

* Analyses performed in presence of TISAB III buffer to give total fluoride concentration.

Autoclaved LG26 released the greatest amount of fluoride to 42 days, however autoclaved LG8 eluted the least amount of fluoride to the same time period. Detection limits of fluoride ion selective electrode were 10 ppm to 100 ppm.

Table 3. 16 Fluoride ion release ($\mu\text{mol g}^{-1}$) over time from discs of monovalent cation based series. $1.5 \text{ SiO}_2 \text{ Al}_2 \text{ O}_3 \text{ 0.5 P}_2 \text{ O}_5 \text{ (1.0-Z) CaO 0.75CaF}_2 \text{ ZNa}_2 \text{ O/K}_2 \text{ O}$

Material	Time (d)			
	7	21	42	84
LG2 Z=0	12.5	28.4	44.1	60.9
LG4 Z=0.025	13.8	26.3	38.9	52.0
LG5 Z=0.05	19.7	37.0	52.2	67.8
LG6 Z=0.1	31.0	54.5	72.4	89.6
LG7 Z= 0.025	15.0	26.7	40.0	53.8
LG8 Z=0.05	20.7	35.8	51.1	66.7
LG10 Z=0.0125/0.0125	16.9	28.3	40.7	54.0
LG11 Z=0.05/0.05	19.3	36.1	51.0	66.1

Data obtained from discs (20 mm by 2 mm) in 50 ml water at 37°C. Release data is the arithmetic mean of one analysis of each of six specimens. The standard deviation did not exceed 10%.

LG6 released the greatest amount of free fluoride up to 84 days, however LG4 eluted the least amount of free fluoride to the same time period. Detection limits of fluoride ion selective electrode were 10 ppm to 100 ppm.

Table 3. 17 Fluoride ion release ($\mu\text{mol g}^{-1}$) over time from discs of apatite stoichiometric based series. $(\text{P})\text{SiO}_2 \text{ 1.5P}_2 \text{ O}_5 \text{ (Q)Al}_2 \text{ O}_3 \text{ (S-X)CaO XCaF}_2$

Material	Time (d)			
	3	7	21	42
LG26 X=2.0	4.2	7.4	13.5	20.2
LG27 X=1.0	2.5	4.4	7.7	11.4
LG28 X=0.5	1.3	2.4	4.2	6.5
LG29 X=0.25	0.9	1.7	3.1	4.6
LG30 X=0	0.1	0.5	0.5	0.6

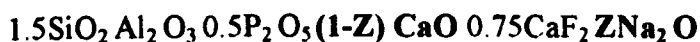
Data obtained from discs (20 mm by 2 mm) in 50 ml water at 37°C. Release data is the arithmetic mean of one analysis of each of six specimens. The standard deviation did not exceed 10%.

LG26 released the greatest amount of free fluoride to 42 days, however LG30 eluted the least amount of free fluoride to the same time period. Detection limits of fluoride ion selective electrode were 10 ppm to 100 ppm.

(b) Sodium by ion selective electrode

A sodium ion selective electrode was used to measure the concentration of ions released from set discs of IC (see section 2.2.1). Sodium release data from all the formulations examined is summarized in Tables 3.18 to 3.19 on the following pages. Particular results of interest of sodium ion release are added as footnotes in Tables 3.18 and 3.19.

Table 3. 18 Sodium ion release ($\mu\text{mol g}^{-1}$) over time from discs of ionomeric cements of the monovalent cation series .



Material	Time (d)			
	7	21	42	84
LG2 Z=0	3.1	4.9	5.1	5.1
LG4 Z=0.025Na	7.5	16.0	20.8	22.9
LG5 Z=0.05Na	9.1	9.1	25.5	28.8
LG6 Z=0.1Na	9.2	23.1	40.2	51.2
LG7 Z=0.025K	4.0	5.2	5.8	5.9
LG8 Z=0.05K	3.4	5.3	5.7	5.8
LG10 Z=0.0125Na/K	7.6	12.3	14.2	15.0
LG11 Z=0.05Na/K	8.0	14.0	17.7	19.2

Data obtained from discs (20 mm by 2 mm) in 50 ml water at 37°C *. Release data is the arithmetic mean of one analysis of each of six specimens. The standard deviation did not exceed 10%.

* Analyses performed in presence of sodium ionic strength adjustor (ISA) buffer to keep a constant background ionic strength and adjust pH.

LG6 released the greatest amount of sodium up to 84 days, however LG2 eluted the least amount of sodium up to the same time period. Detection limits of sodium ion selective electrode were 10 ppm to 100 ppm.

There was a positive relation between sodium glass content and sodium ion release as can be shown in Figure 3.6, with a correlation coefficient of 0.99 and linear regression of 543.4. This indicates that sodium ion release was dependent on sodium glass content.

Figure 3.6 Relation between Sodium glass content and Sodium ion release at 84 days. Linear regression, $y=543.4x+5$. Correlation coefficient=0.99 (n=6)

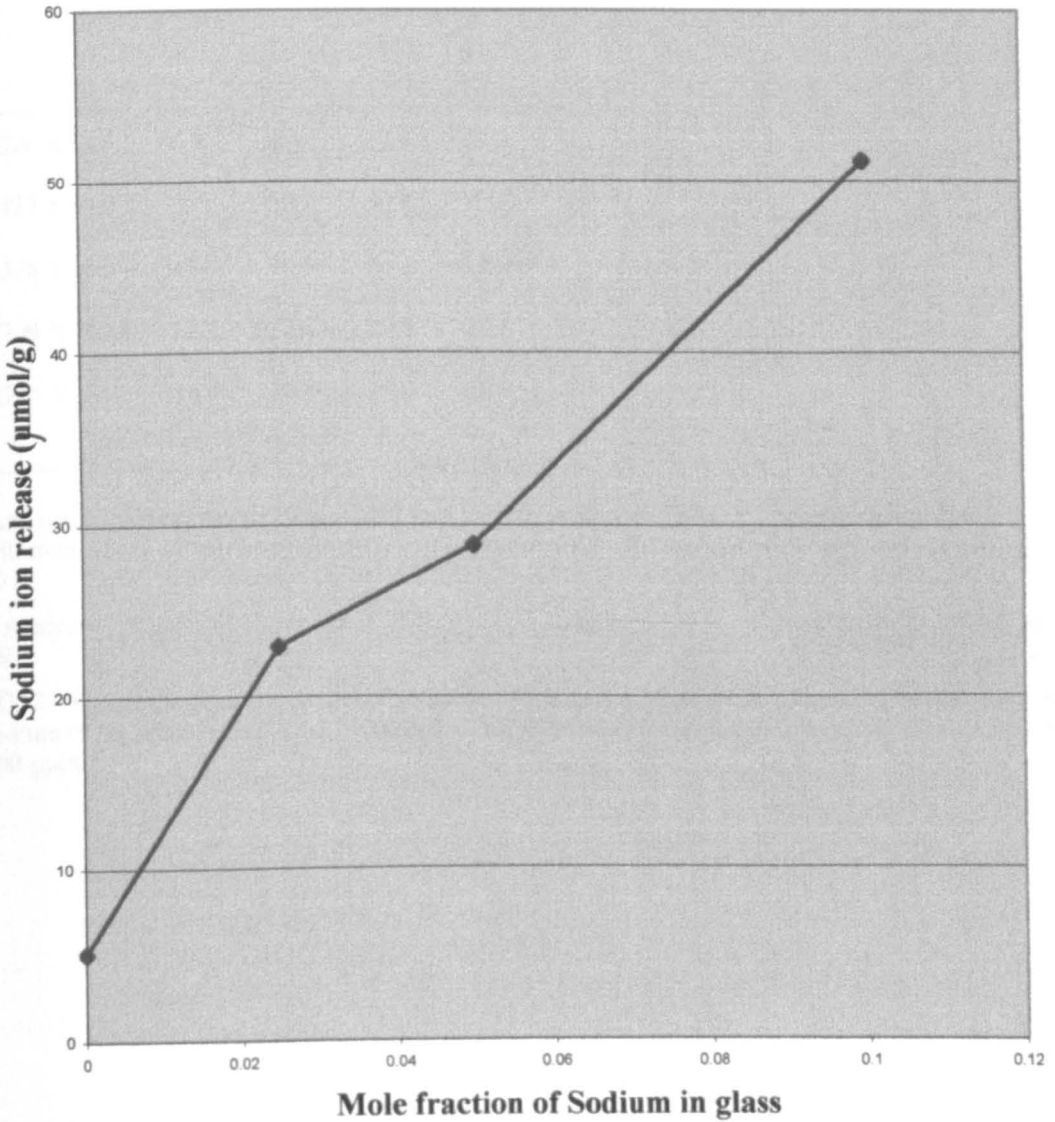


Table 3. 19 Sodium ion release ($\mu\text{mol g}^{-1}$) over time from discs of ionomeric cements of the apatite stoichiometric based series . $(\text{P})\text{SiO}_2$ $1.5\text{P}_2\text{O}_5$ $(\text{Q})\text{Al}_2\text{O}_3$ **(5-X) CaO XCaF_2**

Material	Time (d)			
	3	7	21	42
LG26 X=2.0	6.4	9.3	14.4	17.3
LG27 X=1.0	35.6	36.8	40.6	43.6
LG28 X=0.5	19.8	20.5	24.5	27.9
LG29 X=0.25	35.2	37.4	39.5	41.8
LG30 X=0	16.9	18.6	25.0	25.7

Data obtained from discs (20 mm by 2 mm) in 50 ml water at 37°C *. Release data is the arithmetic mean of one analysis of each of six specimens. The standard deviation did not exceed 10%.

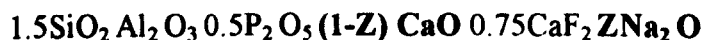
* Analyses performed in presence of ISA to keep a constant background ionic strength and adjust pH.

LG27 released the greatest amount of sodium to 42 days, however LG26 eluted the least amount of sodium to the same time period. Detection limits of sodium ion selective electrode were 10 ppm to 100 ppm.

(c) Potassium by atomic absorption spectroscopy

Atomic absorption spectroscopy was used to measure the concentration of ions released from set discs of IC (see section 2.2.2). Potassium release data from all the formulations examined is summarized in Tables 3.20 to 3.21 on the following pages. Particular areas of interest of potassium ion release results are added as footnotes in Tables 3.20 and 3.21.

Table 3. 20 Potassium ion release ($\mu\text{mol g}^{-1}$) over time from discs of ionomeric cements of the monovalent cation series .



Material	Time (d)			
	7	21	42	84
LG2 Z=0	0.3	0.6	0.7	0.7
LG4 Z=0.025Na	0.1	0.2	0.3	0.4
LG5 Z=0.05Na	0.1	0.2	0.3	0.3
LG6 Z=0.1Na	0.1	0.1	0.2	0.3
LG7 Z=0.025K	5.2	8.5	11.7	14.0
LG8 Z=0.05K	7.1	13.9	19.9	24.6
LG10 Z=0.0125Na/K2.6	4.5	5.7	6.6	

Data obtained from discs (20 mm by 2 mm) in 50 ml water at 37°C . Release data is the arithmetic mean of one analysis of each of six specimens. The standard deviation did not exceed 10%. LG8 released the greatest amount of potassium to 84 days, however LG6 and LG5 eluted the least amount of potassium to the same time period. Detection limits of potassium ion selective electrode were 1 ppm to 10 ppm.

Table 3. 21 Potassium ion release ($\mu\text{mol g}^{-1}$) over time from discs of ionomeric cements of the apatite stoichiometric based series . (P)SiO₂ 1.5P₂ O₅ (Q)Al₂ O₃ (S-X) CaO XCaF₂

Material	Time (d)			
	7	21	42	84
LG26 X=2.0	1.0	1.7	2.3	2.8
LG27 X=1.0	1.2	1.8	2.4	2.8
LG28 X= 0.5	1.2	1.6	1.9	2.1
LG29 X= 0.25	1.6	2.2	2.6	3.0
LG30 X=0	1.6	2.1	2.4	2.7

Data obtained from discs (20 mm by 2 mm) in 50 ml water at 37°C . Release data is the arithmetic mean of one analysis of each of six specimens. The standard deviation did not exceed 10%. LG29 released the greatest amount of potassium to 84 days, however LG28 eluted the least amount of

potassium to the same time period. Detection limits of sodium ion selective electrode were 1 ppm to 10 ppm.

(d) Aluminium by atomic absorption spectroscopy

Atomic absorption spectroscopy was used to measure the concentration of ions released from set discs of IC (see section 2.2.2). Aluminium release data from all the formulations examined is summarized in Tables 3.22 to 3.27 on the following pages. Particular areas of interest are added as footnotes where appropriate.

Table 3. 22 Aluminium ion release (nmol g^{-1}) over time from discs of ionomeric cements of the monovalent cation series (Na^+ and K^+).

$1.5\text{SiO}_2 \text{ Al}_2\text{O}_3 \text{ 0.5P}_2\text{O}_5 \text{ (1-Z) CaO 0.75CaF}_2 \text{ ZNa}_2\text{O}$

Material	Time (d)							
	1	3	5	7	10	14	21	42
LG2 Z=0	na	na	na	0	na	na	0.2	0.4
LG3 Z=0	<0.1	<0.1	<0.1	<0.1	0.1	0.1	0.1	0.2
LG4 Z=0.025Na	na	na	na	<0.1	na	na	0.3	0.3
LG5=0.05Na	na	na	na	0.2	na	na	0.1	0.5
LG6=0.1Na	na	na	na	<0.1	na	na	0.1	0.3
LG7=0.025K	na	na	na	<0.1	na	na	0.3	0.3
LG8=0.05K	na	na	na	0.1	na	na	0.1	0.5
LG10=0.0125Na/K	na	na	na	0	na	na	0.1	0.2
LG11=0.05Na/K	na	na	na	0.1	na	na	0.2	0.5
LG23=0.15Na	<0.1	<0.1	0.1	0.1	0.3	0.3	0.4	0.6
LG63=0.2Na	<0.1	<0.1	0.2	0.2	0.4	0.5	0.6	0.9
LG65=0.1Na	<0.1	<0.1	<0.1	<0.1	0.1	0.2	0.2	0.3
LG66=0.2Na	<0.1	<0.1	0.2	0.2	0.2	0.3	0.3	0.4
LG67=0.3Na	<0.1	0.1	0.2	0.3	0.4	0.5	0.5	0.9
LG68=0.4Na	<0.1	0.2	0.4	0.6	0.7	0.9	1.2	1.5
LG69=0.5Na	0.1	0.3	0.6	0.9	1.4	1.6	2.1	2.6
LG70=0.45Na	0.1	0.2	0.5	0.8	1.2	1.4	1.8	2.3

Data obtained from discs (20 mm by 2 mm) in 50 ml water at 37°C . Release data is the arithmetic mean of one analysis of each of six specimens. The standard deviation did not exceed 10%.

na-Not applied-reading was not taken as there was no sample

LG69 released the greatest amount of aluminium to 42 days, however LG22 eluted the least amount of aluminium to the same time period < 0.1 nmol g^{-1} . Detection limits of the AAS for aluminium were 0.1 ppm to 1 ppm.

Figure 3.7 to Figure 3.9 illustrate aluminium ion release and its positive relation with sodium and potassium solubilising ions from monovalent cation glasses at various time lengths. Figure 3.7 shows a positive relation of aluminium ion release and sodium glass content with a correlation coefficient of 0.97 (n=6). Figure 3.8 shows a positive relation between aluminium ion release and sodium glass content with a correlation coefficient of 0.96 (n=6). Figure 3.9 shows a positive relation between aluminium ion release and potassium glass content with a correlation coefficient =0.87 (n=6). Figure 3.10 shows an increase in aluminium ion release of LG26 up to a period of 42 days showing a relation between aluminium ion release and time as it has a correlation coefficient of 0.82.

LG26 released the greatest amount of aluminium to 42 days with 0.2 nmol g^{-1} . LG28, LG29, and LG30 eluted the least amount of aluminium at the same time period i.e. $< 0.1 \text{ nmol g}^{-1}$. Detection limits of the AAS for aluminium were 0.1 ppm to 1 ppm. Data was obtained from discs (20 mm by 2 mm) in 50 ml water at 37°C . Release data is the arithmetic mean of one analysis of each of six specimens. The standard deviation did not exceed 10%.

LG42 of the series varying in calcium fluoride released the greatest amount of aluminium to 42 days i.e. 0.3 nmol g^{-1} . However, LG44 and LG45 eluted the least amount of aluminium to the same time period i.e. $< 0.1 \text{ nmol g}^{-1}$. Detection limits of the AAS for aluminium were 0.1 ppm to 1 ppm. Data was obtained from discs (20 mm by 2 mm) in 50 ml water at 37°C . Release data is the arithmetic mean of one analysis of each of six specimens. The standard deviation did not exceed 10%.

Figure 3.7 Relation between Aluminium ion release and Sodium glass composition at 7 days. Linear regression, $y=0.67x+0$. Correlation coefficient=0.97 (n=6)

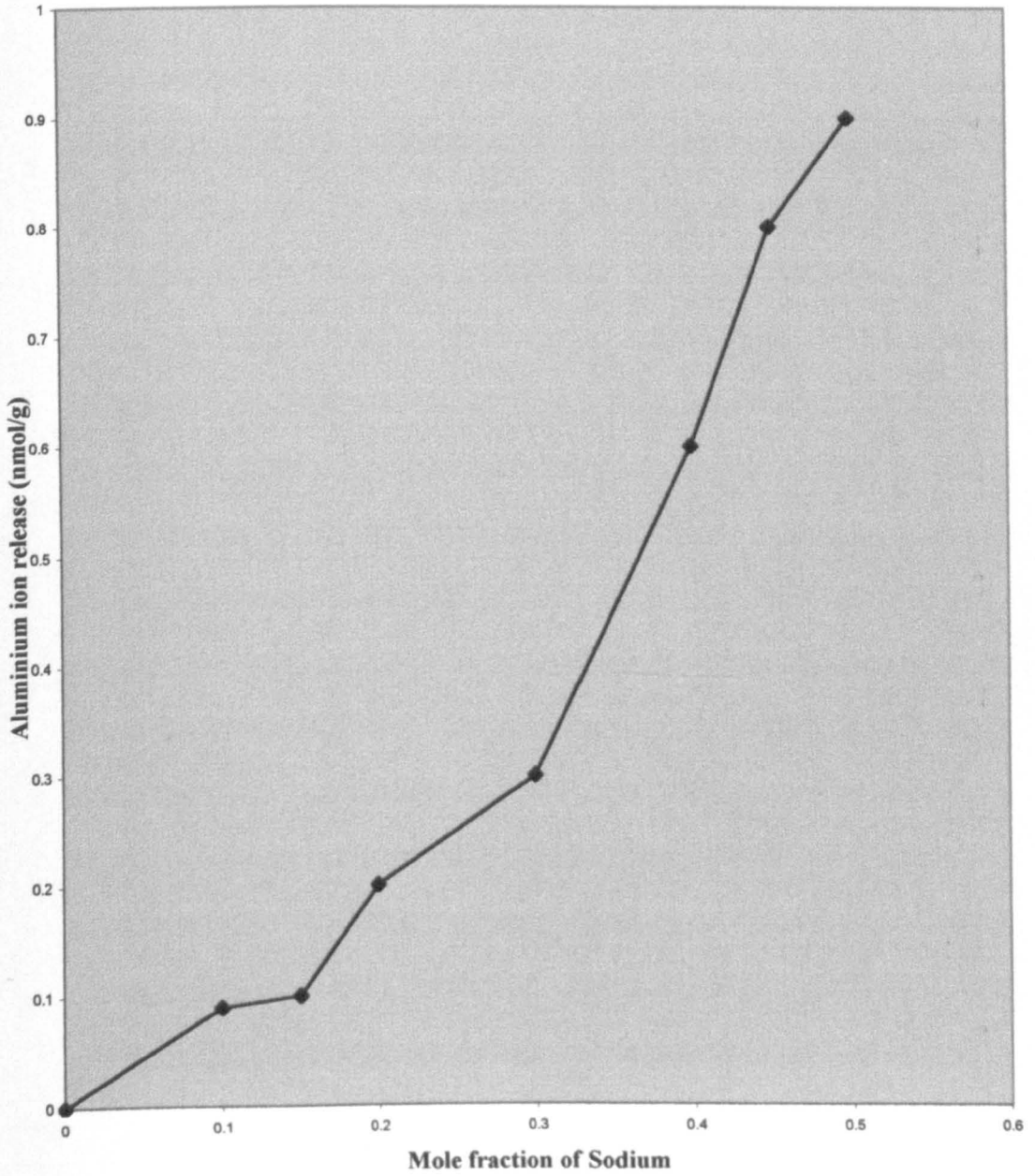


Figure 3.8 Relation between Aluminium ion release and Sodium glass composition at 21 days. Linear regression, $y=3.89x+0.22$. Correlation coefficient=0.96 (n=6)

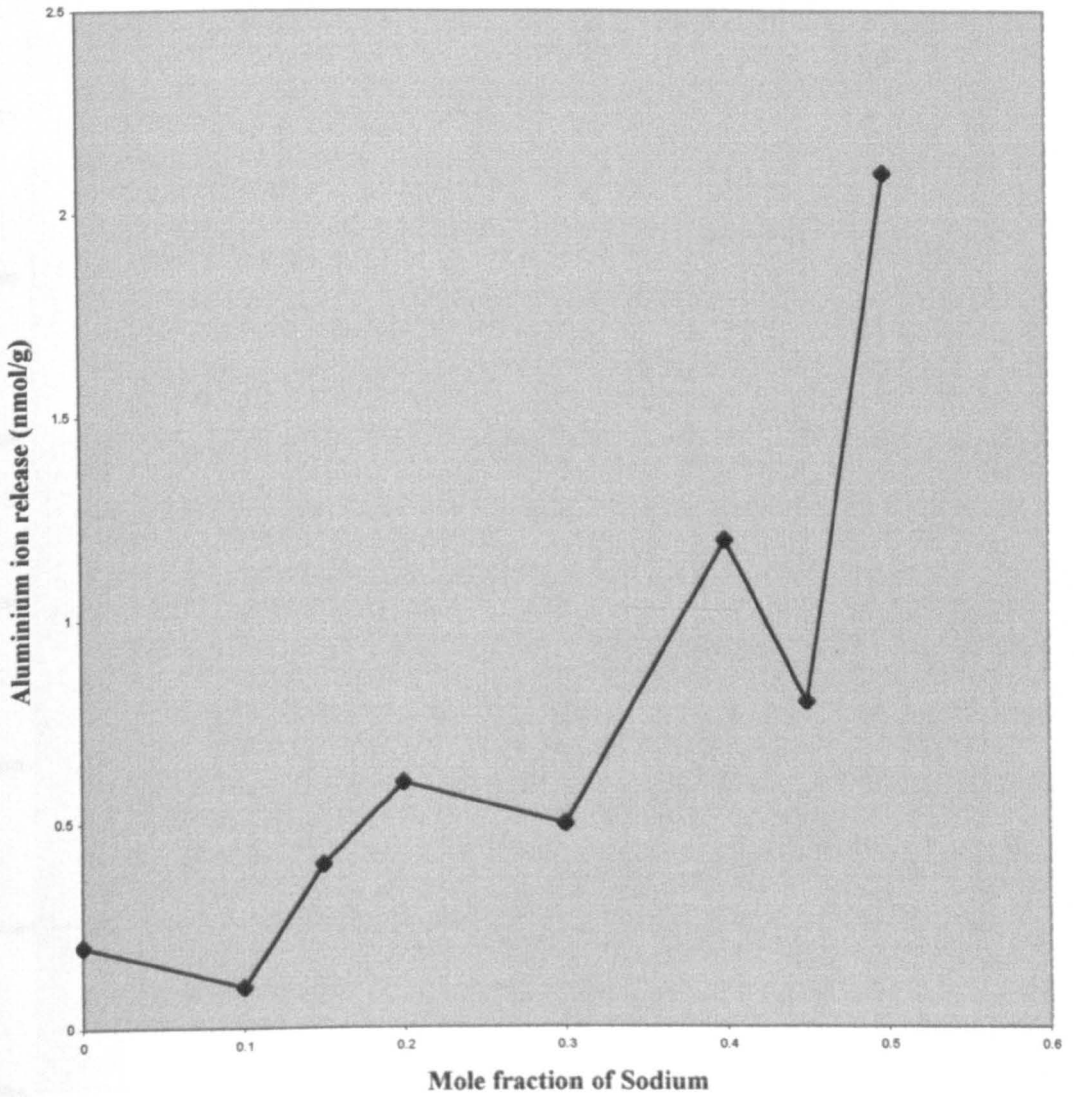


Figure 3.9 Relation between Aluminium ion release and Potassium glass composition at day7. Linear regression, $y=2.32x+0.09$. Correlation coefficient= 0.87 (n=6).

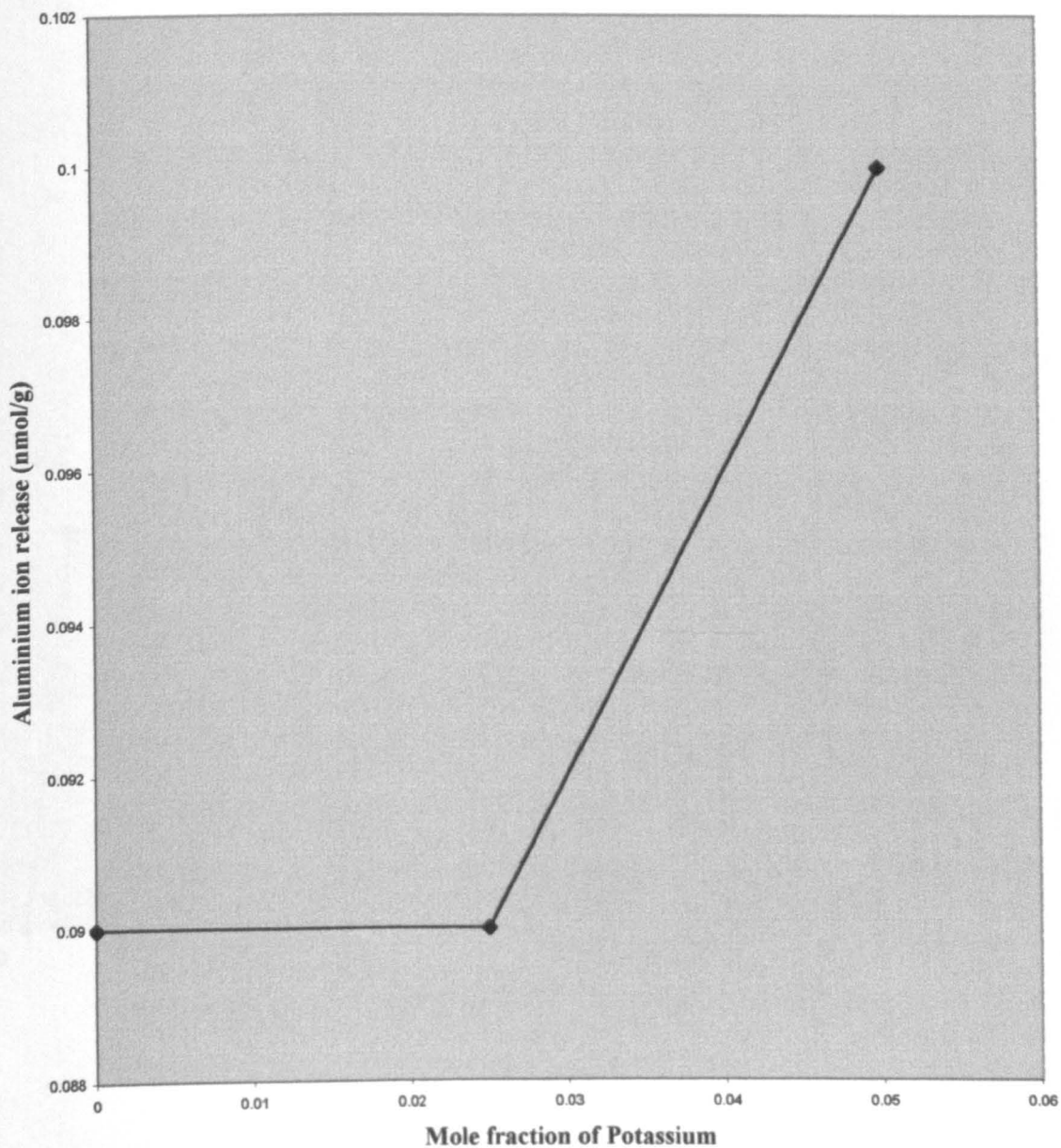


Figure 3.10 Aluminium ion release of LG26 up to a period of 42 days. Linear regression, $y=0.032x-0.05$. Correlation coefficient=0.82 (n=6)

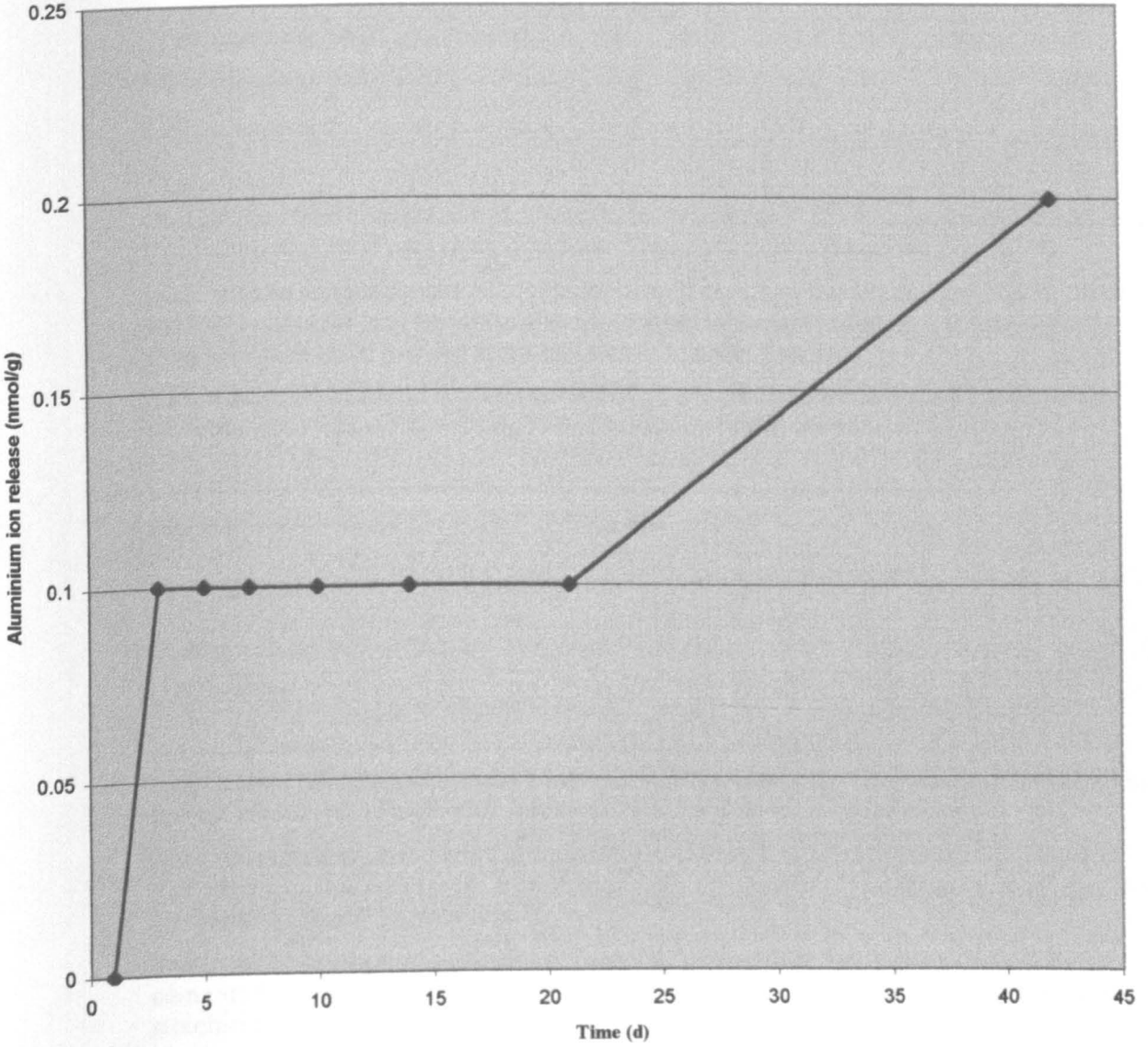


Table 3.23 Aluminium ion release (nmol g^{-1}) over time from discs of ionomeric cements from the series varying in silica:alumina and calcium .

Material	Time (d)							
		3	5	7	10	14	21	42
$(\text{SiO}_2:\text{Al}_2\text{O}_3:\text{CaF}_2)1$								
LG53 (4.5:3.0:2.0)	<0.1	<0.1	<0.1	0.2	0.2	0.2	0.3	0.4
LG54 (6.0:4.0:1.0)	<0.1	<0.1	<0.1	<0.1	<0.1	<0.1	0.1	0.2
LG72 (6.0:4.0:2.0)	0	<0.1	<0.1	<0.1	0.1	0.2	0.2	0.3

Data obtained from discs (20 mm by 2 mm) in 50 ml water at 37°C . Release data is the arithmetic mean of one analysis of each of six specimens. The standard deviation did not exceed 10%.

LG53 released the greatest amount of aluminium to 42 days, however LG55, LG56, LG57, LG74 and LG75 eluted the least amount of aluminium to the same time period i.e. $<0.1 \text{ nmol g}^{-1}$. Detection limits of the AAS for aluminium were 0.1 ppm to 1 ppm.

Table 3.24 Aluminium ion release (nmol g^{-1}) over time from discs of ionomeric cements from the series varying in silica:alumina ratio based .

Material	Time (d)							
	$\text{SiO}_2:\text{Al}_2\text{O}_3,1$	3	5	7	10	14	21	42
LG80 (6.7:3.3)	0.2	0.3	0.3	0.3	0.3	0.4	0.4	0.4
LG81 (6.75:3.25)	0.1	0.2	0.2	0.2	0.2	0.2	0.3	0.3

Data obtained from discs (20 mm by 2 mm) in 50 ml water at 37°C . Release data is the arithmetic mean of one analysis of each of six specimens. The standard deviation did not exceed 10%.

LG80 released the greatest amount of aluminium to 42 days, however LG77 and LG78 eluted the least amount of aluminium to the same time period i.e $<0.1 \text{ nmol g}^{-1}$. Detection limits of the AAS for aluminium were 0.1 ppm to 1 ppm.

Table 3.25 Aluminium ion release (nmol g^{-1}) over time from discs of ionomeric cements from the series varying in generic compositions derived from the apatite-stoichiometric based glass LG26.

Material	Time (d)							
	$\text{SiO}_2:\text{P}_2\text{O}_5:\text{CaO}$ 1	3	5	7	10	14	21	42
LG26 (4.5:1.5:3.0)0		0.1	0.1	0.1	0.1	0.1	0.1	0.2
LG83 (4.1:1.7:2.8)<0.1	<0.1	<0.1	0.1	0.1	0.1	0.2	0.2	0.3
LG84 (3.7:1.9:2.6)0.1	0.1	0.2	0.2	0.3	0.3	0.4	0.4	0.5
LG85 (3.3:2.1:2.4)0.2	0.2	0.3	0.3	0.3	0.4	0.4	0.4	0.4

Data obtained from discs (20 mm by 2 mm) in 50 ml water at 37°C . Release data is the arithmetic mean of one analysis of each of six specimens. The standard deviation did not exceed 10%.

LG84 released the greatest amount of aluminium to 42 days, however LG83 eluted the least amount of aluminium to the same time period. Detection limits of the AAS for aluminium were 0.1 ppm to 1 ppm.

There was a positive relation between aluminium ion release and phosphate glass content. For example a phosphate mole fraction of 2.1 gave a high amount of aluminium ion release i.e. 0.2 nmol/g. However, a phosphate mole fraction of 1.5 gave an aluminium ion release of 0 nmol/g. Graphs were not included for this observation as a wider range of phosphate glass concentrations were required for adequate plots.

Table 3.26 Aluminium ion release (nmol g⁻¹) over time from discs of ionomeric cements from the calcium based series

Material	Time (d)							
	CaO:CaF ₂ 1	3	5	7	10	14	21	42
LG95 (2.8:2.2)	0.1	0.2	0.3	0.3	0.4	0.5	0.6	0.7
LG96 (2.6:2.4)	0.1	0.2	0.3	0.3	0.4	0.5	0.5	0.7
LG97 (2.4:2.6)	<0.1	0.1	0.2	0.3	0.3	0.4	0.4	0.6
LG98 (2.2:2.8)	<0.1	0.2	0.2	0.3	0.3	0.4	0.5	0.7
LG99 (2.0:3.0)	0.1	0.2	0.3	0.3	0.4	0.4	0.5	0.7

Data obtained from discs (20 mm by 2 mm) in 50 ml water at 37°C . Release data is the arithmetic mean of one analysis of each of six specimens. The standard deviation did not exceed 10%.

LG95 released the greatest amount of aluminium to 42 days, however LG97 eluted the least amount of aluminium to the same time period. Detection limits of the AAS for aluminium were 0.1 ppm to 1 ppm.

Table 3. 27 Aluminium ion release (nmol g^{-1}) over time from discs of glass ionomeric cements controls .

Material	Time (d)							
	1	3	5	7	10	14	21	42
Chemfil	0.5	0.7	1.1	1.3	1.7	1.9	2.3	2.9
Chemfil Express	0.1	0.3	0.4	0.5	0.6	0.7	0.8	0.9

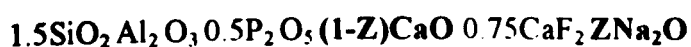
Data obtained from discs (20 mm by 2 mm) in 50 ml water at 37°C . Release data is the arithmetic mean of one analysis of each of six specimens. The standard deviation did not exceed 10%.

Chemfil released more aluminium to 42 days than Chemfil Express to the same time period. Detection limits of the AAS for aluminium were 0.1 ppm to 1 ppm.

(e) Silicon by atomic absorption spectroscopy

Atomic absorption spectroscopy was used to measure the concentration of ions released from set discs of IC (section 2.2.2). Silicon release data from all the formulations examined is summarized in Tables 3.28 to 3.35 on the following pages. Particular results of interest are added as footnotes where appropriate.

Table 3. 28 Silicon release ($\mu\text{mol g}^{-1}$) over time from discs of ionomeric cements of the monovalent cation series (Na^+ and K^+).



Material	Time (d)								
	1	3	5	7	10	14	21	42	84
LG3 Z=0	4.7	10.1	14.7	17.9	21.7	26.3	33.3	55.9	na
LG4 Z=0.025Na	na	na	na	46.8	na	na	68.0	108.7	156.2
LG5 Z=0.05Na	na	na	na	80.6	na	na	122.0	173.1	194.2
LG6 Z=0.1Na	na	na	na	78.2	na	na	119.0	149.6	208.4
LG7 Z= 0.025K	na	na	na	51.3	na	na	76.0	108.0	128.8
LG8 Z= 0.05K	na	na	na	58.8	na	na	na	na	na
LG10 Z=0.0125Na/K	na	na	na	55.4	na	na	na	na	na
LG11Z=0.05Na/K	na	na	na	3.3	na	na	48.0	84.1	102.4
LG22 Z=0.05K	3.4	7.5	11.8	13.5	18.9	26.8	30.5	42.7	na
LG23 Z=0.15Na	4.9	9.6	15.4	16.5	24.8	32.5	40.4	53.2	na
LG63 Z=0.2Na	7.1	14.0	19.0	23.0	31.0	38.8	47.8	65.8	na
LG65 Z=0.1Na	5.3	11.6	16.3	20.0	24.0	28.2	36.0	60.8	na
LG66 Z=0.2Na	5.2	10.2	15.3	19.0	23.1	28.1	35.5	59.1	na

LG67 Z=0.3Na	4.6	9.3	14.2	17.8	22.0	27.4	35.2	58.6	na
LG68 Z= 0.4Na	4.6	8.3	15.0	18.9	22.7	28.4	35.7	50.6	na
LG69 Z=0.5Na	7.8	15.6	24.0	30.7	39.1	48.4	60.7	98.2	na
LG70 Z=0.45Na	6.4	12.8	19.6	25.3	31.2	38.6	49.9	85.3	na

Data obtained from discs (20 mm by 2 mm) in 50 ml water at 37°C . Release data is the arithmetic mean of one analysis of each of six specimens. The standard deviation did not exceed 10%.

na-Not applied- reading not taken as there was no sample.

LG5 released the least amount of measured silicon to 42 days, however LG22 eluted the least silicon to the same time period. Detection limits of the AAS for silicon were 100 ppm to 500 ppm.

Figure 3.11 (next page) shows that there was no relation between measured silicon release and sodium glass content ions from the glass of the monovalent cation series at 42 days. There was a drop in measured silicon release after 0.1 mole fraction of sodium (see Figure 3.9) thereafter there was no pattern emerging from the data.

Measured silicon ion release and sodium glass content ions from monovalent cation series of ICs had a correlation coefficient of -0.3 . However, there may be a positive relation between release and potassium ions from LG7, LG8 and LG22 glass composition however a wider range of potassium based glasses were required to confirm this and to obtain an adequate plot.

Figure 3.11 Relation between measured Silicon release and Sodium glass composition at day 42. Linear regression, $y=222.0x+49$. Correlation coefficient=-0.3 (n=6).

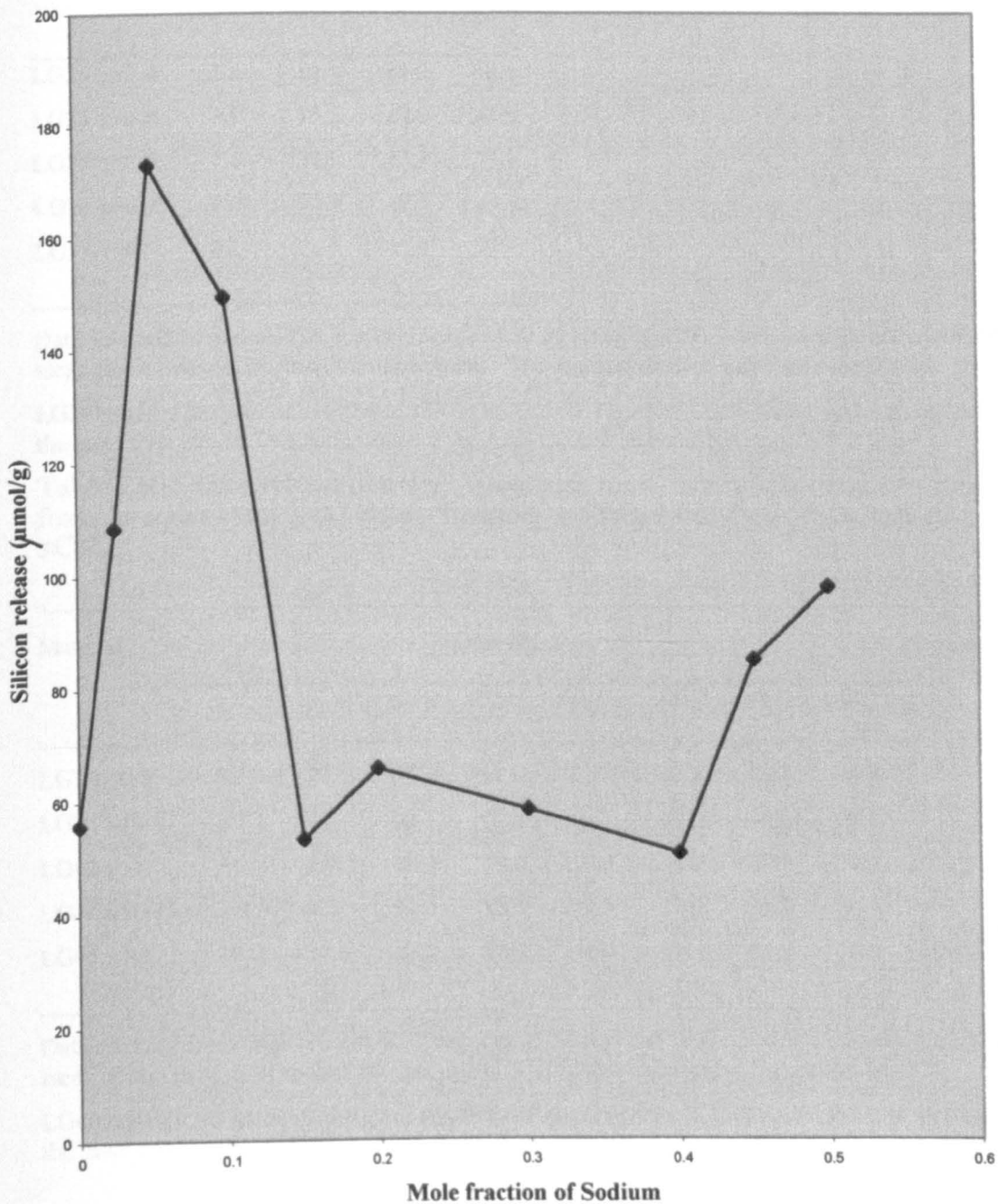


Table 3.29 Silicon release ($\mu\text{mol g}^{-1}$) over time from discs of ionomeric cements from the apatite stoichiometric series ($\text{Ca:P} \sim 1.66$). $(\text{P})\text{SiO}_2$ 1.5 P_2O_5 (Q) Al_2O_3 (5-x) CaO x CaF_2

Material	Time (d)			
	1	7	21	42
LG26 x=2.0	2.3	10.6	23.6	50.1
LG27 x=1.0	6.3	15.2	29.6	52.5
LG28 x=0.5	7.1	18.9	42.3	70.1
LG29 x=0.25	8.6	24.3	47.3	86.5
LG30 x=0	8.2	21.6	45.4	77.0

Data obtained from discs (20 mm by 2 mm) in 50 ml water at 37°C. Release data is the arithmetic mean of one analysis of each of six specimens. The standard deviation did not exceed 10%.

LG29 released the greatest amount of silicon to 42 days, however LG26 eluted the least amount to the same time period. Detection limits of the AAS for silicon were 100 ppm to 500 ppm.

Table 3.30 Silicon release ($\mu\text{mol g}^{-1}$) over time from discs of ionomeric cements from the series varying in calcium fluoride. 1.5 SiO_2 1.0 Al_2O_3 0.5 P_2O_5 1.0 CaO x CaF_2

Material	Time (d)							
	1	3	5	7	10	14	21	42
LG3 x=0.5	4.7	10.1	14.7	17.9	21.7	26.3	33.3	55.9
LG26 x=0.67	2.3	na	na	10.6	na	na	23.6	50.1
LG42 x=1.0	3.4	7.0	10.0	11.8	16.9	21.0	25.2	35.3
LG44 x=0.25	3.9	8.2	11.5	13.7	19.5	27.0	34.7	50.8
LG45 x=0	10.0	17.0	22.2	27.7	51.9	51.9	58.0	76.9

Data obtained from discs (20 mm by 2 mm) in 50 ml water at 37°C. Release data is the arithmetic mean of one analysis of each of six specimens. The standard deviation did not exceed 10%.

LG45 released the greatest amount of silicon to 42 days, however LG42 eluted the least amount to the same time period. Detection limits of the AAS for silicon were 100 ppm to 500 ppm.

Table 3.31 Silicon release ($\mu\text{mol g}^{-1}$) over time from discs of ionomeric cements from the series varying in silica:alumina and calcium .

Material ($\text{SiO}_2:\text{Al}_2\text{O}_3:\text{CaF}_2$)1	Time (d)							
	3	5	7	10	14	21	42	
LG53 (4.5:3.0:2.0)	5.0	10.0	14.7	17.2	21.9	25.7	30.6	41.3
LG54 (6.0:4.0:1.0)	4.5	9.1	13.8	17.2	21.4	25.2	30.5	41.8
LG55 (6.75:4.5:0.5)	5.8	11.9	17.7	21.2	25.8	27.3	36.8	49.9
LG56 (7.125:4.75:0.25)	20.5	43.5	63.0	79.6	92.4	111.7	132.1	179.0
LG57 (7.5:5.0:0)	5.6	11.9	17.7	21.8	26.1	30.9	37.1	46.5
LG72 (6.0:4.0:2.0)	7.6	14.7	21.5	26.9	32.0	37.3	44.2	55.4
LG73 (7.5:5.0:1.0)	8.3	16.2	24.3	39.9	37.7	43.7	52.7	64.1
LG74 (8.25:5.5:0.5)	8.2	15.2	23.2	28.9	36.6	42.9	50.0	78.6
LG75 (8.625:5.75:0.25)	9.6	18.0	27.7	33.8	42.4	49.8	59.4	78.6

Data obtained from discs (20 mm by 2 mm) in 50 ml water at 37°C . Release data is the arithmetic mean of one analysis of each of six specimens. The standard deviation did not exceed 10%.

LG56 releases the greatest amount of silicon to 42 days, however LG53 elutes the least amount of silicon to the same time period. Detection limits of the AAS for silicon were 100 ppm to 500 ppm.

Table 3.32 Silicon release ($\mu\text{mol g}^{-1}$) over time from discs of ionomeric cements from the series varying in silica:alumina ratio based .

Material $\text{SiO}_2:\text{Al}_2\text{O}_3$ 1	Time (d)							
	3	5	7	10	14	21	42	
LG77 (6.25:3.75)	3.4	7.4	11.2	14.0	17.1	20.4	25.3	40.9
LG78 (6.5:3.5)	3.6	9.3	13.7	17.3	22.1	25.9	31.6	50.6
LG80 (6.7:3.3)	5.1	11.8	17.7	21.4	27.9	34.4	42.8	79.1
LG81 (6.75:3.25)	6.5	9.5	12.3	15.0	18.3	25.5	36.5	66.9

Data obtained from discs (20 mm by 2 mm) in 50 ml water at 37°C . Release data is the arithmetic mean of one analysis of each of six specimens. The standard deviation did not exceed 10%.

LG80 releases the greatest amount of silicon to 42 days, however LG77 elutes the least amount of silicon. Detection limits of the AAS for silicon were 100 ppm to 500 ppm.

Figure 3.12 Relation between Phosphorus pentoxide glass composition and Silicon release at 42 days. Linear regression, $y=28.8x+46.5$. Correlation coefficient=0.96 (n=6)

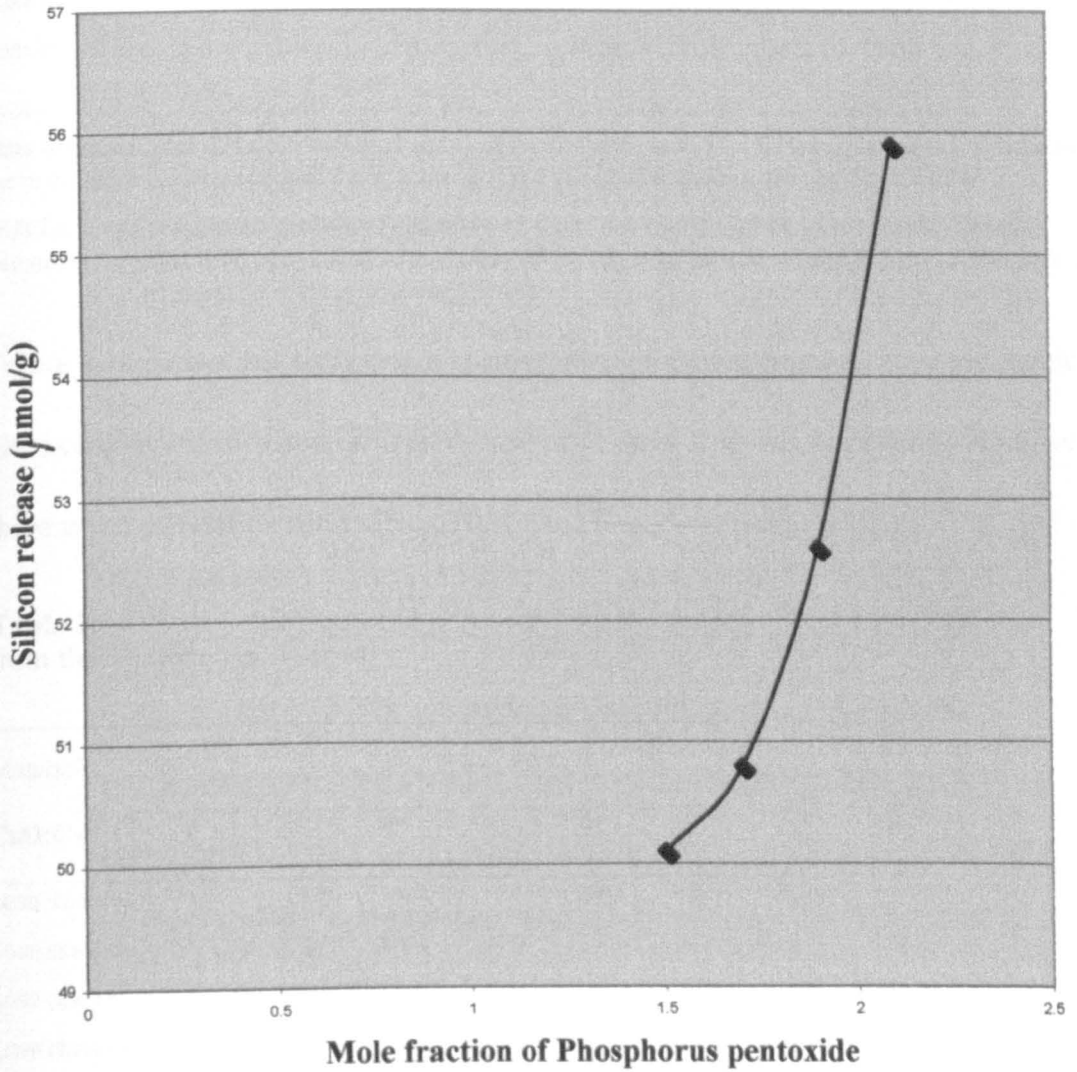


Table 3.33 Silicon release ($\mu\text{mol g}^{-1}$) over time from discs of ionomeric cements from the series varying in generic compositions derived from the apatite-stoichiometric based glass LG26.

Material	Time (d)							
	1	3	5	7	10	14	21	42
SiO₂:P₂O₅:CaO								
LG26 (4.5:1.5:3.0)	2.3	na	na	na	na	na	23.6	50.1
LG83 (4.1:1.7:2.8)	2.9	9.2	14.5	15.7	21.4	29.3	35.4	50.8
LG84 (3.7:1.9:2.6)	6.3	10.8	14.6	18.2	1.5	28.1	37.9	52.6
LG85 (3.3:2.1:2.4)	5.8	11.9	15.5	21.6	24.9	29.7	36.1	55.9

Data obtained from discs (20 mm by 2 mm) in 50 ml water at 37°C. Release data is the arithmetic mean of one analysis of each of six specimens. The standard deviation did not exceed 10%.

LG85 releases the greatest amount of silicon to 42 days, however LG83 elutes the least amount of silicon to the same time period. Detection limits of the AAS for silicon were 100 ppm to 500 ppm.

Figure 3.12 shows that there was a positive relation between phosphorus pentoxide glass content and measured silicon release at 42 days, that was detected by AAS, as there was a correlation coefficient of 0.96 (and linear regression =28.8).

Table 3.34 Silicon release ($\mu\text{mol g}^{-1}$) over time from discs of ionomeric cements from the calcium based series.

Material	Time (d)							
	1	3	5	7	10	14	21	42
CaO:CaF₂								
LG95 (2.8:2.2)	4.5	10.0	18.1	23.0	29.8	35.9	43.3	52.3
LG96 (2.6:2.4)	5.1	10.5	18.3	23.0	27.9	34.0	41.3	52.5
LG97 (2.4:2.6)	4.1	8.7	12.6	16.8	21.7	27.3	35.7	47.5
LG98 (2.2:2.8)	5.4	10.7	16.2	20.8	26.6	32.9	42.8	54.7
LG99 (2.0:3.0)	4.6	8.7	14.0	18.1	23.2	29.6	39.2	50.8

Data obtained from discs (20 mm by 2 mm) in 50 ml water at 37°C. Release data is the arithmetic mean of one analysis of each of six specimens. The standard deviation did not exceed 10%.

LG95 releases the greatest amount of silicon to 42 days, however LG97 elutes the least amount of silicon to the same time period. Detection limits of the AAS for silicon were 100 ppm to 500 ppm.

Table 3. 35 Silicon release ($\mu\text{mol g}^{-1}$) over time from discs of glass ionomeric cements controls .

Material	Time (d)							
	1	3	5	7	10	14	21	42
Chemfil	3.6	7.7	11.0	11.6	16.2	21.6	25.3	36.0
Chemfil Express	3.5	6.1	8.6	10.6	11.8	14.8	20.6	27.2

Data obtained from discs (20 mm by 2 mm) in 50 ml water at 37°C . Release data is the arithmetic mean of one analysis of each of six specimens. The standard deviation did not exceed 10%.

Chemfil released more silicon to 42 days than Chemfil Express. Detection limits of the AAS for silicon were 100 ppm to 500 ppm.

From these tables of results it may be shown that there is a relation between the sodium, potassium and phosphorus pentoxide glass content increase and measured silicon release.

(f) Calcium by atomic absorption spectroscopy

Atomic absorption spectroscopy was used to measure the concentration of ions released from set discs of IC (section 2.2.2). Calcium release data from all the formulations examined is summarized in Tables 3.36 to 3.42 on the following pages. Particular results of interest are added as footnotes where appropriate.

Table 3. 36 Calcium ion release ($\mu\text{mol g}^{-1}$) over time from discs of ionomeric cements of the monovalent cation series (Na^+ and K^+).

1.5SiO₂ Al₂ O₃ 0.5P₂ O₅ (1-Z)CaO 0.75CaF₂ ZNa₂O

Material	Time (d)								
	1	3	5	7	10	14	21	42	84
LG3 Z=0	0.5	0.9	1.6	2.2	2.9	4.2	5.9	8.4	na
LG4 Z=0.025Na	na	na	na	2.0	na	na	6.5	12.0	14.5
LG6 Z=0.1Na	na	na	na	0	na	na	0.3	2.4	4.1
LG7 Z=0.025K	na	na	na	2.6	na	na	5.6	12.3	15.1
LG8 Z=0.05K	na	na	na	2.6	na	na	6.2	12.0	14.9
LG10 Z=0.0125Na/K	na	na	na	1.5	na	na	3.6	10.1	12.8
LG11 Z=0.05Na/K	na	na	na	2.6	na	na	6.4	12.2	14.8
LG22 Z=0.05K	<0.1	<0.1	<0.1	0.1	0.1	0.2	1.3	1.2	na
LG69 Z=0.5Na	0.3	<0.1	na	na	na	na	na	na	na

Data obtained from discs (20 mm by 2 mm) in 50 ml water at 37°C. Release data is the arithmetic mean of one analysis of each of six specimens. The standard deviation did not exceed 10%.

na-Not applied-reading not taken as there was no sample.

LG11 released the greatest amount of calcium to 84 days, however LG6 elutes the least amount of calcium to the same time period. LG67 and LG68 eluted $<0.1 \mu\text{mol g}^{-1}$ throughout the time of the experiment. Detection limits of the AAS for calcium were 1 ppm to 10 ppm.

There was no relation between calcium ion release and sodium glass composition.

There is no relation between calcium ion release and potassium glass content. There

was no relation between sodium ions of monovalent cation ICs and calcium ion

release. A wider range sodium based glasses were required for plots and to confirm

a definite relation between sodium based ICs and calcium ion release. There was

also no relation between potassium ions in the monovalent cation ICs and calcium

ion release. A greater range of potassium based glasses were required for a definite relation to be confirmed. Hence calcium was not influenced by increasing sodium and potassium ions of the monovalent cation based series of glasses.

Table 3.37 Calcium ion release ($\mu\text{mol g}^{-1}$) over time from discs of ionomeric cements from the apatite stoichiometric series (Ca:P~1.66). (P)SiO₂ 1.5P₂O₅ (Q)Al₂O₃ (5-x)CaO xCaF₂

Material	Time (d)			
	3	7	21	42
LG26 x=2.0	0.9	1.8	3.3	4.9
LG27 x=1.0	0.7	1.4	2.4	3.6
LG29 x=0.5	1.0	1.4	1.9	2.6
LG30 x=0	0.8	1.1	1.3	1.6

Data obtained from discs (20 mm by 2 mm) in 50 ml water at 37°C. Release data is the arithmetic mean of one analysis of each of six specimens. The standard deviation did not exceed 10%.

na-Not applied- reading not taken as there was no sample.

LG26 released the greatest amount of calcium to 42 days, however LG30 eluted the least amount of calcium. Detection limits of the AAS for calcium were 1 ppm to 10 ppm.

Table 3.38 Calcium ion release ($\mu\text{mol g}^{-1}$) over time from discs of ionomeric cements from the series varying in calcium fluoride upto the same time period. 1.5SiO₂ 1.0Al₂O₃ 0.5P₂O₅ 1.0CaO xCaF₂

Material	Time (d)							
	1	3	5	7	10	14	21	42
LG3 x=0.5	0.5	0.9	1.6	2.2	2.9	4.2	5.9	8.4
LG26 x=0.67	na	0.9	na	1.8	na	na	3.3	4.9
LG42 x=1.0	0.7	1.0	1.4	1.7	2.2	2.9	3.9	6.3
LG44 x=0.25	<0.1	0.2	0.3	0.5	0.8	1.2	1.8	3.9
LG45 x=0	0.8	1.5	1.5	2.1	2.8	3.9	5.0	7.8

Data obtained from discs (20 mm by 2 mm) in 50 ml water at 37°C. Release data is the arithmetic mean of one analysis of each of six specimens. The standard deviation did not exceed 10%.

na-Not applied- reading was not taken as there was no sample.

LG45 released the greatest amount of calcium to 42 days, however LG44 eluted the least amount of calcium. Detection limits of the AAS for calcium were 1 ppm to 10 ppm.

Table 3.39 Calcium ion release ($\mu\text{mol g}^{-1}$) over time from discs of ionomeric cements from the series varying in silicate:alumina and calcium .

Material	Time (d)								
	Si:Al:Ca	1	3	5	7	10	14	21	42
LG33 (4.5:3.0:2.0)		1.5	3.2	5.4	6.2	8.4	10.3	12.9	17.9
LG34 (6.0:4.0:1.0)		0.4	0.9	1.9	2.6	3.3	4.3	5.4	8.1
LG35 (6.75:4.5:0.5)		0.3	0.7	1.4	1.9	2.5	3.2	4.4	6.8
LG36 (7.125:4.75:0.25)	0.4		0.7	1.3	1.8	2.5	3.2	4.2	6.5
LG37 (7.5:5.0:5.0)		0.1	0.3	0.7	1.1	1.6	2.1	2.9	4.9
LG72 (6.0:4.0:4.2)		0.5	1.2	1.9	2.8	3.5	4.3	5.6	8.2
LG73 (7.5:5.0:1.0)		0.5	1.3	1.9	2.6	3.5	4.6	5.9	8.5
LG74 (8.25:5.5:5.0)		0.6	1.3	2.0	2.8	3.7	4.9	5.9	7.4
LG75 (8.625:5.75:0.25)	0.6		1.7	2.6	3.3	4.2	4.9	5.4	6.2

Data obtained from discs (20 mm by 2 mm) in 50 ml water at 37°C . Release data is the arithmetic mean of one analysis of each of six specimens. The standard deviation did not exceed 10%.

na-Not applied-reading was not taken as there was no sample.

LG53 released the greatest amount of calcium to 42 days, however LG57 eluted the least amount of calcium to the same time period. Detection limits of the AAS for calcium were 1 ppm to 10 ppm.

Table 3.40 Calcium ion release ($\mu\text{mol g}^{-1}$) over time from discs of ionomeric cements from the series varying in Silica:Alumina ratio based .

Material	Time (d)								
	SiO ₂ :Al ₂ O ₃	1	3	5	7	10	14	21	42
LG77 (6.25:3.75)		<0.1	0.2	0.2	0.3	0.4	0.9	1.5	2.6
LG78 (6.5:3.5)		<0.1	0.3	0.7	0.9	1.5	1.8	2.3	3.2
LG80 (6.7:3.3)		0.4	0.8	1.4	1.9	2.5	3.9	5.6	7.5
LG81 (6.75:3.25)		0.3	0.4	0.5	0.6	0.8	2.3	3.9	5.8

Data obtained from discs (20 mm by 2 mm) in 50 ml water at 37°C . Release data is the arithmetic mean of one analysis of each of six specimens. The standard deviation did not exceed 10%.

LG80 released the greatest amount of calcium to 42 days, however LG77 elutes the least amount of calcium to the same time period. Detection limits of the AAS for calcium were 1 ppm to 10 ppm.

Table 3.41 Calcium ion release ($\mu\text{mol g}^{-1}$) over time from discs of ionomeric cements from the series varying in generic compositions derived from the apatite-stoichiometric based glass LG26.

Material	Time (d)							
	1	3	5	7	10	14	21	42
$\text{SiO}_2:\text{P}_2\text{O}_5:\text{CaO}$								
LG26 (4.5:1.5:3.0)	na	0.9	na	1.8	na	na	3.3	4.9
LG83 (4.1:1.7:2.8)	0.1	0.8	1.4	1.9	2.8	3.3	4.0	5.4
LG84 (3.7:1.9:2.6)	0.7	0.8	0.9	1.0	1.2	2.9	4.9	7.4
LG85 (3.3:2.1:2.4)	0.2	0.4	0.6	0.9	1.2	1.8	2.8	4.3

Data obtained from discs (20 mm by 2 mm) in 50 ml water at 37°C. Release data is the arithmetic mean of one analysis of each of six specimens. The standard deviation did not exceed 10%.

LG84 released the greatest amount of calcium to 42 days, however LG85 eluted the least amount of calcium to the same time period. Detection limits of the AAS for calcium were 1 ppm to 10 ppm.

There was a relation between decreasing calcium ion release with an increase in phosphorus pentoxide glass content. A wider range of phosphate glasses were required for an adequate plot (correlation coefficient = -0.87 and linear regression = 0.38).

Table 3.42 Calcium ion release ($\mu\text{mol g}^{-1}$) over time from discs of ionomeric cements from the Calcium based series.

Material	Time (d)							
	1	3	5	7	10	14	21	42
$\text{CaO}:\text{CaF}_2$								
LG95 (2.8:2.2)	1.4	3.1	4.9	6.2	8.1	9.9	12.5	15.1
LG96 (2.6:2.4)	0.8	2.1	3.2	4.3	5.8	7.3	9.6	12.8
LG97 (2.4:2.6)	0.7	1.6	2.5	3.3	4.5	5.6	7.5	10.5
LG98 (2.2:2.8)	1.7	3.6	5.2	6.6	8.8	10.6	13.4	16.9
LG99 (2.0:3.0)	1.2	2.5	3.6	4.8	6.4	8.3	11.2	14.8

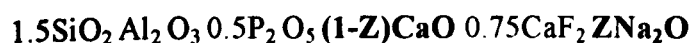
Data obtained from discs (20 mm by 2 mm) in 50 ml water at 37°C. Release data is the arithmetic mean of one analysis of each of six specimens. The standard deviation did not exceed 10%.

LG98 released the greatest amount of calcium to 42 days, however LG97 eluted the least amount of calcium to the same period of time. Detection limits of the AAS for calcium were 1 ppm to 10 ppm.

(g) Phosphate by high pressure liquid chromatography

High pressure liquid chromatography was used to measure the concentration of ions released from set discs of IC (section 2.2.2). Phosphate release data from all the formulations examined is summarized in Tables 3.43 to 3.49 on the following pages. Particular areas of interest are added as footnotes where appropriate.

Table 3. 43 Phosphate ion release ($\mu\text{mol g}^{-1}$) over time from discs of ionomeric cements of the monovalent cation series (Na^+ and K^+).



Material	Time (d)								
	1	3	5	7	10	14	21	42	84
LG2 z=0	na	na	na	na	na	na	6.3	8.8	11.2
LG3 z=0	0.2	0.4	0.5	0.6	0.7	0.8	0.9	1.2	na
LG4 z=0.025Na	na	na	na	2.4	na	na	3.9	4.9	5.9
LG6 z=0.1Na	na	na	na	5.5	na	na	8.1	9.7	11.7
LG7 z=0.025K	na	na	na	1.3	na	na	1.9	2.5	3.4
LG8 z=0.05K	na	na	na	2.4	na	na	2.6	4.8	6.0
LG10 z=0.0125Na/K	na	na	na	1.7	na	na	2.1	2.7	3.5
LG11 z=0.05Na/K	na	na	na	2.6	na	na	4.1	5.3	6.5
LG22 z=0.05K	0.2	0.3	0.4	0.5	0.5	0.6	0.7	0.9	na
LG67 z=0.3Na	0.4	0.7	0.8	0.9	1.1	1.3	1.7	2.2	na
LG68 z=0.4Na	0.5	0.8	1.1	1.3	1.6	1.8	2.1	2.7	na
LG69 z=0.5Na	1.7	2.7	3.6	4.0	4.7	5.3	6.4	8.2	na

Data obtained from discs (20 mm by 2 mm) in 50 ml water at 37°C. Release data is the arithmetic mean of one analysis of each of six specimens. The standard deviation did not exceed 10%.

na-Not applied-reading not taken as there was no sample.

LG6 released the greatest amount of phosphate to 42 days, however LG22 eluted the least amount of phosphate to the same time period. Detection limits of the HPLC for phosphate were 5 ppm to 40 ppm.

Table 3.42 shows that there was no relation between phosphate ion release and sodium solubilising ions of the monovalent cation based series of ICs hence no plots were included. There may be a relation between phosphate ion release and

potassium glass content however more potassium based glasses were required for analysis to confirm this.

Table 3.44 Phosphate ion release ($\mu\text{mol g}^{-1}$) over time from discs of ionomeric cements from the apatite stoichiometric series ($\text{Ca:P}\sim 1.66$). $(\text{P})\text{SiO}_2 1.5\text{P}_2\text{O}_5 (\text{Q})\text{Al}_2\text{O}_3 (5-x)\text{CaO } x\text{CaF}_2$

Material	Time (d)			
	3	7	21	42
LG26 $x=2.0$	0.1	1.7	2.6	3.8
LG27 $x=1.0$	1.2	1.9	2.7	3.5
LG28 $x=0.5$	1.6	2.0	2.8	3.7
LG29 $x=0.25$	3.3	4.1	5.5	7.7
LG30 $x=0$	2.2	2.9	4.0	5.8

Data obtained from discs (20 mm by 2 mm) in 50 ml water at 37°C. Release data is the arithmetic mean of one analysis of each of six specimens. The standard deviation did not exceed 10%.

LG29 released the greatest amount of phosphate to 42 days, however LG27 eluted the least amount of phosphate to the same time period. Detection limits of the HPLC for phosphate were 5 ppm to 40 ppm.

Table 3.45 Phosphate ion release ($\mu\text{mol g}^{-1}$) over time from discs of ionomeric cements from the series varying in calcium fluoride. $1.5\text{SiO}_2 1.0\text{Al}_2\text{O}_3 0.5\text{P}_2\text{O}_5 1.0\text{CaO } x\text{CaF}_2$

Material	Time (d)							
	1	3	5	7	10	14	21	42
LG2 $x=0.75$	na	na	na	na	na	na	6.3	8.8
LG3 $x=0.5$	0.2	0.4	0.5	0.6	0.7	0.8	0.9	1.2
LG26 $x=0.67$	na	0.1	na	1.7	na	na	2.6	3.8
LG42 $x=1.0$	0.5	0.2	0.3	0.3	0.3	0.4	0.4	0.4
LG44 $x=0.25$	0.4	0.6	0.8	0.9	0.1	1.2	1.4	1.9
LG45 $x=0$	1.6	2.5	2.9	3.4	3.8	4.6	5.3	6.4

Data obtained from discs (20 mm by 2 mm) in 50 ml water at 37°C. Release data is the arithmetic mean of one analysis of each of six specimens. The standard deviation did not exceed 10%.

LG45 released the greatest amount of phosphate to 42 days, however LG42 eluted the least amount of phosphate to the same time period. Detection limits of the HPLC for phosphate were 5 ppm to 40 ppm.

Table 3.46 Phosphate ion release ($\mu\text{mol g}^{-1}$) over time from discs of ionomeric cements from the series varying in silica:alumina and calcium .

Material	Time (d)							
	3	5	7	10	14	21	42	
SiO₂:Al₂O₃:CaF₂1								
LG53 (4.5:3.0:2.0) 0.1	0.2	0.3	0.3	0.3	0.3	0.4	0.5	
LG54 (6.0:4.0:1.0) 0.1	0.1	0.2	0.2	0.2	0.2	0.2	0.4	
LG55 (6.75:4.5:0.5) 0.2	0.3	0.4	0.4	0.5	0.5	0.6	0.8	
LG56 (7.125:4.75:0.25)0.2	0.4	0.5	0.5	0.5	0.5	0.6	0.8	
LG57 (7.5:5.0:0) 0.2	0.3	0.4	0.4	0.4	0.5	0.5	0.6	
LG72 (6.0:4.0:2.0) 0.8	1.4	1.6	1.8	1.9	2.1	2.3	2.8	
LG73 (7.5:5.0:1.0) 0.8	1.2	1.5	1.7	1.9	2.1	2.4	2.7	
LG74 (8.25:5.5:0.5) 0.7	1.0	1.3	1.4	1.5	1.7	1.9	2.3	
LG75 (8.625:5.75:0.25)0.9	1.4	1.8	1.9	2.1	2.3	2.6	3.1	

Data obtained from discs (20 mm by 2 mm) in 50 ml water at 37°C . Release data is the arithmetic mean of one analysis of each of six specimens. The standard deviation did not exceed 10%.

LG72 released the greatest amount of phosphate to 42 days, however LG54 eluted the least amount of phosphate to the same period of time. Detection limits of the HPLC for phosphate were 5 ppm to 40 ppm.

Table 3.47 Phosphate ion release ($\mu\text{mol g}^{-1}$) over time from discs of ionomeric cements from the series varying in silica:alumina ratio based .

Material	Time (d)							
	1	3	5	7	10	14	21	42
SiO₂:Al₂O₃								
LG77 (6.25:3.75) 0.3	0.5	0.7	0.8	0.8	0.9	0.9	1.1	
LG78 (6.5:3.5) 0.4	0.8	1.2	1.3	1.5	1.6	1.7	1.9	
LG80 (6.7:3.3) 1.0	1.6	2.0	2.2	2.5	2.7	3.0	3.6	
LG81(6.75:3.25) 1.1	1.3	1.4	1.5	1.7	2.0	2.5	2.9	

Data obtained from discs (20 mm by 2 mm) in 50 ml water at 37°C . Release data is the arithmetic mean of one analysis of each of six specimens. The standard deviation did not exceed 10%.

LG80 released the greatest amount of phosphate to 42 days, however LG77 eluted the least amount of phosphate to the same time period. Detection limits of the HPLC for phosphate were 5 ppm to 40 ppm.

Table 3.48 Phosphate ion release ($\mu\text{mol g}^{-1}$) over time from discs of ionomeric cements from the series varying in generic compositions derived from the apatite-stoichiometric based glass LG26.

Material	Time (d)							
	1	3	5	7	10	14	21	42
SiO₂:P₂O₅:CaO								
LG26 (4.5:1.5:3.0)	na	0.1	na	1.7	na	na	2.6	3.8
LG83 (4.1:1.7:2.8)	0.3	1.1	1.6	1.8	2.2	2.4	2.5	2.9
LG84 (3.7:1.9:2.6)	1.0	1.6	2.1	2.4	2.6	3.0	3.7	4.7
LG85 3.3:2.1:2.4)	1.6	1.9	1.9	2.1	2.4	2.7	2.9	3.9

Data obtained from discs (20 mm by 2 mm) in 50 ml water at 37°C . Release data is the arithmetic mean of one analysis of each of six specimens. The standard deviation did not exceed 10%.

LG84 released the greatest amount of phosphate to 42 days. however LG83 eluted the least amount of phosphate. Detection limits of the HPLC for phosphate were 5 ppm to 40 ppm.

Figure 3.13 shows a positive relation between phosphorus pentoxide glass content and PO_4^{3-} ion release at 3 days, where the parameters have a correlation coefficient of 0.97 (linear regression =0.69). There is an increase in PO_4^{3-} release as phosphorus pentoxide glass content increases.

Figure 3.13 Relation between Phosphorus pentoxide glass composition and phosphorus ion release at 3 days. Linear regression, $y=0.69x-6$. Correlation coefficient=0.97 (n=6)

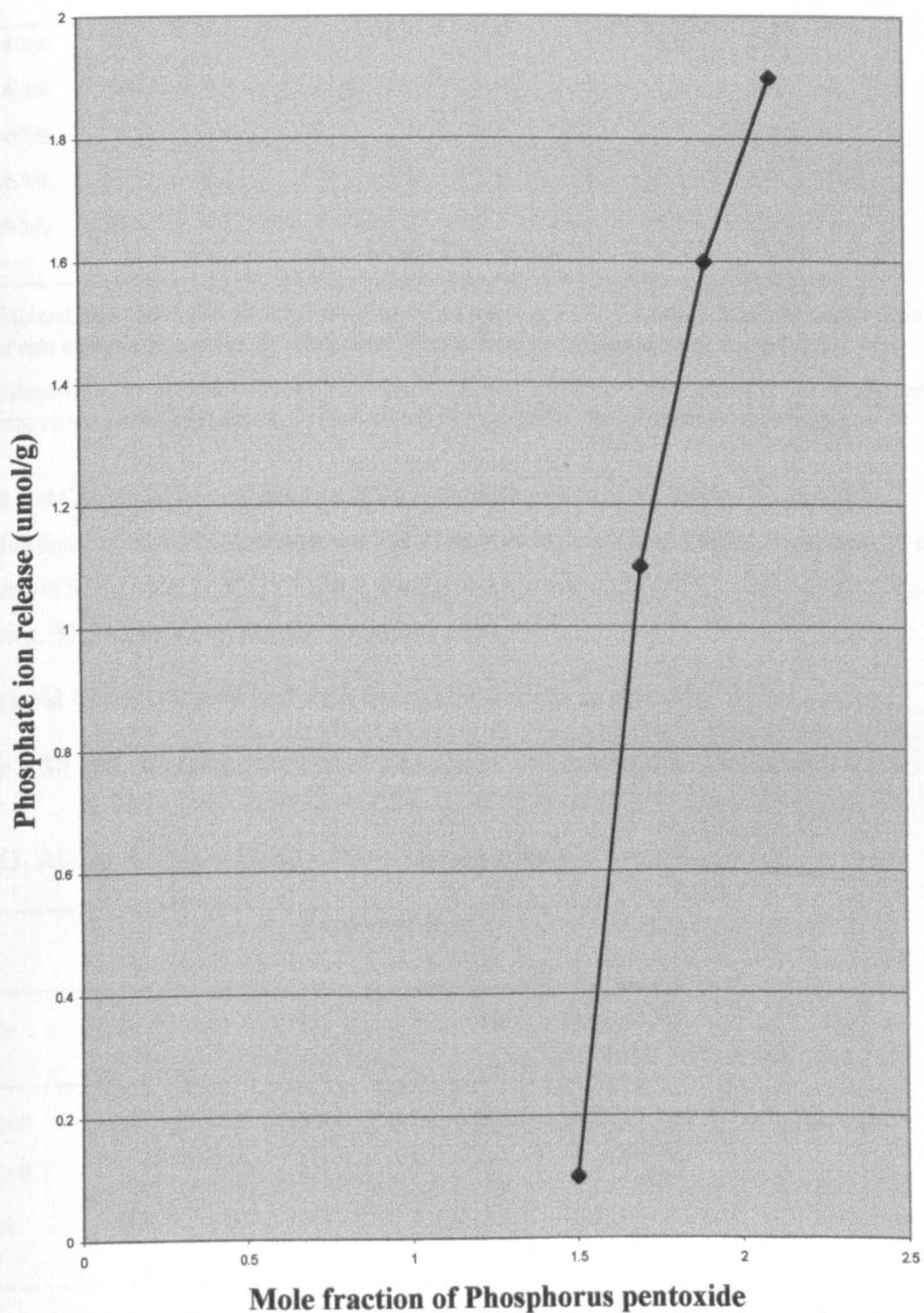


Table 3.49 Phosphate ion release ($\mu\text{mol g}^{-1}$) over time from discs of ionomeric cements from the Calcium based series .

Material	Time (d)							
	1	3	5	7	10	14	21	42
CaO:CaF₂								
LG95 (2.8:2.2)	0.6	0.9	1.2	1.0	1.4	1.7	2.0	2.6
LG96 (2.6:2.4)	0.6	0.9	1.1	1.3	1.4	1.6	1.8	2.3
LG97 (2.4:2.6)	0.5	0.8	0.9	1.0	1.2	1.2	1.4	1.9
LG98 (2.2:2.8)	0.5	0.7	0.9	0.9	1.1	1.3	1.5	1.9
LG99 (2.0:3.0)	0.6	0.9	1.1	1.2	1.2	1.3	1.5	1.9

Data obtained from discs (20 mm by 2 mm) in 50 ml water at 37°C . Release data is the arithmetic mean of one analysis of each of six specimens. The standard deviation did not exceed 10%.

LG95 released the greatest amount of phosphate to 42 days, however LG98 eluted the least amount of phosphate to the same time period. Detection limits of the HPLC for phosphate were 5 ppm to 40 ppm.

Chemfil and Chemfil Express released equal amounts of phosphate to 42 days i.e. $0.1 \mu\text{mol g}^{-1}$.

Detection limits of the HPLC for phosphate were 5 ppm to 40 ppm. Data obtained from discs (20 mm by 2 mm) in 50 ml water at 37°C . Release data is the arithmetic mean of one analysis of each of six specimens. The standard deviation did not exceed 10%.

3.2 (h) pH of autoclaved and non-autoclaved discs in solution

Table 3.50 pH of eluting water as a function of cement disc immersion time

1.5SiO₂ Al₂ O₃ 0.5P₂ O₅ (1-Z) CaO 0.75CaF₂ ZNa₂O

Sample	Number of Days					
	1	3	5	7	10	14
LG2 Z=0	7.6	6.8	6.5	6.7	6.7	6.8
LG6 Z=0.1	7.7	7.4	6.9	7.0	7.3	7.2
Control	5.7	5.6	5.6	5.4	5.5	6.0

Data obtained from discs (20 mm by 2 mm) in 50 ml water at 37°C. Data is the arithmetic mean of one analysis of each of six specimens. The standard deviation did not exceed 10%. Water treated with LG6 is less acidic than water treated with LG2.

Table 3.51 Mean pH of eluted water of autoclaved ICs at 7 days

LG7 and LG8 are from the monovalent cation based series of ICs with the following formulae: $1.5\text{SiO}_2 \text{Al}_2\text{O}_3 \cdot 0.5\text{P}_2\text{O}_5 \cdot (1-Z) \text{CaO} \cdot 0.75\text{CaF}_2 \cdot Z\text{Na}_2\text{O}$
 LG26 from the apatite stoichiometric has the following formulae series (Ca:P~1.66). $(\text{P})\text{SiO}_2 \cdot 1.5\text{P}_2\text{O}_5 \cdot (\text{Q})\text{Al}_2\text{O}_3 \cdot (5-x)\text{CaO} \cdot x\text{CaF}_2$

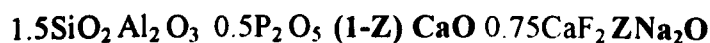
Sample		Mean pH
LG7	Z=0.025K	6.6
Autc LG7	Z=0.025K	6.4
LG8	Z=0.05K	6.7
Autc LG8	Z=0.05K	6.5
LG26	x=2.0	6.4
Autc LG26	X=2.0	6.0
Control		6.2

Autc-autoclaved

Data obtained from discs (20 mm by 2 mm) in 50 ml water at 37°C. Data is the arithmetic mean of one analysis of each of six specimens. The standard deviation did not exceed 10%. pH measurements were taken using a pH electrode attached to an Orion AS 720pH/ISE direct readout meter (USA). Water treated with autoclaved ICs showed a reduction in pH.

Table 3.52 pH of LG2 and LG26 in 50ml of water

LG2 is a monovalent cation with the following formula:



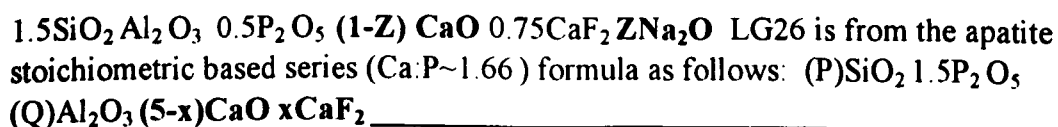
LG26 is from the apatite stoichiometric based series (Ca:P~1.66) formula as follows: $(P)\text{SiO}_2 \cdot 1.5\text{P}_2\text{O}_5 \cdot (Q)\text{Al}_2\text{O}_3 \cdot (5-x)\text{CaO} \cdot x\text{CaF}_2$

Sample	Number of Days		
	1	3	7
LG2 Z=0	6.4	6.6	6.6
LG26 x=2.0	4.7	5.4	5.4
Control	5.4	5.4	5.4

Data obtained from discs (20 mm by 2 mm) in 50 ml water at 37°C. Data is the arithmetic mean of one analysis of each of six specimens. The standard deviation did not exceed 10%. Water treated with LG26 was more acidic compared to water treated with LG2.

Table 3.53 pH of LG2 and LG26 in 50ml of α -minimal essential media

LG2 is a monovalent cation with the following formula:



Sample	Number of Days		
	1	3	7
LG2	8.1	6.8	6.9
LG26	6.4	6.5	6.4
Control	7.1	7.0	7.0

Data obtained from discs (20 mm by 2 mm) in 50 ml α -minimal essential media at 37°C. Data is the arithmetic mean of one analysis of each of six specimens. The standard deviation did not exceed 10%. α -MEM treated with LG26 was more acidic than α -MEM treated with LG2.

Ion balance calculation for LG26:

LG26 :4.5 SiO₂. 3Al₂O₃. 1.5P₂O₅. 3.0 CaO. 2.0CaF₂

Anions

6Al³⁺

(3Ca³⁺) (2Ca²⁺)

Cations

(9O²⁻) (3O²⁻)

1.5PO₄³⁻

4F⁻

Total of anions 28 μ moles of a charge + total of cations -32.5 μ moles of a charge gave -4.5 μ moles of a charge for LG26.

LG63 :1.5 SiO₂. Al₂O₃. 0.5P₂O₅. 0.8 CaO. 0.75CaF₂ 0.2Na₂O

Anions

2Al³⁺

(0.8Ca³⁺) (0.75Ca²⁺)

0.4Na⁺

Cations

(3O²⁻) (0.8O²⁻) (0.2O²⁻)

0.5PO₄³⁻

1.5F⁻

Total of anions 9.5 μ moles of a charge + total of cations -11 μ moles of a charge gave -1.5 μ moles of a charge for LG63.

By totaling the number of positive and negative ions released and calculating the cumulative ion balance there was a surplus of negative ions over positive ions leaving the cement at all times, as can be shown for the above examples LG26 and LG63 . As a result of this outflow of negative ions the surrounding fluids, i.e. α -MEM in cell culture, shows a colour change from red to yellow, indicating a drop in pH (Table 3.50). The ion balance thus strongly indicates that fluoride ions released were mediated by an exchange of hydroxyl ions from the elution fluid leaving H^+ ions resulting in a drop in pH.

3.3 Tissue culture results

3.3.1 Bone marrow cell culture

Scanning electron microscopical examination of cultures.

Osteoblast-like cells were found on the surfaces of the IC disc LG27 after 14 days (see Figure 3.14). Cracking did appear for some of the IC discs. Defects did appear on the IC disc LG26 (see figure 3.15) as were used for tissue culture. Confluent cell monolayers formed on the discs as can be seen with LG6 (see Figure 3.16).

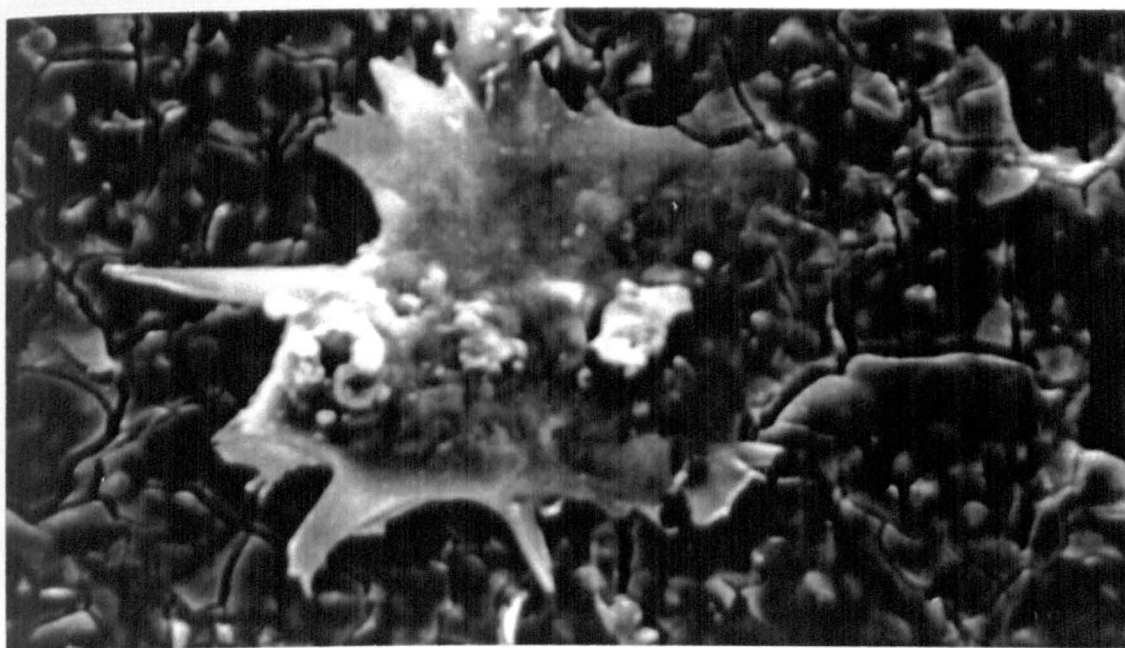


Figure 3.14 Scanning electron micrograph of a 14 day rat osteoblast-type cell derived from bone marrow cell culture: disc of ionomeric cement (LG27). Cell processes in close apposition to surface of IC (Field of width 40 μ m)
Original magnification x 1000 .

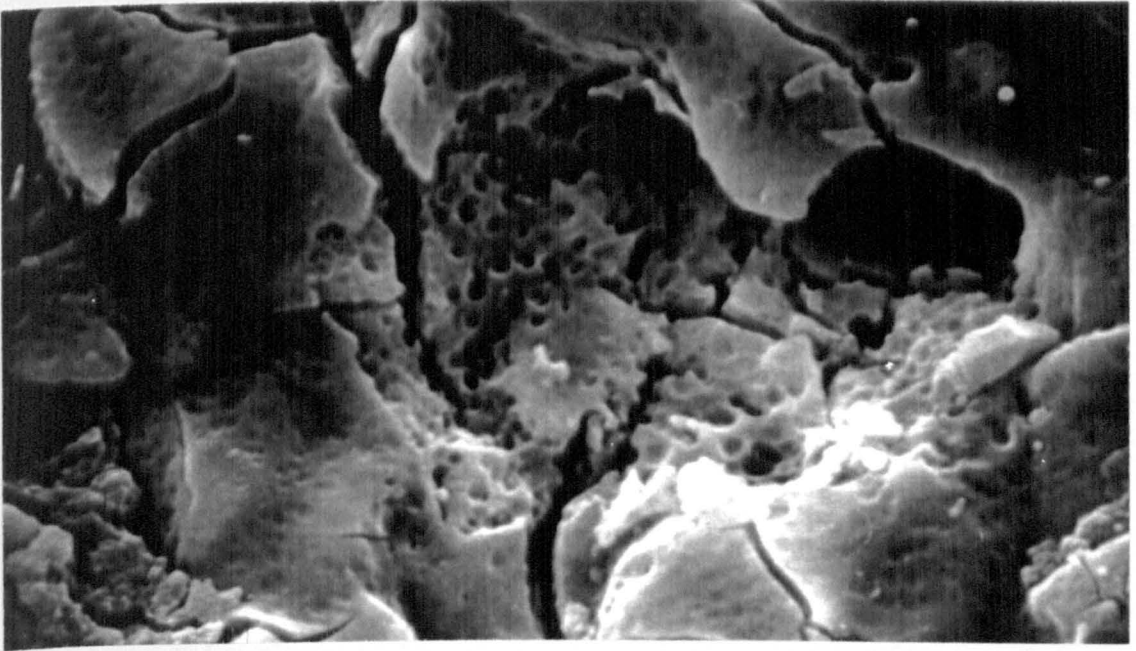


Figure 3.15 Scanning electron photomicrograph at high power showing defect on surface of typical set ionomeric cement as used for cell culture (LG26) after 14 days (Field width 200 μ m) Original magnification x1850.

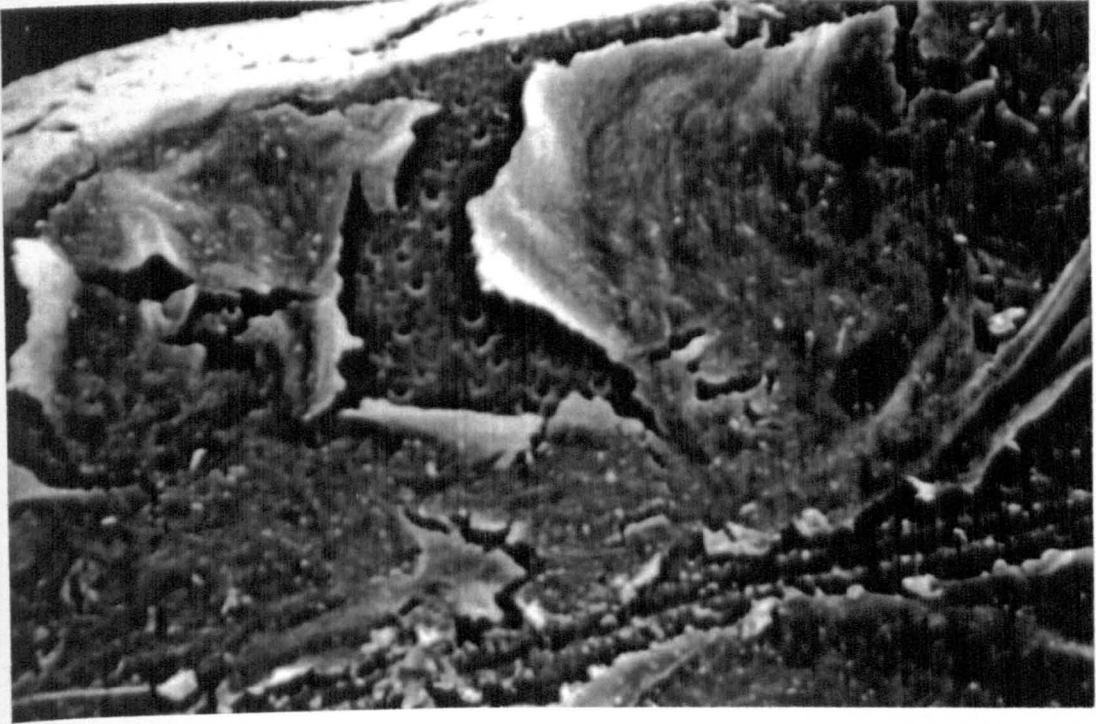


Figure 3.16 Scanning electron photomicrograph showing confluent osteoblast-like cells (from bone marrow cell culture) on the surface of set ionomeric cement (LG6) after 14 days cell culture (Field width= $120\mu\text{m}$) Original magnification x 800.

3.3.2 Quantitative assessment of Cytocompatibility Results

3.3.2 (a) Total protein and MTT results for bone marrow cell cultures

Figures 3.17 to 3.22 present data clearly showing the difference between the different ICs performance in the MTT test and Protein assays for rat bone marrow cell cultures. Particular results of interest are added as footnotes.

3.3.2 (b) Total protein and MTT results for Ros cell cultures

Figures 3.23 to 3.30 present data clearly showing the difference between the various ICs performance in the MTT and Protein assays for Ros cell cultures. Particular results of interest are added as footnotes.

Total Protein of bone marrow cells cultures with monovalent cation series of ICs

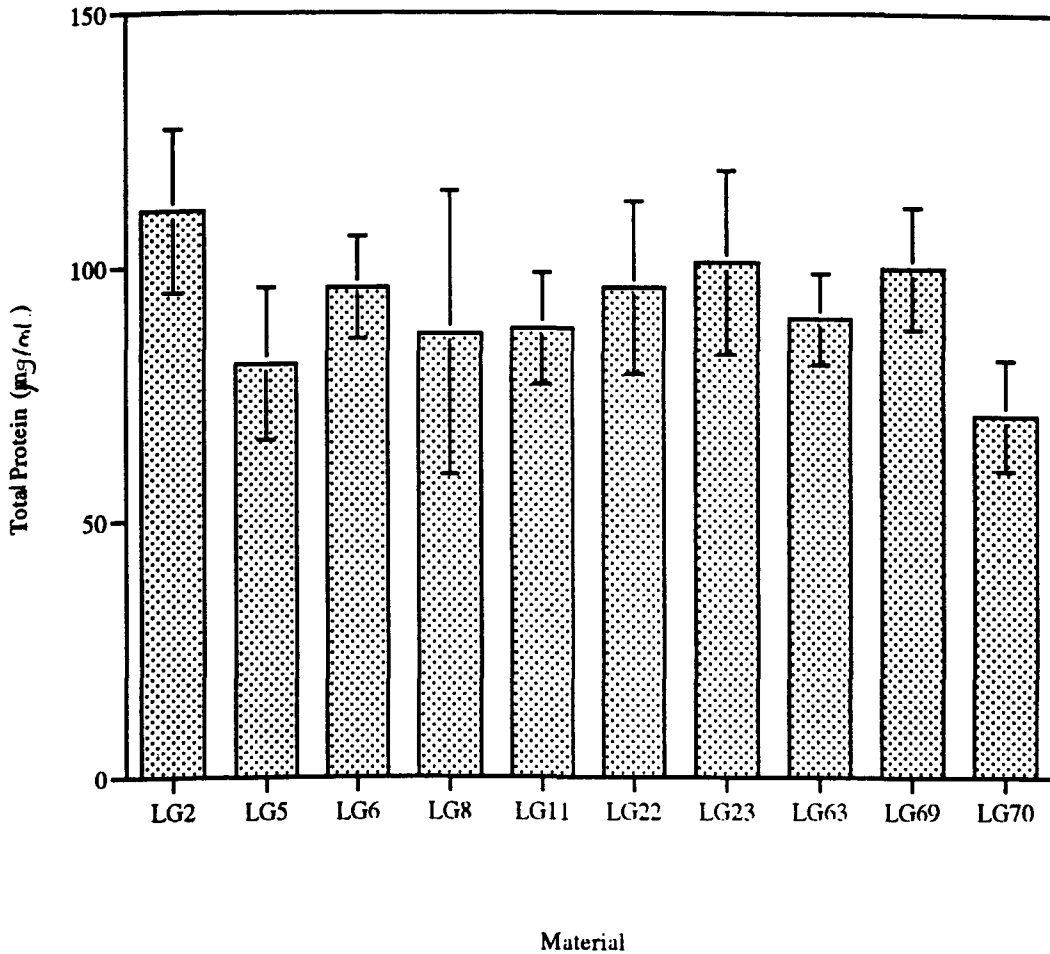


Figure 3.17 BMC cultures associated with the monovalent cation series IC LG2 had the greatest concentration of total protein. BMC cultures associated with LG70 had the least concentration of total protein from all the monovalent cation based ICs. This was determined by using the protein assay (as described in chapter 2.0 Materials and Method section 2.2.3i). LG2 BMC cultures compared to LG70 BMC cultures were statistically significant by using the Student t-Test (N=6, Error bar 1SD) as $P < 0.05$. LG8 BMC cultures compared to LG11 BMC cultures were not significantly different as the Student t-Test showed that they had a $P > 0.05$. LG23 BMC cultures compared to LG69 BMC cultures were not significantly different as the Student t-Test showed that $P > 0.05$. All other BMC cultures exposed to monovalent cation ICs were significantly different e.g. LG5 BMC cultures compared to LG70 BMC cultures had a $P < 0.05$ and were thus significantly different.

Cell activity of Bone marrow cell cultures with Monovalent cation ICs

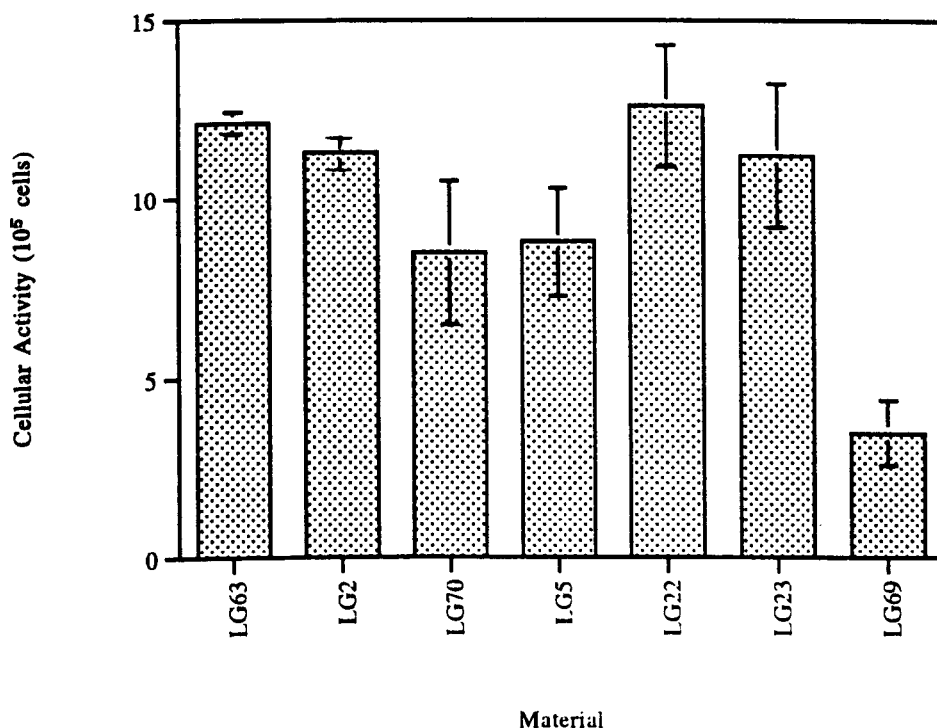


Figure 3.18 LG22 associated BMC cultures were the most active (12×10^5 cells) from all the monovalent cation based ICs used in this study. LG69 BMC cultures were the least active from all the monovalent cation based ICs. This was determined using the MTT assay (as described in chapter 2.0 Materials and Method section 2.2.3 ii). LG22 BMC culture activity compared to LG69 BMC culture activity were statistically significantly different with $P < 0.05$ using the Student t-Test ($N=6$, Error bar 1SD). All BMC cultures associated with ICs were compared against each other and were all found to be significantly different with $P < 0.05$.

Total Protein of Bone marrow cell cultures with Apatite-stoichiometric based ICs

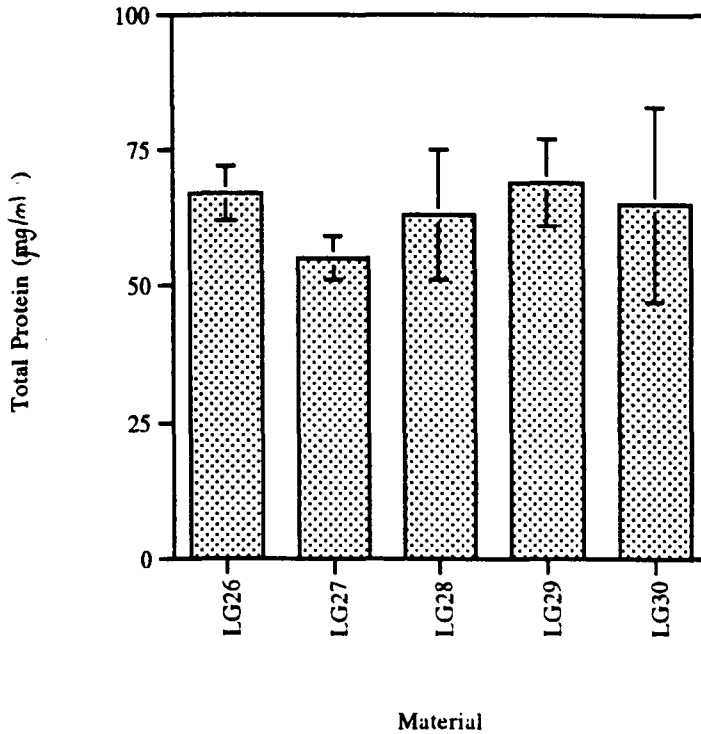


Figure 3.19 BMC cultures associated with the apatite-stoichiometric based IC LG29 had the greatest concentration of total protein. BMC cultures associated with LG27 had the least concentration of total protein from all the apatite-stoichiometric based ICs. This was determined using the protein assay as described in chapter 2.0 section 2.2.3 ii. LG27 BMC cultures compared to LG29 BMC cultures were significantly different as $P < 0.05$ using the Student t-Test ($N=6$, Error bar 1SD). All IC-BMC cultures were compared to each other and were all found to be significantly different with $P < 0.05$.

Cell activity of Bone marrow cell cultures with Apatite-stoichiometric based ICs

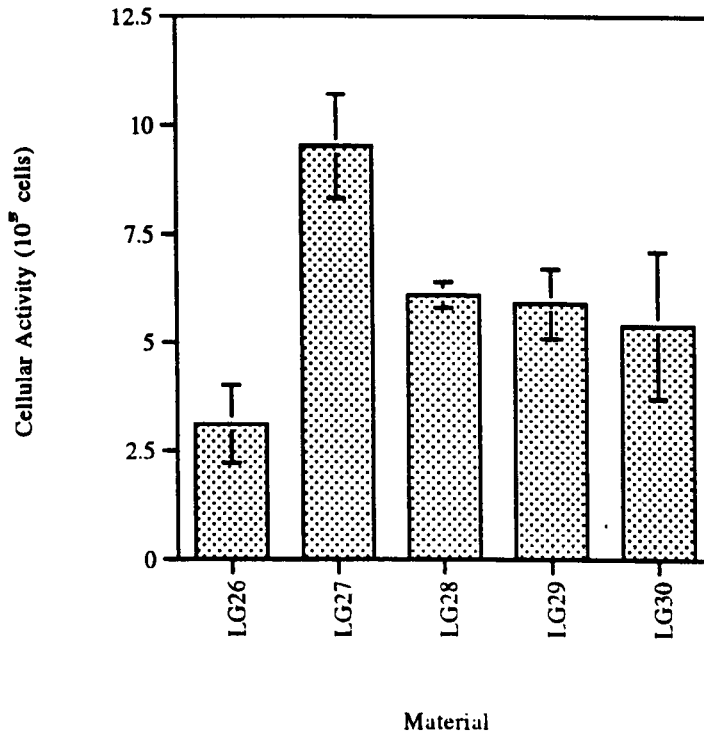


Figure 3.20 LG27 associated BMC cultures were the most active (9.5×10^5 cells) from all the apatite-stoichiometric based IC cultures used in this study. LG26 associated BMC cultures were the least active from all the apatite-stoichiometric based IC cultures. This was determined using the MTT assay (as described in chapter 2.0 Materials and Method section 2.2.3 ii). LG27 BMC culture activity was compared to LG26 BMC culture activity and were found to be significantly different with $P < 0.05$ using the Student t-Test ($N=6$, Error bar 1SD). LG28 BMC culture activity and LG29 BMC culture activity were compared using the Student t-Test and were also found to be significantly different with $P < 0.05$.

Total protein of Bone marrow cell culture with Commercial based cements

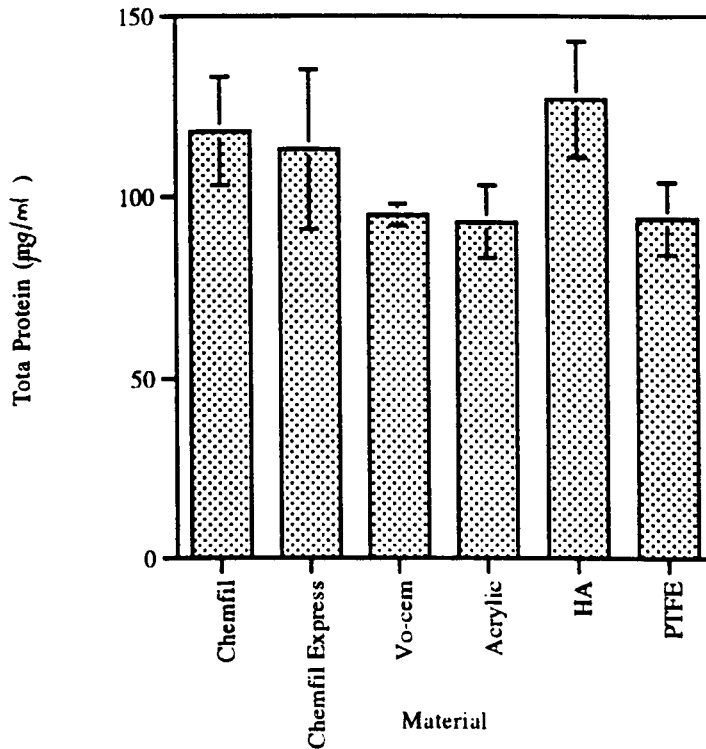


Figure 3.21 BMC cultures associated with the commercial cement hydroxyapatite had the greatest concentration of total protein compared to all the commercial cements used in this study. BMC cultures associated with acrylic had the least concentration of total protein from all the commercial based cements. HA BMC cultures were compared to Acrylic BMC cultures and were found to be significantly different with $P < 0.05$ using the Student t-Test ($N=6$, Error bar 1SD). Vo-cem BMC cultures were compared to Acrylic BMC cultures and were significantly different ($P < 0.05$). PTFE BMC cultures were compared to Acrylic BMC cultures and were significantly different with $P < 0.05$. Vo-cem BMC cultures were compared to PTFE BMC cultures and were significantly different ($P < 0.05$). All comparisons were made using the Student t-Test.

Cell activity of Bone marrow cell cultures with Commercial cements

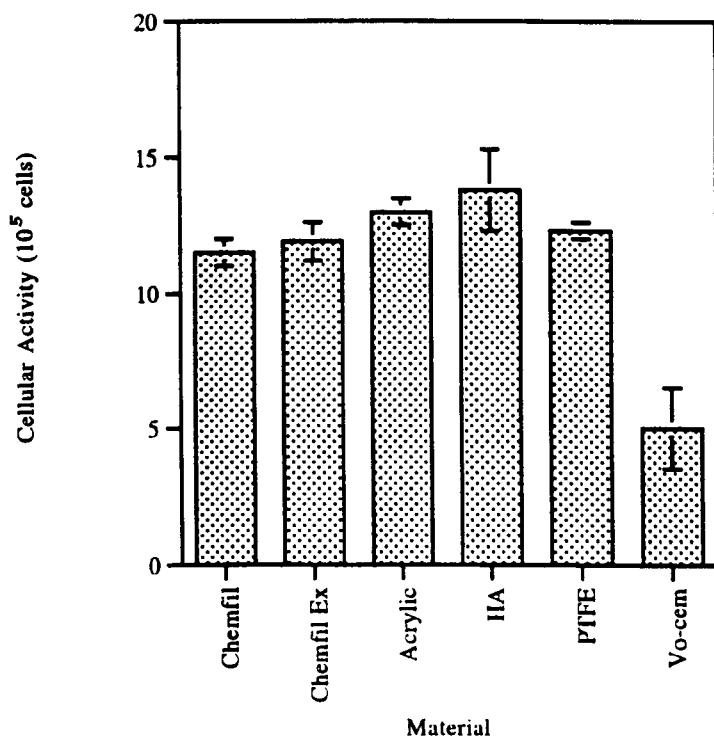


Figure 3.22 HA associated BMC cultures were the most active cells (13.8×10^5 cells) from all the BMC cultures associated with commercial based materials. This was determined using the MTT assay (as described in chapter 2.0 of the Materials and Method section 2.2.3 ii). HA BMC culture activity was compared to Vo-cem BMC culture activity by using the Student t-Test and were found to be statistically significant ($N=6$, Error bar 1SD) with $P<0.05$. Acrylic BMC culture activity was compared to PTFE BMC culture activity by using the Student t-Test and were not significantly different from each other as $P>0.05$. Chemfil BMC culture activity was compared to Chemfil Express BMC culture activity but were found to be significantly different with $P<0.05$ using the Student t-Test. Chemfil Express BMC culture activity was compared to Acrylic BMC culture activity and were significantly different using the Student t-Test as $P<0.05$.

Total protein of Ros cell cultures with monovalent cation series of ICs

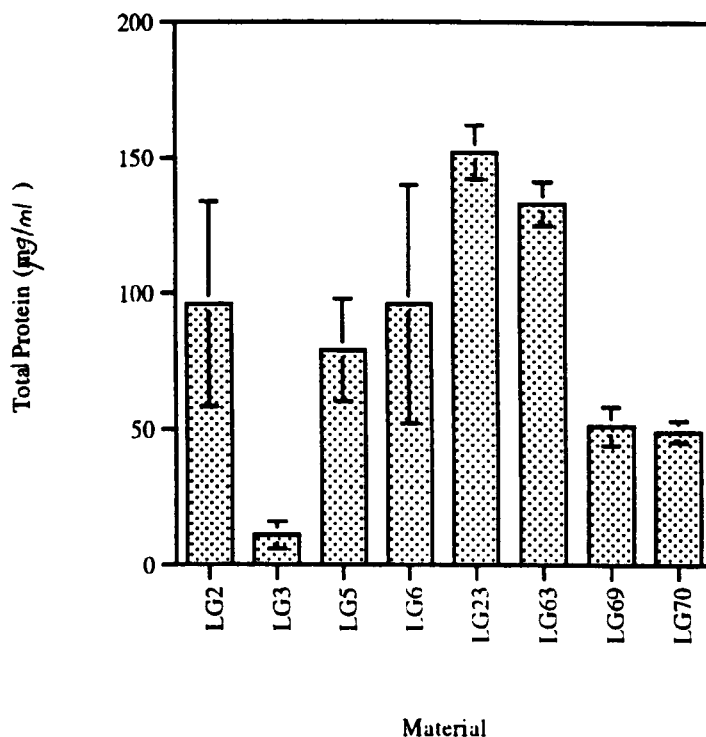


Figure 3.23 Ros cell cultures associated with the monovalent cation series IC LG23 had the greatest concentration of total protein. Ros cell cultures associated with LG3 had the least concentration of total protein from all the monovalent cation based ICs. This was determined using the protein assay (as described in chapter 2.0 of the Materials and Method section 2.2.3 ii). LG23 associated Ros cell culture protein concentrations were compared to LG3 Ros cell culture protein concentrations and were significantly different as $P < 0.05$ using the Student t-Test ($N=6$). LG69 Ros cell culture protein concentrations were compared to LG70 Ros cell culture protein concentrations using the Student t-Test and were significantly different. LG2 Ros cell culture protein concentrations were compared to LG6 Ros cell culture protein concentrations using the Student t-Test and were not significantly different as $P=1$.

Cell activity of Ros cell cultures with monovalent cation ICs

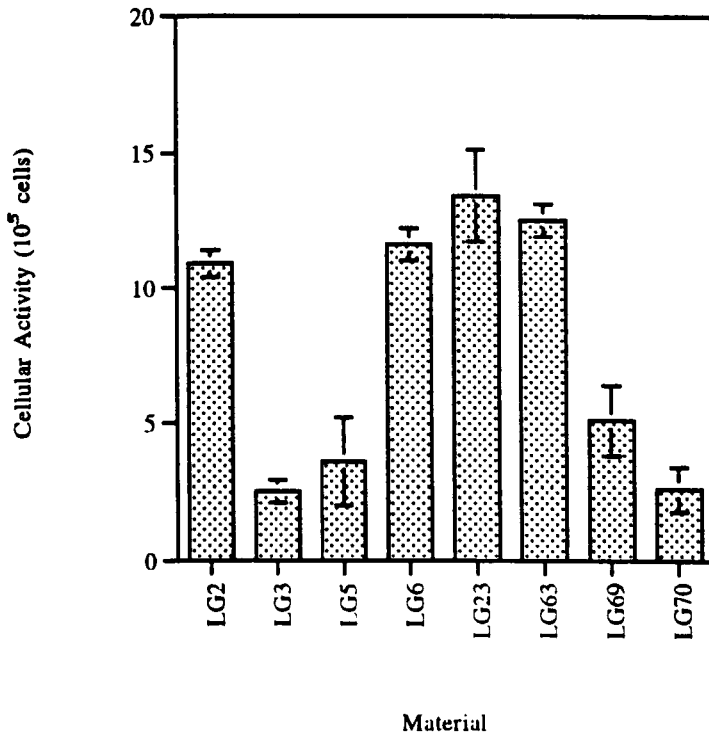


Figure 3.24 LG23 associated Ros cell cultures were the most active (13×10^5 cells) from all the Ros cell cultures associated with monovalent cation based ICs. LG3 Ros cell cultures were the least active compared to all other Ros cell cultures associated with monovalent cation based ICs. These were determined by using the MTT assay (as described in Chapter 2.0 of the Materials and Method section 2.2.3 ii). Ros cell culture activity associated with LG23 was compared to Ros cell culture activity associated with LG3 using the Student t-Test ($N=6$, Error bar 1SD) and were significantly different as $P<0.05$. LG2 Ros cell culture activity was compared to LG6 Ros cell culture activity using the Student t-Test and were significantly different as $P<0.05$. LG63 Ros cell culture activity was compared to LG6 Ros cell culture activity and were significantly different as $P<0.05$. LG5 Ros cell culture activity was compared to LG69 Ros cell culture activity and were significantly different as $P<0.05$. LG3 Ros cell culture activity was compared to LG70 Ros cell culture activity and were not significantly different as $P>0.05$.

Total protein of Ros cell cultures with varying silica/alumina and calcium based ICs

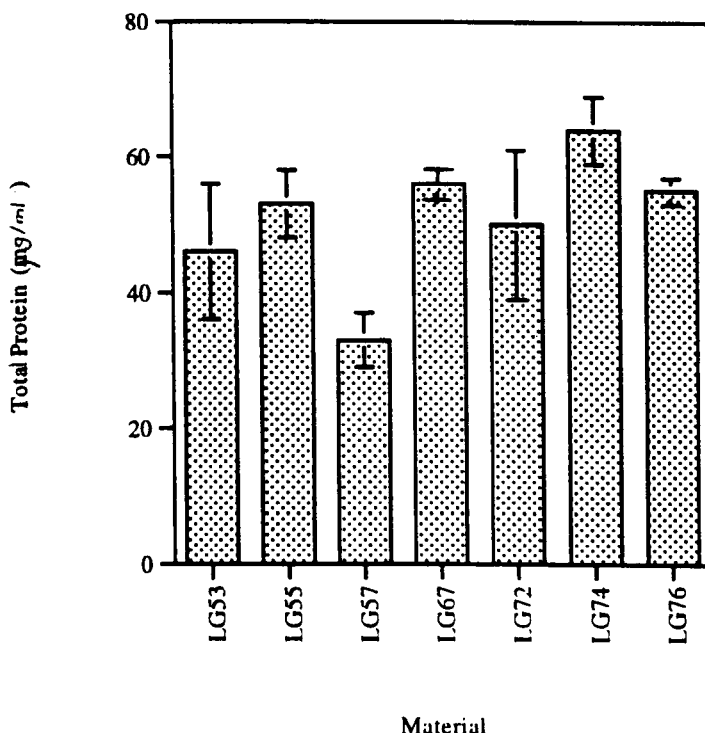


Figure 3.25 LG74 Ros cell cultures had the greatest concentration of total protein from all the Ros cell cultures associated with ICs varying in silica/alumina and calcium. LG57 Ros cell cultures had the least concentration of total protein compared to all the ICs varying in silica/alumina and calcium concentration. The protein concentration was determined by using the protein assay (as described in chapter 2.0 of the Materials and Method section 2.2.3 ii). LG74 Ros cell culture protein concentrations were compared with LG57 Ros cell culture protein concentrations by using the Student t-Test (N=6, Error bar 1SD) and were significantly different as $P < 0.05$. LG72 Ros cell culture protein concentrations were compared to LG53 Ros cell culture protein concentrations and were significantly different as $P < 0.05$. LG55 Ros cell culture protein concentrations were compared to LG67 Ros cell culture protein concentrations and were also significantly different with $P < 0.05$. However, LG67 Ros cell culture protein concentrations were compared to LG76 Ros cell culture protein concentrations and were not significantly different as $P > 0.05$.

Cell activity of Ros cell cultures with varying silica/alumina and calcium based ICs

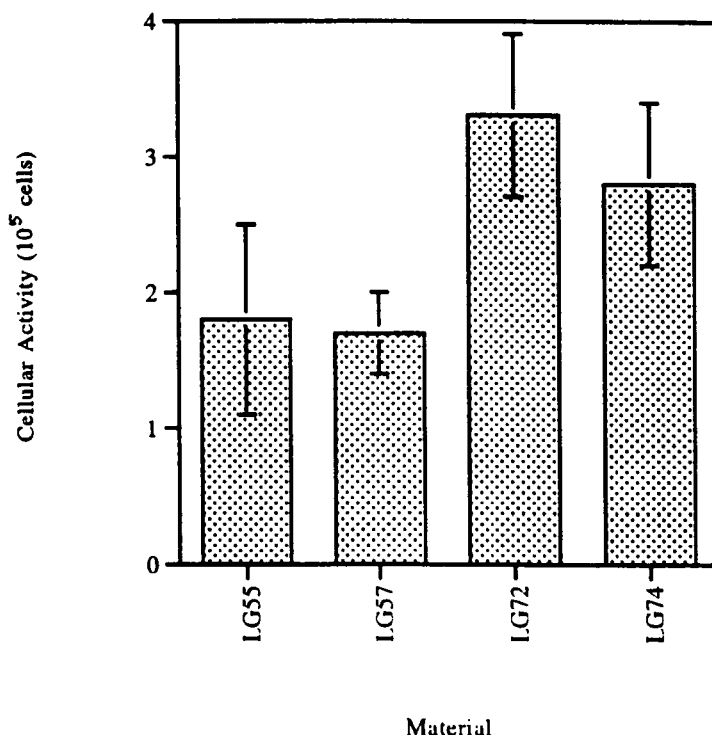


Figure 3.26 LG72 associated Ros cell cultures were the most active (11×10^5 cells) from all the other cultures associated with ICs varying in silica/alumina and calcium. LG57 associated Ros cell cultures were the least active from this series. These were determined using the MTT assay (as described in chapter 2.0 of the Materials and Method section 2.2.3. ii). LG72 Ros cell culture activity was compared to LG57 Ros cell culture activity by using the Student t-Test ($N=6$, Error bar 1SD) and were significantly different as $P<0.05$. LG55 Ros cell culture activity compared to LG57 Ros cell culture activity using the Student t-Test showed that the cell activities of these Ros cell cultures were significantly different as $P<0.05$.

Total Protein of Ros cell cultures with ICs varying in calcium fluoride

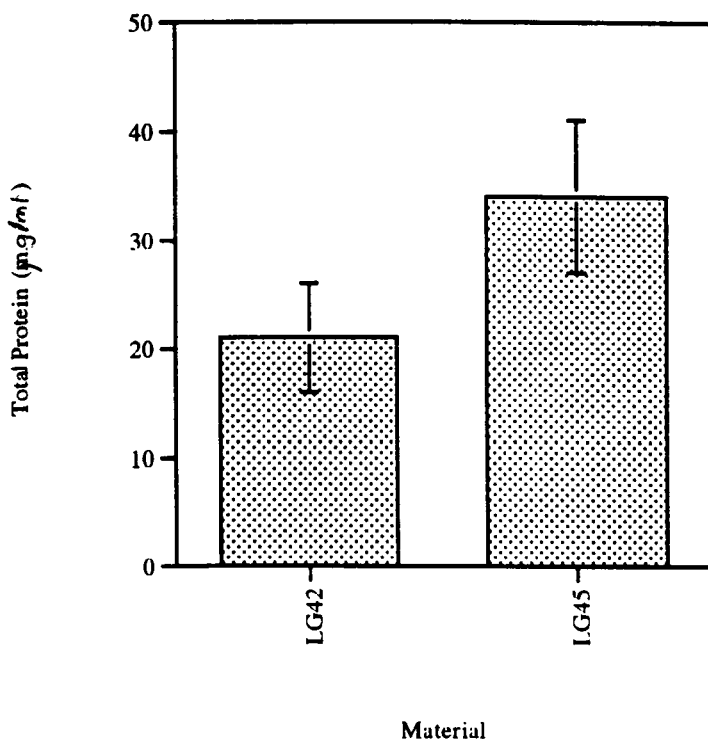


Figure 3.27 LG45 Ros cell cultures had greater total protein concentrations than LG42 Ros cell cultures total protein concentrations. The protein concentration was measured by using the Protein assay (as described in chapter 2.0 Materials and Method section 2.2.3 ii). LG45 Ros cell culture total protein concentrations were compared to LG42 cell culture total protein concentrations by using the Student t-Test (N=6, Error bar 1SD) and were significantly different as $P < 0.05$.

Cell activity of Ros cell cultures with ICs varying in calcium fluoride

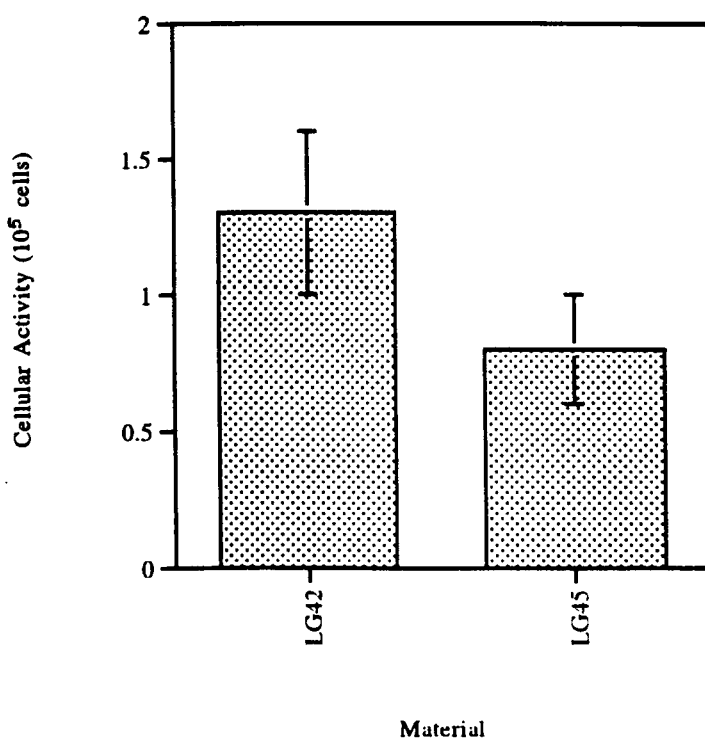


Figure 3.28 LG42 associated Ros cell cultures (1.3×10^5 cells) were more active than LG45 associated Ros cell cultures (0.8×10^5 cells) from the ICs varying in calcium fluoride. The cell activity was measured using the MTT assay (as described in chapter 2.0 of the Materials and Method section 2.2.3 ii). LG42 Ros cell culture activity was compared to LG45 Ros cell culture activity by using the Student t-Test ($N=6$, Error bar 1SD) and were significantly different as $P<0.05$.

Total protein of Ros cell cultures with commercial cements

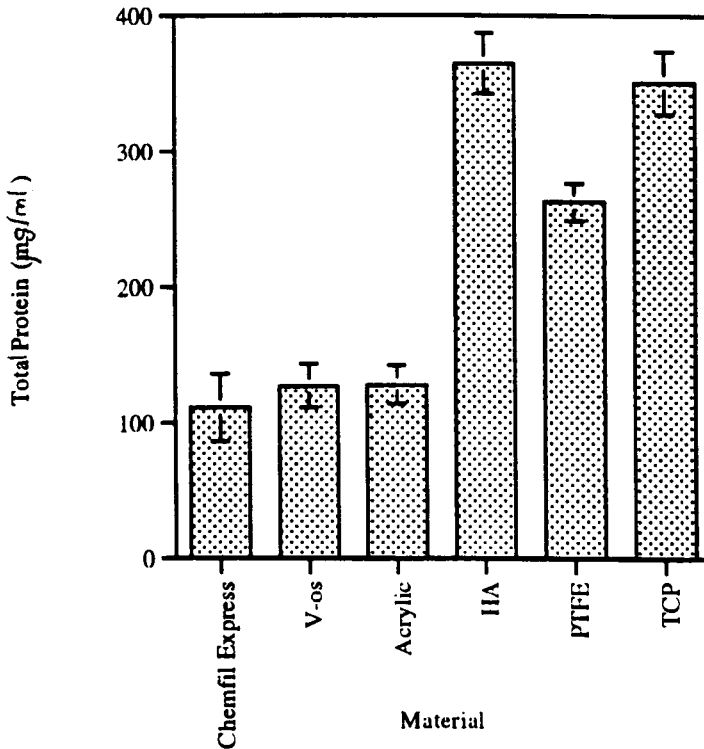


Figure 3.29 Ros cell cultures associated with the commercial cement HA had the greatest concentration of total protein (365 µg/ml) from all the commercial based materials analysed. Ros cell cultures associated with the commercial cement Chemfil Express had the least concentration of total protein (111 µg/ml). This was determined using the protein assay (as described in chapter 2.0 of the Materials and Method section 2.2.3 ii). HA Ros cell culture total protein concentrations were compared to Chemfil Express Ros cell culture total protein concentrations using the Student t-Test (N=6, Error bar 1SD) where they were significantly different as $P < 0.05$. V-os Ros cell culture total protein concentrations were compared to acrylic Ros cell culture total protein concentrations and were significantly different as $P < 0.05$. Chemfil Express Ros cell culture total protein concentrations were compared to acrylic and V-os Ros cell culture total protein concentrations and were both significantly different as $P < 0.05$.

Cell activity of Ros cell cultures with commercial cements

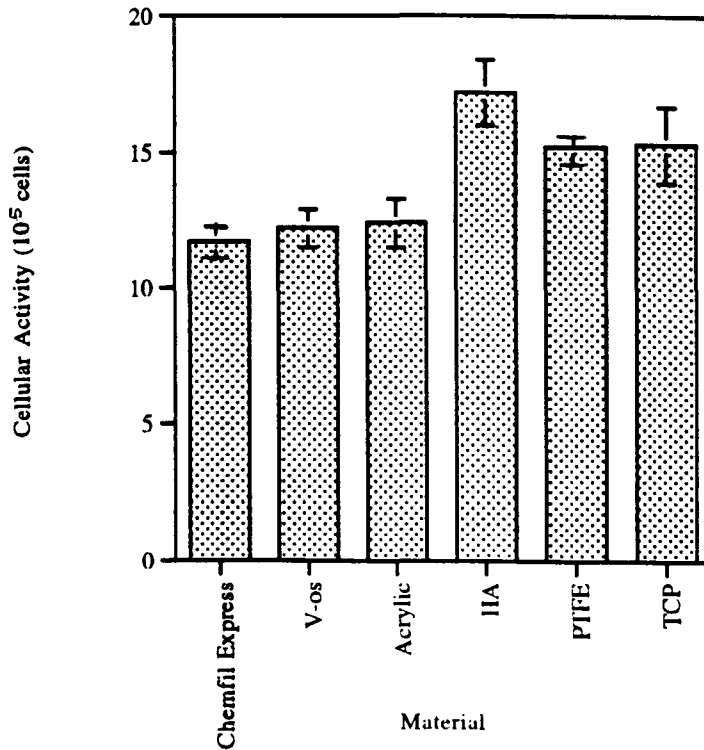


Figure 3.30 HA associated Ros cell cultures were the most active (17.2×10^5 cells) compared to all other Ros cell cultures associated with commercial materials. Chemfil Express associated Ros cell cultures were the least active from all the commercial materials analysed (11.7×10^5 cells). These were determined using the MTT assay (as described in chapter 2.0 of the Materials and Method section 2.2.3 ii). HA Ros cell culture activity was compared to Chemfil Express Ros cell culture activity by using the Student t-Test ($N=6$, Error bar 1SD) and were significantly different with $P<0.05$. V-os Ros cell culture activity was compared to acrylic Ros cell culture activity and were significantly different with $P<0.05$. Chemfil Express Ros cell culture activity was compared to V-os Ros cell culture activity and were significantly different as $P<0.05$. However, PTFE Ros cell culture activity and TCP Ros cell culture activity were compared and were not significantly different as $P>0.05$. Chemfil Express Ros cell culture activity was compared to acrylic Ros cell culture activity and were not significantly different as $P>0.05$.

3.4 *In vivo* Results

3.4.1 Histological assessment of *In vivo* surgical implantation

Of the 144 operations all healed uneventfully except for one with the IC LG119. In this case at day 7 a large swelling had developed around the area of the implant. The abdominal muscle was damaged by the reaction and torn and this could not be repaired. It was concluded by Dr Brian Howard, the University Vet, that the rat should be put to rest.

The controls (with no surgery, Figure 3.31 and 3.32) showed normal marrow and mature cancellous trabeculae through the mid-shaft of the femur. All the set ICs exhibited formation of new bone on their surfaces and generally new bone was formed in continuity with the implant surface from the woven bone at the surgical site into the marrow space as was with the set IC LG63 with a high sodium content (Figure 3.33).

Histological examination of ICs in the midshaft of the femur at four weeks revealed healed bone with no great difference in biological response subjectively as are shown in Figures 3.33 to 3.39. At the same time the response of the tissues to wet ICs was more varied as assessed subjectively and objectively as are presented in Figures 3.40 to 3.46 and Tables 3.54 and 3.56. Only the ICs LG26 and LG30 were used set

and wet. The set ICs were significantly more osteoconductive and better integrated than the wet ICs (Tables 3.54 and 3.55).

The remodelling of bone at four weeks served to repair damaged tissue and establish a new bone /IC interface. When the wet IC is first introduced to bone in the *in vivo* situation the IC is acidic and toxic to soft and hard tissue.^{34, 46} however by four weeks the rat bone has time to repair as shown in Figure 3.33.

In most cases, the interface between set implants and host was characterized by a layer of notably cellular and, variably mineralized immature bone as with the set IC LG26, which has a high calcium fluoride content as shown in Figure 3.35 and Figure 3.36. In demineralized sections variably mineralized tissues were judged by pale pink staining of hematoxylin and eosin that signifies non-mineralized bone tissue and the darker pink staining represents mineralized bone, thus variably mineralized bone tissue as can be shown in Figure 3.36. In places the cellularity of newly formed bone resulted in woven bone : marrow spaces close to the interface were lined by prominent osteoblasts. Judged subjectively, the layer of new bone varied in thickness for different ICs, for example LG63 with a high concentration of sodium (Figure 3.33 and Figure 3.34) showed less bone thickness than the apatite-stoichiometric glass LG26 with no sodium and high calcium fluoride concentration (Figure 3.36 and 3.37).

In all cases, the periosteal end of the implant was covered by a layer of partly remodelled woven bone for set ICs LG2 to LG63 of the sodium based ICs and LG26 to LG30 of the apatite-stoichiometric based series (Figure 3.36). Similarly, that portion of each implant which projected endosteally (Figure 3.37) was separated from the adjacent vital marrow tissue by a thin layer of mineralized woven bone (Figure 3.38) as is specified with LG26 as a set IC (with a high calcium fluoride content). In demineralized sections mineralized tissue is dark pink using haematoxylin and eosin staining and non-mineralized tissue in comparison is much paler in appearance.

Compared to set ICs particles of wet ICs were less frequently surrounded by newly formed bone and separated from the adjacent healthy marrow tissue as was with the wet IC LG125 which has a high strontium concentration (Figure 3.39). In some cases, wet ICs such as LG125 with a high strontium concentration were surrounded by a combination of woven and more mature bone with partly mineralized osteoid situated more peripherally (Figure 3.40 and Figure 3.41). Some wet ICs such as LG119 with a low strontium concentration appeared to be still evoking a vigorous response at four weeks and were surrounded by combinations of mature bone, osteoid and cellular osteogenic connective tissue (Figure 3.42). The interface

between these wet ICs with a low strontium concentration is demonstrated with LG119 showing cellular osteogenic connective tissue (Figure 3.43).

In places, wet ICs with a high zinc concentration, such as LG130, were surrounded by compressed cellular connective tissue with minimal evidence of new bone apposition (Figure 3.44). Additionally, wet ICs with a high calcium fluoride concentration from the apatite-stoichiometric series, such as LG26, were also surrounded by acellular connective tissue (Figure 3.45).



Figure 3.31 Transverse section through mid-shaft of femur showing extent of normal marrow and minimal cancellous trabeculae; Haematoxylin and Eosin x 42.

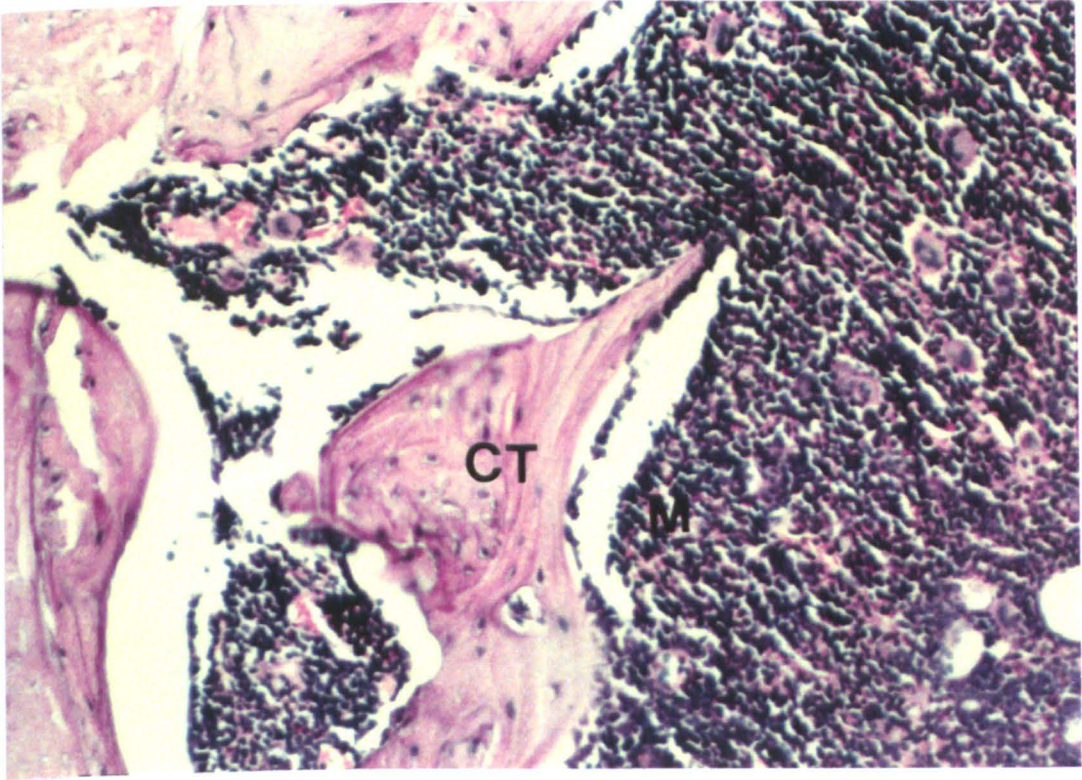


Figure 3.32 Detail from Figure 3.31 showing the surface between normal marrow tissue and mature cancellous trabeculae (CT); Haematoxylin and Eosin x 212.



Figure 3.33 Transverse section of femur showing a rod of ionomeric cement LG63 (IC) completely surrounded by bone; arrows depict six points around the perimeter at which osteoconduction might be evaluated; Haematoxylin and Eosin x 16.

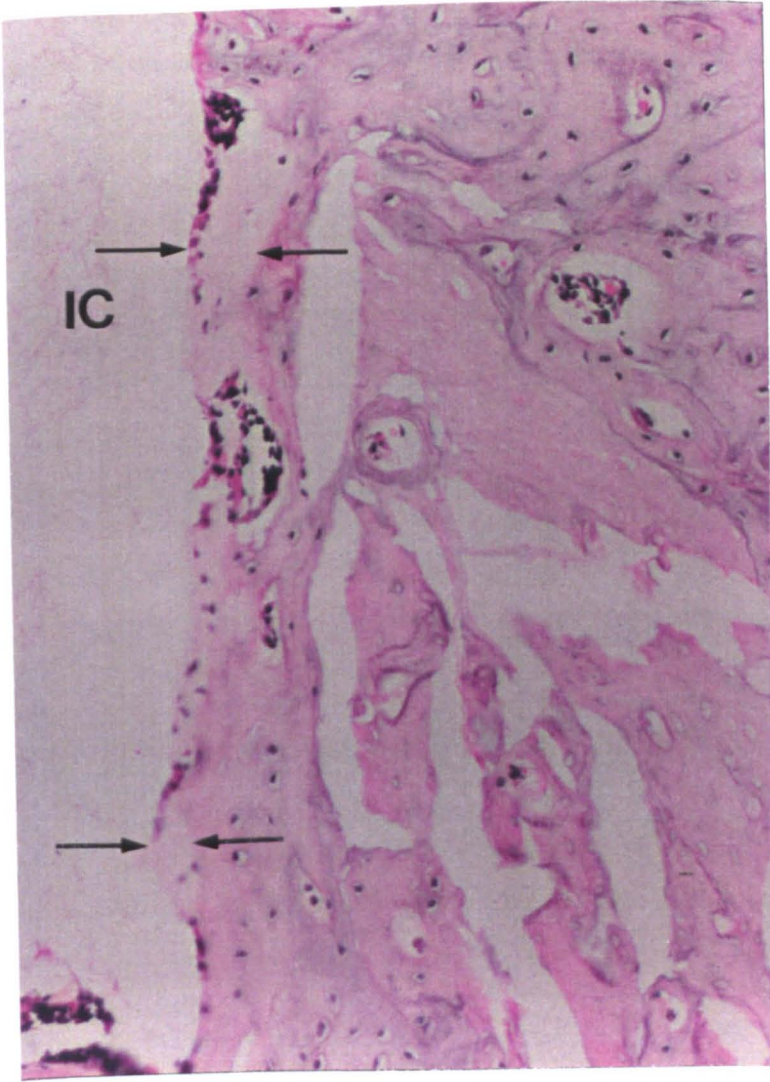


Figure 3.34 Interface between “set” ionomeric cement LG63 (IC) and bone; the opposing arrows demarcate the thickness of newly formed bone and its measurement formed the basis for evaluating osteoconductive potential; Haematoxylin and Eosin x 162.

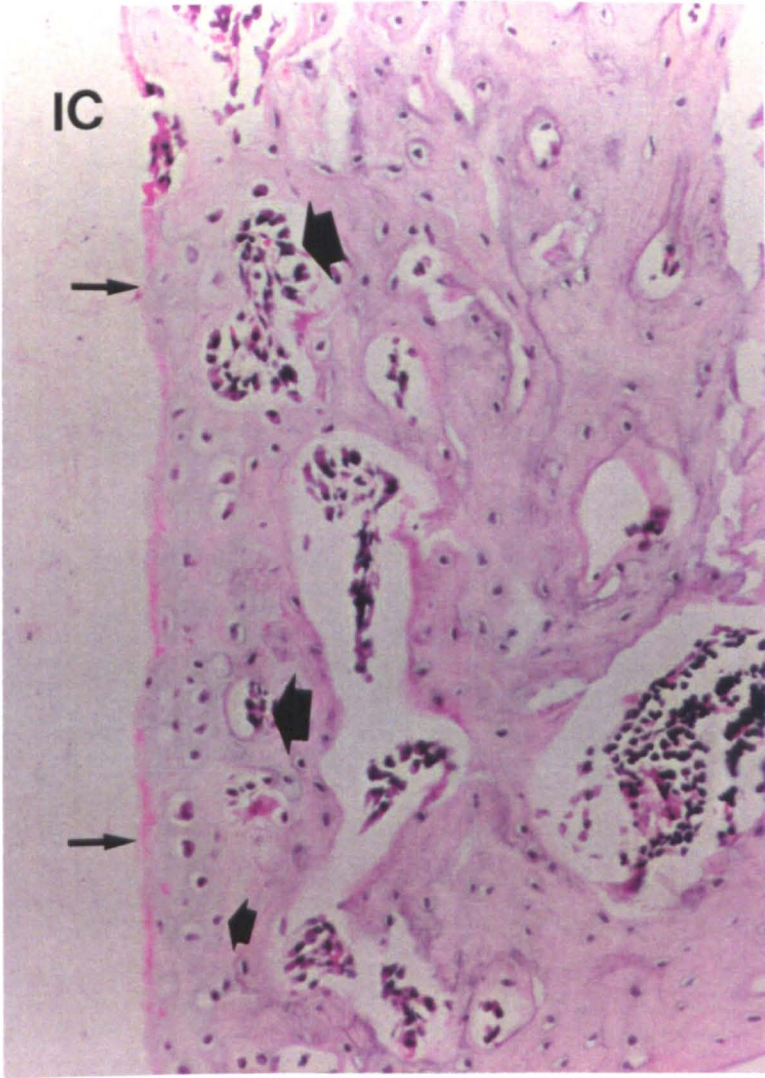


Figure 3.35 Interface (narrow arrows) between the set ionomeric cement LG26 (IC) and newly formed bone; note its cellularity and the chondroid appearance seen focally (small wide arrow); osteoblasts line marrow spaces adjacent to the interface (large wide arrow); Haematoxylin and Eosin x 162.



Figure 3.36 Partly remodelled cortex and new bone (arrows) at the periosteal interface of the set IC implant LG26 (IC); P = periosteum; M = skeletal muscle; Haematoxylin and Eosin x 162.

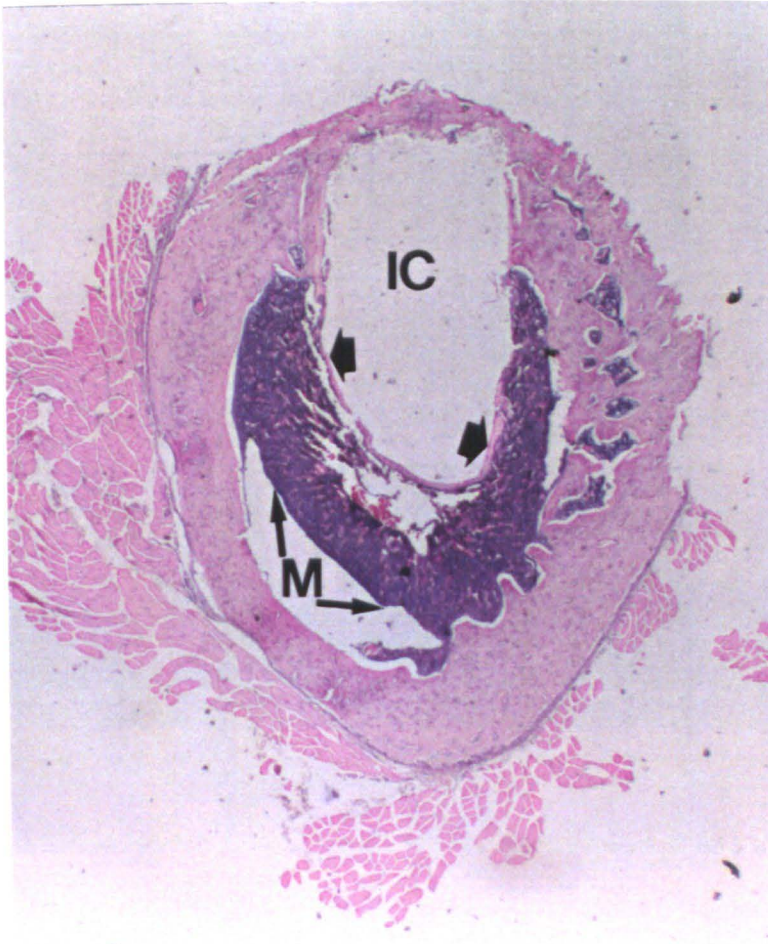


Figure 3.37 Set IC implant LG26 (IC) projecting into marrow cavity and separated from vital marrow (M) by a thin layer of new bone (wide arrows); Haematoxylin and Eosin x 16.

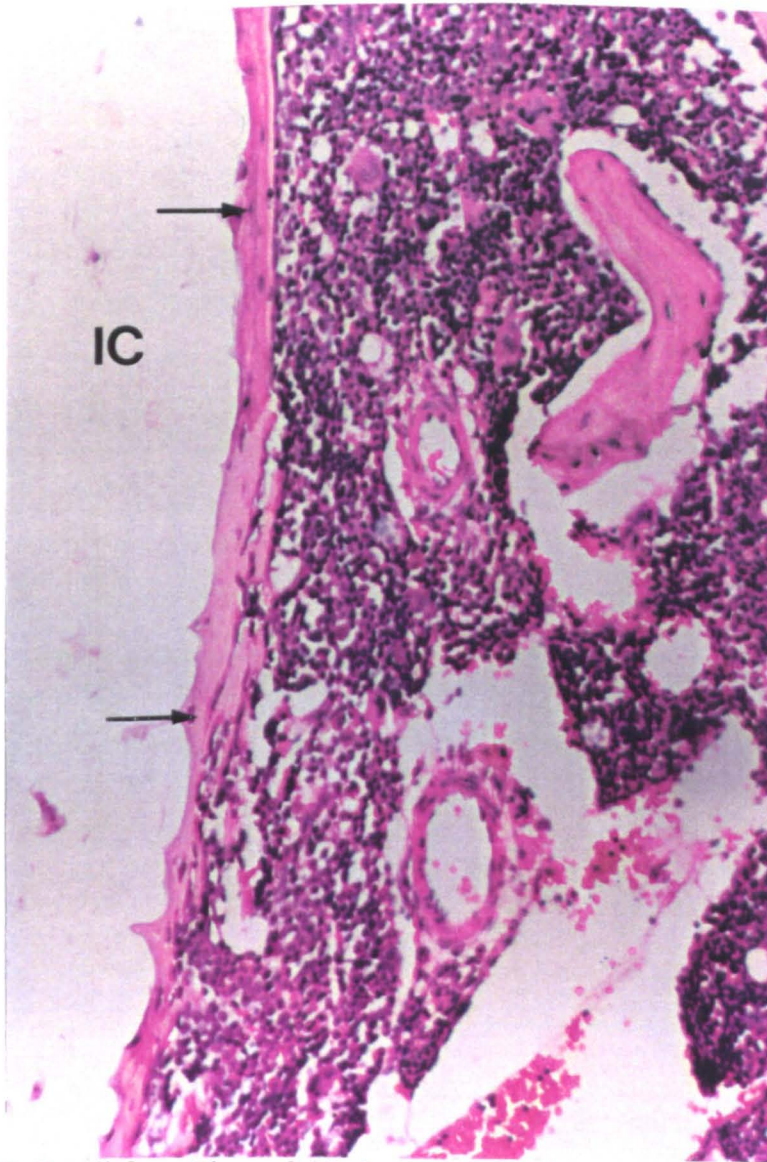


Figure 3.38 Detail from Figure 3.37 showing a thin layer of partly mineralized woven bone (arrows) separating the set implant LG26 (IC) from vital marrow tissue; Haematoxylin and Eosin x 162.

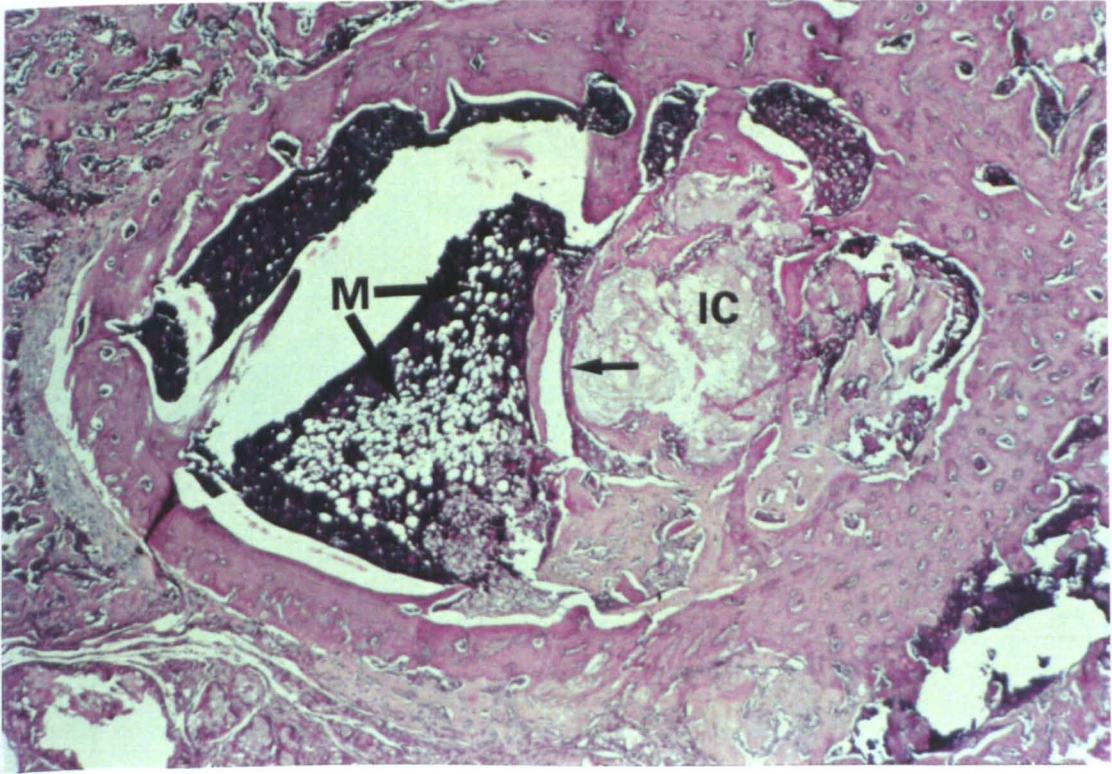


Figure 3.39 Particles of the wet cement LG125 (IC) surrounded by newly formed bone (arrow) and separated from the adjacent healthy marrow tissue (M); Haematoxylin and Eosin x 42.

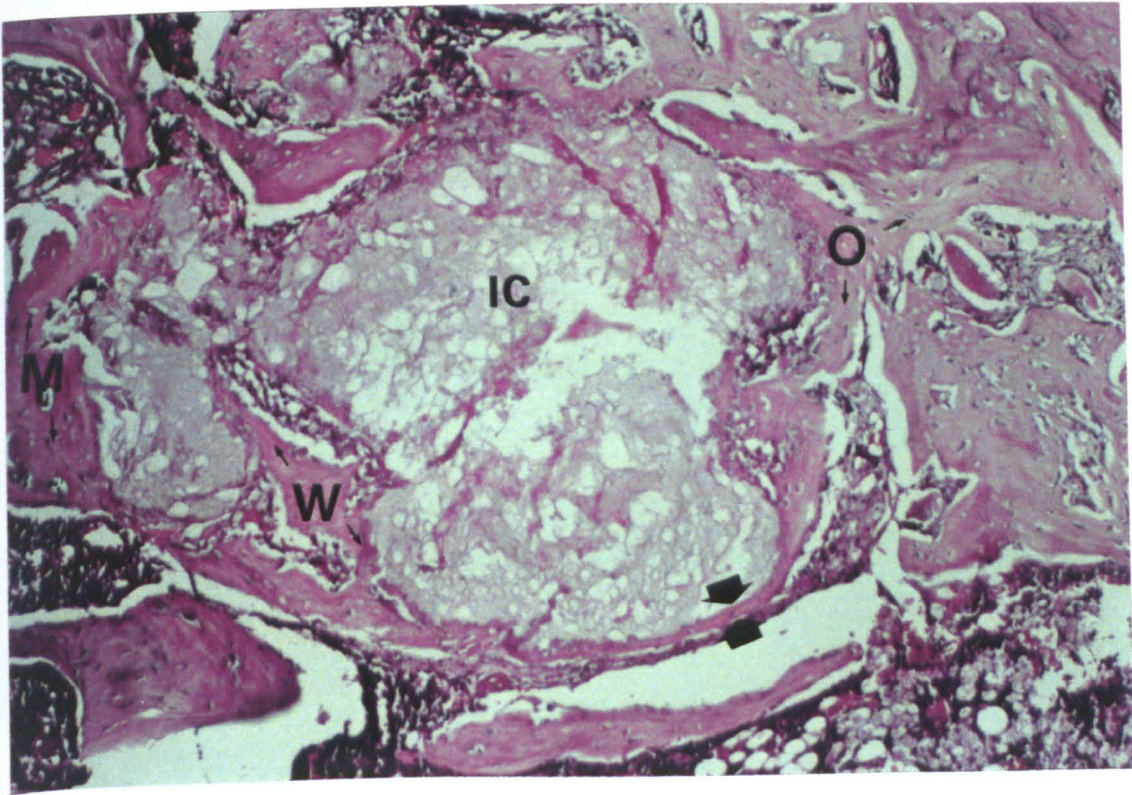


Figure 3.40 Higher power view of Figure 3.39 showing the wet cement LG125 (IC) surrounded by a combination of woven (W) and more mature bone (M) with partly mineralized osteoid (O) situated more peripherally. The wide arrows demarcate the thickness of newly formed bone and its measurement formed the basis for evaluating osteoconductive potential; Haematoxylin and Eosin x 106.

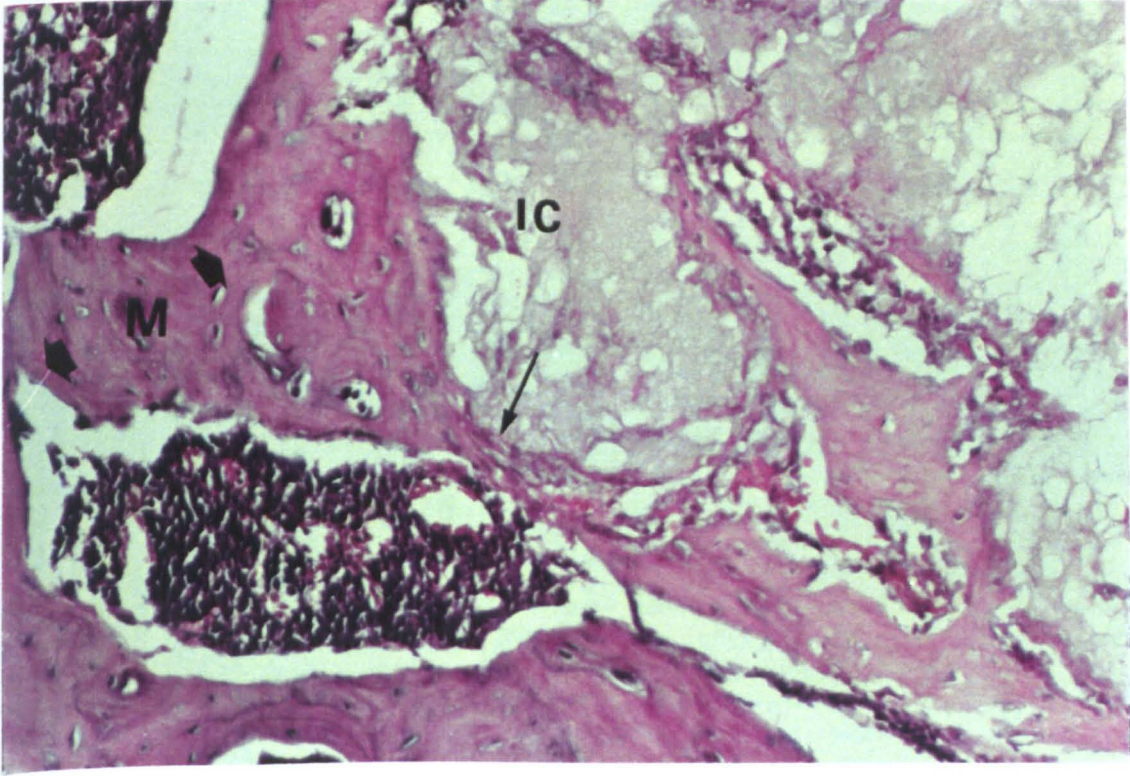


Figure 3.41 Detail from Figure 3.40 showing interface between the wet cement LG125 (IC) and relatively mature bone (M); Haematoxylin and Eosin x 212.

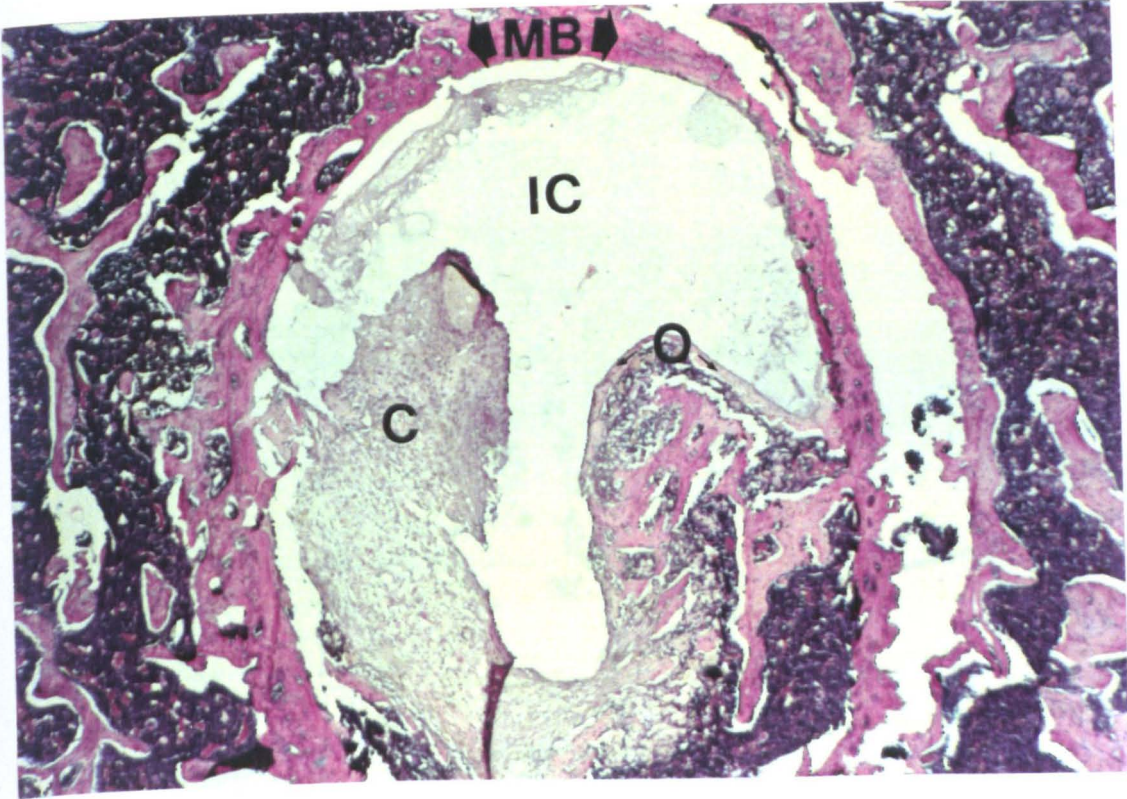


Figure 3.42 Wet cement LG119 (IC) surrounded by a combination of mature bone (MB), osteoid (O) and cellular osteogenic connective tissue (C); Haematoxylin and Eosin x 42.

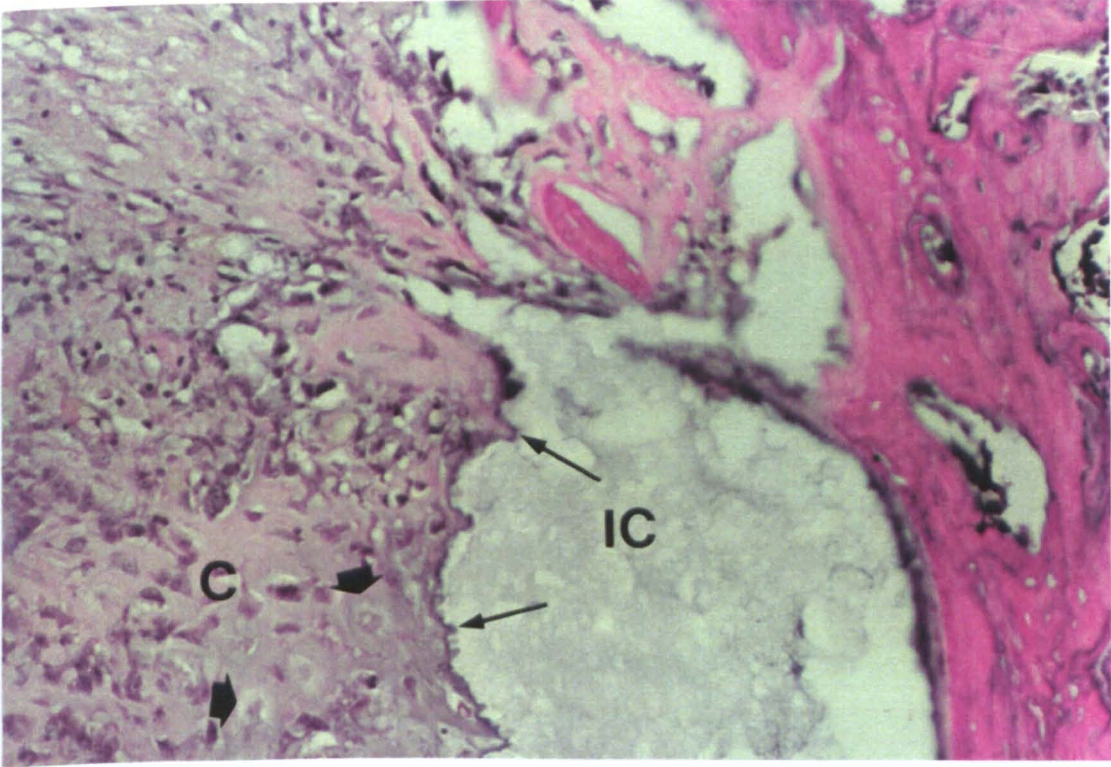


Figure 3.43 Interface between the wet cement LG119 (IC) and notably cellular osteogenic connective tissue (c) (bold arrow); Haematoxylin and Eosin x 212.

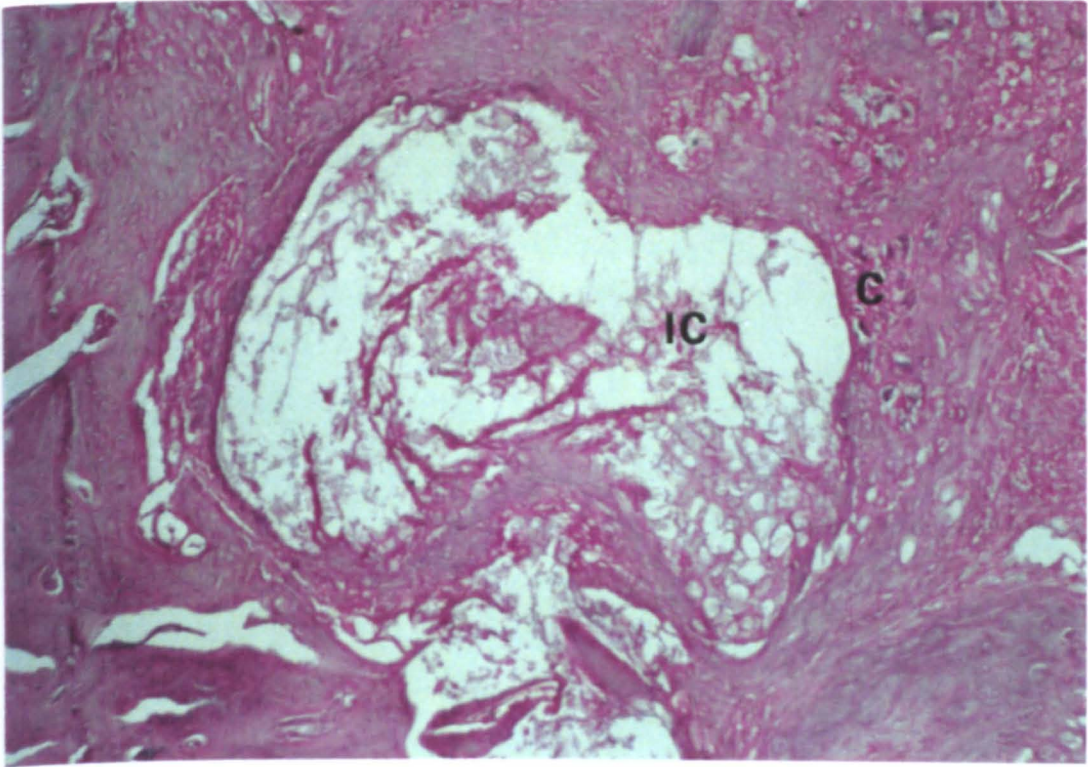


Figure 3.44 Particle of the wet cement LG130 (IC) surrounded by compressed cellular connective tissue (C) with minimal evidence of new bone apposition; Haematoxylin and Eosin x 106.

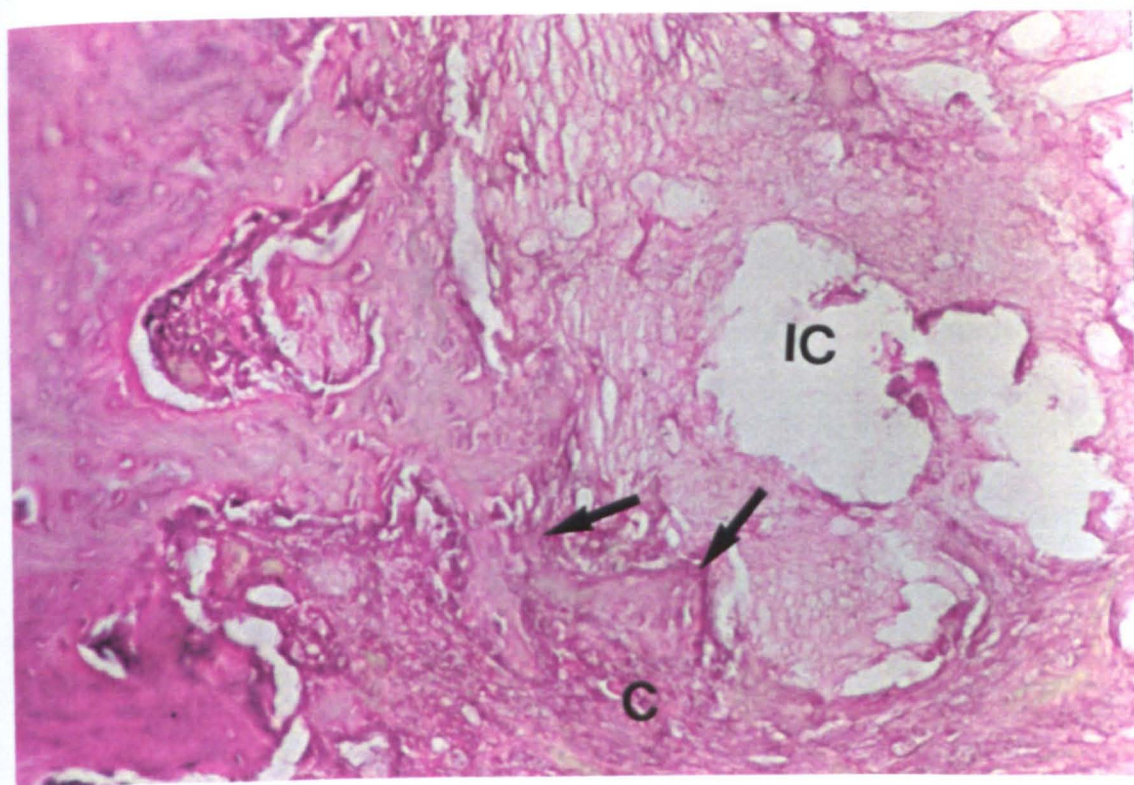


Figure 3.45 The wet cement LG26 (IC) surrounded by acellular connective tissue (C); new bone formation is present peripherally (arrow); Haematoxylin and Eosin x 212.

3.4.2 Histomorphometric results

There were differences in the amount of new bone in contact with the implanted ICs i.e. with the length of the bone/implant interfacial contact (osseointegration) and in the amount of bone formed adjacent to the implants (osteoconduction) as assessed after four weeks (Turn to Appendix and see Tables A1-A16).

Table 3.54 Summary of mean and SD of each set Ionomeric cement at four weeks implantation N=5

Ionomeric cement	% Osseointegration	Osteoconduction (mm)
LG2	37.0 ± 0.8	0.05 ± 0.02
LG6	61.0 ± 2.6	0.09 ± 0.06
LG63	68.0 ± 0.8	0.1 ± 0.03
LG26	80.8 ± 2.6	0.16 ± 0.2
LG27	78.2 ± 1.3	0.08 ± 0.02
LG30	70.6 ± 2.3	0.07 ± 0.02

LG26 had the greatest % osseointegration and osteoconductive values, whereas LG2 has the least % osseointegration and osteoconductive values.

Table 3.55 Summary mean and SD of each wet Ionomeric cement at four weeks implantation N=5

Ionomeric cement	% Osseointegration	Osteoconduction (mm)
LG23 1:2:3	65.5 ± 3.5	0.04 ± 0.03
LG23 1:2:2	50.6 ± 2.9	0.02 ± 0.01
LG26	67.1 ± 1.9	0.06 ± 0.02
LG30	54.5 ± 3.3	0.04 ± 0.03
LG119	56.2 ± 3.8	0.05 ± 0.02
LG125	77.0 ± 2.6	0.08 ± 0.01
LG130	72.4 ± 3.3	0.05 ± 0.03
LG132	42.5 ± 1.3	0.05 ± 0.01

LG125 had the greatest % osseointegration and osteoconductive values. LG132 had the least value for % osseointegration, however, LG23 1:2:2 IC had the least osteoconductive value.

Table 3.56 Summary mean and SD of each of the Acrylic cements at four weeks implantation N=5

Acrylic type	% Osseointegration	Osteoconduction (mm)
Acrylics set	29.9 ± 2.3	0.05 ± 0.02
Acrylics wet	25.9 ± 2.8	0.03 ± 0.02

Acrylic set cements had greater % osseointegrative and osteoconductive values than the wet cements.

The following are all based on the paired Student's t-Test:

-Rods of LG26 (apatite-stoichiometric based cement) were significantly better integrated than the other set rods ($p < 0.05$ in all cases)

-Rods of LG2 (sodium based cement) were significantly less well integrated than other set rods ($p < 0.05$ in all cases).

-Rods of LG26 (apatite-stoichiometric based cement) were significantly more osteoconductive than the other set rods ($p < 0.05$ in all cases).

-Rods of LG2 (sodium based cement) were significantly less osteoconductive than other set rods ($p < 0.05$ in all cases)

-Rods of LG125 (radiopaque strontium based cement) were significantly better integrated than the other wet cements ($p < 0.05$ in all cases)

-Rods of LG23 high powder/liquid ratio (sodium based cement) were significantly less osteoconductive than the other wet cements ($p < 0.05$ in all cases).

-Rods of LG125 (radiopaque strontium based cement) were significantly more osteoconductive than the other wet cements ($p < 0.05$ in all cases).

3.3.2 Immunohistochemical evaluation

3.3.2.1 General Histology

Of the 15 implant sites all healed uneventfully. All the ionomeric cements exhibited formation of new bone on their surface and generally new bone was formed in continuity with the implant surface from the woven bone at the surgical site into the marrow space (Fig 3.31). The operation site was entirely healed and the cortex was repaired. In places the cellularity of the newly formed bone resulted in a chondroid-like appearance: marrow spaces close to the interface were lined by prominent osteoblasts. Even as judged subjectively, the layer of new bone varied in thickness for different ionomeric cements. In all cases, the periosteal end of the implant was covered by a layer of partly remodelled woven bone.

3.3.2.3 Immunohistochemical assessment

LG23

The greatest amount of osteopontin staining (OPN) was in bone associated with the IC LG23 (Figure 3.46). Demineralization of the sections had little effect on OPN, FN and TN staining. There was a significant amount of differential staining of the

reversal lines (Figure 3.47) that were densely thread-like in appearance. Reversal lines indicate the borders between new layers of bone that have been formed on old layers. The brighter staining signified the new woven bone in comparison to the less dense staining showing the mature bone, as OPN was staining the reversal lines but with less intensity.

FN was clearly present as it was staining the woven bone associated with the implant surface of LG23 (Figure 3.48) and megacaryocytes. FN was found in the mineralized matrix of woven bone in a diffuse granular or fibrous arrangement. TN was distributed in soft tissues in the periphery of the endosteum in a diffuse granular pattern immediately adjacent to and within sites of ossification.

LG6

Reversal line staining was apparent at the regions of woven bone greater than that of mature bone. However, the amount of OPN staining was less than that of LG23 associated woven bone (Figure 3.49). FN was again abundant at the implant-bone interface, and in woven bone, staining megacaryocytes. TN was present in the bone associated with the implant interface (Figure 3.50), clearly showing intense staining at the periphery of the endosteum.

LG2

There was less OPN thread-like fluorescence in woven bone associated with LG2, the control, (Figure 3.51) in comparison to LG23 and LG6. Intense staining was

situated at the woven bone in contact with the implant. FN was stained for at the megacaryocytes and was abundant in the bone. TN again stained the bone adjacent to the IC-implant, LG2, at the periphery of the endosteum (Figure 3.52).

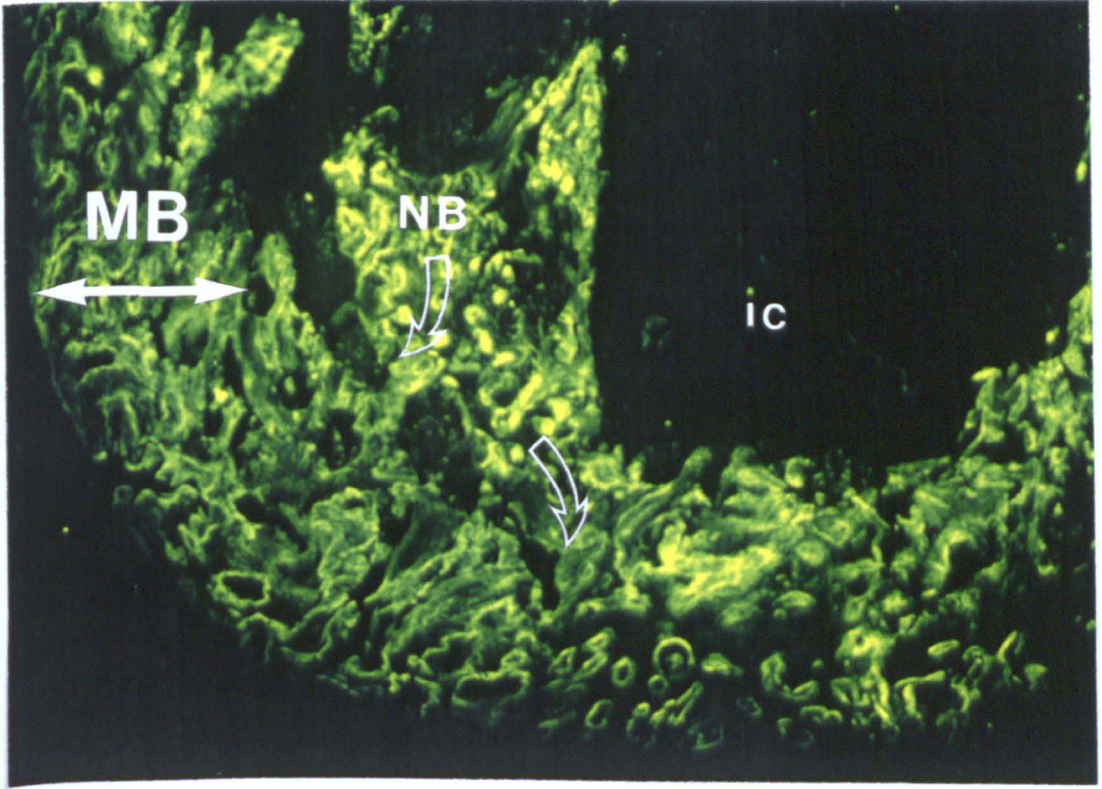


Figure 3.46. OPN immunofluorescence stain at the new woven bone (NB) and with less brightly stained mature bone (MB) with the IC-implant LG23 (IC); x 200.

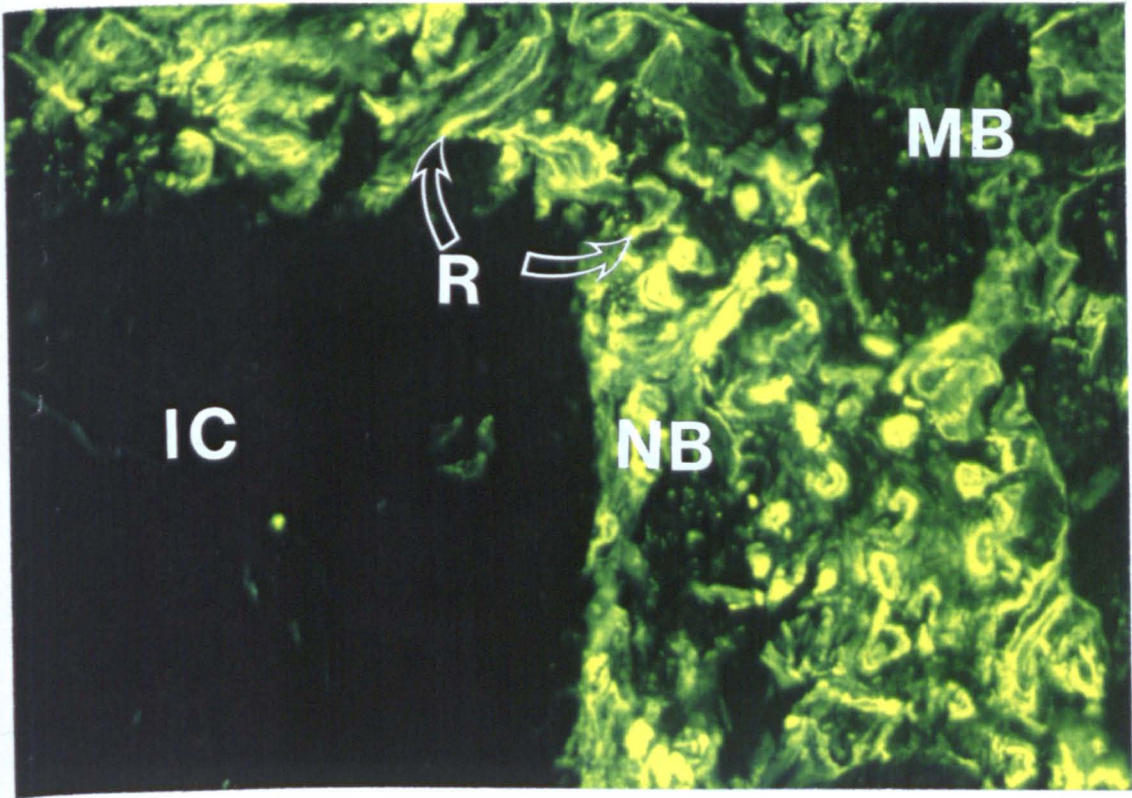


Figure 3.47. OPN immuofluorescence stain at new woven bone densely staining the reversal lines (R) signified by pointed arrows in new bone (NB) and to a lesser degree staining mature bone (MB) with the IC-implant LG23; x 400.

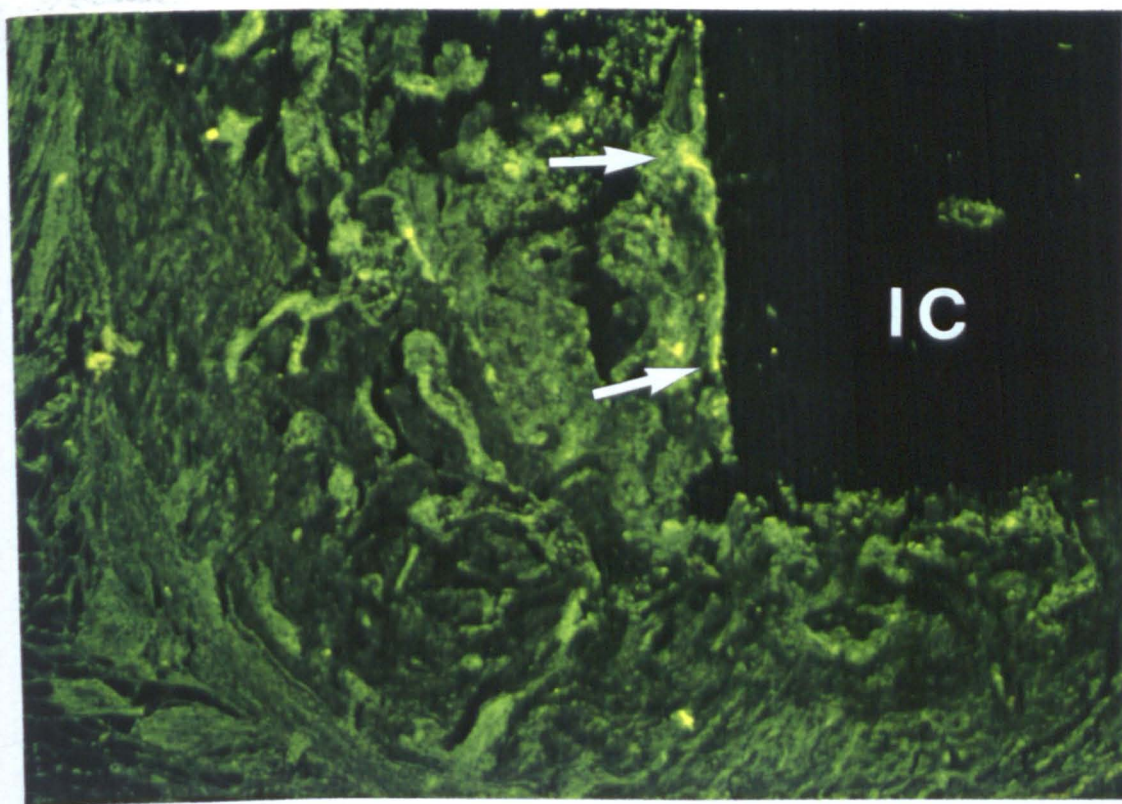


Figure 3.48. FN immunofluorescence stain at the mineralized matrix of woven bone diffuse granular arrangement indicated by arrows pointing at the new woven bone in contact with the IC-implant LG23; x 200.

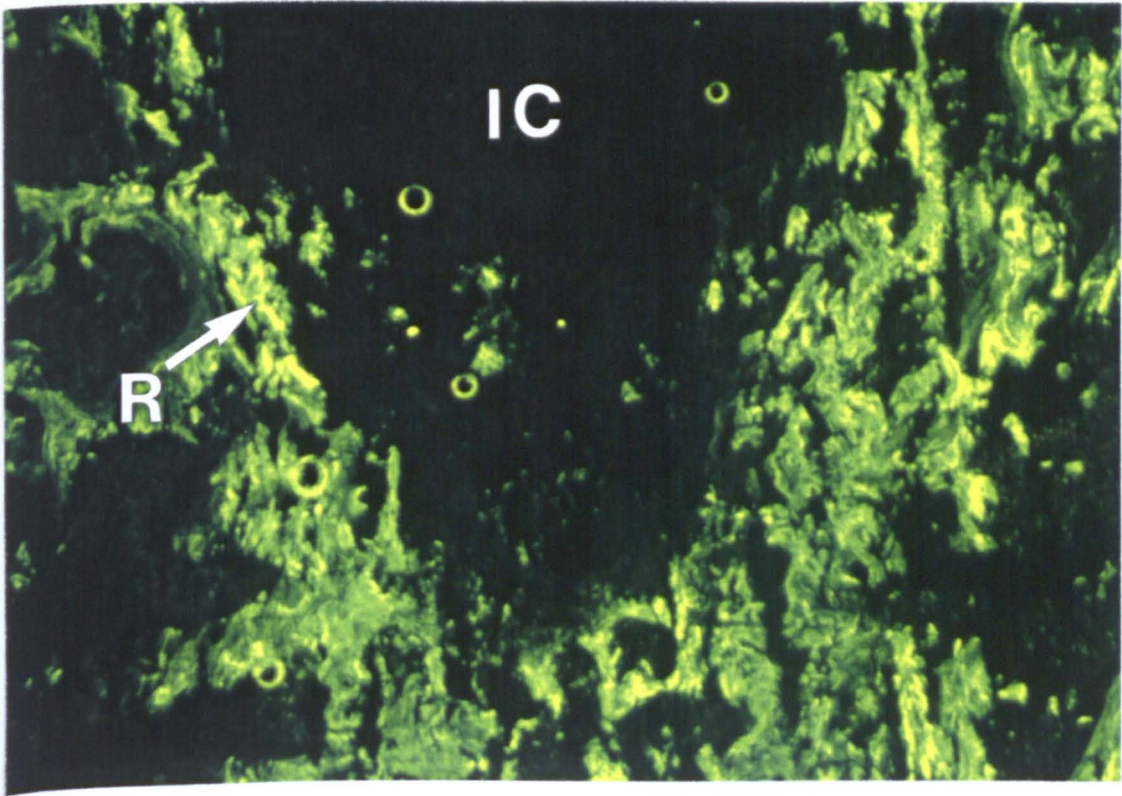


Figure 3.49. OPN immunofluorescence stain at the reversal line (indicated by arrow) in close proximity to the IC-implant LG6; x 200.

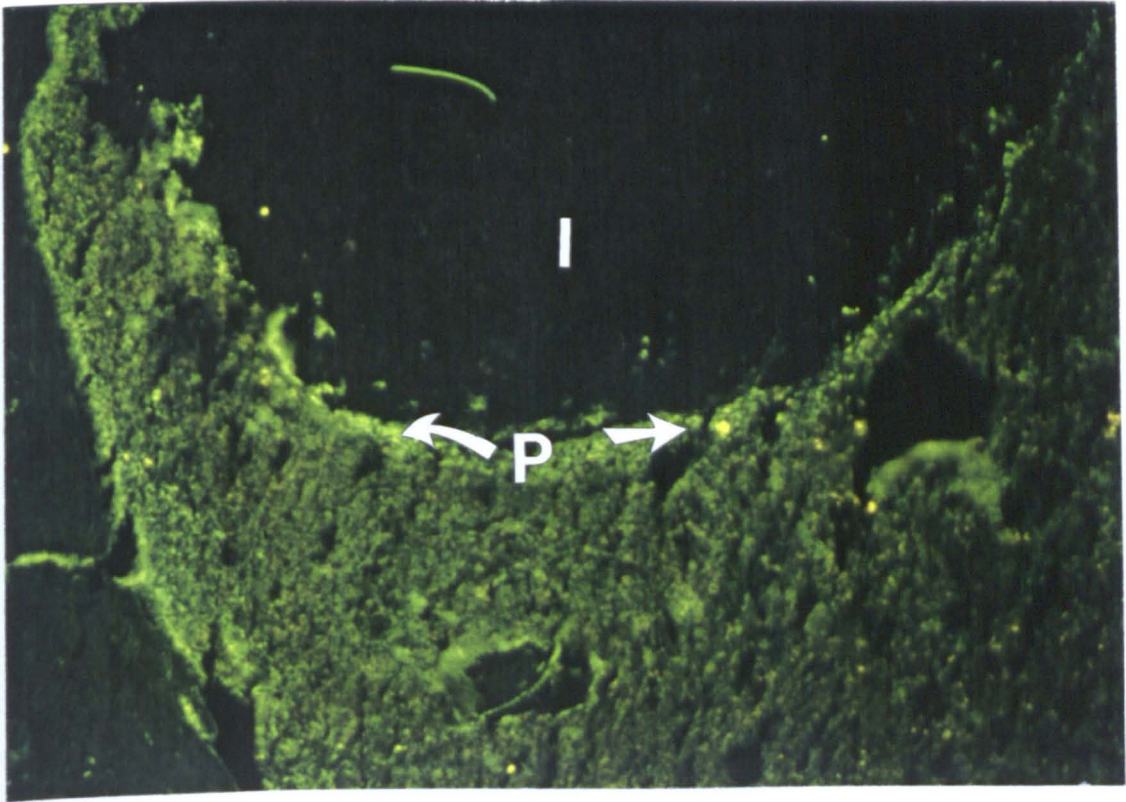


Figure 3.50. TN immunofluorescence stain at the periphery of the endosteum (P), arrows indicate the granular appearance with close contact to the bone associated with the IC- implant (I) LG6; x 100.

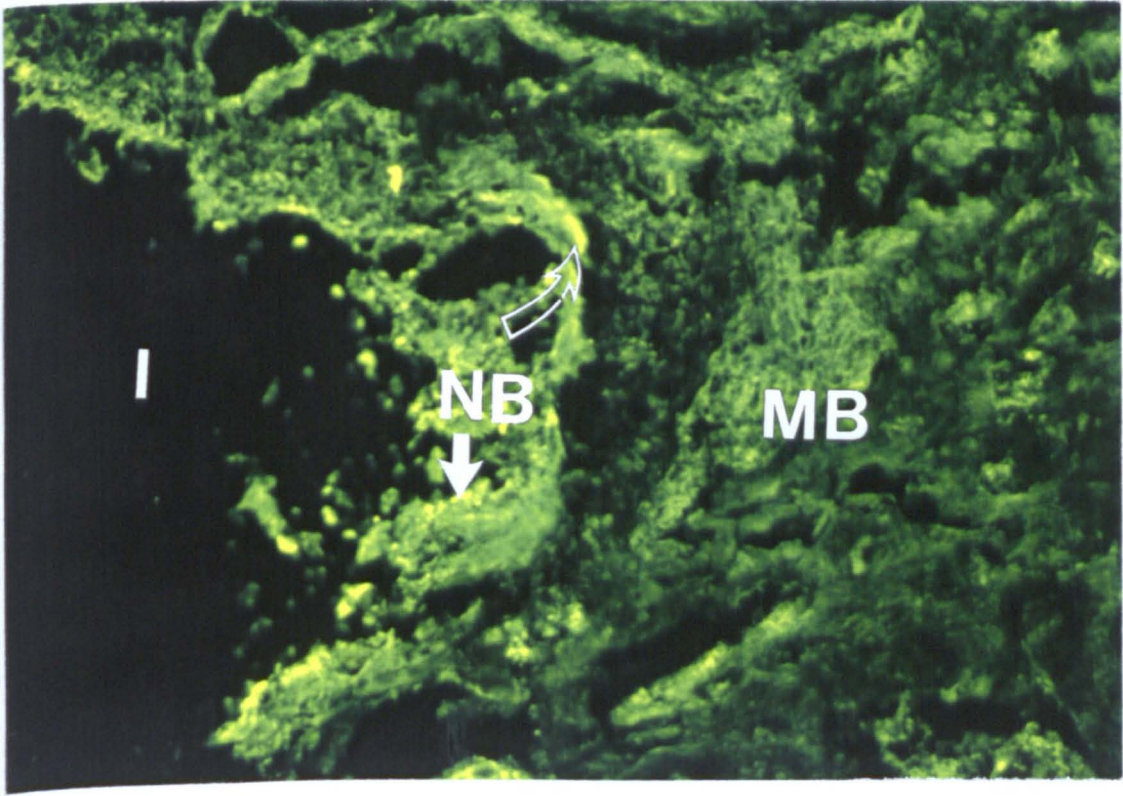


Figure 3.51. OPN immunofluorescent stain in new woven bone (NB) in comparison to mature bone (MB) with the IC implant (I) LG2; x 300.

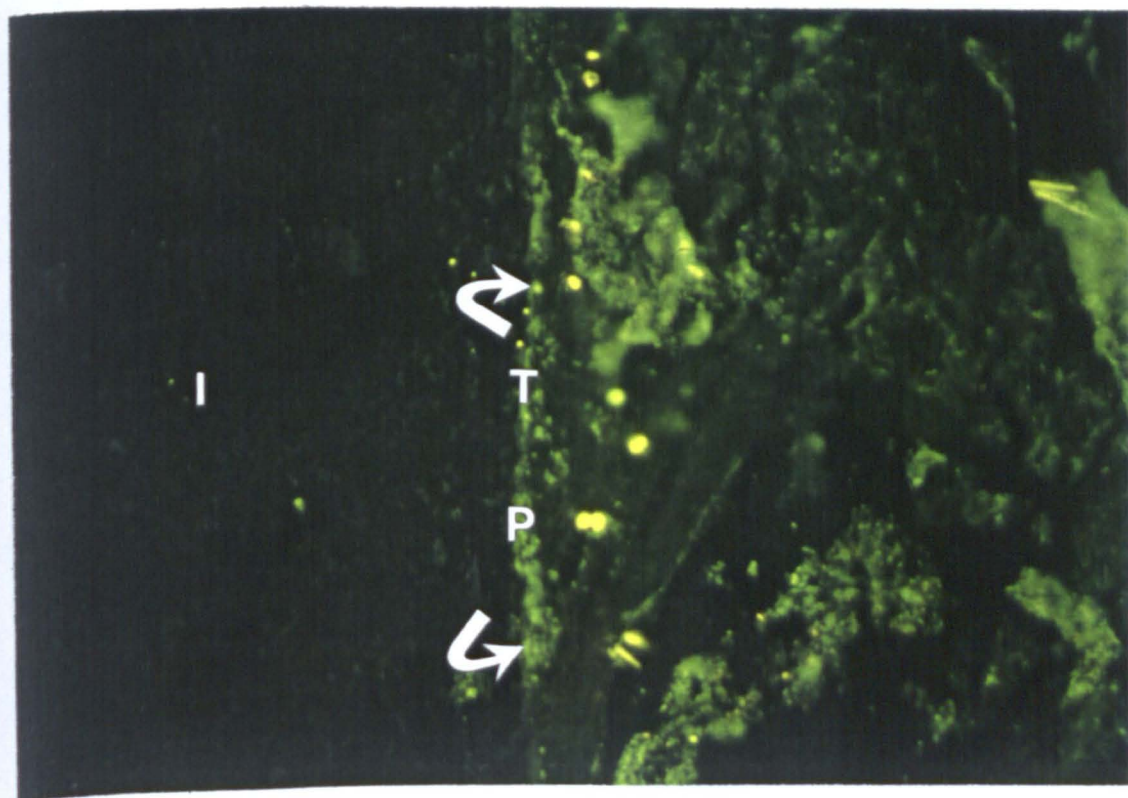


Figure 3.52. TN (T) immunofluorescent stain at the periphery of the endosteum. Note a diffused granular appearance of the new woven bone (NB) associated with the IC-implant LG2 (I) (indicated by arrows), 400

4. GENERAL DISCUSSION

From the review presented in Chapter One (pages 1-22), it is clear that certain formulations of IC have potential as osteoconductive bone substitutes and cements.^{34, 35, 45, 46, 48, 57, 72, 77, 80, 82} The evidence presented in previous studies has relied largely on the use of commercial dental materials or minor variations in formulation.^{35, 45, 48, 81} A minority of groups have had access to experimental materials from the Laboratory of the Government Chemist and industry (e.g. MP4 from Pilkingtons), but precise and reliable data on composition is again lacking.^{34, 46, 62} The situation is further complicated by very recent reports that aluminium ions leached from ICs may be undesirable, inhibiting local bone tissue mineralization¹⁹⁰ and even causing patient death after inappropriate placement.¹⁰⁸

Despite the inadequate data on IC formulation, most authors agree that glass composition is an important factor determining both biocompatibility and osteoconduction. However, to date no reports on the biological response to IC's for biomedical application have been based on a series of defined glass formulations. The development of a large number of well defined materials by Hill *et al* (University of Limerick) presented an excellent opportunity to address this issue. The experiments presented in Chapters Two and Three were designed specifically to investigate the relationship between formulation and biocompatibility. In addition, the potential for clinical use of ICs as bone substitutes and cements was addressed. The following sections discuss the relationship between glass

composition, ion release and biological response *in vitro* and *in vivo*. Clinical handling characteristics are also important and these are discussed first.

4.1 Setting and working times

Setting and working times are very important characteristics. If the material is difficult to handle in the operating theatre or sets too quickly, it will be totally unsuitable for use as a bone cement. To date, no appropriate times have been described for IC bone cements, although these parameters have been defined for acrylic bone cements (4 to 15 min by the “International Standard Organisation” (ISO). Some attempt has been made by the author to define the needs in an IC system (Section 2.2.1). In brief, it was decided that a material required a working time >150 seconds to have a practical application in the operating theatre.

The setting and working times required for the surgical placement of ICs for use as a bone substitute in maxillofacial surgery or as a hip replacement were studied. No attempt was made during this study to modify the setting and working times of cements. There is however potential to modify the setting characteristics of these ICs by the addition of tartaric acid, which may improve the manipulation of the cement paste, sharpen the set by accelerating the precipitation process, and may increase the cements strength. The addition of tartaric acid would be suitable for cements with less fluoride.

Other factors affecting the setting time would be the glass composition, especially with the alumina/silicate ratio and fluoride content. Particle size of the glass powder

is important as the finer the powder the faster the set and the shorter the working time. The relative proportions of the constituents in the cement mix i.e. glass, poly(acrylic) acid and water are important as the greater the proportion of the glass and the lower the proportion of water the faster the set and the shorter the working time. On mixing, all the ICs, with the exception of LG23 at a low powder /liquid ratio, were sufficiently viscous to prevent flow and loss from the surgical field during placement. This would assist the surgeon and avoid displacement of material into adjacent tissues.

Some of the glasses evaluated did not form a cement at the ratios investigated. After being mixed with 0.2 g of poly(acrylic) acid, 0.3 ml water the 1g of the glass powder, LG94, LG93, LG92 and LG91 had not undergone gelation after 40 min. It has been reported that fluoride prolongs working time,⁵¹ glasses LG91-LG94 had a high calcium fluoride content (2.2-2.6 mole fractions) which may explain their poor cement forming properties. The glasses used in Tables 3.1-3.5 had fluoride mole fractions of less than 2.0, which may explain why they had shorter setting and working times.^{52,191} Formulation clearly has an effect on the mixing and working properties of ICs (Introduction, page 8).

The acrylic cements had the longest setting time (540 seconds) (Table 3.5) and were found to be the least biocompatible (Table 3.56) this could be from the exothermic setting reaction that may cause thermal necrosis or the release of monomer.²⁸⁻³²

Despite their poor performance in this study, many surgeons are familiar with the behaviour of this biomaterial in the theatre.

Of the materials tested under simulated surgical conditions, those with setting times >150 seconds and working times >120 seconds might be considered most suitable for use as an *in situ* setting bone substitute or cement for low-load bearing applications. Materials that met this requirement were LG26, LG27, LG30 and the acrylics. LG26 had a longer working time as it had a greater concentration of fluoride than LG27 and LG30. ^{51, 191}

4.2 Relationship between glass composition and ion release

Ion release is believed to be an important determinant of biocompatibility of ICs. Ion release experiments were designed to model these events prior to cell culture experiments. The results of extensive ion release studies are given in Chapter Three (Tables 3.6 to 3.49).

In general, it was observed that the ions released from a set IC reflected closely to the cement formulation. However, a number of subtle but important deviations from this trend were observed. There was a relation between calcium and phosphate with some of the ICs. In that as the calcium content of the glass increased there was less phosphate released (see Table 3.45 of Results chapter).

The importance of some of these deviations will be more clear in the discussion of biocompatibility (Section 4.3). The influence of composition on the release of each ion will be considered separately before looking at the effect of this phenomenon on biocompatibility.

4.2.1 Fluoride ion release

Ion release experiments were carried out by placing various glasses as set IC discs (see Chapter 2, Materials and Method section 2.1.1) into 50 ml of pure water.

While fluoride ion release is clearly one of the critical factors determining biocompatibility and osteoconduction, no groups have yet reported an optimum range for elution of this ion. In this study, LG26 and LG125 were found to perform best in the *in vivo* implantation experiments (see Tables 3.54 and 3.55). It is not unreasonable to assume that fluoride release was near optimum for this animal model.

Care must be taken when extrapolating these results to the human clinical situation. Firstly, the young rat model may have a different metabolism to an adult human who may be compromised by trauma or disease. The shape of set IC bone cement in the body would be of an irregular shape and would present a greater surface area for ion release. Therefore further experiments are required to optimise the release of fluoride for a medical grade IC. It is important to remember that a range of other ions such as aluminium, silicate, calcium and phosphate have biological activity and

are implicated in the osteoconductive behaviour of ICs (see Section 1.1.4).^{34-36, 46, 81, 84, 92-99, 114, 192-195}

Much evidence suggests that there is more than one mechanism responsible for fluoride ion release. The most accepted theory to date is the counter ion mechanism.⁵⁰ The counter ion mechanism involves the simultaneous release of an alkali metal cation, for example a sodium counter ion.⁵⁰ The monovalent sodium cation and the negative fluoride ions have a charge balancing effect, where fluoride is released as sodium fluoride. LG6 with a high sodium concentration released the greatest amount of free fluoride (section 2.1.1a and Table 3.16). This also applied to LG69 (Table 3.6 and section 2.1.1 a ii) from the monovalent cation based ICs, releasing the greatest initial burst of fluoride from all the ICs used in this study (Table 3.6) and has a high sodium content (0.5 mole fraction, Figure 3.1 to Figure 3.3) relating ion release to cement formulation.

The ion exchange mechanism explains how cements with no alkali metal content are still able to release fluoride indicating that a soluble counter ion is not always required. At all times the cements in this study demonstrated a negative ion balance where there were more negative ions leaving the cement than positive ions. While this experiment was not designed to specifically study ion release mechanism the results (Table 3.6 to 3.49) indicate that the cements may also release fluoride ions by an ion exchange mechanism where the fluoride ion in the cement would be exchanged for a hydroxyl group from the water in the elution medium.¹⁹⁵

Glasses containing a low fluoride concentration released a low concentration of fluoride ions, for example LG45 (Table 3.8 and section 2.1.1 h) showing a positive relation between fluoride ion release and cement formulae i.e. less fluoride in the cement resulted in less fluoride ion release. Figure 3.5 showed a strong correlation coefficient of 1 between fluoride glass content and fluoride ion release. Fluoride ion release was found to increase as the sodium or calcium fluoride content of the glass increased.

There was a greater fluoride release in glasses with an increased silica concentration and decreasing aluminium concentration glass composition, for example, LG81 (Table 3.10 and section 2.1.1 k). While fluoride ion release was clearly one of the critical factors determining biocompatibility and osteoconduction, no groups have yet reported an optimum range for elution of this ion.

The total and free fluoride ion results for the monovalent cation series (Table 3.6 and Table 3.16) and apatite-stoichiometric based series (Table 3.7, Table 3.17 and Figure 3.4) showed no significant difference between the measurements made with and without TISAB III indicating that virtually all the fluoride ions eluted were released as free fluoride ions and were not chelated to metal cations, such as with aluminium.

4.2.1 b) Fluoride ion release of LG2 and LG26 in alpha-minimal essential medium and autoclaving

ICs were placed in α -Minimal essential media (α -MEM) to determine the amount of fluoride eluted in simulated body fluid. α -MEM contained inorganic ions close in concentration to those in human blood plasma. LG26 had a high calcium fluoride concentration and for this reason released more fluoride (see Table 3.13 and section 2.1.1 b) than LG2. This was beneficial as fluoride ions at certain concentrations are potentially osteoconductive.^{34-36, 46, 84, 92-95}

Less fluoride ions were released by LG2 and LG26 α -MEM (Table 3.13) than in water (Table 3.6 and 3.7). Autoclaving effects of the ICs were investigated because the set rods were sterilised by autoclaving. There was an initial burst of fluoride ions in the water during autoclaving. Contact with aqueous fluids must be avoided, for these removed ions such as fluoride⁵¹ and prior to placing IC discs into α -MEM. The fluoride release from a material depends upon the length of maturation of the matrix prior to first exposure to moisture. The shorter the maturation period the greater the fluoride ion release.¹⁹⁶ The maturation time for these cements was 24 hours therefore a low amount of fluoride was released. This also applied to results in Table 3.15. An alternative method to sterilise ICs to avoid water contact would be to γ -irradiate the ICs.

During setting of an IC a paste was formed where the basic glass powder reacted with poly(acrylic) acid to form a salt hydrogel. This hydrogel was the cement binding matrix. This ionic reaction took place in three stages. Firstly, a surface decomposition of the glass particles by hydronium ions (H_3O^+) from poly(acrylic) acid solution took place. This resulted in the release of Al^{3+} and Ca^{2+} leading to the aqueous phase. Fluoride ions in the form of sodium fluoride were also released from the IC for a sustained period of time.¹⁹⁷

Secondly, a calcium poly(acrylic) gel resulted from reaction of calcium with poly(acrylic) acid. The final reaction was the formation of aluminium poly(acrylic) acid which cross-linked the poly(anion) chains. The diffusion of Ca^+ and Al^{3+} ions from the glass into the aqueous phase was facilitated by formation of fluoro-complexes.¹⁹⁷ Only a thin surface layer of glass particles was involved in the cement formation reaction. The set cement consisted of a solid insoluble aluminium-calcium poly(acrylic) matrix in which non-reacted glass powder particles were surrounded by a thin silica gel layer (filling materials) and water molecules. In the early stage of setting, a proportion of the cement-forming aluminium, calcium and fluoride ions were present in soluble form and could be dissolved out of the cement by aqueous fluids. Once these ions were leached out, they were unavailable for matrix formation and the surface was softened. The cement was sensitive to loss of water during the third step of the setting reaction and for some time in its set form, which may have lead to shrinkage and surface cracking.¹⁹⁷ Under conditions of

complete desiccation the cement was dramatically weakened. In a biological system, for instance in the bone cavity, this could not happen. Al^{3+} and Ca^{2+} were solidly fixed in the cement phase and only appeared as trace elements.¹⁹⁷

4.2.2 Sodium ion release

The sodium (Na^+) monovalent cation is an important charge balance in the counter ion mechanism proposed to account for fluoride ion release from ICs⁵⁰ and does have some physiological importance.⁹¹ Increasing sodium glass content lead to increased sodium ion release in the monovalent cation series of ICs relating to cement formulation(Section 2.1.1 a). For example, LG6 released the most sodium ($51.2 \mu\text{molg}^{-1}$ of sodium at 84 days) and had a high sodium glass content (see Table 3.18 and Chapter 2, section 2.1.1, Figure 3.1 to Figure 3.3). There was a strong correlation between sodium glass content and sodium ion release as shown in Figure 3.6 where the correlation coefficient was 0.99. This indicted that sodium ion release was dependent on the sodium glass content.

Sodium ion release was detected from all ICs, even the apatite stoichiometric series of glasses, that had a non-sodium formula (Chapter 2, section 2.1.1 and Table 3.19 of Results chapter). The sodium ion release from this series was explained by possible contamination during glass preparation, grinding, washing or handling of the glass. LG6 released a high concentration of fluoride and sodium from the monovalent cation series of ICs (see Tables 3.6 and 3.18). It may be that fluoride is partially released as sodium fluoride via the counter ion mechanism.⁵⁰

4.2.3 Potassium ion release

The potassium(K^+) monovalent cation may be considered a charge balance in the counter ion mechanism. However, no group as yet has demonstrated the ability of potassium to be released with fluoride via the counter ion mechanism.⁵⁰ Selected ICs were measured for potassium ion release as it does have some physiological importance⁹¹ and is considered important in the body with respect to cell mass.⁹¹ LG8 eluted a greater amount of fluoride ions than LG7 showing a possible relation between fluoride ion release (Table 3.6) and potassium ion release (Table 3.20) with the monovalent cation series. LG8 has a greater potassium glass content than LG7 showing a relation to cement formulation, and for this reason it may be the potassium ion, a monovalent cation, that could be partially eluted with fluoride by the counter ion mechanism⁵⁰ as a counter ion.

Aluminium ion release

Aluminium is important in the formation of ICs and with their biological properties. Aluminium in ICs determined whether the glass network would breakdown at all when exposed to acids, and the rate at which the breakdown occurred⁵¹ and was an important constituent for cement formation.⁵¹ ICs that were high in aluminium content are opaque.⁵¹ Alumina reduces the setting time of the cements⁵¹ and increases their compressive strength.⁵¹ Although strength may be increased by these means it is achieved at the expense of translucency,⁵¹ which is an important factor in dental applications. It has been reported that aluminium ions are released for a short period and can be absorbed by tooth enamel, conferring acid-resistance.

Aluminium has many disadvantages and advantages in a physiological system (see Section 1.1.4 d). It has been reported to bind to constituents of bone tissue such as collagen that may build a positive potential on collagen fibrils and prevent mineralization.^{190, 192} The binding of aluminium on HA crystals and bone constituents, such as collagen, may be building a positive surface potential which is responsible for the inhibition of HA crystal growth and bone mineralization.¹⁹²

In addition to this aluminium has been reported to enhance the mobilisation of calcium from bone by a cell-independent mechanism¹⁰⁷ and can disrupt the conversion of the initial formed soluble amorphous bone mineral to its crystalline form. If this occurs, the amorphous form of the mineral could be readily dissolved and eluted from the tissue.¹⁰⁷ Chronic aluminium toxicity has been reported to have lead to Alzheimer's disease⁸¹ and aluminium encephalopathy.¹⁰⁸

By contrast, other groups have found that aluminium at low concentrations have stimulated the expansion of osteoblast (and the subsequent apposition of lamellar bone).^{102, 103} These conflicting results may be from small variations in aluminium concentration. Trabecular generation has been reported¹⁰¹ and may be an indication of a latent potential for skeletal regeneration without re-enacting *de novo* processes. For these reasons it would be safer if aluminium levels were kept low. Recently it has been reported that in fish silicic acid protects against the toxicity of aluminium

by the formation of hydroxyaluminosilicates (HAS) and a mechanism of formation of these species has been suggested.²⁰⁰⁻²⁰²

While aluminium ion release is a major factor in determining biocompatibility and perhaps osteoconduction, no groups have yet reported an optimum range for elution of this ion. In this study, LG26 and LG125 were found to perform best in the *in vivo* implantation experiments (Table 3.54 and 3.55). It is not unreasonable to assume that aluminium release was near optimum for this animal model. These materials were expected to be suitable at aluminium levels less than 0.2 nmol g^{-1} as this was the maximum aluminium ion release from the ICs tested (Chapter 3, Table 3.22 to Table 3.27 and Figure 3.10). However, care must be taken when extrapolating these results to the human clinical situation as with fluoride.

Aluminium is recommended to be kept at low levels as the binding of aluminium ions to hydroxyapatite nuclei in bone can inhibit further precipitation and crystal growth.^{190, 192}

The monovalent cation based IC LG69 eluted the greatest amount of aluminium from all the ICs tested in this study (2.6 nmol/g in 42 days). There was no distinctive relation as to why there was a higher aluminium elution from LG69 than the other ICs tested, only that there was a higher sodium concentration (0.5 mole fractions) in LG69 glass than others tested that can be shown in Figure 3.7 (Results chapter) where there was a relation between increased sodium glass composition and

positive correlation with aluminium ion release with a correlation coefficient of 0.97. This strong correlation of aluminium ion release increase was evident in Figure 3.8 with increasing sodium glass content at 21 days showing a relation to its IC formulation. Figure 3.9 showed a positive correlation between increasing potassium glass content and aluminium release increase (correlation coefficient=0.87).

The low aluminium release from the set cements indicated that there was no significant dissolution of the cement matrix and that ion release occurred largely by a diffusion process, rather than by surface dissolution. Aluminium ions were small and of high charge (Al^{3+}) and were strongly chelated by the poly(acrylic) acid of the polysalt matrix and were bound in the cement reducing diffusion. Diffusion is the process by which matter is transported from one part of the system to another as a result of random molecular motion. The diffusional aspects in polymer systems have been strongly related to the fractional free volume present. In polymers, segmental molecular motion allowed diffusion of molecules to jump from one sorption site to the next. Diffusive motion depends on penetrant size, shape and concentration, component interactions and temperature. The morphology and the number or type of structural defects in the polymer were also important. Ficks first law was the rate of transport of a diffusing substance through a unit area into an absorbing solid or fluid is:

$$J = -D \frac{dc}{dx} \quad (203)$$

Where J is the rate of transfer of diffusing substance,

C is the concentration .

X is some distance into absorbing solid or fluid and

D is the diffusional coefficient.

Frequently diffusion occurs in one direction only. Hence, a concentration gradient exists only along the x-axis. In such cases the rate of mass transfer was given by Ficks second law which stated:

$$dC/dt = D \frac{d^2 C}{dx^2} \quad (203)$$

where t is the time. The most common equation used for the absorption/desorption processes, for short times was:

$$M_t/M_\infty = 4(Dt/\pi h^2)^{1/2}$$

Where M_∞ is the equilibrium mass uptake,

M_t is the mass uptake at time t and

H is the thickness. (203)

H was usually small to minimise edge effects and to permit one dimensional penetrant diffusion. In general, the diffusional behaviour and transport mechanisms in glass polymers were classified according to the relative rates of mobility of the penetrant and the polymer segments. Three basic categories exist, which may be described as follows:-

- (1) Fickian Diffusion was where the rate of penetrant diffusion was much less than that of the polymer segmental mobility. Sorption equilibrium was rapidly obtained, with no dependence on swelling kinetics being observed. In mass

uptake profiles, a linear relationship was seen between $M_t/M_\infty \sim 0.6$. D , diffusional coefficient, may be calculated from the linear slope.

(2) Extreme Fickian diffusion occurred when the penetrant mobility was much greater than the polymer relaxation process. Here sorption processes were found to be strongly dependent on swelling kinetics and mass uptake profiles showed a linear relationship with time. The diffusing penetrant moved as a sharp front of constant velocity. Many polymeric systems exhibit this type of behaviour, especially the alcohol/glass polymer systems e.g. methanol/PMMA.

(3) Non-Fickian or anomalous diffusion occurs when the penetrant mobility and the polymer segmental relaxation were comparable. (1) and (2) may be as the two limiting types of transport behaviour, with anomalous diffusion being between them. They could be distinguished by the slope of the sorption-time curve represented as follows: $-M_t/M_\infty = Kt^n$

Where M_t is the relative weight gain at time t ,

M_∞ is the equilibrium relative weight gain and

K and n are constants.

For (1) $n=1/2$

(2) $n=1$

(3) $1/2 < n < 1$.

Permeation was a three part process, involving

(a) a solution of small molecules in a polymer,

(b) molecule migration or diffusion through the polymer according to the concentration gradient and

(c) the molecule emergence at the outer surface.

Permeability, P , was the product of the solubility, S , and diffusivity, D , and where solubility obeys Henry's law $P=DS$.²⁰⁴ The permeation of water molecules varied greatly from polymer to polymer. This variation was greatly influenced by the degree of interaction which was possible between the water molecule and polar substitutes of the polymer chains. If mass, as in ions, were transferred from an IC to an immersion medium and vice versa as in IC fluoride uptake studies, the mechanism by which this process occurred could only be by diffusion.

If ICs were partly insoluble due to a combination of thermodynamic, kinetic and structural factors, the only mechanism which will allow structural degradation to occur in water would be by diffusion. Water molecules, which are relatively small in contrast with macromolecules, were strongly associated through hydrogen bond formation, in both the liquid and solid states. In polar molecules, strong localised interactions may develop while in non-polar materials, clustering or association of the absorbed water molecules may have occurred.²⁰³

As aluminium release from the set cements was negligible and there was no significant difference between the free fluoride and the total fluoride released. This suggests that little or no fluorine was released in the form of aluminium complexes.

The cements with no alkali metal content still released fluoride indicating that a soluble counter ion is not required.⁵⁰ At all times the cements demonstrated a negative ion balance where there were more negative ions leaving the cement than positive ions (see Results chapter 3.0 page 114-115). The results demonstrated that the ion exchange mechanism may be responsible whereby the fluoride ion in the cement is exchanged for a hydroxyl group from water in the elution medium.¹⁹⁵ It must also be pointed out that cement discs were allowed to set for 24 hours prior to elution. Exposure to water at earlier times may have lead to possible dissolution and greater ion release. The aluminium results (see Table 3.22-3.27) showed that the ICs used in this study would not be expected to reach a level to cause problems.^{81, 108, 190}

Ion release levels were probably dependent on the mass of the cement material implanted. Dissolution at the cement surface in setting cements was a factor in ion elution. Protecting the cement surface or extending the time prior to immersion had been shown to reduce ion elution. In addition, for any given IC system, the total loss in mass terms due to ion elution was negligible.

Long term changes in the properties of ICs were generally regarded as being due to continued degradation of the glass and a cross-linking reaction that took place over an extended time period exceeding one year. Thus the concentration of ions, including fluoride ions in the polysalt matrix was likely to increase with time. The

low release of aluminium from the set cements indicated that there was no significant dissolution of the cement matrix and that ion release occurred largely by the diffusion process.

Erbe *et al* reported that the most striking feature of the IC-group was the abundant amount of osteoid tissue seen one year post-operatively. This was probably an expression of a disturbance of mineralization comparable to the osteomalacia produced by administration of aluminium and magnesium antacids²⁰⁵ Carter DH *et al* concluded that the defect in mineralization in the bone apposed to the implant could then be attributed to the eluted ions and that aluminium ions have stimulated the apposition of lamellar bone.²⁰⁶

Blades *et al* 1997 reported that the interface tissue of these ICs showed good integration but poor mineralized tissue and osteoid-like in appearance.²⁰⁷ Two possible local mechanisms were acting to upset normal bone mineralization. The release of H⁺ ions from unpolymerised poly(acrylic) acid component of the wet ICs would have created a locally low pH environment, or set cement and would have incorporated into mineralizing osteoid that may be responsible for the inhibition of mineralization observed in all ICs implanted (LG26 and LG30). Further optimisation of cement formulation to minimise aluminium and H⁺ release from the setting cement may improve the biocompatibility and mechanical properties of the

bone-IC interface.²⁰⁷ This may have indicated that the effect of the aluminium ion depended upon small variations in its concentration.²⁰⁶

4.2.5 Silicate release

It was important to keep the silicate release levels low as high levels of silicon have been related to autoimmune diseases²⁰⁸ and as Meyer *et al* concluded silicon may lead to disturbances in mineralization.¹⁰² It has been reported that silicic acid prevents aluminium toxicity in fish.²⁰⁰⁻²⁰² The protection by silicic acid is believed to involve the formation of hydroxyaluminosilicate (HAS) and a mechanism of formation of these species has been suggested.²⁰² HAS remains sufficiently stable on a biological time scale and to have significant influence upon the toxicity of aluminium in fish and in biological systems in general.^{201, 202} From this it can be concluded that silicon at low concentrations is non-harmful.²⁰⁰⁻²⁰² The greater the silica content of the glass the greater the amount of silicate ion release from the cement matrix.

While silicate release was a critical factor determining biocompatibility, no groups have yet reported an optimum range for the elution of this ion. In this study, LG26 and LG125 were found to perform best in the *in vivo* osteoconductive experiments (Table 3.54 and Table 3.55). It is not unreasonable to assume that silicate release was near optimum for this animal model. In the elution experiments LG26 (Table 3.29) silicon was detected early on in the experiment. At day one $2.3 \mu\text{molg}^{-1}$ was released and at day forty-two $50.1 \mu\text{molg}^{-1}$ of silicon was measured. Perhaps silica

IC concentrations of 4.5 mole fractions could be suitable and be a safe range for silicate release as a dental material and as an orthopaedic cement. However, care must be taken when extrapolating these results to the human clinical situation.

No relation was found between sodium glass composition and measured silicon release as shown in Figure 3.11, that had a correlation coefficient of 0.3. There was no relation between potassium glass composition and silicon release (Table 3.38). However, a wider range of potassium glass concentrations would have confirmed this confidently. There was a relation between increasing silicon release and decreased CaF_2 in glasses (Table 3.29 and Table 3.30) e.g. LG45 had no CaF_2 and eluted the greatest amount of silicon measured at 42 days compared to all other glasses tested (Table 3.30). Measured silicon, as expected showed a relation to silica glass composition e.g. at day 1 LG81, containing a mole fraction of 6.75 of SiO_2 eluted the greatest levels of measured silicon from the series varying in silica :alumina ratio showing a relation between ion release and IC formulation. As aluminium glass composition increased less silicon levels were detected (Table 3.32).

Measured silicon release increased as phosphorus pentoxide composition increased for generic compositions derived from the apatite stoichiometric based glass LG26, as shown in Figure 3.12, where there was a strong correlation of 0.96 correlation coefficient (Table 3.33). However, silica glass composition also increased making it difficult to conclude whether improved phosphorus pentoxide glass composition

increased the measured silicon release from these ICs. The testing of phosphorus pentoxide based glasses may have concluded this. There was no relation between the calcium based series and measured silicon release (Table 3.34).

A possible pattern emerges with some ICs releasing low levels of measured silicon and aluminium from the same ICs. For example, LG22 was measured as eluting the least amount of aluminium and silicon from the monovalent cation series (Tables 3.22 and 3.28). This pattern also applied to LG77 of the series varying in silica:alumina ratios, which released the least amount of measured silicon (Table 3.32) and aluminium (Table 3.24).

4.2.6 Calcium ion release

Calcium is important as it is a constituent of teeth and bones as hydroxyapatite⁹¹ is responsible, partially, for the release of fluoride ions from ICs.⁵¹ Calcium is both physiologically useful and highly mobile in the human body. Osteoclast activity is thought to be partially activated by the level of ionised calcium generated locally as a result of bone resorption.^{110, 209}

Calcium ion release from IC was largely dependent on the calcium concentration of the glass.^{50, 51} For example, LG7 of the monovalent cation based series, released the greatest amount of calcium from this series of ICs as it had a high composition of calcium in its glass (Table 3.36 in Results section). Calcium ion release increased as

the calcium fluoride content in the apatite stoichiometric based glasses increased (section 2.1.1b in Materials and Methods section and Table 3.37 in Results section).

The series varying in silica:alumina ratios all had the same calcium concentration (see section 2.1.1 k and Table 3.40) and yet showed an increase in calcium ion release as the silica IC content increased and the alumina content decreased. These results implicated that calcium ion release was also dependent on the concentration of silica and alumina in the glasses for this series (Table 3.42).

While fluoride, aluminium and silicate ions are critical factors determining biocompatibility, and in the cases of fluoride and aluminium, osteoconduction, no groups have yet reported on an optimum range for elution for the calcium ion. In this study, LG26 and LG125 were found to perform best in the wet and set *in vivo* implantation experiments (see Tables 3.54 and 3.55). It is not unreasonable to assume that calcium release was near optimum for this animal model. These materials had an early calcium elution of $0.9 \mu\text{molg}^{-1}$ at day 3, increasing to $4.9 \mu\text{molg}^{-1}$ at day 42 in the ion release experiments (Table 3.37). Another IC with two mole fractions of calcium was LG53 that eluted the greatest amount of calcium for the series varying in silica, alumina and calcium.

There was no relation between sodium glass composition and calcium ion release (Table 3.36 showing calcium ion release of the monovalent cation series). An increase in phosphorus pentoxide glass composition showed a decrease in

calcium ion release (Table 3.41) from analysis of the series varying in generic compositions derived from the apatite stoichiometric based glass LG26. However, the mole fraction of CaO in this range of glasses increases and calcium ion release increases showing a positive relation between calcium ion release and calcium IC formulation.

4.2.7 Phosphate ion release

Phosphorus is important as it is involved with the mineral hydroxyapatite.

Phosphorus improves translucency and adds body to ICs.⁵¹ Phosphorus is assumed to leave the cement as PO_4^{3-} . Phosphorus influences alkaline phosphatase activity.²¹⁰

There was no relation between sodium glass composition and phosphate ion release (Table 3.43). There may be a relation between potassium glass composition and phosphate ion release from these results (Table 3.43). However, by analysing a wider range of potassium based glasses it may be shown that there was a definite relation between potassium glass composition and phosphate ion release. Table 3.47 at day 1 showed that there was a relation between phosphate ion release and silica glass composition and decreasing alumina glass composition.

There was a relation between calcium and phosphate with some of the ICs. In that as calcium glass content increased there was less phosphate released (Table 3.48 of Results chapter). Phosphate (PO_4^{3-}) ion release increased as phosphorus pentoxide concentration of ICs increased as was shown in Figure 3.13 where there

was a strong correlation (0.97). This showed a positive relation between phosphate ion release and IC formulation. For example, the ICs LG83 to LG85, derivatives from LG26 at day 3, showed an increase in phosphate ion release as the phosphorus pentoxide content increased (Table 3.48 and section 2.1.1 e). All the Limerick based glasses released greater phosphate ion release levels than the controls Chemfil and Chemfil Express (Table 3.51).

Phosphate ion release was one of the critical factors determining biocompatibility and osteoconduction, no groups have yet reported an optimum range for elution of this ion. In this study LG26 and LG125 were found to perform best in the *in vivo* implantation experiments (see Tables 3.54 and 3.55) and it may be added that perhaps an IC with the same mole fraction of phosphorus pentoxide, i.e. 1.5 as that of LG26 may perhaps be a suitable concentration for a bone cement or bone substitute.

4.2.8 pH effects on the IC discs

Extracellular fluid (ECF) has a hydrogen ion concentration of about 4×10^{-8} mol/L (pH 7.4) which is slightly alkaline. Intracellular fluids tend to be slightly more acidic than ECF. In ECF the pH, ranges from 6.8 to 7.8 and is compatible with human life. Even small changes in the hydrogen ion concentration can greatly change the physiological functioning of the body even for a brief period of time.²¹¹ Buffering prevents large changes in hydrogen ion concentration when hydrogen ions are added to or removed.²¹¹

The fluoride ion exchange mechanism does have important consequences for biocompatibility studies particularly in cell culture, the measurement of fluoride ion release and its clinical significance. The pH fell as fluoride ions were exchanged with the hydroxyl ions¹⁹⁵ (Table 3.50). The pH reduction depended on time, but also on the mass of the cement, its surface area, the quantity of water used and how frequently the water was changed.⁸³ A small pH reduction reduced the ion exchange process by reducing the number of hydroxyl ions available for ion exchange. The effects of pH changes on fluoride ion release were therefore likely to be complex.

Cell culture studies (see Results section 3.3, Figures 3.17 and 3.30) indicated that increasing sodium content of ICs and increasing ion release were beneficial for the cells. For these reasons two glasses, LG2 and LG6, were monitored over 14 days for pH changes in the eluting water. There was a reduction in pH, where LG6 was in the biocompatible pH range, but LG2 fell outside the acceptable pH range for biocompatibility.

LG6 released more fluoride ions (Table 3.6) than LG2. Ions were released from the matrix of bone cement by either counter ion mechanism⁵⁰ or by the ion exchange mechanism.¹⁹⁵ There was an imbalance of the measured anions to cations released from the set cements with an excess of negative ions (Results section pp 114), which strongly indicated that fluoride ions were exchanged for hydroxyl ions.¹⁹⁵

This was supported by a reduction of pH in tissue culture indicated by its colour change (from red-orange to yellow). LG2 (no sodium) showed a greater pH reduction than LG6 (contained sodium and fluoride) because of the effect of monovalent ions, e.g. Na^+ , enhanced their uptake and re-release of ions e.g. fluoride, which may explain why there was less of a pH reduction with LG6, because of the possible uptake of fluoride ions, than with LG2 which had no sodium and therefore no enhanced amount of fluoride and sodium re-release or uptake (Table 3.6 and Table 3.18).²¹²

A drop in the pH (Table 3.51) was expected for the autoclaved ICs as the initial burst of fluoride ions was eluted into the water from autoclaving,⁵¹ (Ion balance calculation pp 114). Fluoride and hydroxyl ions were exchanged in this early contact with water in the autoclave.¹⁹⁵

Table 3.52 and Table 3.53 showed that the ICs LG2 and LG26 in α -MEM had higher pH's than those tested in water and there was a pH rise in water but released less fluoride in α -MEM (see Table 3.13). Prior to placing IC discs into α -MEM, the IC discs were autoclaved. This would have lead to an initial burst of fluoride ions from the IC discs in the water from autoclaving.⁵¹ The low pH is a critical factor responsible for microbial inhibition by these materials.²¹³

The ICs LG2 and LG26 in α -MEM were both biocompatible when compared to the intracellular fluid pH limits. There was a pH drop in α -MEM which may indicate

fluoride ion exchange with the hydroxyl ion as was the situation in cell culture where fluoride elutes into the α -MEM.

LG2 and LG26 in water (Table 3.52) showed a pH rise. This could be from the uptake of fluoride ions ^{213,214} as the initial burst of fluoride ions occurred before 24 hours and these fluoride ions may have been exchanged back into the IC in exchange for the hydroxyl ion back into the water and as a result showing a pH rise.

The pH of LG26 in α -MEM pH 6.0 - 7.0 could perhaps be suitable as LG26 was one of the most biocompatible ICs. The pH range of LG26 could be the most osteoconductive where it may inhibit microbial activity. As a dental cement LG26 would be expected as having anti-caries properties. It could be used as an orthopaedic cement and having such anti-microbial properties would expect the IC to reduce infection after bone implantation.

4.3 Total protein and MTT assays for bone marrow cells and Ros cells

An adequate intake of protein is essential for higher animals since only the simple forms of life are able to synthesise their protein from other nitrogen sources. The protein content of cell culture is widely used for estimating total cellular material ²¹⁵ and was used to determine the total protein concentration in cultures containing ICs using two different cell lines. The MTT method (see Section 2.2.3c iii) was used to determine the cellular activity (mitochondrial respiration) after prolonged exposure

to the IC. Cell activity is defined as the retention of metabolic or proliferative ability of a cell population as a whole.²¹⁵

The effect of ions on biocompatibility was complex depending on the ion mix and concentration of specific ionic species. Fluoride as mentioned earlier in this chapter (Section 4.2.2, Fluoride ion release) has been reported to be osteoconductive.^{34-36, 46, 48, 87, 90, 93-95} The ICs giving the best cellular response were LG22, LG63, LG6, LG23 and LG2 with bone marrow cells and Ros cells (Figure 3.14, Figure 3.15, Figure 3.17 and Figure 3.23). Fluoride elution levels for some of these ICs were relatively high (Table 3.6).

However, LG2, LG6, LG23 and LG63 all eluted low levels of aluminium ions (Table 3.22 & Figures 3.17 and Figure 3.23). The results for protein and MTT assays showed that there was an inverse relationship between the aluminium ion release (Table 3.22) from ICs and cellular activity (Figure 3.18 and Figure 3.24).

Interestingly, LG6 had a low aluminium ion release (Table 3.22) in combination with a high fluoride ion release (Table 3.6) and showed a good cellular response, indicating that it may not be fluoride that was responsible for *in vitro* toxicity as was shown by other studies.³⁴

LG69 eluted the greatest amount of aluminium having a low cell activity count in both types of cells (Figure 3.18 and Figure 3.20 and Table 3.22), whereas LG2,

LG6, LG23, LG69 and LG22 eluted very low levels of aluminium (Table 3.22) and were well tolerated by cells in culture (Figure 3.18 and Figure 3.24). A low level of aluminium ion release appeared beneficial in our culture studies. It has previously been reported that low levels of aluminium ions showed stimulation of cell growth.^{102-107, 216}

However, aluminium ions have been reported to be cytotoxic at high levels.^{102, 104, 105, 108} From these results the toxic effects of high concentrations of aluminium^{102, 104, 105, 108} restricted the growth of Ros cells. The effect of aluminium ions on bone metabolism is an area of continuing debate as at low concentrations it is beneficial.^{101-108, 200, 205-207}

All the apatite-stoichiometric based ICs had released very low levels of aluminium where LG26 eluted the most from this series (Figure 3.10). This higher aluminium ion release from LG26 compared to LG27, LG28, LG29 and LG30 was the reason why bone marrow cell cultures exposed to LG26 were less active (Figure 3.20) as aluminium was reported as potentially damaging.^{103, 105, 106, 108}

LG72 in with Ros cell culture gave positive cell activity results (Figure 3.26). LG72 had a lower mole fraction of alumina than LG73-LG75, and eluted low concentrations of aluminium (see Table 3.23) and a high level of fluoride (see Table 3.9). LG74 also eluted very low levels of aluminium (<0.1 nmol/g) (see Table 3.23)

this added to its good biocompatibility of Ros cell cultures.^{103, 105, 106, 108} Greater cell activity and thus biocompatibility of cell cultures was associated with decreasing alumina concentrations with regards to ion release and glass content. The alumina glass content and its low release levels in the region of $<0.2 \text{ nmolg}^{-1}$ from ICs may have determined the biocompatibility of the IC with respect to Ros and bone marrow cell activity.

Silicon could be harmful but its exact effect on bone-forming cells is unknown. It has been reported to be linked to autoimmune diseases at high levels²⁰⁸ for this reason the amount in the IC should be low. LG27 and LG26 were detected eluting low amounts of silicon which was perhaps why bone marrow cell cultures associated with LG27 and LG26 produced greater protein concentrations (see Table 3.29 and Figure 3.19).^{34, 81, 109}

LG72 was well tolerated in cell culture and had a low mole fraction of silica (see section 2.1.1 l) and was measured as eluting less silicon than the other ICs from the same series of ICs varying in alumina and silica and calcium^{34, 109} (Table 3.31). LG72 did however have a low alumina glass content than others in this series and this may have contributed to the positive biocompatibility result (see Figure 3.25 and Figure 3.26).

There was a relation between high phosphate ion release of ICs LG6 and LG2 (Table 3.43) and bone marrow cell cultures associated with LG2 and LG6 producing high concentrations of protein (Figure 3.17 and Figure 3.23). Phosphorus is potentially beneficial as it is a constituent of the mineral hydroxyapatite in bone, the IC was thus acting as a source of phosphate for the production of natural mineralized tissue and was reported to regulate the level of skeletal ALP.²¹⁰

The high phosphate ion release of apatite-stoichiometric based IC LG29 (Table 3.44) may have resulted in the higher protein production of the BMC cultures (Table 3.44, and Figure 3.19).²¹⁰ LG27 eluted the least amount of phosphate which perhaps explained the reduced protein production in the BMC cultures.²¹⁰

The most promising *in vitro* results from the series varying in silica / alumina and calcium were with cell cultures associated with LG74, LG72 and LG55 (see Figure 3.25 and 3.26) where LG74 associated Ros cell cultures (Figure 3.25) produced high concentrations of protein perhaps from the high amount of phosphate ion release.²¹⁰ Cell cultures associated with HA produced the best response *in vitro* testing for protein production and cell activity compared to all the other materials used in this study (Figure 3.21, Figure 3.22, Figure 3.29 and Figure 3.30).

The response of the bone marrow cell cultures and Ros cell cultures to HA confirmed the inert nature of this material and its good *in vitro* response (Figure

3.21, Figure 3.22, Figure 3.29 and Figure 3.30). In addition to this, recent studies suggest that the possibility of non-biological precipitation of mineral^{216, 217} as hydrolysis of β -glycerophosphate produced high local concentrations of phosphate ions.²¹⁷ HA consisting of calcium phosphate showed osteoconductive potential¹³⁻¹⁵ TCP with Ros cell culture produced very high protein concentrations and cell activity results (Figure 3.29 and Figure 3.30).

The *in vitro* cell culture results confirmed that ICs were not inert and that their ability to leach ions,^{50, 51} affected the *in vitro* response of cells dependent upon the type, amount and combination of ions released.

Recently, Oliva *et al* found that certain commercial ICs were biocompatible when tested using human osteoblasts *in vitro*.²¹⁸ The results from this thesis support that there was an exchange of ions with adjacent tissues at the implant site, which was the basis of osteoconduction and bone-bonding properties of ICs.^{81, 219} The *in vitro* cell culture results lead to the next step of which glasses to use for *in vivo* implantation studies.

4.4 *In vivo* evaluation of ICs

ICs in the set and wet form were osteoconductive and can therefore be used as bone cements and/or bone substitutes. The integration and interaction of these ICs with bone is of importance for clinical application which is why bone proteins, such as osteopontin, fibronectin and tenascin are important to show normal bone

development. However, it must be taken into account that observations made were in a healing (three week old) rat model where the metabolism differs to that of the human body.

4.4 (a) Evaluation of set Ionomeric cements

Semi-quantitative histomorphometric analysis and histological evaluation revealed that there was a more positive response from the surrounding bone associated with the IC implants in the apatite-stoichiometric based IC series as compared to those in the monovalent cation series (Table 3.54). LG26 was the most osteoconductive (0.16 mm) and was the most integrated (80.8%, Figure 3.35 to Figure 3.38) whereas LG2 was the least osteoconductive (0.05 mm) and least integrated (37%) from all the ICs used in this study (Table 3.54). Sodium fluoride at low levels has been shown to have pronounced effects on the skeleton, it may be possible to modify the therapeutic use of fluoride in osteoporosis and other brittle bone.^{35, 36, 46, 48, 87, 90-95}

The results (Table 3.54) appeared to be correlated with the composition of the ICs (Section 2.1.1). Increasing the fluoride content in the apatite-stoichiometric based series (LG30 to LG26) was associated with increased bone formation (Figure 3.35- Figure 3.38) and confirms the results seen in this study and by others as to the beneficial effect of this ion in appropriate concentration on bone formation.^{46, 81}

Work previously reported on this series of glasses has demonstrated that increasing

the sodium content of IC increases the rate and amount of fluoride release from the cement matrix. This has been proposed to be due to increasing the mobility of fluoride ions in the matrix and by facilitating an ion exchange mechanism between the IC and the environment.¹⁹⁵ From analysing ion release from ICs taken together with those of this study demonstrate that while the total amount of fluoride present is an important determinant of biological response, the mobility of ions within the cement matrix and their release characteristics are significant factors affecting the induced biological response.

In the apatite-stoichiometric based series (see section 2.1.1.b) the fluoride content was increased in order to investigate osteoconductive effects i.e. bone growth and osseointegration and ensure glass formation. The mole fraction of alumina was increased throughout the series with LG26 containing 3 mole fractions, LG27 with 4 mole fractions, and LG30 containing 5 mole fractions. The amount of new bone was thus negatively correlated with alumina content, LG30 being associated with the least amount of new bone formation. Increasing aluminium ion release from ionomeric materials has been demonstrated to be negatively correlated with the *in vitro* response of osteoblasts⁸¹ as was found in this study (see Figure 3.17 to 3.30).

The effect of aluminium ions on bone metabolism is however an area of continuing debate.¹⁰⁵ Aluminium ions have been shown to reduce new bone formation¹⁰¹ and

inhibit bone mineralization.^{193, 205, 206, 207} There is evidence that aluminium can enhance the mobilisation of calcium from bone by a cell-independent mechanism.¹⁰⁷ In contrast, low concentrations of aluminium have been reported by Lau *et al* to stimulate the proliferation and differentiation of osteoblasts *in vitro*.¹⁷⁰ While *in vivo*, administration of aluminium has been shown to increase bone volume by positively influencing trabecular networking in the axial skeleton.¹⁰¹ The set IC LG26 shows that aluminium at a low concentration, e.g. 3 mole fractions of aluminium, positively influenced osteoconduction.

The results of the set ICs show that biological response was reduced with increased alumina content associated with reduced fluoride content. Thus, the effects of aluminium and fluorine are likely to be dependent on the concentration of their ions. The beneficial effects of fluoride were thought to be due to promotion of osteoblastic activity and increasing trabecular bone density.⁸¹ However, the effects of fluorine, like aluminium, appear to be dose-dependent *in vitro*⁹³ and *in vivo*.²²⁰ The formulation of defined ICs enables controlled evaluation of the parameters that effect the biological response of bone to ICs.

The biocompatibility and composition of ICs are of great importance because they need to be in direct contact with bone for any chemical adhesion to occur. These model IC formulations induced favourable biological response from the tissues of the implant bed. Improved osseointegration and osteoconduction being associated

with increased calcium fluoride or sodium content and reduction in alumina content. *In vitro* work from this thesis demonstrated a link between glass composition, and ion release, with fluoride ion release increasing as the sodium or calcium fluoride content of the glass increases. Improved osseointegration and osteoconduction appear to be mediated by increased fluoride ion release. Increased calcium fluoride content and fluoride release were positively correlated with osteoconduction.

Calcium also plays an important role with osteoconduction as it is also used in the prevention of osteoporosis and in protecting what bone mass a woman may have at her current age. The evidence is strong that prevailing calcium intakes contribute to the low bone mass component of osteoporotic fragility and that increases in intake would reduce the osteoporotic fracture burden.²²¹

The most osteoconductive set IC was LG26 of the apatite stoichiometric based series that has the same calcium:phosphate ratio as bone (1.66). It also had a high calcium fluoride content of 2 mole fractions. LG26 consisted of an alumina content of 3.0 mole fractions, and eluted a low amount of aluminium ($<0.2 \text{ nmol g}^{-1}$). At these levels LG26 influenced cell activity *in vivo* to an extent where maximum osteoconduction and maximum osseointegration of bone was produced. As an *in situ* setting bone substitute or as a bone cement, the setting and working time made the IC LG26 the most manageable and workable cement as a bone substitute and as a potential bone cement.

4.4 (b) Evaluation of wet Ionomeric cements used for surgical implantation

LG125 had the greatest amount of bone-implant contact (77.0%) (Table 3.55, Figure 3.39 to Figure 3.41) and the greatest amount of bone growth (0.08 mm) from all other wet ICs. LG132 had the least amount of bone-implant contact (42.5%) and LG23 with a 1:0.2:0.2 composition (0.2 ml water) was the least osteoconductive (0.02 mm). LG125 has a strontium oxide mole fraction of 3, whereas LG119 has a strontium mole fraction of 1.5 (section 2.1.1c, Figure 3.42 and 3.43). From these results it would suggest that strontium has a strong osteoconductive influence.^{112-114, 222-225}

More importantly, it has been reported that low doses of strontium and fluoride increases the number of bone forming sites and vertebral bone volume in rats, but does not have detectable adverse effects on the mineralization of bone.²²⁵

Strontium may be able to prevent the changes in bone turnover by oestrogen deficiency.²²³ Strontium at low doses has been used to treat osteoporosis.¹¹³

The potentially positive effects of strontium on bone appear to be dose-dependent as it has also been found that treatment of mineralizing tissues with strontium both *in vitro* and *in vivo* may result in defective mineralization and an accumulation of complexed acidic phospholipid.²²⁶ Strontium appears to perturb mineralization, partly by a direct effect on the cells of mineralizing tissues. Excessive doses of

strontium can disturb calcium metabolism.¹¹¹ Strontium must only be used at low levels to avoid these excessive defects in bone.²²⁵

Fluoride has also contributed to the osteoconductive properties^{34-36, 46, 48, 96-99, 110} of LG125 and LG119 (Figure 3.43 and Figure 3.42), as well as strontium and with this chemical composition of LG125 the greatest amount of bone formation and integration was formed. Fluoride has been associated with an increase in periosteal bone formation and an increase in endosteal bone resorption.⁹⁹

Zinc plays an important role in the growth and stimulation of bone formation^{184, 194} and as a ceramic was considered an osteoconductive agent.¹⁹⁴ The results of LG130 and LG132 from this study confirmed its osteoconductive property (Table 3.55). LG130 was significantly better integrated with bone than LG132 (figure 3.44). This is probably because LG130 had a greater zinc oxide mole fraction (1.5) than LG132¹⁹⁴ (section 2.1.1d).

LG23 in the 1:0.2:0.3 ratio was significantly better integrated and osteoconductive than the LG23 1:0.2:0.2 ratio as there was less water (0.2 ml) to mix the 1 g glass and 0.2 g of poly(acrylic) acid. ICs are water based materials, and as water played an important role in their setting and structure. Water was the reaction medium into which the cement forming cations, i.e. calcium and aluminium are leached and in which they are transported to react with the polyacid to form a poly(acrylate)

matrix. Water also served to hydrate the siliceous hydrogel and the metal poly(acrylate) salts formed. It was an essential part of the cement structure. If there was less water or if water was lost from the cement by desiccation while it was setting, the cement forming reactions would stop.²²⁷

As cement aged, the degree of hydration increased. This was accompanied by an increase in strength and modulus and a decrease in plasticity.^{228, 229} This was why the 1:0.2:0.3 ratio composition for IC formation was important to maintain. More importantly, lack or loss of water retarded cement formation and prevented the strength of the IC from fully developing as it was a requirement for the hydration of the matrix salts.⁵¹

LG26 (Figure 3.35-3.38) and LG30 set rod cements were more osteoconductive and better integrated than LG26 (Figure 3.45)and LG30 wet cements. This is probably because of the 'toxic' responses when the ICs were placed 'wet' during the early phases of gelation. Preformed IC bone cement induced a favourable response from hard tissues or are inert.^{34, 35, 46, 48} It was this 'toxic' phase of the IC that has to be understood by the surgeon, for while an improved bone substitute has some clinical value the main clinical need was for an improved cement, which would induce a predictable healing response and maintain a long term functional bond with bone.

However, it must be noted that the IC implants in the rat femur were observed at a duration of 4 weeks. This concealed early i.e. 1-2 weeks, damage associated with the implant in the wet and set IC usually at the 2 week stage, progresses to encapsulation by a layer of new bone at the 4 week stage of bone growth.

Initially, after direct surgical placement an unset IC bonds to the underlying bone. This was followed by a period of remodelling and periosteal reaction prior to stabilisation of the interface.^{46, 82} The effect of the wet cement was probably mediated by a combination of reduction of tissue pH, thus an acidic environment, due to the release of free poly(acrylic) acid, release of glass particles and metal ions from wet cements contaminated by tissue fluid/blood. Set cement rapidly became surrounded by a layer of relatively mature bone.^{35, 48, 82}

LG125 and LG26 have similar chemical formulae with the exception of LG125 having an additional 3 mole fractions of Strontium. However, LG125 had a working and setting time of less than 150 seconds. This faster working and setting time made it a less manageable and workable cement as a bone cement or bone substitute. LG125 had a calcium:phosphate ratio that was the same as that of bone (1.66). It had a high calcium fluoride content of 2 mole fractions. LG125 consisted of an alumina mole fraction of 3. From LG26 and LG125 osteoconductive and integration results it seemed that these quantities were the appropriate levels that influenced

maximum bone growth *in vivo*. LG26 seemed to be the most manageable and workable cement.

The control acrylic set rods (Table 3.56) were significantly more osteoconductive and better integrated in bone than the acrylic wet cements. However, neither acrylic set nor wet control cements were as osteoconductive or as well integrated with bone than any of the implanted ICs. The poor response was probably related to the exothermic polymerisation and by the leaching effects of residual monomer²⁹⁻³¹ causing thermal^{27, 28} and chemical necrosis.^{29, 30}

Problems did arise and were as follows:

- a) Difficulty in recognising the wet implant as it was irregularly shaped and not rod shaped.
- b) Sometimes difficulty arose in drilling the hole into the midshaft of the femora. For example, the hip joint was drilled, as some rats had very narrow femurs.
- c) When paraffin sectioning the knife would sometimes leave grazed marks on the section, and on a few occasions it damaged the whole bloc because of a fault in the microtome and damage the section.
- d) When handling paraffin sections, the implant would sometimes lift off the rest of the section when placed in warm water to expand the section. Only after staining and mounting would this absence of the implant and tearing in the section be observed microscopically.

e) When placing the paraffin section on the glass slide, sections occasionally left creases. When attempting to displace the crease from the section sometimes the section would be ruined.

f) The paraffin blocks with bone had to be cooled for at least 15 min to produce a lean, non-creased bone section with the implant, and if the room temperature was above 21°C, it took longer to cool the block.

4.4 (c) Bone Proteins

The amount of new bone formation (% integration) was ordered LG23>LG6>LG2. This trend was applicable with the amount of OPN staining (Figure 3.46 to Figure 3.47, Figure 3.49 and Figure 3.51). The control material, LG2 with no sodium, showed the least bone formation and least staining for OPN (Figure 3.51), while LG23 (Na⁺=0.15M) with the greatest new bone formation, showed the most staining (Figure 3.46 and Figure 3.47).

This suggested that more bone had more OPN as the sodium content increased (Figure 3.46, Figure 3.47, Figure 3.49 and Figure 3.51). OPN staining was prominent in the new bone formed adjacent to the IC-implants where it was concentrated at the reversal lines. The reversal line is found between the edge of a resorption cavity that will become a new haversian system in new bone in bone remodelling.

The remodelling of bone can only be achieved by bone resorption. The association of OPN, with IC-implants, integrated with bone may explain their osteoconductive properties and the differences that occur with varying IC formulations. From these observations and past studies¹⁷¹⁻¹⁷³ it can be suggested that OPN is involved in initial bone formation with these IC-implants.

The amount of staining with FN and TN did not increase with more sodium. FN was widely distributed staining regions of woven bone with all the IC-implants (Figure 3.48). However, this does correlate with past immunohistochemical *in vitro* studies that have located FN and TN on fibers that were aligned within the plane in which bone formation was occurring, in areas of intramembranous osteogenic differentiation.¹⁷⁴ From the results in this study it may be suggested that FN was involved in the initial ECM-cell interactions involved in endochondral bone development¹⁷⁴⁻¹⁷⁷ with these IC-implants. It would also relate to what Yamada *et al* reported that FN, as adhesive protein, influenced cell migration *in vivo*.²³⁰

TN was distributed in the periphery of the endosteum (Figure 3.50 and Figure 3.52) a site of osteogenesis with all the IC-implants used in this study. The presence of TN on the fibers in a beaded pattern may also be related as it has been found to be important in normal bone formation,²³¹ as its absence seems to be characteristic of dysplastic bone development. This correlates with proposed functions of TN, that it is involved in wound healing and tissue remodelling¹⁷⁸⁻¹⁸³ with these IC-implants.

Problems did arise with immunohistochemical techniques. For example, the sections slid off the glass slide after fixing the sections with neutral buffered formalin for 3 min. The problem was with the temperature of the room, as it was 35°C. Sections had to be cut again on a cooler day.

5. FINAL DISCUSSION

Materials designed for use in the construction of medical devices must be biocompatible. Furthermore, it is important to consider their interaction with the biological environment following surgical implantation. The study of implant-tissue interaction is therefore essential to gain an understanding of those factors which may ultimately determine clinical success. Cell activity, interfacial interaction and implant material toxicity are factors that have been amenable to the *in vitro* cell culture study. *In vivo* evaluation was undertaken to determine the initial response of bone and the interface between bone and implant materials.²³²⁻
²³⁴ The *in vivo* model used provided a rapid assessment of the initial response and healing of bone around the implanted material.²³²⁻²²⁸

As mentioned earlier in Chapter 1 (Section 4.2) it is difficult to define levels of elution for the ions fluoride, aluminium, silicate, calcium and phosphate. There are differences (between the two organisms) in metabolism between rat and man because of size and other differences such as bone turnover and metabolic rate would be less in a rodent e.g. rat. The chronology of healing in the rodent model can be related to the clinical situation. The events of healing are the same for both the rodent model and for humans, that is the proliferation of fibroblasts and capillary sprouts grow into a blood clot and injured area forming granulation tissue. The area is also invaded by polymorphonuclear leukocytes and later by macrophages that phagocytize the tissue debris. The granulation tissue gradually becomes denser and cartilage forms. This newly formed connective tissue and

cartilage is callus. It serves temporarily in stabilizing and binding together the fractured bone. At the same time, the dormant osteogenic cells of the periosteum enlarge and become active osteoblasts. Osseous tissue is deposited. This formation of new bone continues toward the fractured ends of the bone and finally forms a sheathlike layer of bone over the fibrocartilaginous callus. As the bone increases in amount. Osteogenic buds invade the fibrous and cartilaginous callus and replace it with a bony tissue. The cartilage undergoes calcification and absorption. The newly formed bone is spongy which later becomes transformed into a compact type, and the callus becomes reduced in diameter. At the time when this subperiosteal bone formation is taking place, bone also forms in the marrow cavity. The medullary bone growing centripetally from each side of the fracture unites, thus aiding the bony union. Healed bone in young individuals assumes its original contour which applies in both the rodent model and in humans.

In a three week old rat this healing process will be faster than the healing process in a three year old rat. This correlates with the fact that a 6 year old child will have a faster bone turnover than a 60 year old adult, hence the age of the subject was of importance with respect to healing time. In some cases the protein anabolic functions are poor so that the bone matrix cannot be deposited satisfactorily in some old people which as a result can then be diagnosed as osteoporosis. In the bones of children, in whom the rates of deposition and absorption are rapid, brittleness is evident in comparison with bones of old age, at which time the rates of deposition and absorption are slow.

The elution data were obtained from water *in vitro*, and differences in surface areas for the models exist. However, some conclusions can be made when combined with *in vitro* cell culture results and from the various IC formulations. It can be said that ion release concentrations were dependent on IC chemical formulations, for example, an IC with a high phosphorus pentoxide content eluted high levels of phosphate.

Aluminium ions appear to be the determining ions influencing cell activity (see section 3.3.2 and Figures 3.7-3.20). From these results the biocompatibility of ICs as assessed by *in vitro* cell growth is inversely proportional to aluminium ion release. Fluoride may also have been effective as an influencing agent in the activity of cells studied.^{35-36, 46, 50, 87, 90, 93-100} Phosphate appears to be influencing protein concentration in the cells used (see Section 3.2.1g and Figures 3.8-3.20) The results obtained show that as the elution of phosphate from ICs increases there is a positive correlation with the cells protein concentration.

From the Results presented in Chapter 3.0 and the General Discussion in Chapter 4.0 it can be determined that the *in vivo* method and *in vivo* results were more reliable than the *in vitro* cell culture method and cell culture results. The *in vivo* animal implantation model is still required to investigate the response of a whole animal to a material.²³⁹ From successful *in vivo* surgical implantation results positive conclusions can be made to use these IC implants in humans leading to clinical success of the IC as a bone substitute or bone cement. Using the *in vivo* model accurate measurements of bone growth and intimate bone-implant surface

contact were determined using histomorphometric analysis. In addition to this, by using the *in vivo* method pathological reactions can be identified by histologically examining other organs of the same animal, for example, the kidney.

However, a combination of *in vitro* (ion release and cell culture) and *in vivo* (surgical implantation and immunohistochemistry) techniques have produced conclusions that are confident in this study. LG26 was the most osteoconductive and well integrated IC implant in bone from all the ICs used in this study. LG125 was also osteoconductive and well integrated in bone. However, LG26 was *in vitro* tested for its ion elution and cell culture using bone marrow cells and Ros cells. LG26 was also tested *in vivo* for surgical implantation in its set and wet form. Hence, confident conclusions can be made about LG26. LG125 was not *in vitro* tested which gives less firm conclusions as no comments can be made on its ion release qualities which are important, e.g. when determining the aluminium ion release, or by cell culture.

For these reasons, and as it is the most workable and manageable cement with suitable working and setting times, LG26 would be the most well recommended IC as a bone substitute or bone cement as good results were obtained in most tests. If time permitted it would have been useful to determine the localisation of the bone proteins OPN, FN and TN for the IC implants LG26 and LG125 to show that there was interaction of these non-collagenous ECM proteins with these chosen IC implants during hard tissue healing.

6. CONCLUSION

Conclusions were made as follows:

(i) Of the materials tested, those with setting times >150 seconds and working times > 120 seconds were considered most suitable for use as an *in situ* setting bone substitute or bone cement for low-load bearing applications. Materials that met this requirement were LG26, LG27 and LG30. LG26 was the most manageable and workable IC as a bone substitute, as a potential bone cement for orthopaedic use and as a dental cement.

(ii) As fluoride, sodium, potassium, alumina, silica, calcium and phosphorus pentoxide glass contents increased the corresponding ions also increased in elution. Ion release levels for small mammals may be considered as follows:

Fluoride ion measurements carried out were considered to be of levels up to $26 \mu\text{molg}^{-1}$. Aluminium ion measurements carried out may be considered to be of levels $< 0.2 \text{ nmolg}^{-1}$. Silicon ion measurements carried out were considered to be of levels $< 50.1 \mu\text{molg}^{-1}$. Silica levels in ICs used as bone cements or bone substitutes should be kept low. Calcium ion measurements carried out were considered to be of levels up to $4.9 \mu\text{molg}^{-1}$. Phosphate ion measurements carried out were considered to be of levels up to $3.8 \mu\text{molg}^{-1}$.

(iii) The most biocompatible ICs as evaluated from *in vitro* cell culture assays were LG22, LG63, LG6, LG23 and LG2. All of these ICs were also from the monovalent cation based series of ICs.

(iv) The total protein produced by cultures of rat bone marrow cells and Ros cells increased as phosphate and fluoride ion levels increased. It could be the phosphate ion that encourages cell protein production. Cell activity was also inversely proportional to aluminium ion release. It could therefore be the aluminium ion that is the dominant ion determining cell activity.

(v) LG26 set rods were the most well integrated and osteoconductive in this study. LG125 wet ICs with high mole fractions of radiopaque constituents (SrO and ZnO) were the most well integrated and osteoconductive wet ICs in this study.

(vi) Set ICs were significantly better integrated and osteoconductive than wet ICs.

(vii) LG26 and LG125 had the same calcium:phosphate ratio (1.66) as that of bone and with 2 mole fractions of calcium fluoride. LG26 and LG125 had the same alumina composition (3 mole fractions). From these studies it might be concluded that the compositions of LG26 and LG125 are approaching the ideal as bone cement and bone substitutes in non-load bearing situations.

(viii) From *in vitro* and *in vivo* studies it may be concluded that LG26 is the most promising IC of the formulations tested in this thesis for clinical evaluation as a bone cement and substitute.

(ix) *In vitro* and *in vivo* studies suggest that a high aluminium concentration is associated with toxicity and poor biocompatibility. Taken in addition to our knowledge of inhibition of calcium/phosphate mineralization, this component should be reduced in future developments.

(x) OPN is involved in initial bone formation with the IC-implants. There was an increase in OPN as sodium content in ICs increased. FN and TN did not increase with more sodium and as a result with more bone growth. All the IC-implants integrated with bone and ECM proteins FN, TN and OPN were prominently found in new bone suggesting that they play an important role in the interactions of the healing of hard tissues with the IC implants.

(xi) ICs have potential for use as bone cements and bone substitutes, however further work is required.

7. FUTURE CONSIDERATIONS

The following points can be considered for future work:

(i) Aluminium free materials or aluminium-reduced materials are required as bone response was found to be negatively correlated with increasing aluminium.

(ii) To further investigate chemical and surface analysis that forms an integral part of the development or manufacture of any material. A number of techniques are available that enable characterisation of the surface of a material. These techniques include x-ray photoelectron spectroscopy (XPS).

(iii) To further investigate IC implants *in vivo* at longer lengths of time to give clear indications of how biocompatible the IC implants are after 12 weeks, 24 weeks, 52 weeks and 2 years in larger mammals.

(iv) To further investigate ICs with bovine bone morphogenetic protein and other growth factors at varying concentrations to determine the rate of osteoconduction. To further immunohistochemical work, e.g. to determine the amount of osteocalcin and osteonectin. To identify osteopontin on non-decalcified bone tissue and compare with decalcified bone tissue and measure the areas of fluorescence by confocal microscopy.

(v) Further ion release studies are required in larger volumes of water and in simulated body fluid after γ -irradiating the set IC discs to imitate a larger mammal.e.g. human.

(vi) To use more cell lines, e.g. calvarial osteoblast culture model to evaluate biocompatibility and biodegradation of ICs to give confident biocompatibility results.

(vii) Further attempts at observing the ultra structural interactions of IC implants in bone *in vivo* using TEM and SEM and investigate bone-implant bonding, hence the bone-implant interface.

REFERENCES

1. Charnley J. Anchorage of the femoral head prosthesis to the shaft of the femur. *J. Bone Joint Surg.* **42B**: 28-30, 1960.
2. Charnley J. Arthroplasty of the hip- a new operation. *Lancet.* **1**: 1129-32, 1961.
3. Charnley J. The long-term results of low friction arthroplasty of the hip performed as a primary intervention. *J. Bone Joint Surg.* **54B**: 61-76, 1972.
4. Charnley J. Risks of total hip replacement. *Br. Med. J.* **4**: 101, 1975.
5. Convey FR; Gunn DR; Hughes JD & Martin WE. The relative safety of polymethylmethacrylate. *J. Bone Joint Surg.* **57a**: 57-64, 1975.
6. Capocasale L and Beramini M. Biocompatibilita dell idrossiapatite e del fosfato tricalcico col tessuto osseo. *Dent. Cadmos.* **4**: 55, 1987.
7. Passi P; Miotti A and Terribile Wiel Marin V. Tricalcium phosphate ceramics in periodontal therapy: Histological results, in Pizzoferrato A: *Biomaterials and clinical applications.* Amsterdam, Elsevier Science Publishers. 189, 1987.
8. De Groot K. Degradable ceramics in Williams DF: *Biocompatibility of clinical implant materials.* Boca Raton, Fla, CRC Press. **1**: 199-222, 1981.
9. Jarcho M. Biomaterial aspects of calcium phosphates: Properties and Applications. *Dent. Clin. North Am.* **30(1)**: 25-47, 1986.
10. Denissen HW; Makkes PC & Van den Hoof A. Dense apatite implants: The bonding to alveolar bone. *Implantologist.* **2**: 56.
11. Williams DF. Definitions in Biocompatibility Proceedings of a consensus conference of the European Society for Biomaterials, 3-5 March 1986, Chester, UK. *Progress in Biomedical Engineering.* **4**. Elsevier Science Publishers, London, 1987.
12. Williams DF. *Definitions in Biomaterials, Progress in Biomedical Engineering.* Elsevier, Amsterdam. **4**: 9-44, 1987.
13. Jarcho M. Calcium phosphate ceramics as hard tissue prosthetic. *Clinical Orthopaedics.* **157**: 259-278, 1981.
14. De Bruijn, Klein C, De Groot K & Van Blitterswijk C. The ultrastructure of the bone-HA interface *in vitro.* *J. Biomed. Mater. Res.* **26**: 1365-1382, 1992.

15. Basle M, Rebell A, Grozon F *et al.* Cellular response to calcium phosphate ceramics implanted in rabbit bone. *J. Mater. Sci. Mater. Med.* **4**: 273-280, 1993.
16. Veerman ECI, Suppers RJF, Klein CPAT, de Groot K, Nieuw Amerongen AV. SDS-PAGE analysis of the protein layers adsorbing *in vivo* and *in vitro* to bone substituting materials. *Biomaterials.* **8**: 442-448, 1987.
17. Müller-Mai C, Voigt C & Gross UM. Incorporation and degradation of HA implants of different surface roughness and surface structure in bone. *Scanning Microscopy.* **4**: 613-624, 1990.
18. Van Blitterswijk CA, Kuijpers W, Daems WT & de Groot. Macropore tissue in growth: a quantitative and qualitative study on HA ceramic. *Biomaterials.* **7**: 137-143, 1986.
19. Kwong CH, Burns WB & Cheung HS. Solubilization of HA crystals by murine bone cells, macrophages and fibroblasts. *Biomaterials.* **10**: 579-584, 1989.
20. Hench LL, Spilman DB & Noletti DR. Fluoride bioglasses. In *Biological and Biomechanical performance of Biomaterials* Eds P Christel, A Meunier, AJC Lee) Elsevier, Amsterdam. 99-104, 1986.
21. Hench LL. Investigations of bonding mechanisms at the interface of prosthetic material. In: *US Army Med. Res. and Development Command, Contract No. DADA 17-70-C-0001.* **1-6.** 1970-75.
22. Hench LL, Splinter RJ, Allen WC & Greenlee TK. Bonding mechanism at the interface of ceramic prosthetic materials. *J. Biomed. Mater. Res.* **2(1)**: 117-141, 1971.
23. Hench LL & Wilson J. Surface-active biomaterials. *Science.* **226**: 630-636, 1984.
24. Hench LL, Paschall HA. Direct chemical bond of bioactive glass-ceramic materials to bone and muscle. *J. Biomed. Mater. Res. Symp.* **4**: 25-42, 1973.
25. Vrouwenvelder WCA, Groot CG, de Groot K. Better histology and biochemistry for osteoblasts cultured on titanium-doped bioactive glass: Bioglass 45S5 compared with iron-, titanium-, fluorine-, and boron-, containing bioactive glasses. *Biomaterials.* **15(2)**: 97-105, 1994.
26. Di Pisa JA, Sih GS & Berman AT. The temperature problem at the bone-acrylic cement interface of the total hip replacement. *Clin. Orthop.* **121**: 95-8, 1979.

27. Mjöberg B, Selvik G, Hansson LI, Rosenqvist & Rönnerfolt. Mechanical loosening of total hip prostheses. *J. Bone Joint Surg.* **68B(5)**: 770-7, 1986.
28. Feith R. Side effects of acrylic cement implanted into bone. *Acta Orthop. Scand. Suppl.* **161**: 1-36, 1975.
29. Petty W. Methylmethacrylate concentrations in tissues adjacent to bone cement. *J. Biomed. Mater. Res.* **14**: 88-95, 1980.
30. Thompson LR, Miller EG & Bowles WH. Leaching of unpolymerized materials from orthodontic bonding resins. *J. Dent. Res.* **61(8)**:989-92, 1982.
31. Pople IK & Philips H. Bone cement and the liver. A dose-related effect? *J. Bone Joint Surg.* **70B(3)**: 364-366, 1988.
32. Rotter MA, Gioe TJ & Sieber JM. Systemic effects of polymethylmethacrylate: Increased serum levels of γ -glutamyltranspeptidase following arthroplasty. *Acta Orthop. Scand.* **55**: 441-413, 1984.
33. Fleck C; Eifler D; Ondracek G & Watts JF. In: *Krawczynski J, Ondracek G, eds. Biomaterials Scientific series of the International Bureau.* **16**: 18-81, 1993.
34. Brook IM, Craig GT & Lamb DJ. *In vitro* interactions between primary bone organ cultures, glass-ionomer cements and hydroxyapatite & tricalcium phosphate ceramics. *Biomaterials.* **12**: 179-86, 1991.
35. Jonck LM, Grobelaar CJ & Starting H. Biological evaluation of glass-ionomer cement (Ketac-O) as an interface material in joint replacement: A screening test. *Clinical Materials.* **4**: 201-224, 1989.
36. McElveen JT. Ossiculoplasty with polymaleinate ionomeric prostheses. *Otolaryngol. Clin. North Am.* **27(4)**: 777-784, 1994.
37. Geyer G, Helms J. Reconstructive measures in the middle ear and mastoid using a biocompatible cement-preliminary clinical experience. *Clinical implant materials ed. Heimke E, Soltese U, Lee A.J.C. Advances in biomaterials.* Amsterdam, Elsevier. **10**: 529-535, 1990.
38. Babighan G. Use of a glass ionomer cement in otological surgery. A preliminary report. *J. Laryng. Otol.* **106**: 954-959, 1992.
39. Ramsden RT; Herdman RCD; Lye RH. Ionomeric bone cement in neuro-otological surgery. *J. Laryng. Otol.* **106**: 949-953, 1992.

40. Geyer G, Helms J. Ionomer-based bone substitute in otologic surgery. *Eur. Arch. Otorhinolaryngol.* **250(5)**: 253-256, 1993
41. Müller J; Geyer G; Helms J. Ionomer cement in cochlear implant surgery. *Laryngorhinootologie.* **72(1)**: 36-38, 1993.
42. Babighian G; Dominguez M; Pantano N; Tomasi P. Multichannel cochlear implant: personal experience. *Acta Otorhinolaryngol Ital.* **14(2)**: 107-125, 1994.
43. Müller J; Geyer G; Helms J. Restoration of sound transmission the middle ear by reconstruction of the ossicular chain in its physiologic position. Results of incus reconstruction with ionomer cement. *Laryngorhinootologie.* **73(3)**: 160-163, 1994.
44. Nordenvall KJ. Glass-ionomer cement used as surgical dressing after radical surgical exposure of impacted teeth. *Swed. Dent. J.* **16(3)**: 87-92, 1992.
45. Jonck LM & Grobelaar CG. Ionos bone cement (glass-ionomer): An experimental and clinical evaluation in joint replacement. *Clin. Mats.* **6**: 323-359, 1990.
46. Brook IM; Craig GT & Lamb DJ. Initial *in vivo* evaluation of glass-ionomer cements for use as alveolar bone substitutes. *Clin. Mats.* **7**:295-300, 1991.
47. Svanberg M; Krasse B & Ornerfeldt HO. *Mutans streptococci* in interproximal plaque from amalgam and glass ionomer restorations. *Caries Res.* **24**:133-136, 1990.
48. Jonck LM; Grobelaar CJ & Strating H. The biocompatibility of glass-ionomer cements in joint replacement: Bulk testing. *Clin. Mater.* **4**: 85-107, 1989.
49. Nicholson JW; Braybrook JH & Wasson EA. The biocompatibility of glass ionomer cements. A review. *J. of Biomater Sci. Polymer.* **2(4)**: 277-85, 1991.
50. Wilson AD; Groffman DR & Kuhn AT. The release of fluoride and other chemical species from a glass-ionomer cement. *Biomaterials.* **6**: 431-433, 1985.
51. Wilson AD & McLean JW. Glass-ionomer cement. *Quintessence Publishing Co. Inc. Chicago, Illinois.* 1988
52. Wilson AD & Kent BE. The glass-ionomer cement: A new translucent dental filling material. *J. Appl. Chem. Biotechnol.* **21**: 313, 1971
53. Powis DR, Folleras T, Merson SA & Wilson AD. Improved adhesion of a glass-ionomer cement to dentine and enamel. *J. Dent. Res.* **61**: 1416-1422, 1982.

54. Wilson AD & Crisp S. Poly(carboxylate) cement. *Br. Pat.* **1**: 422, 377, 1972.
55. McLean JW & Wilson AD. The clinical development of the glass-ionomer cement I. Formulations and properties. *Aust. Dent. J.* **22**: 31-36, 1977.
56. Aboush Y EY & Jenkin CBG. An evaluation of the bonding of glass-ionomer restorative to dentine and enamel. *Br. Dent. J.* **161**: 179-184, 1986.
57. Brook IM; Craig GT; Hatton PV & Jonck LM. Bone cell interactions with a granular glass-ionomer bone substitute material: *in vivo* and *in vitro* culture models. *Biomaterials.* **13(10)**: 721-725, 1992.
58. Hatton PV & Brook IM. Characterization of the ultrastructure of glass-ionomer (poly-alkenoate) cement. *Br. Dent. J.* **173**: 275-277, 1992.
59. Hatton PV, Craig GT & Brook IM. Characterization of the interface between bone and glass-ionomer(polyalkenoate) cement using transmission electron microscopy and x-ray microanalysis. *Advances in Biomaterials.* **10**: 331-336, 1992.
60. Crisp S; Lewis BG & Wilson AD. Characterisation of glass-ionomer cements. Effect of powder:liquid ratio on the physical properties. *J. Dent. Res.* **4**: 287-290, 1976.
61. Williams JA & Billington RW. Increase in compressive strength of glass-ionomer restorative materials with respect to time: a guide to their suitability for use in posterior primary dentition. *J. Oral Rehabilitation.* **16**: 475-479, 1989.
62. Wood D; Hill R. Structure-property relationships in ionomer glasses. *Clin. Mater.* **7**: 301-312, 1991.
63. Piotrowski G; Hench LL; Allen WC & Miller GJ. Mechanical studies of the bone bioglass interfacial bond. *J. Biomed. Mater. Res. Symp.* **6**: 47-61, 1975.
64. Gross UM & Strunz V. The anchoring of glass ceramics of different solubility in the femur of the rat. *J. Biomed. Mater. Res. Symp.* **14**: 607-618, 1980.
65. McLean JW. Glass-ionomer cements. *Br. Dent. J.* **164**: 293-300, 1988.
66. Loescher AR; Robinson PP; Brook IM. The immediate effects of implanted ionomeric and acrylic bone cements on peripheral nerve function. *J. Materials Sci. in Med.* **5**: 551-556, 1994.
67. Bodell SM; Brook IM & Hatton PV. *In vitro* biomechanical evaluation of glass-ionomer and polymethylmethacrylate cements. *J. Dent. Res.* **73**: 740, 1993.

68. Crisp S & Wilson AD. Reactions in glass-ionomer cements: Decomposition of the powder I. *J. Dent. Res.* **53**: 1408-1413, 1974.
69. Barry TI; Clinton DJ & Wilson AD. The structure of a glass-ionomer cement and its relationship to the setting process. *J. Dent. Res.* **58**: 1072-1079, 1979.
70. Forsten L. Fluoride release and uptake by Glass-ionomers. *Scand. J. Dent. Res.* **99**: 241-5, 1991.
71. Yoshii S; Kakutani Y; Nakamura T; Kitsugi T; Oka T; Kokubo T; Takagi M. *J. Strength of bonding between A-W glass ceramic and the surface of bone cortex. Biomed. Mater. Res. Appl. Biomater.* **22(A3)**: 327-38, 1988.
72. Wilson AD & Kent BE. Surgical cement. *Br. Patent.* **129**: 1316, 1973.
73. Seppä L; Torppa-saarinen E; Luoma H. Effect of different glass-ionomers on the acid production and electrolyte metabolism of *Streptococcus mutans* Ing Britt. *Caries Res.* **26**: 434-438, 1992.
74. Swift Jr ER. *In vitro* caries-inhibitory properties of a silver cermet. *J. Dent. Res.* **68**: 1088-1093, 1989.
75. Forss H; Seppä L. Prevention of enamel demineralization adjacent to glass-ionomer filling materials. *Scand. J. Dent. Res.* **98**: 173-178, 1990.
76. Wittwer C; Devlin AJ; Hatton PV; Brook IM & Downes S. The release of serum proetins and dye from glass-ioomer (polyalkenoate) and acrylic cements: A pilot study. *Jn. of Mats. Science: Mats. in Medicine.* **5**: 711-714, 1994.
77. Helms J; Geyer G. Closure of the perous apex of the temporal bone with ionomeric cement following translabyrinthine removal of an acoustic neuroma. *J. Laryngol. Otol.* **108(3)**: 202-205, 1994.
78. Loescher AR; Robinson PP; Brook IM. The immediate effects of implanted ionomeric and acrylic bone cements on peripheral nerve function. *J. Materials Sci. in Med.* **5**: 108-112, 1994.
79. Renard JL; Felten D; Bequet D. Post-otoneurosurgery aluminium encephalopathy. *Lancet.* **344**: 63-64, 1994.
80. Brook IM; Lamb DJ. Clinical evaluation of ionogran for use in the restoration and treatment of alveolar bone atrophy. *Proc 11th European Conf. on Biomaterials.* Pisa, Tipografia Vigo Cursi, 466-468, 1994.

81. Sasanaluckit P; Albustany KR; Dockerty PJ; Williams DF. Biocompatibility of glass-ionomer cements. *Biomaterials*. **14(12)**: 906-916, 1993.
82. Hatton PV; Brook IM. X-ray microanalysis of bone and implanted bone substitutes. *Micron et Microscopica Acta*. **23**: 363-364, 1992.
83. Mallakh BF; Sarker NK. Fluoride release from glass-ionomer cements in de-ionized water and artificial saliva. *Dent. Mater.* **6**: 118-122, 1990.
84. Swartz ML; Phillips RW & Clark HE. Long-term fluoride release from glass-ionomer cements. *J. Dent. Res.* **63**: 158-160, 1984.
85. Shimokobe H; Komatsu H & Matsui I. Fluoride content in human enamel after removal of the applied glass-ionomer cements. *J. Dent. Res.* **66**:131, 1982.
86. Wesenberg G & Hals E. The *in vitro* effect of a glass-ionomer cement on dentine and enamel walls. *J. Oral Rehabil.* **7**: 35-42, 1980.
87. Riggs BL & Melton III J. Involutional osteoporosis. *New England. J. Med.* **314**: 1676-1686, 1986.
88. Sögaard CH; Mosekilde L; Schwartz W; Leidig G; Minne HW; Ziegler R. Effects of fluoride on rat vertebral body biomechanical competence and bone mass. *Bone*. **16**: 163-169, 1995.
89. Reed BY; Zerwekh JE; Antich PP; Pak CY. Fluoride-stimulated [³H] thymidine uptake in a human osteoblastic osteosarcoma cell line is dependent on transforming growth factor beta. *J. Bone Miner. Res.* **8(1)**: 19-25, 1993.
90. Smith DC & Peltomiemi A. In Biocompatibility of Dental Materials, *Characteristics of Dental Tissues and their Response to Dental Materials*, ed DC Smith & DF Williams. CRC Press, Boca Raton, Florida. **1**, 1982.
91. Guyton AC. *Textbook of medical physiology*. WB Saunders Co. 1986.
92. Frost HM. Coherence treatment of osteoporosis. *Orthopaedic Clinics of North America*. **12**: 649-69, 1981.
93. Farley JR; Wergedal JE; Baylink DJ. Fluoride directly stimulates proliferation and ALP activity of bone-forming cells. *Science*. **222**: 330-332, 1983.
94. Lundy MW; Fraley JR; Baylink DJ. Characterization of a rapidly responding animal model for fluoride-stimulated bone formation. *Bone*. **7**: 289-293, 1986.

95. Turner RT; Francis R; Brown D; Garand J; Hannon KS; Bell NH. The effects of fluoride on bone and implant histomorphometry in growing rats. *J. Bone Miner. Res.* **4(4)**: 477-484, 1989.
96. Zipkin I; McClure FJ & Lee WA. Relation of the fluoride content of human bone to its chemical composition. *Arch. Oral. Biol.* **2**: 190, 1960.
97. Charen J; Taves DR; Stem JW & Parkins FM. Bone fluoride concentrations associated with fluoroiodated drinking water. *Calcif. Tissue. Int.* **27**: 95, 1979.
98. Zipkin I; McClure FJ; Leone NC & Lee WA. Fluoride deposition in human bone after prolonged ingestion of fluoride in drinking water. *US Public Health Rep.* **73**: 732, 1958.
99. Baylink D; Wergdal J; Stauffer M & Rich C. Effects of fluoride on bone formation, mineralization and resorption in the rat, in fluoride in medicine. *Visscher Th. Ed. Huber, Bern.* 37, 1970.
100. Licata AA. Therapies for symptomatic primary osteoporosis. *Geriatrics.* **46(11)**: 62-3, 66-7, 1991.
101. Quarles LD; Murphy G; Vogler JB; Derzner MK. Aluminium induced neogenesis. A generalised process affecting trabecular networking in the axial skeleton. *J. Bone Mineral Res.* **5**: 652-635, 1990.
102. Meyer U; Szulczewski DH; Barckhaus RH; Atkinson M; Jones DB. Biological evaluation of an ionomeric bone cement by osteoblast cell culture methods. *Biomaterials.* **14(12)**: 917-924, 1993.
103. Szulczewski DH; Meyer U; Moller K; Startmann U; Doty SD; Jones DB. Characterisation of bovine osteoclasts on an ionomeric cement *in vitro*. *Cells and Materials.* **36**: 438-441, 1984.
104. Blumenthal NC; Posner AS. *In vitro* model of aluminium-induced osteomalacia inhibition of hydroxyapatite formation and growth. *Calc. Tissue Int.* **36**: 438-441, 1984.
105. Quarles LD. Paradoxal toxic and trophic osseous actions of aluminium: potential explanations. *Miner. Electrolyte Metab.* **17**: 233-239, 1991.
106. Goodman WG. Bone disease and aluminium: pathogenic considerations. *Am. J. Kidney Res.* **6**: 330-335, 1986.
107. Goodman WG; O'Connor J. Aluminium alters calcium influx and efflux from bone *in vitro*. *Kidney Inter.* **39**: 602-607, 1991.

108. Renard JL; Fettes D; Bèquet D. Post-otoneurosurgery aluminium encephalopathy. *The Lancet*. **344**: 63-64, 1994.
109. Kitsugi T; Nakamura T; Oka M; Cho SB; Muiyaji F; Kokubo T. Bone-bonding behaviour of three heat-treated silica gels implanted in mature rabbit bone. *Calcif. Tissue Int.* **57 (2)**: 155-160, 1995.
110. Driessens FCM & Verbeeck RMH. The effect of fluoride on calcium phosphates and calcified Tissues. *Biomaterials*. *CRC Press, Boston*. 1990.
111. Morohashi T; Sano T; Yamada S. Effects of strontium on calcium metabolism in rats I. A distinction between the pharmacological and toxic doses. *Jpn. J. Pharmacol.* **64(3)**: 155-62, 1994.
112. Reeve SH; Heso R and Wootton R. A new tracer method for the calculation of rates of bone formation and breakdown in osteoporosis and their generalized skeletal disorders. *Calcif. Tissue Res.* **22**: 191, 1976.
113. Dow EC & Stanbury JB. Strontium and calcium metabolism in metabolic bone diseases. *J. Clin. Invest.* **39**: 385, 1960.
114. McCredic D & Retenberg E. Strontium kinetic studies in children with bone disorders. *Austr. Paediatr. J.* **3**: 327, 1972.
115. Hinoura K; Moore BK & Phillips RW. Tensile bond strength between glass ionomer cement and composite resins. *J. Am. Dent. Assoc.* **114**: 167-172, 1987.
116. McCulloch AL & Smith BGN. *In vitro* studies of cusp reinforcement with adhesive restorative material. *Br. Dent. J.* **161**: 450-452, 1986.
117. Williams D. An introduction to medical and dental materials, In: *Williams D (ed) Concise encyclopaedia of medical and dental materials*, Pergamon Press, Oxford. 134-139, 1991.
118. Pillar RM. Modern metal processing for improved load-bearing surgical implants. *Biomaterials*. **12**: 95-100, 1991.
119. McDonald DJ; Sui FH; McLeod RA & Dahlin DC. Giant-cell tumor of bone. *J. Bone Joint Surg.* **68A(2)**: 235-42, 1986.
120. DeLeeuw HW & Pottenger LA. Osteonecrosis of the acetabulum following radiation therapy. *J. Bone Joint Surg.* **70A(2)**: 293-9, 1988.

121. Harris WH & Penenberg BL. Further follow-up on socket fixation using a metal-backed acetabular component for total hip replacement. *J. Bone Joint Surg.* **69A(8)**: 1140-3, 1987.
122. Dorr LD; Takei GK & Conaty JP. Total hip arthroplasties in patients less than forty-five years old. *J. Bone Joint Surg.* **65A(4)**: 474-9, 1983.
123. Ortman BL & Pack LL. Aseptic loosening of a total hip prosthesis secondary to tophaceous gout. *J. Bone Joint Surg.* **69A(7)**: 1096-9, 1987.
124. Callaghan JJ; Salvati EA; Pellicci PM; Wilson DD & Ranawat CS. Results of revision for mechanical failure after cemented total hip replacement, 1979 to 1982. *J. Bone Joint Surg.* **67A(7)**: 1074-85, 1985.
125. Kavanagh BF & Fitzgerald RH. Multiple revisions for failed total hip arthroplasty not associated with infection. *J. Bone Joint Surg.* **69A(8)**: 1144-9, 1987.
126. Cheung LK; Sammon Nabil & Tideman H. The use of mouldable acrylic for restoration of the temporalis flap donor site. *J. Cran. Max. Fac. Surg.* **22**: 335-341, 1994.
127. Belligoi ME; Peade PC. The effect polymethylmethacrylate as an alloplastic on lay graft on rat calvarial bone. *Abstract in 15th ANZAOMS Biennial Conference, Melbourne 14*, 1993.
128. Kavanagh B; Devitz M; Ilstrup D; Stauffer R & Coventry M. Charnley total hip arthroplasty with cement. *J. Bone Joint Surg.* **71A**: 1496, 1989.
129. Salvati E; Wilson P; Jolley M; Vakili F; Aglietti P & Brown G. A ten-year follow up study of our first hundred consecutive Charnley total hip replacements. *J. Bone Joint Surg.* **63A**: 753, 1981.
130. Stauffer R. Ten-year follow-up study of total hip replacement with particular reference to roentographic loosening of the components. *J. Bone Joint Surg.* **64A**: 983, 1982.
131. Sutherland C; Wilse A; Borden L & Marks K. A ten-year follow-up of one hundred consecutive Muller curved-stem total hip replacement arthroplasties. *J. Bone Joint Surg.* **64A**: 970, 1982.
132. Wroblewski BM. 15-21-year results of the Charnley low-friction arthroplasty. *Clin. Orthop.* **211**: 30, 1986.

133. Fischer AA. Reactions to acrylic bone cement in orthopaedic surgeons and patients. *Cutis*. **37**: 425-426, 1986.
134. Tallroth K; Eskola A; Santavirta S; Kontinen YT; Lingholm TS. Aggressive granulomatous lesions after hip arthroplasty. *Br. J. Bone Joint Surg.* **71**: 571-575, 1989.
135. Frame JW; Rout PGJ & Browne RM. Ridge augmentation using solid and porous HA particles with and without autogenous bone or plaster. *J. Oral Maxillofacial. Surg.* **45**: 771-775, 1987.
136. White E & Shors EC. Biomaterial aspects of interpore-200 porous HA. *Dental clinics N. America.* **30**: 49-67, 1986.
137. Klein CPAT; Abe Y; Hosono H & de Groot K. Comparison of calcium phosphate glass ceramics with apatite ceramics implanted in bone. An interfacial study II. *Biomaterials.* **8**: 234-236, 1987.
138. Kitsugi T; Yamamuro T; Nakamura T; Kotani S; Kokubo T & Takeuchi H. Four calcium phosphate ceramics as bone substitutes for non-weight-bearing. *Biomaterials.* **14**: 216-224, 1993.
139. Davies JE & Matsuda T. Extracellular matrix production by osteoblasts on bioactive substrata *in vitro*. *Scanning Microscopy.* **2(3)**: 1445-1452, 1983.
140. de Putter C; de Lange GI & de Groot K. Perimucosal dental implants of dense HA, evaluation and prognosis of their retention in alveolar bone. In: *Biological and biomechanical performance of biomaterials.* Ed. P. Christel et al. Elsevier Sci. Amsterdam. 111-116, 1986.
141. Van Blitterwijk; Grote JJ; Kwijpers CJG; Van Hock B & Daems WH. Bioreactions at the tissue hydroxyapatite interface. *Biomaterials.* **6**: 241-251, 1986.
142. Craig GT; Brook IM & Lamb DJ. Tissue response to subperiosteal implantation of dense hydroxyapatite. *Biomaterials.* **10**: 133-135, 1989.
143. Metsger DS; Driskell TD & Paulsrud RJ. Tricalcium phosphate ceramics a resorbable bone implant. *Review and current status.* *J. Am. Dent. Assoc.* **105**: 1035-8, 1982.
144. de Groot K. Bioceramics of calcium phosphate. *CRC Press, Boca Raton, Florida.* 1983.

145. Jarcho M; Kay JF & Gumaer KI. Tissue cellular and subcellular events at a bone ceramic hydroxyapatite interface. *J. Bio. Eng.* **1**: 79-92, 1977.
146. Van Blitterswijk CA; Hessling SC; Grote JJ; Koerten HK & de Groot. The biocompatibility of hydroxyapatite ceramic: A study of retrieved human middle ear implants. *J. Biomed. Mat. Res.* **24**: 433-453, 1990.
147. Scherft JP. The lamina limitans of the organic matrix of calcified cartilage and bone. *J. Ultrastructural Research.* **38**: 318-331, 1972.
148. Ham AW & Cormack DH. *Histology. Pub. J. B. Lippincott, Philadelphia, 396*, 1979.
149. Ogiso M; Kaneda H; Arasali J & Tabata T. Epithelial attachment and bone tissue formation on the surface of hydroxyapatite ceramics dental implants, In: *Biomaterials 1980, Winter GD et al (eds), John Wiley & Sons Ltd, London 59-64*, 1982.
150. Jansen JA; de Wijn JR; Wolters-Lutgerhorst JML & Van Mullen PJ. Ultrastructural study of epithelial cells attachment to implant materials. *J. Dent. Res.* **64**: 891-896, 1985.
151. Driskell JD; Hassler CR; Tennery VJ; McCoy IR & Clarke WJ. Calcium phosphate resorbable ceramic: A potential alternative for bone grafting. *J. Dent. Res.* **52**: 123-131, 1973.
152. LeGeros RZ; Daculsi G; Orly I; Gregorie M; Heughebaert M; Gineste M; Kijkowska. Formation of carbonate apatite on calcium phosphate materials: Dissolution/precipitation processes, In: *Bone-bonding biomaterials, Ducheune P et al (Eds), Reed Healthcare Communications, Leiderdorp, The Netherlands, 112-120*, 1992.
153. Van Blitterswijk CA & Grote JJ. Biological performance of ceramics during inflammation and infection, In: *CRC Critical Reviews in Biocompatibility, 5*: 13-43, 1989.
154. Shirota T; Ohno K; Michi K; Tachikawa T. An experimental study of healing around hydroxyapatite implants installed with autogenous iliac bone grafts for jaw reconstruction. *J. Oral Maxillofac. Surg.* **49**: 1310-1315, 1991.
155. Brook IM; Craig GT *et al*. Management of the mobile fibrous ridge in atrophic maxilla using porous hydroxyapatite blocks. *Br. Dent. J.* **162**: 413-420, 1987.

156. Brook IM & Lamb DJ. The use of particulate and block forms of hydroxyapatite for local augmentation. *Int. J. Oral and Maxillofac. Implants.* **2**: 85-89, 1987.
157. Frame JW & Brady CL. Augmentation of an atrophic edentulous mandible by interpositional grafting with hydroxyapatite. *J. Oral Maxillofac. Surg.* **43**: 89-92, 1984.
158. Terry BC; Albright JE & Baker RD. Alveolar ridge augmentation in the edentulous maxilla with use of autologous ribs. *J. Oral Surg.* **32**: 429-433, 1974.
159. Topazian RG; Hammer WB & Boucher IJ *et al.* Use of alloplastic for ridge augmentation. *J. Oral Surg.* **29**: 792-796, 1971.
160. Ducheyne D; Hench LL; Kagan A; Martens M; Burssens A & Mulier JK. Effects of hydroxyapatite impregnation on skeletal bonding of porous coated implants. *J. Biomed. Mater. Res.* **14**: 225-337, 1980.
161. Takagi M; Mochida M; Uchida N; Saito K & Uematsu K. Filter cake forming and hot isotactic pressing for TZP-dispersed Hydroxyapatite composite. *J. Mater. Med.* **3**: 199-203, 1992.
162. Klein CPAT. Calcium phosphate implant materials and biodegradation, *PhD Thesis, Free University, Amsterdam, The Netherlands*, 1983.
163. Klein CPAT; Driessen AA; de Groot K & Van den Hooff A. Biodegradation behaviour of various calcium phosphate materials in bone tissue. *J. Biomed. Mater. Res.* **17**: 769-782, 1983.
164. Klein CPAT; Patka P; Van der Lubbe HBM; Wolke JGC; de Groot K. Plasma-sprayed coatings of tetracalcium, hydroxyapatite and tricalcium phosphate on titanium alloy: an interface study. *J. Biomed. Mater. Res.* **25**: 53, 1991.
165. Van Blitterswijk CA; Grote JJ; Koerten HK & Kuijpers W. Biological performance of β -Whitlockite. A study in the non-infected and infected rat middle ear. *J. Biomed. Mater. Res.* **20**: 1197-1217, 1986.
166. Dhert WJA. Plasma-sprayed coatings and hard tissue compatibility. A comparative study on fluorapatite, magnesium whitelockite and hydroxyapatite, *PhD Thesis, Leiden University, The Netherlands*, 1993.
167. Gross U; Schmitz HJ; Kinne R; Fendler FR & Struntz V. Tissue or cell culture versus *in vivo* testing of surface reactive biomaterials, In: *Biomaterials and clinical applications*, Ed. Pizzoferrato, Ravaglio & Lee. Elsevier Science Pub. BV; Amstredam, The Netherlands. 547-556, 1987.

168. Szulczewski DH; Meyer U; Moller K; Stratmann U; Doty SD & Jone DB. Characterisation of bovine osteoclasts on an ionomeric cement *in vitro*. *Cells and Materials*. **3**: 83-92, 1993.
169. Kawahara H; Imanishi Y & Tomaka K. Dental application of a glass-ionomer cement. *Dental Outlook*. **50**:623-633, 1977.
170. Lau William KH; Yoo A & Wang SD. Aluminium stimulates the proliferation and differentiation of osteoblasts *in vitro* by a mechanism that is different from fluoride. *Mol. Cell Biochem*. **105**: 93-105, 1991.
171. Nomura S; Willis AJ, Edwards DR; Heath JK & Hogan BLM. development expression of 2ar (osteopontin) and SPARC (osteonectin) RNA as revealed by *in situ* hybridisation. *J. Cell Biol*. **106**: 441-450, 1988.
172. Mark MP; Butler WT; Prince CW; Finkleman RD & Ruch JV. Developmental expression of 44kDa bone phosphoprotein (osteopontin) and bone q-carboxyglutamic acid (Gla)-containing protein (osteocalcin) in calcifying tissues of rat. *Differentiation*. **37**: 123-136, 1988.
173. Hirakawa Y; Ikeda T; Yamaguchi A; Hirota S; Takemura T; Kitamura K & Nomura S. Localization of the mRNA for bone matrix proteins during fracture healing as determined by *in situ* hybridization. *J. Bone Miner. Res*. **9(10)**: 1551-1557, 1994.
174. Akiyama S & Yamada KM. Fibronectin and disease, In *Connective Tissue and Diseases of connective tissues*, ed Wagner B; Mayer RF. Baltimore: Williams & Wilkins, 1993.
175. Reddi AH. Regulation of bone differentiation by local and systemic factors. In *Bone and mineral Reserach*. Vol 3. Ed Peck WA. Pub Elsevier, Amsterdam. 1985.
176. Weiss RE & Reddi AH. Appearance of fibronectin during the differentiation of cartilage, bone and marrow. *J. Cell Biol*. **88**: 630, 1980.
177. Weiss RE & Reddi AH. Role of fibronectin in collagenous matrix-induced mesenchymal cell proliferation and differentiation *in vivo*. *Exp. Cell Res*. **133**:247, 1981.
178. Erikson HP; Bourdon MA. Tenascin: an extracellular matrix protein prominent in specialized embryonic tissues and tumors. *Ann. Rev. Cell Biol*. **5**: 71-92, 1989.

179. Tervo K; Van Setten GB; Beuerman RW; Virtanen I; Tarkkanen A; Tervo T. Expression of tenascin and cellular fibronectin in the rabbit cornea after anterior keratectomy. Immunohistochemical study of wound healing dynamics. *Invest. Ophthalmol. Vis. Sci.* **32**: 2912-2918, 1991.
180. Van Setten Gb; Koch JW; Tervo K; Lang GK; Tervo T; Naumann GDH *et al.* Expression of tenascin and fibronectin in the rabbit cornea after laser excimer laser surgery. *Graefes. Arch. Clin. Exp. Ophthalmol.* **230**: 178-83, 1992.
181. Mackie EJ; Thesleff II & Chiquet-ehrisman R. Tenascin is associated with chondrogenic and osteogenic differentiation *in vivo* and promotes chondrocytes *in vitro*. *J. Cell Biol.* **105**: 2569-2579, 1987.
182. Howedy AA; Virtanen I; Laitinen L; Goud NS; Koukolis GK; Gould VE. Differential distribution of tenascin in the normal, hyperplastic and neoplastic breast. *Lab. Invest.* **63**: 798-806, 1990.
183. Chuong CM; Chen HM. Enhanced expression of neural cell adhesion molecules and tenascin (cytotactin) during wound healing. *Am. J. Pathol.* **138**: 427-440, 1991.
184. Olsen FK; Austin BP; Walia H. Osseous reaction to implanted Zinc oxide-eugenol retrograde filling materials in the tibia of rats. *J. Endod.* **20**(8); 389-94, 1994.
185. Majeska RJ; Rodan SB & Rodan GA. Parathyroid Hormone-responsive clonal cell lines from rat osteosarcoma. *Endocrinology.* **107**(9): 1494-1503, 1980.
186. Lowry ON; Roseburgh NJ; Farr AL; Randall RJ (1951). Protein measurement with the folin phenol reagent. *J. Biol. Chem.* **193**: 265-275.
187. Mosmann T (1983) Rapid colorimetric assay for cellular growth and survival: Application to proliferation and cytotoxicity assays. *J. Immunol. Methods.* **65**:55-63.
188. Albrektsson T & Johansen C. Quantified bone tissue reactions to various metallic implants with reference to the so called osseointegrated concept. In: *The bone biomaterial interface*, ed. JE Davies, University Toronto Press, 257-363, 1991.
189. Pizzoferrato A; *et al.* Quantitative biocompatibility our experience. In: *Biomaterial tissue interfaces* ed. P.J Doherty *Advances in Biomaterials.* Pub. Elsevier Science, Amsterdam, 63-72, 1992.

190. Ellis HA; McCarthy JH; Herrington J. Bone aluminium in haemodialysed and in rats injected with aluminium chloride: Relationship to impaired bone mineralisation. *J. Clin. Path.* **32**: 832-844, 1979.
191. Barry TI; Clinton DJ & Wilson AD (1978). The structure of a Glass-ionomer cement and its relationship to the setting process. *J. Dent. R.* **58(3)**: 1072-1079.
192. Zhong JP; LaTorre GP; Greenspan DC & Hench LL. Aluminium inhibitory effect on the formation of hydroxyapatite. In: *Bioceramics ed. Wilson J & Hench LL.* **8**: 489-492, 1995.
193. Bolvin G & Meunier PJ. In: The metabolic and molecular basis of acquired disease, ed. Cohen RD; Lewis B; Albertii KGMM & Denman AM, *Balliere Tindall, London.* 1803-1823, 1990.
194. Moonga BS; Dempster DW. Zinc is a potent inhibitor of osteoclastic bone resorption *in vitro.* *J. Bone Miner. Res.* **10(3)**: 453-7, 1995.
195. Kuhn AT & Wilson AD. The dissolution mechanisms of silicate and glass-ionomer dental cements. *Biomaterials.* **6**: 378-382, 1985.
196. Davies EH; Sefton J; Wilson AD. Preliminary study of factors affecting the fluoride release from glass-ionomer cements. *Biomaterials.* **14(8)**: 636-639, 1993.
197. Gasser O. Glasionomerzemente: Gegenwart und zukunft aus werkstoffkundlicher sicht schweizer. *Monatsschrift f,r Zahnmedizin.* **97**:328-356, 1987.
198. Putt MS & Kleber CJ. Dissolution studies of human enamel treated with aluminium solutions. *J. Dent. Res.* **64**:437-40, 1985.
199. Halse A & Hals E. Electron probe microanalysis of secondary caries lesions adjacent to silicate fillings. *Calcif. Tissue Res.* **21**: 183-93, 1976.
200. Exley C & Birchall JD. A mechanism of hydroxyaluminosilicates formation. *Polyhedron.***12**: 1007-1017, 1993.
201. Exley C & Birchall JD. Silic acid and the biological availability of aluminium. *European J. Soil Sci.* **47**: 137, 1996.2
202. Birchall JD; Exley C; Chappell JS & Phillips MJ. Acute toxicity of aluminium to fish eliminated in silicon-rich acid water. *Nature.* **388**: 146-148, 1989.
203. Atkins PW. *Physical Chemistry.* Third Edition. Oxford University Press. pp 677-681, 1986.

204. Atkins PW. *Physical Chemistry*. Third Edition. Oxford University Press. pp 166-168, 1986.
205. Erbe M; Vandyckerbe RL; Schmitz HJ (1996). Comparison of a Polymethylmethacrylate and glass-ionomer cement using a hemiarthroplasty in the rabbit femur. *J. Mats Science in Med.* 7(8): 517-522.
206. Carter DH; Sloan P; Brook IM and Hatton PV. Role of exchanged ions in the integration of ionomeric (glass polyalkenoate) bone substitutes. *Biomaterials.* 18: 459-466, 1997.
207. Blades MC; Hill R; Morre D; Revell PA. *In vivo* biocompatibility and biomechanically behaviour of two novel glass-ionomer (polyalkenoate) cements for potential use in total joint arthroplasty. *J. Pathology.* 181: A46.
208. Steenland K, Goldsmith DF. Silica exposure & autoimmune disease. *Am. J. Ind. Med.* 28(5): 603-8, 1995.
209. Zaidi M; Kerby J; Huang CL; Alam T; Rathod H; Chambers TJ; Moogna BS. Divalent cations mimic the inhibitory effect of extracellular ionised calcium on bone resorption by isolated rat osteoclasts further evidence for a "calcium receptor". *J. Cell Physiology.* 149(3): 422-7, 1991.
210. Farley JR. Phosphate regulates the stability of skeletal alkaline phosphatase activity in human osteosarcoma (SaOs-2) cells without equivalent effect on the level of skeletal alkaline phosphatase immunoreactive protein. *Calcif. Tissue Int.* 57(5): 371-8, 1995.
211. Vander AJ; Sherman JH; Luciano DS. *Human Physiology: The mechanisms of body function.* McGraw-Hill Book Co. 1986.
212. Hadley P; Billington RW; Pearson GJ. Effect of monovalent ions in glass-ionomer on their uptake/re-release. *J. Dent. Research.* 76(5): 1031, A103, 1997.
213. Hatton PV; Douglas CWI; Benderli Y & Marathakis A. *In vitro* evaluation of the antibacterial activity of glass-ionomer cements. *1st European Union Conference on glass-ionomer cements.* 39-40, 1996.
214. Billington RW; Hadley P and Pearson GJ. Interactions of glass-ionomer cements with alkali metal and fluoride solution. *J. Dent. Res.* 76(5):1031:A102, 1997.
215. Freshney RI. *Culture of animal cells. A manual of Basic Technique.* Third ed. Wiley-Liss Publ. 1994.

216. Boskey AL; Stiner D; Doty S; Bindermann I; Leboy P. Studies of mineralization in tissue culture: Optimal conditions for cartilage calcification. *Bone and Mineral*. **16**: 11-36, 1992.
217. Chung C; Golub EE; Forbes E; Tokuoka T; Shapiro I. Mechanism of action of β -glycerophosphate on bone cell mineralization. *Calcif. Tissue Int.* **51**: 305-311, 1992.
218. Oliva A; Della Ragione F; Aslerno A; Riccio V; Tartaro G; Cozzolina A; D'Amato S; Pontoni G and Zappia V. Biocompatibility studies on glass ionomer cements by primary cultures of human osteoblasts. *Biomaterials*. **17**:1351-1356, 1996.
219. Hatton PV; Craig GT & Brook IM. Glass- polyalkenoate cements. *Biomaterial-Tissue Interfaces*, Doherty PJ et al (Eds.), *Advances in Biomaterials*, Elsevier Science Publishers. **10**:331-336, 1992.
220. Pak CY; Sakhee K; Zerwekh JE; Parcel C; Peterson R & Johnson K. Safe and effective treatment of osteoporosis with slow release sodium fluoride: augmentation of vertebral bone mass and inhibition of fractures. *J. Clin. Endocrine Metab.* **68**: 150-159, 1989.
221. Heaney RP. Life long calcium intake and prevention of bone fragility in the aged. *Calcified Tissue International*. **49**:542-5, 1991.
222. Edwards GK; Sanotoro J; Taylor A Jr. Use of bone scintigraphy to select patients with multiple myeloma for treatment with strontium-89. *J. Nucl. Med.* **35(12)**: 1992-3, 1994.
223. Marie PJ; Hott M; Modrowski D; De Pollak C; Guillermain J; Deloffre P; Tsouderos Y. An uncoupling agent containing Strontium prevents bone loss by depressing bone resorption and maintaining bone formation in estrogen-deficient rats. *J. Bone Miner. Res.* **8(5)**: 607-15, 1993.
224. Morohashi T; Sano T; Harai K; Yamada S. Effects of strontium prevents the increased rate of bone turnover in ovariectomized rats. *Jpn. J. Pharmacol.* **68(2)**: 153-9, 1995.
225. Grynepas MD; Hamilton E; Cheung R; Tsouderos Y; Del Offre P; Hott M; Marie PJ. Strontium increases vertebral bone volume in rats at a low dose that does not induce detectable mineralisation effect. *Bone*. **18(3)**: 253-9, 1996.
226. Neufield BE; Boskey AL. Strontium alters the complexed acidic phospholipid content of mineralizing tissues. *Bone*. **15 (4)**: 425-30, 1994.

227. Wilson AD; Crisp S & Paddon JM. The hydration of a glass- ionomer (ASPA) cement. *Br. Polym. J.* **13**: 66-70, 1981.
228. Hornsby PR. Dimensional stability of glass-ionomer cements. *J. Chem. Tech.* **30**:595-601, 1980.
229. Paddon JM & Wilson AD. Stress relaxation studies on dental materials. *Dental cements J. Dent.* **4**: 183-189, 1976.
230. Yamada KM & Olden K. Fibronectins-adhesive glycoproteins of cell surface and blood. *Nature.* **275**: 179-184, 1978.
231. Carter DH; Sloan P& Aaron JE. Immunolocalization of collagen Types I and III, Tenascin, and fibronectin in intramembranous Bone. *J. Histochem. Cytochem.* **5**: 599-606, 1991.
232. Brook IM. Evaluation of glass-ionomer cements for use as bone substitutes with reference to their value for treatment of atrophic alveolar bone. *PhD thesis.* University of Sheffield. UK. 1993.
233. Winter M; Griss P; De Groot K; Tagai H; Heinke G; Van Zdiijk HJ and Sawaai K. Comparative histocompatibility testing of seven calcium phosphate ceramics. *Biomaterials.* **2**: 159-160, 1981.
234. Vrouwerwelder WC; de Groot CG and de Groot K. Behaviour of fetal rat osteoblasts cultured *in vitro* on bioactive glass and non-active glasses. *Biomaterials.* **13**: 382-392, 1992.
235. Smith KG; Franklin CD; Van Noort R and Lamb DJ. Tissue response to the implantation of two new machinable calcium phosphate ceramics. *Int. J. Oral. Maxillofac. Implants.* **7**: 395-400, 1992.
236. Nakamura M; Kawahara H; Imia K; Tomoda S; Kawata Y and Hikari S. Long-term biocompatibility test of composite resins and glass-ionomer cement *in vitro*. *J. Dent. Mater.* **2(1)**: 100-112, 1983.
237. Gross UM. Biocompatibility. The interaction of biomaterials and the host response. *J. Dent. Ed.* **52**: 798-803, 1988.
238. Kohau D; Schwartz Z; Amir D; Mullermai C; Gross U and Sela J. Effect of titanium implants on primary mineralisation following 6 and 14 days of rat tibial healing. *Biomaterials.* **13**:255-260, 1992.

239. Chaim Brandon. Diffusional transformations in ZrO_2 - Y_2O_3 induced by surface segregation. *Acta Metall.* **34(10)**: 1933-1939, 1986.

APPENDIX

Key to Tables

I = Perimeter of implant (mm)

C = Length of intimate implant/ bone contact (mm)

C/I x 100 = % Osseointegration

T = Thickness of new bone, Osteoconduction(mm)

Distance from implant to mature bone

(New bone / unit length)

Tables A1 to A3 The % osseointegration and the degree of osteoconductivity of the set Sodium based ionomeric cement rods

Table A1 Material : LG2

I	C	C/I	T
3.0	1.1	36.7	0.07
2.9	1.08	37.2	0.04
3.4	1.3	38.2	0.06
5.0	1.8	36.0	0.03
3.5	1.3	37.1	0.03
		Mean=37.04	Mean=0.05
		SD=0.8	SD=0.02

Table A2 Material:LG6

I	C	C/I	T
3.2	1.94	60.6	0.09
2.9	1.8	62.1	0.10
2.3	1.4	60.9	0.17
3.6	2.3	63.9	0.06
3.7	2.1	56.8	0.02
		Mean=61.0	Mean=0.09
		SD=2.6	SD=0.06

Table A3 Material: LG63

I	C	C/I	T
4.7	3.2	68.1	0.09
4.5	3.0	66.7	0.11
4.2	2.85	67.9	0.15
3.5	2.4	68.6	0.09
3.2	2.2	68.8	0.08
		Mean=68.02	Mean=0.10
		SD=0.82	SD=0.03

Tables A4 to A6 The % osseointegration and the degree of osteoconductivity of the apatite-stoichiometric based series (Ca:P~1.66) set rods

Table A4 Material:LG26

I	C	C/I	T
3.5	2.8	80.0	0.14
2.6	2.18	83.8	0.13
5.6	4.3	76.8	0.17
4.8	3.9	81.3	0.16
2.8	2.3	82.1	0.18
		Mean=80.8 SD=2.63	Mean=0.16 SD=0.2

Table A5 Material: LG27

I	C	C/I	T
2.8	2.2	78.6	0.10
5.5	4.2	76.4	0.06
4.5	3.5	77.8	0.08
3.5	2.8	80.0	0.07
3.8	2.98	78.4	0.10
		Mean=78.2 SD=1.31	Mean=0.08 SD=0.02

Table A6 Material: LG30

I	C	C/I	T
5.5	3.7	67.3	0.08
6.1	4.3	70.5	0.06
3.2	2.3	71.9	0.09
3.3	2.3	69.7	0.09
3.1	2.28	73.5	0.05
		Mean=70.6 SD=2.3	Mean=0.07 SD=0.02

Tables A7 to A8 showing the % osseointegration and the degree of osteoconductivity of the sodium based wet ionomeric cements

Table A7 Material: LG23 1:2:3

I	C	C/I	T
8.3	5.8	69.5	0.02
5.7	3.7	65.0	0.03
8.6	5.8	67.4	0.03
2.5	1.5	60.0	0.03
2.6	1.7	65.4	0.09
		Mean=65.5	Mean=0.04
		SD=3.5	SD=0.03

Table A8 Material: LG23 1:2:2

I	C	C/I	T
5.3	2.8	52.8	0.02
3.1	1.5	48.4	0.01
6.7	3.5	52.2	0.04
4.9	2.6	53.1	0.02
4.5	2.1	46.7	0.01
		Mean=50.6	Mean=0.02
		SD=2.9	SD=0.01

Tables A9 to A10 showing the % osseointegration and the degree of osteoconductivity of the apatite-stoichiometric based wet ionomeric cements

Table A9 Material: LG26

I	C	C/I	T
8.4	5.8	69.0	0.07
5.0	3.3	66.0	0.07
10.2	6.9	67.6	0.07
2.8	1.8	64.3	0.03
1.9	1.3	68.4	0.07
		Mean=67.1	Mean=0.06
		SD=1.9	SD=0.02

Table A10 Material: LG30

I	C	C/I	T
3.7	1.9	51.4	0.01
2.2	1.3	59.1	0.05
3.5	1.8	51.4	0.05
3.3	1.8	54.5	0.07
3.2	1.8	56.3	0.01
		Mean=54.5	Mean=0.04
		SD=3.3	SD=0.03

Tables A11 to A12 showing the % osseointegration and the degree of osteoconductivity for the Strontium based radiopaque wet ionomeric cements

Table A11 Material: LG119

I	C	C/I	T
10.9	6.5	59.6	0.06
7.1	4.1	57.7	0.08
2.7	1.6	59.3	0.03
4.0	2.1	52.5	0.04
2.9	1.5	51.7	0.06
		Mean=56.2	Mean=0.05
		SD=3.8	SD=0.02

Table A12 Material: LG125

I	C	C/I	T
1.5	1.1	73.3	0.09
8.5	6.4	75.3	0.07
6.9	5.5	79.7	0.07
6.2	4.8	77.4	0.09
8.1	6.4	79.0	0.08
		Mean=77.0	Mean=0.08
		SD=2.6	SD=0.01

Tables A13 to A14 showing the % osseointegration and the degree of osteoconductivity of the Zinc based radiopaque wet ionomeric cements

Table A13 Material: LG130

I	C	C/I	T
5.6	3.9	69.6	0.04
11.1	8.1	72.9	0.02
3.1	2.3	74.2	0.09
12.5	8.6	68.8	0.05
4.3	3.3	76.7	0.03
		Mean=72.4 SD=3.3	Mean=0.05 SD=0.03

Table A14 Material: LG132

I	C	C/I	T
11.5	4.7	42.3	0.07
18.8	7.6	40.4	0.04
2.8	1.2	42.9	0.06
2.5	1.1	44.0	0.06
2.8	1.2	42.9	0.04
		Mean=42.5 SD=1.3	Mean=0.05 SD=0.01

Tables A15 to A16 showing the % osseointegration and the degree of osteoconductivity of the PMMA controls

Table A15 Materials: Set Acrylic

I	C	C/I	T
22.8	6.9	30.3	0.05
1.4	0.4	28.6	0.02
5.9	1.6	27.1	0.04
2.0	0.6	30.0	0.05
1.2	0.4	33.3	0.07
		Mean=29.9 SD=2.3	Mean=0.05 SD=0.02

Table A16 Materials: Wet Acrylics

I	C	C/I	T
15.7	3.5	22.3	0.03
10.4	2.8	26.9	0.06
7.1	1.7	23.9	0.02
32.6	9.2	28.2	0.01
6.3	1.8	28.6	0.02
		Mean=25.9 SD=2.8	Mean=0.03 SD=0.02

ABBREVIATIONS

HA: Hydroxyapatite

PMMA: Polymethylmethacrylate

ICs: Ionomeric cements

GICs: Glass ionomer cements

XRMA: X-ray microanalysis

P/L: powder/liquid

CFS: Cerebral spinal fluid

Al³⁺: Aluminium

Ca²⁺: Calcium

Ca-P: Calcium-phosphate

CNS: Central nervous system

ALP: Alkaline phosphatase

SaOS-2: Human osteosarcoma cells

Ca₃[PO₄]₂: β-Tricalcium phosphate

β-TCP: Beta-Tricalcium phosphate

TEM: Transmission electron microscopy

ECM: Extracellular matrix

OPN: Osteopontin

FN: Fibronectin

TN: Tenascin

mRNA: Messenger ribonucleic acid

LG: Limerick Glass

PTFE: Poly(tetrafluoroethane)

PMMA: Poly(methylmethacrylate)

Si: Silicon

SiO₂: Silica

O: Oxygen

Al: Aluminium

P: Phosphate

Ca: Calcium

F: Fluoride

Na: Sodium

Fe³⁺: Iron III

K: Potassium

Sr: Strontium

Zn: Zinc

H: Hydrogen

OH: Hydroxide

mm: Millimeters

ml: Milliliters

g: Grammes

ppm: Parts per million

mg/l: Milligramme per liter

MP: MegaPascals

M: Moles

Mf: Mole fraction

AAS: Atomic absorption spectroscopy

ACQ: Analytical quality control

AQCS: Analytical Quality Control Standard

HPLC: High pressure liquid chromatography

°C: Degrees centigrade

%: per cent

SEM: Scanning electron microscopy

kV: Kilo volt

DOC: Deoxycholate

TCA: Trichloroacetic acid

EDTA: Ethyldiaminotetracetic acid

µg/ml: Microgramme per milliliter

µl: Microlitre

**MTT: Methyl tetrazolium test or 3-4,5-[diamethylthiazol-2-yl]-2,5-diphenyl
tetrazolium bromide**

nm: Nanometers

γ: Gamma

w/v: water per volume

M: Molar

SBT: South Bay Technology

FITC: fluorisothiocyanate

s: Seconds

SD: Standard deviation

n: Numbers

na: Not applicable

Ca:P: Calcium phosphate

USA: United States of America

UK: United Kingdom

UV: Ultra violet

autc: Autoclaved

w: Water

m: media

BM: Basic medium

BSM: Basic supplemented medium

DOC: Deoxycholate

TCA: Trichloroacetic acid

HAS: Hydroxyaluminosilicates

α -MEM: Minimal essential media

ECF: Extracellular fluid

XPS: X-ray photoelectron Spectroscopy

I: Perimeter of implant

C: Length of intimate implant/bone contact

T: Thickness of new bone, osteoconduction

NB: New bone

MB: Mature bone

O: osteoid

C: Connective tissue

P: Endosteum

R: Reversal line

I: Implant

M Alpha Medium¹

	Cat No.	22571 1X Liquid	11900 Powder	22551 1X Liquid	12000 Powder	32571 1X Liquid	32551 1X Liquid	
	Component	mg/L	mg/L	mg/L	mg/L	mg/L	mg/L	
ORGANIC SALTS:	CaCl ₂ (anhyd.)	-	200.00	-	200.00	-	-	
	CaCl ₂ • 2H ₂ O	264.00	-	264.00	-	264.00	264.00	
	KCl	400.00	400.00	400.00	400.00	400.00	400.00	
	MgSO ₄ (anhyd.)	-	97.57	-	97.57	-	-	
	MgSO ₄ • 7H ₂ O	200.00	-	200.00	-	200.00	200.00	
	NaCl	6800.00	6800.00	6800.00	6800.00	6800.00	6800.00	
	NaHCO ₃	2200.00	-	2200.00	-	2200.00	2200.00	
	NaH ₂ PO ₄ • H ₂ O	-	140.00	-	140.00	-	-	
	NaH ₂ PO ₄ • 2H ₂ O	158.00	-	158.00	-	158.00	158.00	
SUGAR COMPONENTS:	D-Glucose	1000.00	1000.00	1000.00	1000.00	1000.00	1000.00	
	DL-68 Thioctic Acid	0.20	0.20	0.20	0.20	0.20	0.20	
	Phenol Red	10.00	10.00	10.00	10.00	10.00	10.00	
	Sodium Pyruvate	110.00	110.00	110.00	110.00	110.00	110.00	
	AMINO ACIDS:	L-Alanine	25.00	25.00	25.00	25.00	25.00	25.00
L-Arginine • HCl		127.00	126.98	127.00	126.98	127.00	127.00	
L-Asparagine • H ₂ O		50.00	50.00	25.00	50.00	50.00	25.00	
L-Aspartic Acid		30.00	30.00	30.00	30.00	30.00	30.00	
L-Cystine		24.00	-	24.00	-	24.00	24.00	
L-Cystine • 2HCl		-	31.28	-	31.28	-	-	
L-Cysteine HCl		100.00	100.00	100.00	-	100.00	100.00	
L-Cysteine HCl • H ₂ O		-	-	-	100.00	-	-	
L-Glutamic Acid		75.00	75.00	75.00	75.00	75.00	75.00	
L-Glutamine		292.00	292.00	292.00	292.00	-	-	
L-Alanyl-L-Glutamine		-	-	-	-	434.00	434.00	
Glycine		50.00	50.00	50.00	50.00	50.00	50.00	
L-Histidine HCl • H ₂ O		42.00	41.58	42.00	41.58	42.00	42.00	
L-Isoleucine		53.00	52.40	53.00	52.40	53.00	53.00	
L-Leucine		52.00	52.40	52.00	52.40	52.00	52.00	
L-Lysine • HCl		73.00	72.47	73.00	72.47	73.00	73.00	
L-Methionine		15.00	15.00	15.00	15.00	15.00	15.00	
L-Phenylalanine		32.00	32.00	32.00	32.00	32.00	32.00	
L-Proline		40.00	40.00	40.00	40.00	40.00	40.00	
L-Serine		25.00	25.00	25.00	25.00	25.00	25.00	
L-Threonine		48.00	48.00	48.00	48.00	48.00	48.00	
L-Tryptophan		10.00	10.00	10.00	10.00	10.00	10.00	
L-Tyrosine	36.00	-	36.00	-	36.00	36.00		
L-Tyrosine (disodium salt)	-	52.09	-	52.09	-	-		
L-Valine	46.00	46.00	46.00	46.00	46.00	46.00		
VITAMINS:	L-Ascorbic Acid	50.00	50.00	50.00	50.00	50.00	50.00	
	Biotin	0.10	0.10	0.10	0.10	0.10	0.10	
	D-Ca Pantothenate	1.00	1.00	1.00	1.00	1.00	1.00	
	Choline Chloride	1.00	1.00	1.00	1.00	1.00	1.00	
	Folic Acid	1.00	1.00	1.00	1.00	1.00	1.00	
	D-Inositol	2.00	2.00	2.00	2.00	2.00	2.00	
	Nicotinamide	1.00	1.00	1.00	1.00	1.00	1.00	
	Pyridoxal HCl	1.00	1.00	1.00	1.00	1.00	1.00	
	Riboflavin	0.10	0.10	0.10	0.10	0.10	0.10	
	Thiamine HCl	1.00	1.00	1.00	1.00	1.00	1.00	
	Vitamin B ₁₂	1.40	1.36	1.40	1.36	1.40	1.40	
	RIBONUCLEOSIDES:	Adenosine	10.00	10.00	-	-	10.00	-
		Cytidine	10.00	10.00	-	-	10.00	-
Guanosine		10.00	10.00	-	-	10.00	-	
Uridine		10.00	10.00	-	-	10.00	-	
DEOXYRIBONUCLEOSIDES:	2' Deoxyadenosine	10.00	10.00	-	-	10.00	-	
	2' Deoxycytidine HCl	11.00	11.00	-	-	11.00	-	
	2' Deoxyguanosine	10.00	10.00	-	-	10.00	-	
	2' Deoxythymidine	10.00	10.00	-	-	10.00	-	

¹References:
Murray, *New Biology* (1971) 230, 310.

32 **C W I DOUGLAS, P V HATTON and I M BROOK** (Dental Research Group, School of Clinical Dentistry, University of Sheffield, UK): **Ionomeric cements and Cephalosporins from Ionomer and Acrylic Cements.**

Antimicrobial agents have been successfully used in joint replacement cements. Ionomer cements have several potential advantages over acrylics. The aim of this study was to evaluate the release of two antibiotics from ionomeric and acrylic cements. Discs 12 mm in diameter were prepared from both 19% to 10% w/w of cephalosporin or clindamycin were prepared from both ionomeric and acrylic cements. Discs were placed into phosphate buffered saline (PBS) at 37°C eluted and sampled at 1, 2, 4, 8, 16, 32, 64, 128, 256, 512, 1024, 2048, 4096, 8192, 16384, 32768, 65536, 131072, 262144, 524288, 1048576, 2097152, 4194304, 8388608, 16777216, 33554432, 67108864, 134217728, 268435456, 536870912, 1073741824, 2147483648, 4294967296, 8589934592, 17179869184, 34359738368, 68719476736, 137438953472, 274877906944, 549755813888, 1099511627776, 2199023255552, 4398046511104, 8796093022208, 17592186044416, 35184372088832, 70368744177664, 140737488355328, 281474976710656, 562949953421312, 1125899906842624, 2251799813685248, 4503599627370496, 9007199254740992, 18014398509481984, 36028797018963968, 72057594037927936, 144115188075855872, 288230376151711744, 576460752303423488, 1152921504606846976, 2305843009213693952, 4611686018427387904, 9223372036854775808, 18446744073709551616, 36893488147419103232, 73786976294838206464, 147573952589676412928, 295147905179352825856, 590295810358705651712, 1180591620717411303424, 2361183241434822606848, 4722366482869645213696, 9444732965739290427392, 18889465931478580854784, 37778931862957161709568, 75557863725914323419136, 151115727451828646838272, 302231454903657293676544, 604462909807314587353088, 1208925819614629174706176, 2417851639229258349412352, 4835703278458516698824704, 9671406556917033397649408, 19342813113834066795298816, 38685626227668133590597632, 77371252455336267181195264, 154742504910672534362390528, 309485009821345068724781056, 618970019642690137449562112, 1237940039285380274899244224, 2475880078570760549798488448, 4951760157141521099596976896, 9903520314283042199193953792, 19807040628566084398387907584, 39614081257132168796775815168, 79228162514264337593551630336, 158456325028528675187103260672, 316912650057057350374206521344, 633825300114114700748413042688, 1267650600228229401496826085376, 2535301200456458802993652170752, 5070602400912917605987304341504, 10141204801825835211974608683008, 20282409603651670423949217366016, 40564819207303340847898434732032, 81129638414606681695796869464064, 162259276832213363391593738928128, 324518553664426726783187477856256, 649037107328853453566374955712512, 129807421465770690713274991145024, 259614842931541381426549982290048, 519229685863082762853099964580096, 1038459371726165525706199929160192, 2076918743452331051412399858320384, 4153837486904662102824799716640768, 8307674973809324205649599433281536, 1661534994761864841129919886643072, 3323069989523729682259839773286144, 6646139979047459364519679546572288, 13292279958094918729039359093145776, 26584559916189837458078718186291552, 5316911983237967491615743637258304, 10633823966475934983231487274516096, 21267647932951869966462974549032192, 42535295865903739932925949098064384, 85070591731807479865851898196128768, 170141183463614959731703796392257536, 340282366927229919463407592784515104, 680564733854459838926815185569030208, 1361129467708919677853630371138060416, 2722258935417839355707260742276120832, 5444517870835678711414521484552241664, 10889035741671357422829042969104483296, 21778071483342714845658085938208966592, 43556142966685429691316171876417933184, 87112285933370859382632343752835866368, 174224571866741718765264687505671732736, 348449143733483437530529375011345465472, 696898287466966875061058750022690930944, 1393796574933933750122117500045381861888, 278759314986786750024423500009076373376, 557518629973573500048847000018152746752, 1115037259947147000097694000036305493504, 2230074519894294000195388000072610987008, 4460149039788588000390776000145221974112, 8920298079577176000781552000290443948224, 17840596159154352001563104000580887896448, 35681192318308704003126208001161775792896, 71362384636617408062532416002323551595776, 14272476927323481612506483200464710391552, 28544953854646963225012966400929420783104, 57089907709293926450025932801858841566208, 11417981541858785281005186560371768332416, 228359630837175705620103731207435366466304, 45671926167435141124020746241487073332928, 9134385233487028224804149248297414665856, 18268770466974056449608298496594829331712, 36537540933948112899216596993189658663424, 73075081867896225798433193986379317326848, 14615016373579245159686638797275863465376, 2923003274715849031937327759455172693072, 5846006549431698063874655518910353866144, 11692013098863396127749311037820707732288, 23384026197726792255498622075641415464576, 46768052395453584510997244151282830929152, 9353610479090716902199448830256566185824, 18707220958181433804398897660513132316544, 37414441916362867608797795321026264633088, 74828883832725735217595590642052529266176, 149657767665451470435191181284105058532352, 299315535330902940870382362568210117064704, 598631070661805881740764725136420234128128, 119726214132361176348152945027284046825248, 239452428264722352696305890054568093650496, 478904856529444705392611780109136187300992, 957809713058889410785223560218272374601936, 191561942611777882157044712043654474920384, 383123885223555764314089424087309489840768, 766247770447111528628178848174618979681536, 153249544089422305725635769634923795363072, 306499088178844611451271539269847590726144, 612998176357689222902543078539695181452288, 1225996352715378445805086157079390362904576, 2451992705430756891610172314158780725809152, 490398541086151378322034462831756145161824, 98079708217230275664406892566351228232352, 196159416434460551328813785132702456464704, 392318832868921102657675702265404912928128, 78463766573784220531535140453080982584544, 15692753314756844106307028090616196517088, 31385506629513688212614056181232392314176, 62771013259027376425228112362464784628352, 125542026581854752850456224725129569256704, 251084053163709505700912449450259138513408, 50216810632741901140182489890051826706816, 100433621265483802280364797780103534413632, 200867242530967604560729595560207068827264, 401734485061935209121459191120414137654528, 803468970123870418242918382240828275309056, 1606937940247740836485836644481565506018112, 3213875880495481672971673288963131012032224, 6427751760990963345943346577926262024064448, 1285550352198192669188669315585252404808896, 25711007043963853383773386311705048096177792, 514220140879277067675467726234100963555544, 1028440281758554135350935452468201927111088, 2056880563517108270701870904936403854222176, 4113761127034216541403741809872807708444352, 822752225406843308280748361974561537888704, 16455044508136866165614967239491230757761408, 32910089016273732331229934478982461515542176, 6582017803254746466245986895796492303108512, 13164035606509492932491973791592984606217024, 26328071213018985864983947583185969212434048, 52656142426037971729967895166371938464868096, 1053122848520759434599357903327438769297376, 210624569704151886919871580665477753859472, 421249139408303773839743161330955507718944, 842498278816607547679486322661911015437888, 1684996557633215095358972645323822028876736, 336999311526643019071794529064764405775472, 6739986230532860381435890581295288115550944, 13479972461065720762871781162595776311101888, 2695994492213144152574376232519155262221776, 539198898442628830514875266503830554443552, 107839779688525766102975053300761108887104, 2156795593770515322059501066015222177744176, 431359118754103064411900213203044435488352, 862718237508206128823800426406088870976672, 172543647501641225764760085281217774195344, 345087295003282451529520170562435549068688, 690174590006564903059040341124871091373376, 1380349180013289806118006822249742182646752, 276069836002657961223601364449944354533104, 552139672005315922447202728899888709066208, 1104279344010631844894405457799777418132416, 220855868802126368978881095559955483464432, 441711737604252737957772191119910976888864, 883423475208505475915544382239821957777728, 1766846950417010951831088764479643915555456, 3533693900834021903662177528959278311111008, 7067387801668043807324355057918556622222112, 1413477560333608761464871011583713244444224, 282695512066721752292974203116742648888448, 56539102413344350458594840623348529777696, 11307820482668870091718968124677059555392, 2261564096533774018343793624935411910784, 4523128193067548036687587249870823821568, 9046256386135096073375174499741647643136, 1809251277227019214675034899948329528672, 3618502554454038429350069799896659057344, 723700510890807685870013959979331811488, 14474010217816153717400279199586636228736, 2894802043563230743480055839917327245752, 5789604087126461486960111679834654491504, 11579208174252922973920223359669089823088, 23158416348505845947840446719338179646176, 46316832697011691895680893438676359293312, 9263366539402338379136178687735271858624, 1852673307880467675827235737547054371728, 3705346615760935351654471475094108743456, 741069323152187070330894295018821768912, 1482138646044374140661788590037643537824, 2964277292088748281323577180075287075648, 5928554584177496562647154360150574151296, 11857109168354993125294308720311482322592, 23714218336709986250588617440622964645184, 47428436673419972501177234881245929290368, 94856873346839945002354469762491858580736, 189713746693679890004709395524983717161504, 37942749338735978000941879104967434232208, 758854986774719560018837582099348684664352, 151770997354943912003776564419869739329304, 303541994709887824007553128839739478658608, 607083989419775648015106257679478957317216, 1214167978839551296030212515358979114634432, 242833595767910259206042503071795828268864, 48566719153582051841208500614358166537728, 97133438307164103682417001228716313275456, 194266876614328207364834002457426625551104, 38853375322865641472966800491485325110208, 77706750645731282945933600982970650220416, 1554135012914625658918672019659130004432, 3108270025829251317837344039318260008864, 6216540051658502635674688078636520017728, 12433080103317005271349376157273040035456, 24866160206634010542698752314546080070912, 49732320413268021085397504629092160141824, 99464640826536042170795009258184320283648, 198929281653072084341590018516368640567296, 397858563306144168683180037032737281134592, 79571712661228833736636007406547456226896, 159143425322457667473272014813094912453792, 318286850644915334946544029626189824907584, 636573701289830669893088059252379649815168, 127314740257966133978617611850475929963136, 254629480515932267957235223700951859362704, 509258961031864535914470447401903718725408, 101851792206372907182894094880380737450816, 203703584412745814365788189760761474901728, 407407168825491628731576379521522949803552, 814814337650983257463152759043045899607104, 162962867530196651492630551808611799314208, 325925735060393302985261103617235988628416, 651851470120786605970522207234471977256832, 130370294024157321194104441446873955451364, 260740588048314642388208882893747910902728, 521481176096629284776417765787495821805456, 104296235219325856955283553157599163610912, 208592470438651713910567106315198327221824, 41718494087730342782113421263039665444352, 83436988175460685564226842526079330888704, 166873976350921371128453685052158661777408, 33374795270184274225690737010431733554176, 66749590540368548451381474020863467108932, 133499181080737096902762948041726934177856, 266998362161474193805525896083453868355712, 533996724322948387611051792166907736711424, 106799344864589677522210358433381473422848, 213598689729179355044420716866762846845696, 427197379458358710088841433733525693691392, 854394758916717420177682867467051383827744, 170878951783343484035536573493410276765536, 341757903566686968071073146986820553531072, 6835158071333739361421462939736411070624, 13670316142667478722842925779472222141248, 2734063228533495744568585155894444428496, 54681264570669914891371703117888888569984, 10936252914133982978274340623577777139696, 21872505828267965956548681247155554793952, 43745011656535931913097362494311111587904, 87490023313071863826194724988622223175808, 17498004662614372765238944997724444635168, 34996009325228745530477889995448889270336, 69992018650457491060955779990897778556704, 139984037300914982121911559981795557113408, 27996807460182996424382311996359111422816, 5599361492036599284876462399271822284544, 11198722984073198569752924798543644589088, 22397445968146397139505849597087289177936, 44794891936292794279011699194174773558752, 895897838725855885580233983883495

In vivo response of ionomeric cements: effect of glass composition, increasing soda or calcium fluoride content

K. K. JOHAL, G. T. CRAIG, A. J. DEVLIN, I. M. BROOK*

University of Sheffield, Biomaterials Group, School of Clinical Dentistry, Claremont Crescent, Sheffield. S10 2TA UK

R. HILL

University of Limerick, Department of Materials Science, National Technological Park, Limerick, Ireland

The *in vivo* response of two defined groups of set ionomeric cements (ICs), were evaluated following implantation in the midshaft of three week old Wistar rat femora for four weeks. New bone formation was associated with all the IC implants, the amount of new bone increasing with increasing sodium or calcium fluoride content of the basic glass component. Previous work has shown that there is a link between glass composition and ion release, fluoride ion release increasing as the sodium or fluoride content of the glass increases. It thus appears that in the series studied improved bone formation associated with the ICs was mediated by increased fluoride ion release.

1. Introduction

Ionomer cements are hybrid glass polymer composites formed by the neutralization reaction of a basic ion leachable inorganic glass and an organic polyelectrolyte (polyacrylic) acid. Their properties include a rapid snap set, high compressive strength, adhesion to enamel and dentine, and the release of potentially osteoconductive ions such as fluoride and calcium [1]. Additional properties that make them attractive bone substitutes include a non-exothermic setting reaction, chemical adhesion to bone and metals, and the ability to mould and shape the cement at the implant site with minimal setting shrinkage [2].

Ionomer cements are established restorative dental materials and more recently have been used as preformed implants and cements in otolaryngology and cranial surgery [3,4]. Further development of this group of materials for orthopaedic use is being undertaken [2,5].

Clinical success of biomaterials depends largely upon the structure, composition and stability of the bone/implant interface achieved. The purpose of this study was to evaluate the *in vivo* response of bone to six different formulations of ionomer cements based upon two defined series of ionomeric glasses. The first series had a constant fluoride content but increasing soda content and the other an increasing calcium fluoride content.

2. Materials and methods

2.1. Materials

Six fluoroaluminosilicate glass-based ionomer cements were used in this study. The first series of ionomer cements were sodium based LG2, LG6, and LG63 (Department of Materials Science, University of Limerick, Ireland). They had the following chemical structure, $W\text{SiO}_2 \cdot Y\text{P}_2\text{O}_5 \cdot \text{Al}_2\text{O}_3 \cdot (1-Z)\text{Na}_2\text{O} \cdot \text{CaO} \cdot \text{CaF}_2$ where W, Y and Z are the mole fractions and where Z for ionomer cements LG2 = 0, LG6 = 0.1 and LG63 = 0.2. The second series of ionomeric cements (LG26, LG27 and LG30) with a Ca:P ratio of 1.66 were based on the general formula $(P)\text{SiO}_2 \cdot (Q)\text{Al}_2\text{O}_3 \cdot (5-X)\text{CaO} \cdot 1.5\text{P}_2\text{O}_5 \cdot (X)\text{CaF}_2$. With the production of glasses having a larger content of modifying oxide (CaO) the mole fraction of silica and alumina were increased to ensure glass formation. As the fluoride content of the glass varied by the addition of CaF_2 , the CaO content present was influenced by the variable "X" where X in LG26 = 2, LG27 = 1 and LG30 = 0. The glass LG2 can be considered to be in both series having no soda and a value of X = 0.75.

2.2. Formation of implant rods

Ionomeric cements were produced using a ratio of 1.0 g glass, and 0.2 g freeze dried mercaptan free polyacrylic acid (Advanced Healthcare, UK) and

*To whom correspondence should be addressed

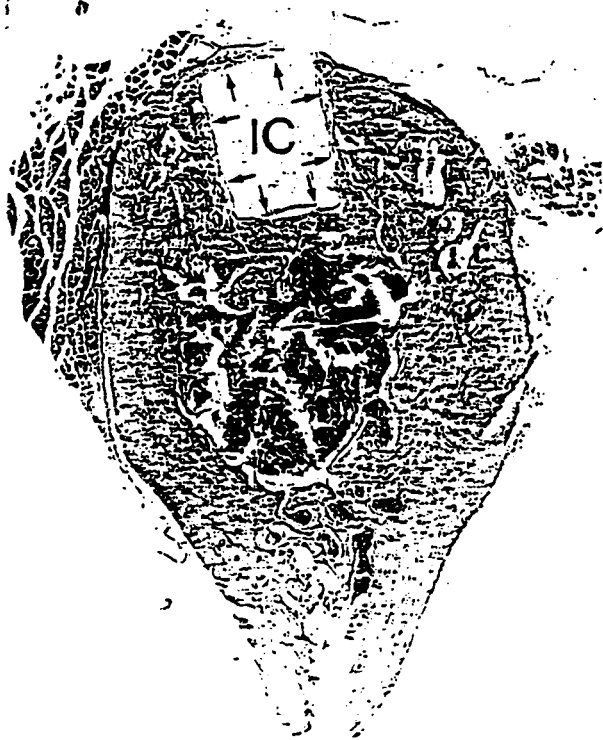


Figure 1 Transverse section of femur showing a rod of ionomeric cement (IC) completely surrounded by bone: arrows depict six points around the perimeter at which osteoconduction might be evaluated: haematoxylin and eosin $\times 16$.

0.3 ml sterile non-pyrogenic water. Smooth rods (nominally 2 mm length \times 1 mm diameter) were produced by placing unset material in silicone moulds. The rods were cured for at least 5 h at 37°C at 100% relative humidity. The rods were then steam sterilized, returned to room temperature and stored overnight at 100% humidity prior to implantation.

2.3. Implantation

For each of the six materials a single rod was implanted, under anaesthesia (Halothane 2% (May and Baker, UK); in oxygen 25% and nitrous oxide 75%), into the midshaft of the femora in groups of five weaned inbred Wistar rats. Under saline irrigation a slow speed 1 mm diameter Tungsten Carbide burr was used to cut a hole matched to the diameter of the implant, through one cortex into the marrow space. Implants were placed to lie level with the surface of the bone penetrating through the cortex into the marrow cavity. The overlying periosteum and soft tissues were replaced and the wound sutured, antibiotics were not used. Post-operatively, wounds were inspected to monitor healing and rats were maintained on a standard laboratory diet. After four weeks, animals were sacrificed and the femora

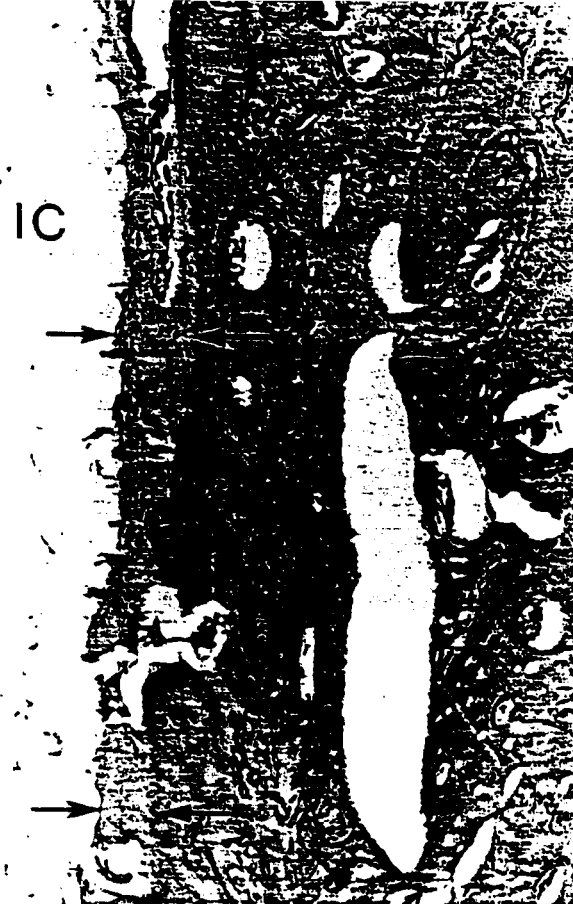


Figure 2 Interface between ionomeric cement (IC) and bone: the opposing arrows demarcate the thickness of newly formed bone and its measurement formed the basis for evaluating osteoconductive potential: haematoxylin and eosin $\times 162$.

removed, fixed in neutral buffered formalin, and decalcified in 4 N formic acid for one week prior to trimming, routine histological processing and paraffin wax embedding.

2.4. Light microscopy/histomorphometry

Five stepped serial sections 7 μ m thick, each separated by 70 μ m, were cut from the implant bed in each femora using a rotary microtome, mounted on glass slides and stained using haematoxylin and eosin. The biological response to the different ionomer implants was studied by determining the degree of osteoconduction and percentage osseointegration, using a transmission microscope linked to an image analyser system (Optimas 5.1, Biosoft, USA). Osteoconduction was determined by taking six points at random around the perimeter of each ionomeric rod and measuring the thickness of new bone formed (Figs 1, 2 and 3). The degree of osteoconduction being taken as the average thickness of new bone produced on the implant surface. Percentage osseointegration was determined by measuring the proportion of the total implant perimeter in contact with bone (Figs 1, 4–6). Statistical analysis was undertaken using the Unistat statistical package (University software, UK) and by applying Student's t-test.



Figure 3 Interface (straight arrows) between ionomeric cement (IC) and newly formed bone; note its cellularity and the chondroid appearance seen focally (curved arrow); osteoclasts line marrow spaces adjacent to the interface (open arrows); haematoxylin and eosin $\times 162$.

3. Results

3.1. Histological assessment

Of the 36 implant sites all healed uneventfully. All the ionomeric cements exhibited formation of new bone on their surface and generally new bone was formed in continuity with the implant surface from the cortical bone at the surgical site into the marrow space (Fig. 1). In most cases, the interface between implant and host was characterized by a layer of notably cellular and, apparently, variably mineralized mature bone (Figs 2 and 3); in places the cellularity of the newly formed bone resulted in a chondroid appearance: marrow spaces close to the interface were lined by prominent osteoblasts. Even as judged subjectively, the layer of new bone varied in thickness for different ionomeric cements. In all cases, the periosteal end of the implant was covered by a layer of partly remodelled cortical bone (Fig. 4). Similarly, that portion of each implant which projected endosteally (Fig. 5) was separated from the adjacent vital marrow tissue by a thin layer of variably mineralized woven bone (Fig. 6).

3.2. Histomorphometry osteoconduction and osseointegration

Increased levels of new bone formation were observed as the soda or calcium fluoride content of the glass

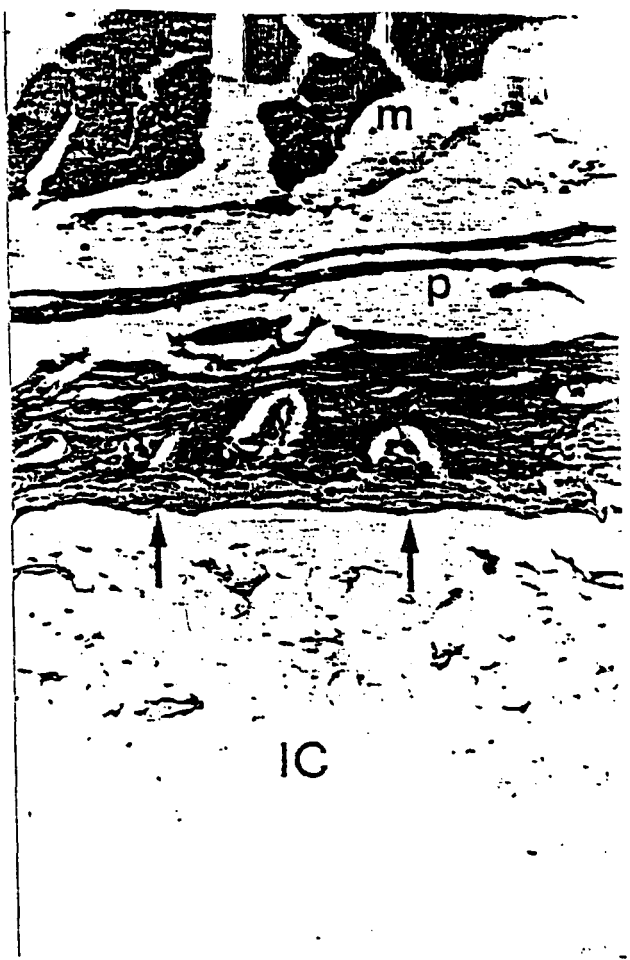


Figure 4 Partly remodelled cortex and new bone (arrows) at the periosteal interface of the implant (IC); p = periosteum; m = voluntary muscle; haematoxylin and eosin $\times 162$.

component of the ionomer cements increased. There was a significant difference in the mean thickness of new bone (degree of osteoconduction) formed adjacent to the soda containing glass based series this being a mean of 0.12 mm for LG63 greatest soda content, 0.07 mm for LG6 and 0.005 mm for LG2 (no soda). The difference between LG63 and LG2 being significant ($t = 5.2$, $df = 3$, $P < 0.007$). In the second series significantly more new bone formation was associated with the ionomer cement LG26 (highest fluoride content) compared to the ionomers in the soda series or other ionomeric cements in the same series ($t = 2.16$, $df = 3$, $P < 0.04$). The mean new bone formation (osteoconduction) observed in the calcium fluoride series being: 1.55 mm for LG26, 0.08 mm for LG27 and 0.07 mm for LG30 with the difference between LG26 and LG27 LG30 being significant ($t = 4.5$, $df = 3$, $P < 0.002$).

The results for the percentage osseointegration of the ionomeric cements showed a similar trend as that seen for osteoconduction with the difference between the calcium fluoride and soda series being significant (LG26 versus LG63 $t = 4.5$, $df = 3$, $P < 0.002$). The soda based ionomeric cements following the order: LG63 > LG6 > LG2 (being 68%, 61% and 37% respectively). The difference between LG2 and LG63 being significant ($t = 37.71$, $df = 3$, $P < 0.0001$). The calcium fluoride based glasses following the order of



Figure 5 Implant (IC) projecting into marrow cavity and separated from vital marrow (m) by a thin layer of new bone (open arrows); haematoxylin and eosin $\times 16$.

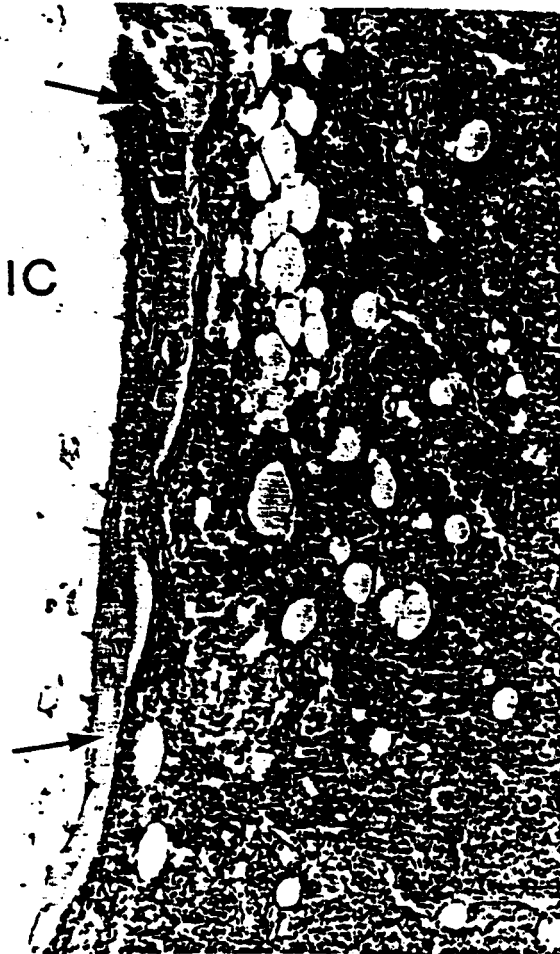


Figure 6 Detail from Fig. 5 showing a thin layer of partly mineralized woven bone (arrows) separating the implant (IC) from vital marrow tissue: haematoxylin and eosin $\times 162$.

LG26 > LG27 > LG30 (being 80.8% > 78.2% > 70.6% respectively). The difference in integration between LG26 and LG30 being significant ($t = 1.953$, $df = 8$, $P < 0.05$).

4. Discussion

Semi-quantitative histomorphometric analysis and histological evaluation revealed that there was a more positive response from the surrounding bone associated with the ionomeric cement implants in the calcium fluoride series as compared to those in the soda containing series. The responses seen appeared to be correlated with the composition of the ionomer glasses. Increasing the fluoride content in the calcium fluoride series (LG30 to LG26) was associated with increased bone formation and confirms the results seen by ourselves and others as to the beneficial effect of this ion in appropriate concentration on bone formation [5-7]. Work previously reported on this series of glasses has however, demonstrated that increasing the soda content of ionomeric cements increases the rate and amount of fluoride release from the cement matrix [6]. This has been proposed to be due to increasing the mobility of fluoride ions in the matrix and by facilitating an ion exchange mechanism between cement and the environment. The results from studying ion release from ionomeric cements [6]

taken together with those of the present study demonstrate that while the total amount of fluoride present is an important determinant of biological response, the mobility of ions within the cement matrix and their release characteristics are significant factors affecting the induced biological response.

In the calcium fluoride series as well as increasing fluoride content in order to ensure glass formation the mole fraction of alumina was increased throughout the series with LG26 containing 3 mole fractions, LG27 with 4 mole fractions, and LG30 containing 5 mole fractions. The amount of new bone was thus negatively correlated with alumina content, LG30 being associated with the least amount of new bone formation. Increasing aluminium ion release from ionomeric materials has been demonstrated to be negatively correlated with the *in vitro* response of osteoblasts [7]. The effect of aluminium ions on bone metabolism is however an area of continuing debate [8]. Aluminium ions have been shown to reduce new bone formation [9], at high concentrations inhibit bone mineralization [10, 11] and there is evidence that aluminium can enhance the mobilization of calcium from bone by a cell-independent mechanism [12]. In contrast, low concentrations of aluminium have been reported to stimulate the proliferation and differentiation of osteoblasts *in vitro* [10]. While *in vivo*, administration of aluminium has been shown to increase

bone volume by positively influencing trabecular networking in the axial skeleton [9]. Such enhancement of bone histogenesis contrasts with the effects of other pharmacologic agents that solely alter the thickness of existing trabecular plates or rods within the vertebral spongiosa [14, 15].

The results of this study show that biological response is reduced with increased alumina content associated with reduced fluoride content. Thus, the effects of aluminium and fluorine are likely to be dependent on the concentration of their ions. The beneficial effects of fluoride are thought to be due to promotion of osteoblastic activity and increasing trabecular bone density [7]. However, the effects of fluoride, like aluminium, appear to be dose-dependent *in vitro* [16, 17] and *in vivo* [18, 19]. The formulation of defined ionomeric cements enables controlled evaluation of the parameters that affect the biological response of bone to ionomeric cements. The biocompatibility and composition of ionomeric cements are of great importance because they need to be in direct contact with bone for any chemical adhesion to occur. The model ionomeric cement formulations studied here induced a favourable biological response from the tissues of the implant bed. Improved osseointegration and osteoconduction being associated with increased calcium fluoride or soda content and reduction in alumina content. Our previous work [6] demonstrated a link between glass composition, and ion release, with fluoride ion release increasing as the sodium or calcium fluoride content of the glass increases. Improved osseointegration and osteoconduction appear to be mediated by increased fluoride ion release.

Acknowledgements

The author would like to thank Denise Teale for her technical advice on histological preparations and David Thompson for preparing photographs, both of whom are in the Department of Oral Pathology and

Dr R Billington for supplying the Polyacrylic acid (Advanced Healthcare, UK). This work was funded by the European Economic Community BRITE/EUR-AM programme Grant No. BRE 2 C7920349.

References

1. P. V. HATTON and I. M. BROOK. *Brit. Dent. J.* 173 (1992) 275-277.
2. L. M. JONCK and C. G. GROBELAAR. *Clin. Mater.* 6 (1990) 323-359.
3. R. T. RAMSDEN, R. C. D. HERDMAN and R. H. LYE. *J. Laryngology Otolaryngology* 160 (1992) 949.
4. G. BABIGHIAN, *ibid.* 160 (1992) 954.
5. I. M. BROOK, G. T. CRAIG and D. J. LAMB. *Clinical Materials* 7 (1991) 295.
6. A. J. DEVLIN, P. V. HATTON, R. HILL, G. HENN, E. DE BARRA, G. T. CRAIG and I. M. BROOK. *Pub. Tipografia Vigo Cursi Pisa*. ISBN. 90-72101-04-3 (1994) 459-462.
7. P. SASANALUCKIT, K. R. ALBUSTANY, P. J. DOHERTY and D. F. WILLIAMS. *Biomaterials* 14 (1993) 906.
8. L. D. QUARLES. *Miner. Electrolyte Metab.* 17 (1991) 233-239.
9. L. D. QUARLES *et al.* *J. Bone Min. Res.* 5 (1990) 625-635.
10. K. H. W. LAU, A. YOO, S. P. WANS. *Mol. and Cell Biochem.* 105 (1991) 93-105.
11. W. G. GOODMAN. *Kidney Int.* 5 (1991) 65-116.
12. A. S. POSNER. *Bone and Min. Res.* 5 (1987) 65-116.
13. H. S. TALWAR *et al.* *Kidney Int.* 29 (1986) 1038-1042.
14. J. REEVE and P. J. MEUNIER. *Brit. Med. Jour.* 294 (1987) 1032-1033.
15. A. M. PARFITT. *Min. Electrolyte Metab.* 4 (1980) 273-287.
16. J. R. FARLEY, J. E. WERGEDAL and D. J. BAYLINK. *Science* 222 (1983) 350.
17. J. E. WERGEDAL, K. H. W. LAU and D. J. BAYLINK. *Clin. Orthop. Rel. Res.* 233 (1988) 274-282.
18. C. Y. PAK, K. SAKAHEE, J. E. ZERWEKH, C. PARCEL, R. PETERSON and K. JOHNSON. *Endocrin. Metab.* 68 150-159.
19. G. BOLVIN and P. J. MEUNIER. in "The metabolic and molecular basis of acquired disease", edited by R. D. Cohen. B. Lewis, K. G. M. M. Alberti and A. M. Denman. (Bailliere Tindall, London, 1990) pp. 1803-1825.

Received 29 June
and accepted 4 July 1995

FLUORIDE RELEASE FROM GLASS POLYALKENOATE (IONOMER) CEMENTS

R.G. Hill, E. De Barra, S.Griffin and G.Henn.

Department of Materials Science and Technology, University of Limerick Limerick
IRELAND

J. Devlin P.V. Hatton I Brook, K. Johal and G. Craig Dental School
University of Sheffield UK.

ABSTRACT

Fluoride release studies from model glass polyalkenoate cements show the release to be proportional to the fluorine content of the glass. The dominant fluoride release mechanism is by an ion exchange mechanism, where fluoride ions are exchanged for hydroxyl ions in water, rather than via a counter ion mechanism involving simultaneous release of an alkali metal ion. The ion exchange mechanism explains the recent reduction in pH observed in cell culture studies. Negligible amounts of aluminium are released and virtually no fluorine is released bound to aluminium from the set cement.

INTRODUCTION

Fluoride ion release and its potential cariostatic role is an attractive feature of glass polyalkenoate dental cements. The fluoride ion is readily exchanged for the hydroxyl ion of hydroxyapatite. Since the fluoride ion is smaller than the hydroxyl ion it packs more readily into the apatite lattice with the result that fluorapatite is chemically and thermodynamically more stable than hydroxyapatite[1]. Fluorapatite is also far less soluble in acidic solution than hydroxyapatite and ion exchange of fluoride ions for hydroxyl ions in teeth makes them far more resistant to decay[2]. In addition fluoride release is thought to have a bacteriocidal action([3].

The importance of fluoride release is becoming of even greater significance with the increasing use of tooth saving preparation methods, such as tunnel and other undermining techniques. In these techniques because of the limited visibility there is a greater risk of leaving carious dentine behind than with conventional box cavities. The increasing use of lasers in dentistry is also likely to facilitate the move towards minimal cavity preparation. The ability of glass polyalkenoate cements to release fluoride ions and remineralise the carious dentin is particularly attractive with these techniques.

There is an extensive literature on fluoride ion release from glass polyalkenoate cements(4) The majority of studies are of fluoride release from commercially available materials in which the glass component is frequently multiphase. The experiments have been performed using widely different procedures, different geometry specimens and the results expressed in numerous different units consequently it is difficult to draw any firm conclusions from the

literature on fluoride release. Furthermore whilst many papers discuss whether fluoride is released by a diffusion or a dissolution process very few papers discuss the possible mechanisms of fluoride ion release or the relationship between glass composition and fluoride ion release.

A second reason for studying fluoride ion release from glass polyalkenoate cements is that these materials are now being developed for use as in situ setting bone cements and preset bone substitutes[5]. In these new applications of glass polyalkenoate cements the biocompatibility of the cement is important. Fluoride ion release is known to stimulate apatite deposition in bone[6] as well as osteoblast mitosis. However excessive fluoride ion release has been associated with a cytotoxic response in cell culture determinations of biocompatibility[7-10]. Furthermore administration of high doses of fluoride in the treatment of osteoporosis is thought to result in bone embrittlement. The ability to control and understand fluoride release are critical to being able to optimise the biocompatibility of glass polyalkenoate cements and their clinical performance.

An understanding of the mechanism of fluoride release and the form in which fluoride is released also has implications for how fluoride release should be measured from glass polyalkenoate cements and may resolve some of the many conflicting reports in the literature.

The present paper investigates the relationship between glass composition and fluoride ion release with the objective of trying to understand and control fluoride ion release. In the present paper a range of specially synthesised fluoro-alumino-silicate glasses were produced. In contrast to the ionomer glasses currently used in commercial materials and early ionomer glasses, the glasses produced for this study were single phase homogenous glasses free of crystalline inclusions or glass in glass phase separation. Synthesis of such homogenous glasses enables the possibility of obtaining correlations between glass composition and cement properties. Many of the glasses used in commercial glass polyalkenoate cements can not be produced reproducibly and this may be a cause of the conflicting results in the literature.

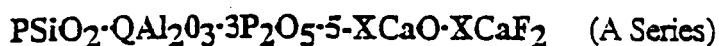
Crisp and Wilson[11] postulated that fluorine is released from glass polyalkenoate cements not only as the free fluoride ion, but also complexed to aluminium so in the present paper not only has both the free fluoride ion concentration, but the complexed fluoride ion concentration released been measured. In addition the release of all other significant ions and species from the set cement has been measured. Thus phosphorous, silicon, aluminium, sodium and calcium release have all been measured from the set cements at the same times as the fluoride release.

The kinetics of fluoride ion release from glass polyalkenoate cements is a complicated phenomena. Glass polyalkenoate cements are not single phase systems, but at least two phase and possibly three phase system systems. The three phases are: glass, polysalt matrix and "silica gel". The latter phase is controversial with a minority of workers regarding the "silica" being dispersed within the polysalt matrix and being responsible for the long term changes in mechanical properties. However the long term changes in the properties of glass polyalkenoate cements are generally regarded as being due continued degradation of the glass and a crosslinking reaction that takes place over an extended time period exceeding one year[12-13]. Thus the concentration of ions, including fluoride ions in the polysalt matrix is likely to increase with time. At the same time the glass transition temperature of the polysalt matrix would be expected to increase and this may reduce the mobility of the fluoride ion in the polysalt matrix and hinder its release.

A full kinetic analysis of fluoride release is therefore premature until an understanding of the basic mechanisms of fluoride release have been established.

EXPERIMENTAL

The glasses used for this study were produced by melting the appropriate amounts of alumina, phosphorous pentoxide, calcium carbonate, calcium fluoride and sodium carbonate in dense sintered mullite crucibles at temperatures between 1300 and 1550°C for two hours. The resulting melts were rapidly shock quenched into demineralised water to prevent phase separation and crystallisation occurring. The glass frit produced was subsequently dried and ground in a vibratory mill. The powder produced was sieved to give particles <45µm, which were used in subsequent cement formation. The composition of the glasses produced was based on previous studies[14-16] and chosen to prevent silicon tetrafluoride formation and loss during melting. Two series of glasses were produced based on the following series:



The first series was designed to study the influence of the fluorine content of the glass, whilst the second series was designed to test the counter ion proposal. The glasses produced differ from the existing commercial glass compositions in having a basic oxide component in the prefired composition. The presence of the basic oxide is thought to result in the fluorine bonding to the aluminium of the glass network rather than to the silicon. The weight loss from the crucible after firing was recorded and in all cases indicated minimal fluorine loss. The prefired compositions can therefore be assumed to be identical to the final glass compositions, which are given in Table 1. The higher fluorine content glass compositions produced for the present paper are however similar to current commercial compositions after they have undergone loss of fluorine during melting.

Cement discs (20mm in diameter x 2mm thick) were prepared by mixing the appropriate glass powder with 40% poly(acrylic acid) in distilled water in a weight ratio of 1:0.5. The cement discs were allowed to set for 24 hours at 37°C before elution under sink conditions into high purity distilled water at 37°C, samples were taken for evaluation at time periods from 3 to 84 days. The free and bound fluoride was measured using a calibrated ion selective electrode both with and without TISAB III. All other ions were determined by atomic absorption spectroscopy

Table 1 Glass Compositions Studied

Glass Code	Series	X	Z
LG26	A	2	-
LG27	A	1	-
LG28	A	0.5	-
LG29	A	0.25	-
LG30	A	0	-
LG2	B	-	0
LG4	B	-	0.025
LG5	B	-	0.05
LG6	B	-	0.10

RESULTS AND DISCUSSION

The results for fluoride release are shown in Tables 2. There was no significant difference between the measurements made with and without TISAB III indicating that virtually all the fluoride released is released as the free fluoride ion and is not chelated to metal cations. Previous studies[11] have suggested that fluoride is released complexed to aluminium ions. All the cements released negligible amounts of aluminium (<0.6 μm moles) and therefore could not release significant amounts of fluoride complexed to aluminium confirming the fluoride data. The low release of aluminium from the set cements indicates that there is no significant dissolution of the cement matrix and that ion release occurs largely by a diffusion process, rather than by surface dissolution. Aluminium ions are small and of high charge and are therefore strongly chelated by the poly(acrylic acid) of the polysalt matrix and are not free to diffuse out of the cement. However it must be pointed out that cement samples were allowed to set for 24 hours prior to elution and exposure to water at earlier times may lead to possible dissolution and greater ion release.

Table 2 Cumulative Fluoride Release ($\mu\text{moles.g}^{-1}$ cement)

Glass	64Hours	1Weeks	3Weeks	6Weeks
LG26	4.2	7.4	13.5	20.2
LG27	2.5	4.4	7.7	11.4
LG28	1.27	2.38	4.2	6.5
LG29	0.95	1.72	3.1	4.6
LG30	0.09	0.47	0.5	0.6
	1Week	3 Weeks	6 Weeks	12 Weeks
LG2	11.8	26.7	43.2	60.1
LG4	13.6	26.1	39.3	53.1
LG5	20.1	36.7	52.7	69.0
LG6	27.1	48.3	66.4	83.8

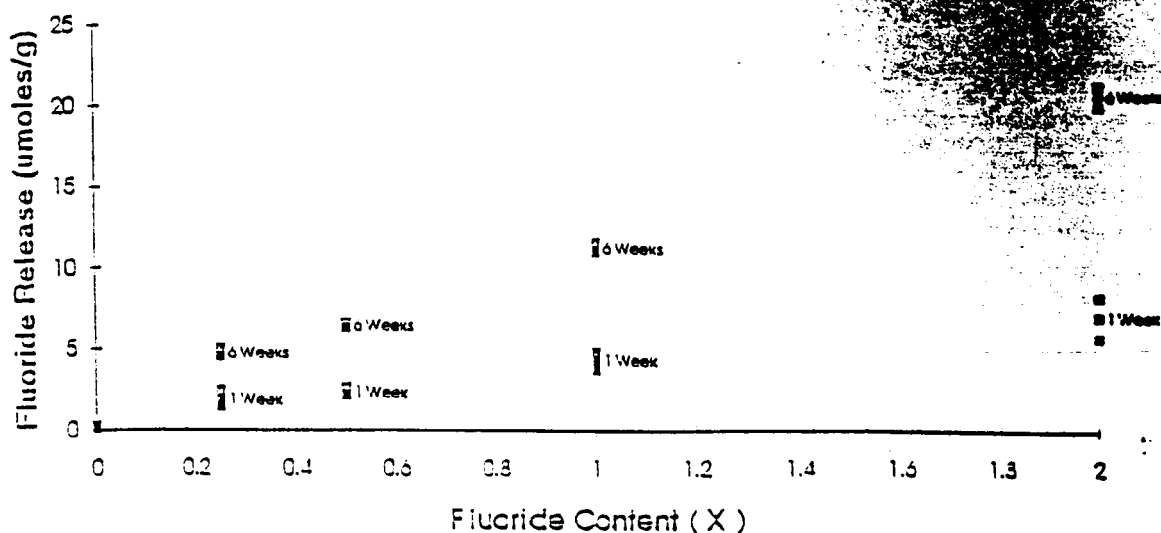
Previous fluoride release studies in the literature have often regarded the release of fluoride as being by a dissolution process, such a view arises from the similarity of glass polyalkenoate cements to the silicate cements formed from similar glasses and orthophosphoric acid. These latter cements were prone to bulk dissolution, which the closely related glass polyalkenoate cements are not because of their high molecular weight poly(acrylic acid) component. Evidence for a diffusion mechanism has previously come from kinetic studies and the fact that the release is proportional to the inverse of the square root of time. However given that the crosslinking reaction is continuing and that the fluoride ion content of the cement matrix is changing by continued reaction such correlations are probably fortuitous.

There is a strong correlation between the fluoride content of the glass and the release of fluoride from the set cements at all measurement times(Figure 1). This result is to be expected, but contrasts with a previous study that indicated no correlation between fluoride release and fluorine content of the glass for commercially available cements[17]. The lack of direct correlation may be a result of some of the fluorine in the commercial glasses being in the form

of crystalline inclusions of fluorite and therefore being unavailable during the cement reaction, as well as differences in the chemistry of the polysalt matrix and its extent of crystallinity.

Figure 1

Cumulative Fluoride Release as a Function of Fluoride Content of the Glass



The release of sodium ions from the second series of glasses correlated with the sodium content of the glass. There was an increase in the amount of fluoride released as the sodium content of the glass was increased, which appeared to support the counter ion mechanism proposed by Wilson and Kuhn[18]. The data is plotted in Figure 2 for the 12 week results. However it is clear that cements with no alkali content release significant quantities of fluoride and even when the data is plotted in terms of μmoles there is no 1:1 correlation between fluoride release and sodium release even for glasses containing sodium. Wilson and Kuhn argued that fluoride was released exclusively in association with a sodium counter ion. Wilson[19] went on to argue that calcium could also act as a counter ion and that fluoride release was restricted by the availability of both calcium and sodium counter ions. Closer examination of the present data indicates a poor correlation, since more fluoride is being released than can be accounted for by a counter ion mechanism involving both sodium and calcium. Totalling the number of positive and negative ions released and calculating the cumulative ion balance indicates that there is a surplus of negative ions over positive ions leaving the cement at all times. In calculating the ion balance it is assumed that phosphorous leaves the cement as $(\text{PO}_4)^{3-}$, calcium as Ca^{2+} , sodium as Na^+ aluminium is neglected and silicon is assumed to leave the cement as a neutral species. It is possible that the silicon leaves the cement as an anionic species thus the actual ion balance will be even more negative than that calculated. The only satisfactory explanation of the ion balance figures is that negative ions are entering the cement from the external solution. The only negative ion present is the hydroxyl ion from the distilled water and the data therefore indicates that fluoride ions are probably being ion exchanged for hydroxyl ions. Such an ion exchange mechanism will result in the external solution increasing in hydrogen ion concentration and reducing in pH. Such pH effects have been observed previously[9].

Figure 2

Fluoride Release Against Sodium Release (12 Weeks)

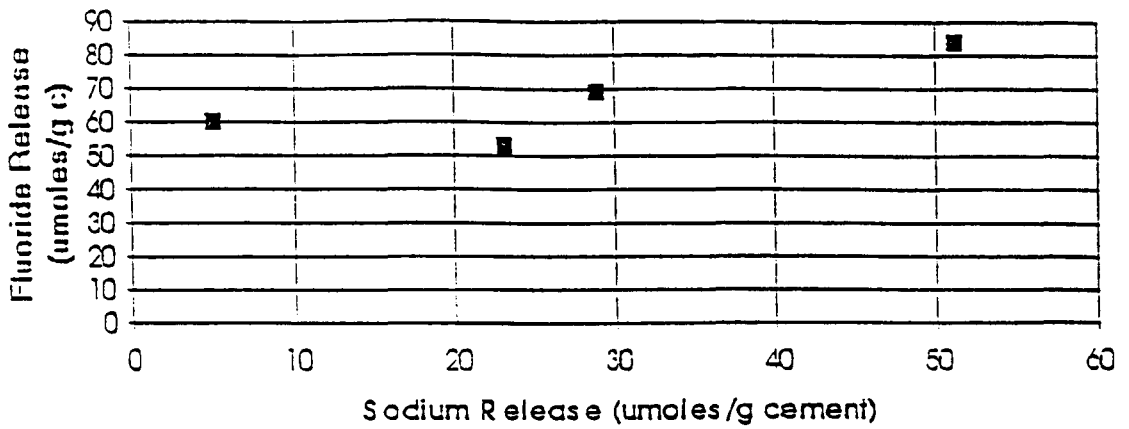
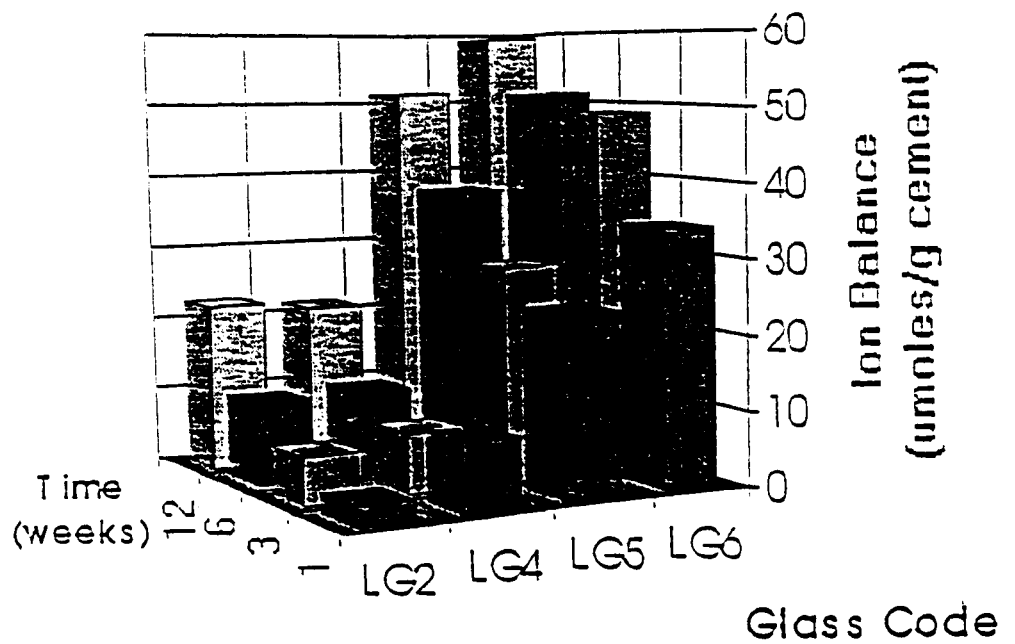


Figure 3

ION BALANCE / TIME



The negative ion balance increases with time and increases as the alkali metal content of the glass is increased (Figure 3). This would indicate that alkali metal ions facilitate fluoride ion release from the set cement by another mechanism other than by providing counter ions. One possibility is that alkali metal ions hinder the crosslinking of the cement matrix, lower the

effective glass transition of the polysalt matrix and facilitate the exchange of fluoride ions for hydroxyl ions by increasing the mobility of these ions in the matrix.

Glass polyalkenoate cements have recently been shown to uptake fluoride ions and subsequently release them by an ion exchange mechanism[20] so the present findings are not surprising. The dominance of the ion exchange mechanism does have important consequences for biocompatibility studies particularly in cell culture, the measurement of fluoride ion release and its clinical significance. Clearly the pH will fall as fluoride ions are ion exchanged. This fall in pH can be very significant and results in the cytotoxic effect observed initially with glass polyalkenoate cements in cell culture[7-10] where the mass of the cement sample is relatively large compared to the volume of culture medium. The pH reduction will depend on time but also on the mass of the cement, its surface area, the quantity of water used and how frequently the water is changed. A large reduction in pH below the pKa of the carboxylic acid functional group is likely to result in dissolution of the cement matrix and therefore an increase in all the ions released as observed in solutions of low pH. In contrast a small pH reduction may reduce the ion exchange process by reducing the number of hydroxyl ions available for ion exchange. The effects of pH changes on fluoride ion release are therefore likely to be complex and it is not surprising that there are markedly different results in the literature for supposedly identical materials.

ACKNOWLEDGEMENTS

The authors would like to thank the European Union for funding under the Brite EuRam Scheme Contract Number BRE2.CT92.0349.

REFERENCES

- 1 Okazaki M. and Sato M. *Biomaterials* 1990 **11** 573-8
2. Okazaki M., Takahashi J., Kimura H. and Aoba T.J. *Biomed Mater. Res.* 1982 **16** 851-60
3. Forss H., Jokinen J., Spets-Happonen S., Seppä L. and Luoma H. *F Caries Res.* 1991 **25** 454-8.
- 4 Forsten L. *Scand. J. Dent. Res.* 1991 **99** 241-5
5. Zollner W. and Rudei C. Medical Applications of glass-ionomers 57-60 in *Glass-ionomers the next generation* Ed P. Hunt International Symposia in Dentistry Philadelphia PA 19103
6. Turner R.T., Francis R., Brown D., Garand J., Hannon K.S. and Beil N.H. *J. Bone Miner. Res.* **4** (1989) 477-84.
7. Docherty P.J. *Clinical Materials* 1991 **7** 335-40
- 8 U. Meyer U., Szulczewski, Barckhaus R.H., Atkinson M. and Jones D.B. *Biomaterials* 1993 **14** 917.
9. Sasanaluckit P., Abustany K.R., Docherty P.J. and Williams D.F. *Biomaterials* 1993 **14** 906
10. Brook I.B., Craig G.T. and Lamb D.J. *Clinical Materials* 1991 **4** 295
11. Crisp S., Lewis B.G. and Wilson A.D. *J. Dent Res.* 1976 **53** 1032-41
12. Crisp S., Abel G. and Wilson A.D. *J. Dent.* 1977 **5** 117
13. Hill R.G. *J. Mater. Sci* 1993 **28** 3851-8
- 14 Hill, R.G., Goat, C. and Wood, D. *J. Amer. Ceram. Soc.* (1992) **75** 778-85
15. Wood, D. and Hill, R.G. *Clinical Materials* (1991) **7** 301-312
16. Wood, D. and Hill, R. *Biomaterials* **12** (1991) 164-70
17. Meryon S.D. and Smith A.J. *Int. Endod J.* 1984 **17** 16-24
- 18 Wilson A.D. Groffman D.R. and Kuhn A.T. 1985 **6** 431-35
19. Wilson A.D. and McLean J.W. *Glass-ionomer cement* Quintessence Publishing Co., Inc. 1988 Chapter 8
20. Billington R.W. *J. Dent Res* (1987) **66** 844

EFFECT OF Na⁺ IONS ON EXTRACELLULAR PROTEINS AROUND IONOMERIC BONE

▲ Johal KK; ⊗ Carter DH; ⊗ Sloan P and ▲ Brook IM

▲ Universities of Sheffield and . ⊗ Manchester UK. [S.C.D. Claremont Cres.
Sheffield S10 2TA. UK. E.mail K.K.Johal@sheffield.ac.uk]

INTRODUCTION

The noncollagenous extracellular matrix proteins (ECMP) osteopontin (OPN), fibronectin (FN), and tenascin (TN) are involved in the integration of biomaterials with bone. OPN is associated with initial bone formation[1]. FN promotes cell adhesion and is thought to influence cell migration *in vivo*[2]. Tenascin is selectively expressed at sites of tissue modelling in developing cartilage and bone to stimulate cell migration and proliferation[3]. TN has also been associated with tissue remodelling, and wound healing. The aim of this study was to determine the distribution of these proteins in bone following implantation of ionomeric (glass-polyalkenoate) cements.

MATERIALS AND METHODS

Three ionomeric cements (IC) produced by reacting mercaptan free polyacrylic acid (Advanced Healthcare, UK.) with ionomer glasses based on the general formula $WSiO_2.YP_2O_5.Al_2O_3.(1.0-ZNa_2O).CaO.CaF_2$ where W, Y and Z are mole fractions and where Z for ICs LG2=0, LG6=0.1, and LG23=0.3 (Department of Materials Science University of Limerick, Ireland) were studied. Under anaesthesia (halothane 2% May & Baker, UK), in oxygen 25% and nitrous oxide 75% sterile set IC rods (2mm x 1mm diameter) were implanted in the midshaft of weaned wistar rats (n=8).

After four weeks, femora were harvested snap frozen in isopentane over liquid nitrogen, and embedded in carboxymethylcellulose at -25°C. Serial cryosections (10µm) were fixed in neutral buffered formalin, decalcified in 20% EDTA and washed in PBS then stained using rabbit polyclonal primary Abs raised against FN (Dako,UK, dilution 1:100), TN (Chemicon, UK, dilution 1:40), using fluorosthioisocyanate (FITC) conjugated secondary Ab raised against rabbit Igs. Monoclonal mouse primary Ab raised against OPN (Ohio Hybridoma Bank, USA, dilution 1:100), using FITC conjugated secondary Abs raised against mouse Igs. Sections

were mounted in DABCO, and examined under UV light using a Zeiss Axoplan microscope. Photographs were taken using Agra 100ASA colour film.

RESULTS / DISCUSSION

The amount of new bone formation (% integration) was ordered LG23>LG6>LG2. The control material (LG2 with Na⁺=0) showed the least bone formation and least staining for OPN, while LG23 (Na⁺=0.3M) with the greatest new bone formation, showed the most staining. This suggested that more OPN differentiated as the sodium content increased. However, the amount of staining with FN and TN did not increase with more sodium. FN was widely distributed staining regions of chondroid bone with all the ICs. TN was distributed in the periphery of the periosteum, a site of osteogenesis with all ICs. OPN staining was prominent in the new bone formed adjacent to the ICs where it was concentrated at the reversal lines. The association of OPN, with ICs, integrated with bone may explain their osteoconductive properties and the differences that occur with varying IC formulations.

CONCLUSION

1. These sodium containing ICs with a set fluoride content exhibited differences in bone formation.
2. All ICs integrated with bone and extracellular matrix proteins FN, TN and OPN were prominently found in new bone suggesting that they play an important role in the interactions of the healing of hard tissues with ICs.

REFERENCES

- [1] Butler WT(1989). *Connect.Tiss. Res.* 23, 123-136.
- [2] Yamada KM; Olden K(1978). *Nature* 275:179-184.
- [3] Shrestha P; Sumitomo S; Ogata K; Yamada K; Takai Yang L; Mori M(1994). *Eur J Cancer B.Oral Oncol.* 30B(6):393-9.

97 Carbohydrate modifications to the RI proteases of *P. gingivalis* W50 assessed by monoclonal antibodies A THICKETT, M RANGARAJAN P SHEPHERD* and M A CURTIS* (MRC Group, SBR/LSMD & Dept Immunol, UMDS, UK)

Immunisation studies in *P. gingivalis* W50 have demonstrated that the *pprRI* gives rise to distinct proteases: RI is a heterodimer composed of the catalytic (α) chain with an adhesion molecule, RIA is the free α chain and RIB a modified form of the α chain which migrates as a band on SDS/PAGE. The maturation pathway of these enzymes may therefore involve transcription of the *pprRI*, proteolytic processing of the initial translation product and post-translational modifications. The aim of the present study was to develop monoclonal antibodies to the α chain of these enzymes in order to examine the maturation in *P. gingivalis*. Previous studies showed that immunisation of experimental animals generates a response which is directed primarily against the β chain. Consequently RIA was the immunogen in the present work. Hybridoma supernatants were screened against recombinant PprRI α chain expressed as an N-terminal (His)₆ fusion protein in *E. coli*. In all cases hybridomas which were positive for RIA were negative for the recombinant but were positive for purified *P. gingivalis* LPS. Immune recognition of RIA by these antibodies was stable to urea, SDS and formic acid treatment but sensitive to periodic acid suggesting heavily linked carbohydrate was the determinant recognised. In contrast to RIA, this antigen was not present on the α chain of RI. These data suggest that the α chains of the RI are differentially modified with carbohydrate common to the LPS of this organism and modifications have a significant effect on the immune recognition of these enzymes.

98 Characterization of lipid A-associated proteins from *Porphyromonas gingivalis* (SHARP* MC CURTIS*, M WILSON*, S POOLE* & B HENGEBOHM* (Dept of Microbiology & Microscopy, EDL, London, London Hospital Medical College, London, NBS/C, Haru.)

Porphyromonas gingivalis is a major periodontal pathogen containing proteolytic and agglutinating proteins. We have previously reported that lipid A-associated proteins (LAPs) of this bacterium, induced L-1 and L-6 production by human cells. The aim of this study was to characterize these LAPs. SDS-PAGE analysis of *P. gingivalis* LAP has shown that the material contains 6 proteins which stimulate the production of L-6 by human monocytes, human gingival fibroblasts (HGFs) and whole blood at concentrations as low as 10ng/ml. Anti-CD14 monoclonal antibodies or polymyxin B did not block this cytokine induction showing that the activity was not due to contaminating lipopolysaccharide (LPS). To identify the cytokine-inducing proteins the LAPs were separated by SDS-PAGE and the individual proteins purified from the gel. Three proteins with molecular masses of 15, 16 and 18kDa were responsible for cytokine production by human monocytes. N-terminal amino acid sequences were obtained for the 15 and 18kDa proteins. The 18kDa sequence was homologous to a conserved region in a number of *P. gingivalis* extracellular molecules including Arg1-gelatinase, Porphyranase and the haemagglutinin HgaA. The 14kDa protein had a novel sequence. In conclusion, induction of cytokine production by human monocytes, HGFs and whole blood was not via the LPS moiety. CD14. The 14kDa protein had a novel sequence and the 18kDa protein was homologous to a number of *P. gingivalis* extracellular molecules. Since these proteins are present on the surface of *P. gingivalis* and induce cytokine production they may be important in the aetiology of the periodontal disease.

99 Strontium oxide as an additive in glass-ionomer cements. S DEB* and JW NICHOLSON (King's Dental Institute, London, SE5 9RW)

Recently reports the effect of strontium oxide (SrO) on the setting kinetics and compressive strength of glass-ionomer cements. SrO is incorporated into certain commercial glasses to confer stability and has been claimed to be a cement forming oxide with aqueous poly(acrylic acid). In the present study, SrO was added to PAA-based glass-ionomers at increasing levels. The experimental glass, G33R, and a commercial glass* Working and setting time were determined by oscillating rheometry and strength at 24 hours. Selected results are shown in the table below.

SrO (by weight)	Working time (min)	Setting time (min)	Compressive strength (MPa)
0%	3.0	7.6	73.0 ± 3.6
5%	3.2	9.4	93.3 ± 3.9
10%	3.4	12.4	73.3 ± 5.0
20%	4.0	14.8	49.8 ± 4.6

Similar results were obtained for the commercial glass. Pure SrO formed a cement with PAA, but ultraviolet and infrared spectroscopy indicated a chemical bond between Sr and the carboxylate. SrO reacts with PAA but reduces the compressive strength with increasing amounts and the setting reaction in glass ionomer cements from Fuji II (ex. GC Corporation)

100 Ion release from novel ionomeric cements related to *in vitro* biocompatibility. A J DEVLIN*, P V RATTON, K K JOHAL, S M BODELL, R G HILL* and I M BROOK (Universities of Sheffield, UK & *Limerick, Ireland.)

Ionomeric cements (ICs) are used as cements and bone substitutes in orthodontology, are widely used as dental materials and are being developed for orthopaedic use. The ability of ICs to exchange ions with tissue has been proposed as the basis for their osteoconductive and bone-bonding properties. The aim of this study was to investigate if ions released from ICs affected their *in vitro* biocompatibility. Selected ions were made from a defined series of glasses with the general formula $1.5SiO_2 \cdot 0.5P_2O_5 \cdot Al_2O_3 \cdot (1.0-2.0)CaO \cdot (0.5-0.75)SrO$, where Z was an alkali metal oxide. Ions were eluted under sink conditions from IC discs (20mm x 2mm) into sterile high purity water at 37°C, samples being collected between 3 and 84 days. Total and free fluoride ion concentrations were determined using a calibrated ion selective electrode with TISAB III buffer. All other ions were determined by atomic absorption spectroscopy. For *in vitro* studies, primary rat bone marrow cells were cultured in supplemented MEM alpha medium in an atmosphere of 5% CO₂. Cells were inoculated at a concentration of 4×10^4 cells/ml into 24 well plates containing tissue sterilised IC, or control discs of dense hydroxyapatite or polymethyl methacrylate (PMMA,ICI U.K.), all discs were 12mm in diameter and 2mm thick. After one week, cell growth was assessed by measuring the total protein content of individual cell cultures using Peterson's modification of the micro-Lowry method. Cell viability was assessed by measuring the mitochondrial activity of the cells. There was an inverse relationship between the aluminium ion release from the ICs and cellular viability. There was no correlation between the cellular response to the ICs studied and their fluoride ion release. The response of cells to HA and PMMA confirmed the inert nature of these materials. *In vitro* biocompatibility of ICs is inversely proportional to aluminium ion release. This aluminium ion release would appear to be more important than fluoride ion release in determining the *in vitro* biocompatibility of ICs.

101 Fluoride release from aesthetic dental materials. A J PRESTON*, L II MAIR*, S M HIGHAM, E A AGALAMANYI (Department of Clinical Dental Sciences, University of Liverpool, UK)

The objective of the study was to investigate the amounts of fluoride released by two glass ionomer cements and to compare this with the amounts of fluoride released by a resin-modified ionomer cement, a compomer and a compomer.

Fluoride release from 3 samples each of 5 aesthetic dental materials was evaluated at 15 minute intervals in deionised water and artificial saliva over a period of 144 at a temperature of 37°C. The materials tested were 2 glass ionomers (1 of which was tested both with and without a surface layer of varnish), a resin-modified glass ionomer, a compomer and a compomer. The data was analysed to show the rate of fluoride release per hour for each material.

The results showed that the fluoride release rate for all the materials in both solutions decreased significantly after one hour. The release rate in artificial saliva was significantly less than in deionised water ($p < 0.05$). The resin-modified glass ionomer consistently displayed the highest fluoride release rate per hour (after 68 hours, water = 1.21 ± 0.11 , artificial saliva = 0.75 ± 0.24 ppm per hour). Dyract and Heliomolar showed the lowest fluoride release rates (after 168 hours, water = 0.020 ± 0.02 ; 0.007 ± 0.006 , artificial saliva = 0.020 ± 0.02 ; 0.020 ± 0.00 ppm F per respectively).

The resin-modified glass ionomer had a higher fluoride release rate than the other materials. The release rate for all the materials decreased dramatically with time.

102 Interactions of glass-ionomer cements with alkali metal fluoride solution RW BILLINGTON*, P HADLEY*, and GJ PEARSON* (Eastman Dental Institute Gray's Inn Rd, London & Advanced Healthcare Ltd, Nr Tonbridge, Kent.)

In a previous study (Billington RW et al J Dent Res 64: 144, 1987) the changes in hardness found in glass-ionomer cements (GIC) discs stored in 2% NaF solution were attributed to the pH changes observed in the NaF. Neither the role of the alkali metal counterion nor the presence or absence of F or alkali metal in the GIC have been reported. To evaluate this interaction K uptake was measured from a 2.75% solution of KF into two GICs, LG30[®] (No Na or F) and AH2[®] (Na and F). This was compared with pH of the solution and surface morphology of the GIC discs. Discs 10mm x 10mm were stored in water at 37°C for 3 days before immersing in KF. Uptake of K was measured (as change in concentration) using an atomic absorption spectrometer in $\mu\text{mol/g}$ and pH with a pH electrode. $N = 3$.

Glass / Time	Initial K pH	3mins K pH	50mins K pH	24hr K pH
LG30	83 6.5	115 6.5	112 6.6	135 7.8
AH2	123 6.7	253 6.6	185 6.7	601 7.6

After 24 hours SEM examination shows the matrix of the AH2 surface was selectively removed exposing the glass particles whereas LG30 was not so affected. Although pH changes were found they were small and similar for AH2 and LG30. It is concluded that F and Na in a GIC make the cement vulnerable to surface attack and such GICs also take up more K ions from solution. Hydroxyapatite on the GIC matrix does not appear a probable mechanism in these conditions.

1 Brite-Euran Programme, Limerick University, 2 Advanced Healthcare Ltd.

103 Effect of monovalent ions on glass-ionomer on their uptake/release P HADLEY*, RW BILLINGTON*, GJ PEARSON*, Advanced Healthcare Ltd, Tonbridge, Kent, Eastman Dental Institute, Gray's Inn Rd, London WC1X 8LD.

Fluoride release of fluoride ion by glass-ionomer cement (GIC) has been the subject of many studies whereas other ions have not been extensively reported. Williams et al (Proc 5th International Conference on Fluoride, 1987) found F release more prolonged with a F-free GIC than with a F-containing GIC (Billington et al Proc 4th World Biomaterials Cong Abs 213).

Researchers studied K re-release, but K was present in neither GIC. This study aims to compare F re-release from GICs made from 4 glasses: LG30[®] (neither Na nor F), LG26[®] (F but no Na), LG27[®] (Na but no F) and AH2[®] (both Na and F). Discs 10mm x 10mm were immersed in water at 37°C for 72 h, then in 10 ml, 2g/L NaF for 24 h. Re-release into 10 ml water, changed as follows, was measured using an atomic absorption spectrometer for Na and a selective ion electrode for F. Results are given as cumulative ion re-release of F & Na in $\mu\text{mol/g}$ compared to unexposed controls for the times in days given below. $N = 3$.

Day	3	6	10	15	23	30	37	1	2	3	6	10	15	23	30	37
Na	73	80	89	95	98	101	102	103	11	38	23	64	74	82	90	93
F	92	103	109	112	113	114	114	25	36	51	60	66	73	78	80	80
Na	58	61	65	67	68	69	70	30	42	51	56	60	66	71	75	79
F	131	136	143	149	153	156	158	160	57	77	84	88	89	94	95	100

The presence of both Na and F in a GIC significantly ($p < 0.01$) enhanced the uptake and release of F and Na re-released from the GIC. Almost all F re-release is complete within 37 days.

1 Brite-Euran Programme, Limerick University, 2 Pilkingtons, 3 Advanced Healthcare Ltd.

104 Confocal imaging of early maturation movements in glass ionomer cements. MA NAASAN*, TF WATSON and M SHERRIFF* (Dept. of Conservative Dentistry, & Dental Materials Science, UMDS, Guy's Hospital, London Bridge, SE1 9RT, UK)

The aim of this study was to image and compare the maturation movements of three 'posterior' glass-ionomer cement restorative materials: Shofu Hi Dense (Shofu UK), Fuji IX (GC Corp, Japan), and Kerac Molar (ESPE, Germany). Extracted third molar teeth were longitudinally sectioned. An 3.0 long x 2.5 wide x 4mm deep cavity was cut into each half tooth, equivalent to a hemisected class I cavity. The polished section surface was firmly clamped against a plastic cover slip. Three groups of 27 samples of each material were placed in the cavities, according to the manufacturer's instructions. The samples were microscopically examined using a confocal microscope (TSM). A x 20 objective lens was used to image for periods up to 135 min, using a video camera, and image capture/analysis system with time lapse (1 frame / minute). After 15 min, the slightly flexible plastic cover slip was removed and the restoration / tooth interface examined with a variety of 'moistening' media below a glass cover slip. These were: 1. glycerine for dehydration; 2. water for rehydration; and 3. oil to give a stable environment for water flux. Crack width and mode of failure were measured over time. Rapid shrinkage movement occurred during the first 15 minutes. Samples showed significant shrinkage with glycerine over the penultimate hour and a healing-swelling movement with water over the final hour period, which was most apparent with Shofu Hi Dense. Shrinkage was reduced when glycerine was placed in the last hour of the experiment. Limited shrinkage occurred under oil. The readily maturing Kerac Molar and Fuji IX showed larger shrinkage rates than Shofu Hi Dense which also swelled more on water uptake to close these gaps.

EPSRC GR/ 01035

DENTSPLY
DE TREY

DENTSPLY DeTrey GmbH
De-Trey-Straße 1
D-78467 Konstanz
Phone: +49-(0)7531-583-0
Fax: +49-(0)7531-583-104
Email: gbb@dentsply.de

TELEFAX

An/To: Dr. I. M. Brook
Zhd./Attn.:
Telefax-No.: 0044 114 271 7863
Von/From: Dr. G.B. Blackwell
Subject: Osseointegration and osteoconduction

Datum/Date: 10.06.1997
Zeichen/Ref.:

Seitenanzahl (inkl. Deckblatt)/
No. of pages (incl. cover page): 3
- Please copy locally -

cc:

I have now had a chance to look through the sheets you passed round at the meeting on Friday, and to do some analysis of the results in my own way. As shown in Tables 1 and 2, this indicates that the osseointegration and osteoconduction (for cured implants) increase with increase in phosphorus and sodium content of the glass, and decrease with increased content of fluoride.

Parameters for osseointegration

Parameter	Estimate	P-value
constant	-447.14	0.0407
ZnO5	1730.84	0.0299
CaF2	-504.60	0.0272
Na+K	155.02	0.0546

Table 1

R² = 95.5

Parameters for osteoconduction

Parameter	Estimate	P-value
constant	-1.62	0.0222
ZnO5	5.60	0.0193
CaF2	-1.54	0.0188
Na+K	0.38	0.0746

Table 2

R² = 88.2

zertifiziert
ISO 9001
certified

This does not agree with your analysis regarding the fluoride, and I have tried to see why this is. Initially I thought the above correlation's must be wrong, but on thinking about it I think they are correct, and that maybe we have been misled by the way the glass compositions are tabulated. I will try to explain this below. The arguments are the same for either osseointegration or osteoconduction.

In Table 3 are the glass compositions and the osseointegration results for the dry specimens as given in your handout.

Batch number		SiO2	Al2O3	P2O5	CaO	CaF2	Na2O	K2O	% osseoint	Osteo - conduction mm
LG	2	1.500	1.000	0.500	1.000	0.750	0.000	0.000	37.00	0.05
LG	6	1.500	1.000	0.500	0.900	0.750	0.100	0.000	61.00	0.07
LG	63	1.500	1.000	0.500	0.800	0.750	0.200	0.000	68.00	0.10
LG	26	4.500	3.000	1.500	3.000	2.000	0.000	0.000	80.80	0.16
LG	27	6.000	4.000	1.500	4.000	1.000	0.000	0.000	78.20	0.08
LG	30	7.500	5.000	1.500	5.000	0.000	0.000	0.000	70.60	0.07

Table 3

At first sight this looks like a series of increasing Na content (glasses 2, 6, and 63), and a series of decreasing CaF2 content (glasses 26, 27, and 30). However it looks different when the compositions are recalculated so that the Al2O3 is always 1, as in Table 4. (All values are divided by the Al2O3 value. The SiO2 content then also becomes constant.)

Batch number		SiO2	Al2O3	P2O5	CaO	CaF2	Na2O	K2O	% osseoint
LG	2	1.500	1.000	0.500	1.000	0.750	0.000	0.000	37.00
LG	6	1.500	1.000	0.500	0.900	0.750	0.100	0.000	61.00
LG	63	1.500	1.000	0.500	0.800	0.750	0.200	0.000	68.00
LG	26	1.500	1.000	0.500	1.000	0.667	0.000	0.000	80.80
LG	27	1.500	1.000	0.375	1.000	0.250	0.000	0.000	78.20
LG	30	1.500	1.000	0.300	1.000	0.000	0.000	0.000	70.60

Table 4

From Table 4 you can see that as well as a trend of decreasing CaF2 in going from LG2 to LG30, there is also a trend of decreasing P2O5. In fact the CaF2 content is highly correlated with the P2O5 content, meaning that when one decreases, so does the other, the only exception to this being LG26. This means that we can't really be sure whether it is the CaF2 or the P2O5 content

which is having the effect on the osseointegration. However LG2 and LG26 form a mini-series in which all components are the same except the CaF2 content. The glass LG26 has a lower CaF2 content than LG2 but the osseointegration is higher, indicating that osseointegration increases with decreasing CaF2 content, as reflected in the negative coefficient for CaF2 in Table 1.

Finally in Table 5 I have sorted the results in order of increasing osseointegration. I think this makes the relationships clearer.

Batch number	SiO2	Al2O3	P2O5	CaO	CaF2	Na2O	K2O	% osseoint	Osteo-conduction
LG 2	1.500	1.000	0.500	1.000	0.750	0.000	0.000	37.00	0.05
LG 6	1.500	1.000	0.500	0.900	0.750	0.100	0.000	61.00	0.07
LG 63	1.500	1.000	0.500	0.800	0.750	0.200	0.000	68.00	0.10
LG 30	1.500	1.000	0.300	1.000	0.000	0.000	0.000	70.60	0.07
LG 27	1.500	1.000	0.375	1.000	0.250	0.000	0.000	78.20	0.08
LG 26	1.500	1.000	0.500	1.000	0.667	0.000	0.000	80.80	0.16

Table 5

I have done a similar analysis with the osteoconduction, and with the same arguments the same conclusions are reached. The results are given in Table 5.

I hope this is useful and not too confusing. Even with the reservations about the P2O5/CaF2 correlation I think you should reconsider your conclusions. Please let me know your thoughts about the above or if you find a flaw in my arguments. I'm not at all familiar with the literature in this area - is there any evidence that the above is wrong? I'm afraid I don't have enough data to do anything with the other series (wet) because these introduce new variables such as strontium.

Regards,

Gordon.

? Ion Release ? \bar{v} content. \bar{v} INT/cont.

Response is under similar F-ALX?

? AL Release